Preclinical validation of antifibrotic implantables for use in bleb-forming glaucoma surgery

Preclinical validation of antifibrotic implantables for use in bleb-forming glaucoma surgery

R.J.S. van Mechelen

Preklinische validatie van fibrose remmende implantaten voor glaucoomchirurgie

R.J.S. van Mechelen

ISBN: 978-94-6419-872-0

Printing: Gildeprint Enschede
Cover design and layout: R.J.S. van Mechelen and Gildeprint Enschede
Chapter 1, Figure 1-1, 1-2, 1-3, 1-4, 5-1: Rogier Trompert Medical Art

Preclinical validation of antifibrotic implantables for use in bleb-forming glaucoma surgery

Proefschrift

ter verkrijging van de graad van doctor aan de Universiteit Maastricht,
op gezag van de Rector Magnificus, Prof. dr. Pamela Habibović
volgens het besluit van het College van Decanen,
in het openbaar te verdedigen
op 16 Oktober om 16:00 uur

door

Radulfus Johannes Stefanus van Mechelen
Geboren 4 Juni 1993 te Heerlen

Promotor
Prof. dr. H.J.M. Beckers

Copromotores
Dr. J.E.J. Wolters
Dr. C.J.F. Bertens

Beoordelingscommissie
Prof. dr. M. van Griensven (voorzitter)
Prof. dr. H.J.M. Smeets
Prof. dr. N.M. Jansonius (Groningen UMC)
Dr. L.J. van Rijn (Amsterdam UMC)

Table of Contents

The research in this thesis was performed under the framework of the Chemelot Institute for Science and Technology (InSciTe).

Chapter 1

General introduction

1. General introduction

The eye is one of the major sensory organs of the body and it plays a very important role in everyday life. If the eye is not functioning properly, visual impairment or blindness can occur. Glaucoma is the leading cause of irreversible blindness worldwide [1]. The etiology and pathogenesis of this disease is complex and not fully elucidated yet. Currently, there is no causative treatment available [2]. Current treatments mainly focus on the reduction of intraocular pressure (IOP), the main risk factor for developing glaucoma. The research in this thesis aims to improve upon the current standard for the surgical treatment of glaucoma, by refining existing treatments and investigating novel antifibrotic treatment modalities. Before going into further detail about glaucoma and its treatment, the following paragraph will give an overview of the anatomy of the eye.

1.1 Anatomy of the eye

The eye consists of several structures as depicted in figure 1-1. The eyeball (*bulbus oculi*) is supported by several surrounding tissues (*adnexa*) *i.e.*, eyelids, conjunctiva, muscles, and the lacrimal system. Intraocular structures are the cornea, trabecular meshwork (TM), iris, ciliary body, lens, vitreous chamber, retina, choroid, and sclera.

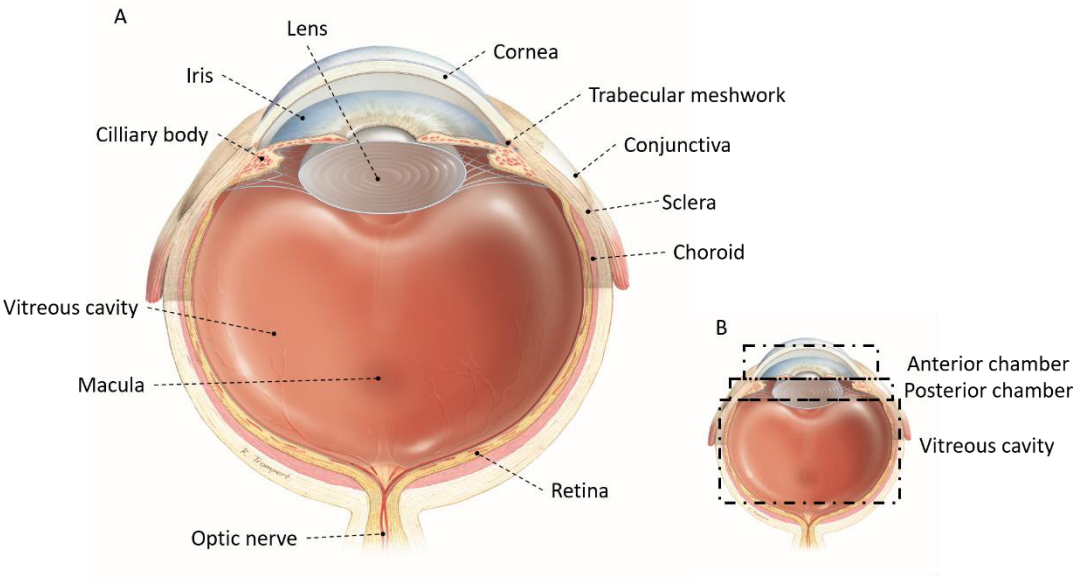

Figure 1-1: Schematic overview of the eye. The eye can be divided into three chambers (see image 1-1B), 1) the anterior chamber, located between the cornea and iris, 2) the posterior chamber between the iris and lens. Both the anterior- and posterior chambers are filled with aqueous humor (AqH), 3) the vitreous cavity, which is covered by the retina. The choroid, a highly vascularized area, is situated between the sclera and retina.

Three chambers can be distinguished within the eye. These are (from front to back) the anterior chamber (area between the cornea and iris), the posterior chamber (area between iris and lens), and the vitreous cavity (area behind the lens) [3]. Figure 1-2 gives a detailed overview of the anterior and posterior chambers which are important regions for the treatment of glaucoma. Aqueous humor (AqH) is produced in the ciliary body, after which it is secreted by the ciliary epithelium. Subsequently, AqH flows from the posterior chamber over the lens into the anterior chamber, providing nutrients to surrounding ocular tissues such as the lens and cornea [3, 4]. In a healthy situation, an equilibrium or homeostasis exists between AqH production and drainage. AqH drains out of the eye through two pathways. Firstly, through the TM and Schlemm's canal which is called the conventional pathway. Secondly, AqH can be reabsorbed through surrounding tissues such as the ciliary muscle, and choroidal vessels. This is called the uveoscleral, or unconventional pathway [5, 6]. In glaucoma, the outflow of AqH is often obstructed, resulting in increased intraocular pressure (IOP), the primary risk factor for glaucoma (IOP higher than 21 mmHg) [7].

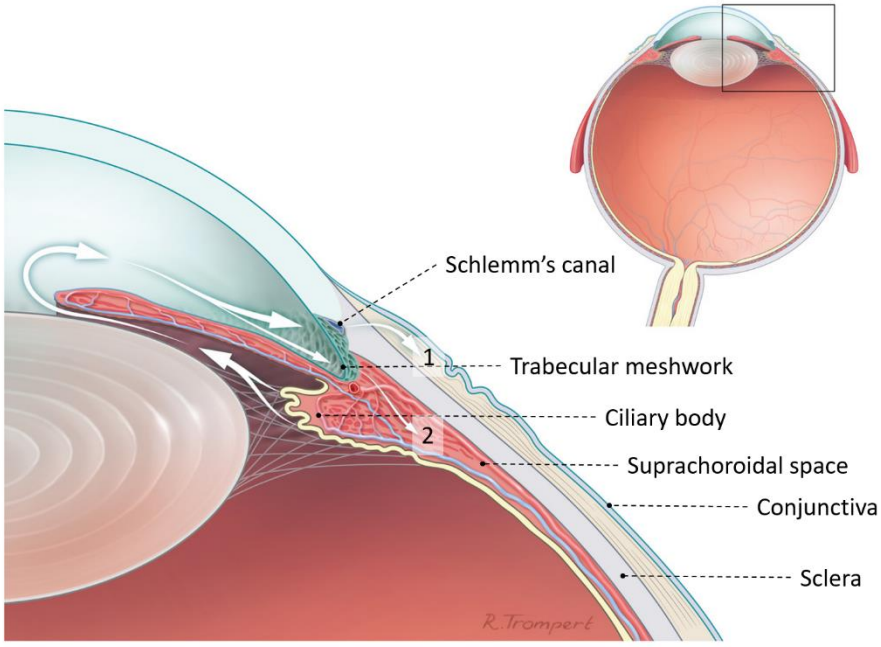

Figure 1-2: Detailed representation of the anterior and posterior chamber of the eye, the white arrows indicate aqueous humor (AqH) flow. AqH is produced in the ciliary body. Hereafter, it travels from the posterior chamber towards the anterior chamber, providing nutrients to the surrounding tissues. AqH drains out of the eye from the trabecular meshwork, after which it is collected in Schlemm's canal (conventional pathway, arrow 1). Alternatively, AqH can also be reabsorbed through the uveoscleral pathway (arrow 2).

Lastly, in the retina light is converted into electrical impulses by photoreceptors (rods and cones), these electrical impulses are conveyed towards retinal ganglion cells (RGCs) through the inner nuclear layer, where signal regulating cells reside (amacrine cells, horizontal cells, and bipolar cells). Nerve fibers of the RGCs converge in the optic nerve head. Hereafter, the optic nerve sends the electrical impulses to the brain where an image is created.

1.2 Glaucoma

Glaucoma is a group of optic neuropathies that are characterized by degeneration of RGCs and the optic nerve (see figure 1-3A) [8]. Glaucoma leads to progressive visual field loss and eventually to blindness if left untreated (figure 1-3B). Glaucoma is the most common cause of irreversible blindness worldwide, and with the ageing population, it is expected that by 2040 approximately 112 million people will suffer from glaucoma [1, 9]. Glaucoma is asymptomatic in its early stages. Approximately 50 to 60% of individuals are unaware of having glaucoma [10, 11]. Several types of glaucoma exist, namely congenital glaucoma, juvenile glaucoma, primary open angle glaucoma (POAG), secondary open angle glaucoma, primary angle closure glaucoma, secondary angle closure glaucoma, and normal pressure glaucoma. The most common form of glaucoma is POAG, in which outflow of AqH is blocked at the level of the TM. As mentioned previously, the primary risk factor for glaucoma is elevated IOP (> 21 mmHg). Other risk factors include age, race, smoking, obesity, and genetic background. Although risk factors for the disease are known, the complete pathophysiology is currently unknown. Glaucoma can be diagnosed with several clinical examinations *i.e.*, IOP measurements (tonometry), assessment of morphological changes to the anterior chamber, optic nerve, and retinal thickness (gonioscopy, funduscopy, and optical coherence tomography, respectively), and visual field testing, which is regularly performed on glaucoma patients to monitor the progression glaucomatous visual field loss [11].

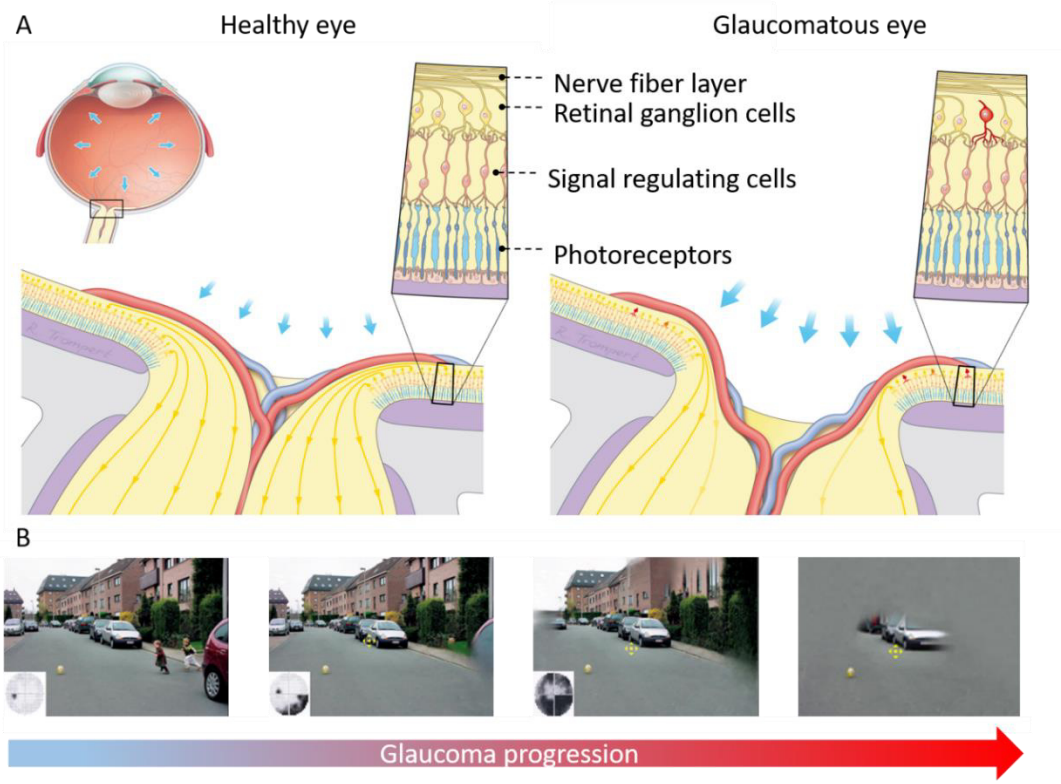

Figure 1-3 (A) Schematic comparison between a healthy (left image) and glaucomatous (right image) eye. In a healthy eye light is converted into electrical impulses by photoreceptors. Signal regulating cells (such as amacrine cells, bipolar cells, and horizontal cells) propagate the signals towards retinal ganglion cells (RGCs). The nerve fibers of the RGCs converge in the optic nerve, which subsequently sends the electrical signal towards the brain to create an image. In a glaucomatous eye, RGCs are damaged and so called “cupping” of the optic nerve occurs, resulting in vision loss. (B) Vision is normal in the early stages of glaucoma. However, as glaucoma progresses and more damage to the RGCs and the optic nerve occurs, visual field defects occur. Progressive visual field loss may lead to severe visual impairment and, finally, blindness. Images courtesy of Ann Hoste, Belgium ©.

1.3 Glaucoma treatment

After diagnosis, glaucoma needs careful monitoring since, even with treatment, visual field loss can still progress. Therefore, treatment of a glaucoma patient is an intensive process in need of continuous adjustments over a patient's lifetime [12]. Currently, IOP reduction is the only proven method to treat glaucoma and reduce progression of visual field loss. Although some clinical trials have tested neuroprotective drugs to find a therapy that can help cure glaucoma, none of them have been successful yet [13, 14]. IOP can be decreased by either reducing the production of AqH or increasing the outflow of AqH. Treatments can be divided into three categories; eye drops (topical medication), laser treatment, and incisional surgery. The latter includes glaucoma filtration surgery (GFS) and minimally invasive glaucoma surgery (MIGS) [9].

1.3.1 Topical medication

Treatment of glaucoma usually starts with eye drops to lower IOP. Several types of drugs can be used including prostaglandin analogues, beta-blockers, carbonic anhydrase inhibitors, and alpha agonists [9, 15, 16]. In case monotherapy is ineffective, a combination of multiple eye drops with different mechanisms can be given to the patient [9]. Unfortunately, adherence to topical therapy is low. Roughly 45% of patients do not consistently take their eye drops [17], which compromises the effectiveness of the prescribed therapy, and subsequently leads to raised IOP. Reasons for nonadherence include suboptimal instillation techniques due to tremors or other physical barriers, poor understanding of treatment aims, and side effects such as irritation of the eye and/or blurred vision [18-21].

1.3.2 Laser treatment

If topical medication does not induce significant IOP reduction, laser treatment can be performed. Laser therapy can also be offered as initial therapy [22], especially when side effects or problems with adherence are expected. During this treatment AqH outflow is increased by burning the TM with a laser, which scars the tissue and afterwards tightens the TM, opening up surrounding structures (pores) and increasing the outflow of AqH [23]. Selective laser trabeculoplasty (SLT) is currently the most used method since it is less destructive to the TM compared to argon laser trabeculoplasty (ALT) [24, 25]. Although SLT is effective in reducing IOP in 80% of patients and reducing the need for topical medications, roughly 50% of all procedures fail within 2 years [24].

1.3.3 Incisional surgery

Surgical intervention is usually resorted to when the aforementioned techniques are insufficient to stop progression of the disease and a low target IOP needs to be reached. Although many variations of surgical techniques exist, they all aim to create an alternative pathway for AqH to exit the eye and reduce IOP. Conventional methods for GFS are trabeculectomy or tube-shunt surgery. The current gold standard for GFS is trabeculectomy. It is a technique that is already decades old but has been refined over the years. During a trabeculectomy a small hole or "fistula" is created between the anterior chamber and the subconjunctival/sub-Tenon's space. AqH will flow under the overlying conjunctiva and the accumulation of fluid there will create a small pouch, called a filtering bleb [26]. Although highly effective in reducing IOP, blebs tend to fail due to the formation of a fibrotic scar (due to an excessive wound healing response) at the filtering bleb, hampering outflow. Therefore, antifibrotic drugs have been implemented to reduce fibrosis. Antimetabolites, such as mitomycin C (MMC) and 5-fluorouracil (5-FU) have been widely used for their antifibrotic efficacy [27]. However, use of these drugs has been associated with severe vision threatening complications such as hypotony, hyphema, bleb leakage, blebitis, and endophthalmitis [9, 26]. Despite the use of antimetabolites, surgeries still tend to fail in 10% of cases per year due to formation of fibrotic tissue [28].
Conventional tube-shunt surgery is the preferred method in cases where trabeculectomy has failed, in refractory glaucoma, or in patients that are prone to develop fibrotic tissue [29]. During tube-shunt surgery a long-tube glaucoma drainage device (GDD) is implanted between the anterior chamber and the subconjunctival space (comparable to trabeculectomy). A GDD typically consists out of a silicone tube and a plate at the end of the tube (made from either silicone or polypropylene). The tube is implanted into the anterior chamber, and the plate will be placed subconjunctivally and sutured onto the sclera to prevent displacement [26]. Trabeculectomy remains the gold standard for incisional surgery in treating POAG. However, as a second option, tube-shunt surgeries are gaining more and more popularity, also for primary cases [30]. Although GFS is highly effective in reducing IOP, clinicians will withhold patients from surgery due to considerable postoperative care and possible vision-threatening complications [12].

The second decade of the 2000s witnessed a tremendous growth in the development of new methods, the so called minimally invasive glaucoma surgery (MIGS) [31, 32]. MIGS claim to have a shorter surgical time, higher safety, faster recovery, and an easier implantation procedure [12]. Whereas during conventional GFS the subconjunctival area is targeted to create a filtering bleb, MIGS procedures can also be directed towards different types of outflow areas. Trabecular meshwork tissue can be either ablated, dilated (Schlemm's canal) or implanted with a small

stent to increase outflow of the TM, implants are currently under investigation to be placed in the suprachoroidal space (increasing outflow of the uveoscleral pathway), and small tubes can be placed into the subconjunctival space (comparable to GFS procedures where AqH flows into a bleb) [32]. This latter form of treatment is currently often referred to as less invasive bleb-forming surgery, as there is more tissue dissection/work needed compared to an ab-interno MIGS procedure, for which usually a small corneal incision is sufficient. Regardless of the advantages of MIGS, the evidence of their IOP lowering efficacy is limited. It has been shown that the new procedures that drain AqH into the subconjunctival space and create a bleb, may have better IOP outcomes compared to ab-interno MIGS techniques [33-39]. However, postoperative complications such as hyphema, hypotony, and the formation of fibrosis can still occur [31, 37-40].

Despite the many available treatment modalities, 25% of all glaucoma patients will ultimately go blind in one eye, and 10% of patients will even become totally blind before the end of their life due to glaucoma [41]. These figures clearly indicate the importance and unmet need for refinement and development of novel treatment modalities that will result in safer and more reliable, stable, and low IOP outcomes.

1.4 Fibrosis

As stated before, about 10% of surgeries fail yearly due to the formation of fibrotic tissue within the filtering bleb [28]. The formation of fibrotic tissue can severely hamper the outflow facilitation of AqH into the bleb, resulting in a decreased outflow of AqH and subsequently an increase in IOP. If this happens, patients will often need to restart or increase their use of topical medication or undergo additional surgery. Fibrosis is not a disease in itself but rather an overstimulated wound healing response. The wound healing response is a normal reaction within the body used to heal tissue damage and form new (healthy) tissue. However, when the wound healing response is overstimulated, a fibrotic response occurs, creating scar tissue [42]. The wound healing response can be divided into four distinct but overlapping phases; hemostasis (first few hours after injury), inflammatory phase (0 - 3 days after injury), proliferative phase (12 hours - 21 days after injury), and tissue remodeling (21 days to a year after injury) [43, 44]. A broad overview of the wound healing response after placement of a subconjunctival tube is given in Figure 1-4.

1.4.1 Hemostasis

After injury, for example due to a surgical procedure, damage to the tissue and surrounding blood vessels will induce a process called hemostasis. During hemostasis, vessels will constrict, and platelets will congregate and form a blood clot by coagulation factors. Subsequently, thrombin induces the formation of fibrin from

fibrinogen [45-47]. Platelets will recruit immune cells by secretion of a secretome with chemokine attractants upon degranulation (chemotaxis), or by directly capturing immune cells in the formed blood clot [48]. Additionally, platelets will release growth factors that can stimulate fibroblasts, endothelial cells, and keratinocytes to aid tissue repair [46]. When a stable blood clot is formed, the coagulation process will be inhibited to prevent excessive thrombosis [49].

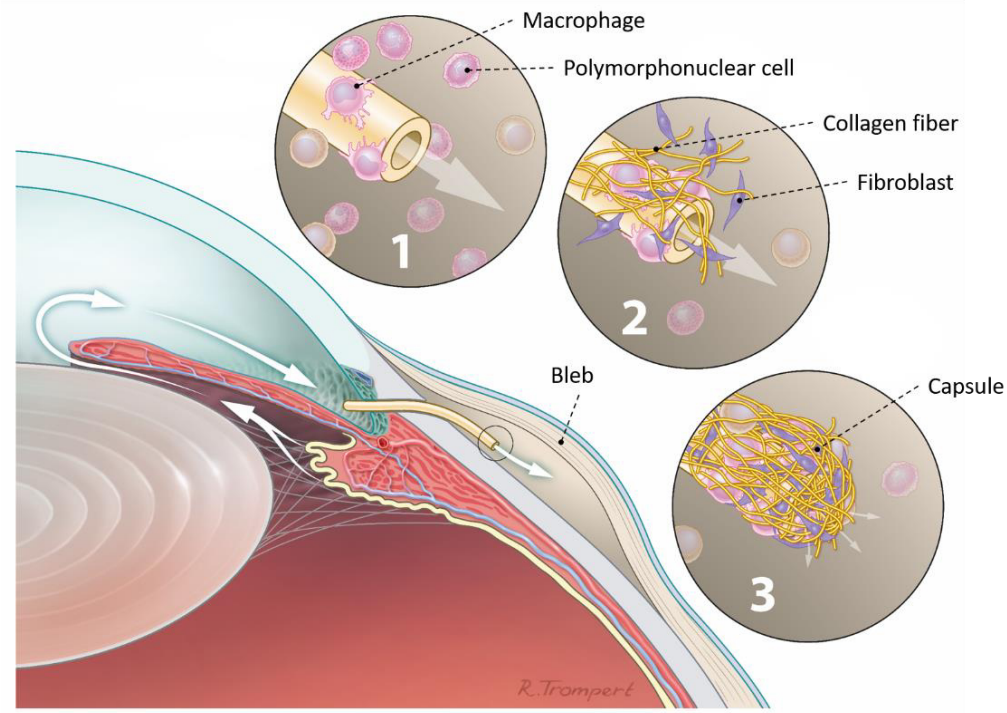

Figure 1-4: Overview of the wound healing response after implantation of a small glaucoma implant into the subconjunctival space. Fluid flow is indicated by white arrows, Aqueous humor (AqH) is produced in the ciliary body, after which it flows towards the anterior chamber and drains out of the eye into a bleb through the implanted microshunt. In short, (1) after surgery an influx of macrophages and polymorphonuclear cells (PMNs) indicate the start of the inflammatory phase. These will start to secrete cytokines and growth factors. (2) Fibroblasts will proliferate and produce extra cellular matrix and collagen fibers to heal the wound. (3) Ultimately, when the wound healing response is complete a fibrotic capsule will be left, limiting the functionality of the bleb.

1.4.2 Inflammatory phase

The loss of blood, plasma proteins, and the release of chemokine attractants from activated platelets induce a local inflammatory response and immune cells such as T cells, mast cells, and resident macrophages are activated [46]. Additionally, immune cells such as neutrophils (or alternatively called polymorphonuclear cells

(PMNs)) and monocytes are attracted from the blood stream towards the site of injury through a process called chemotaxis [50]. PMNs will start to release enzymes and reactive oxygen species (ROS) to clear up tissue debris and eliminate bacteria. Monocytes entering from the blood stream can transdifferentiate into different subsets of macrophages *e.g.*, pro-inflammatory macrophages (previously called M1-macrophages) or anti-inflammatory/alternatively activated macrophages (previously called M2-macrophages). Although this is a simplified representation of the real process, it provides a basic outline of what happens during the inflammatory phase. Pro-inflammatory macrophages will promote inflammation by releasing ROS, inflammatory cytokines, and growth factors. In turn these macrophages will phagocytose apoptotic neutrophils and replace them as the primary inflammatory cell within a wound. Under the influence of environmental changes such as a switch in cytokines, micro-RNAs, transcription factors, and changes in receptors, pro-inflammatory macrophages or monocytes can undergo transdifferentiation into anti-inflammatory (alternatively activated) macrophages [46]. Anti-inflammatory macrophages will release cytokines to resolve inflammation and release growth factors to promote re-epithelialization, fibrosis and angiogenesis [51].

1.4.3 Proliferative phase

Within 12 hours after initial injury, the proliferative phase starts. The main cells involved in this process are keratinocytes, endothelial cells (angiogenesis), macrophages (angiogenesis), and fibroblasts [52]. Keratinocytes get activated by cytokines and growth factors, after which they will undergo partial epithelial mesenchymal transition. Then they start to migrate across the wound to form a new epidermal layer (re-epithelialization) [46]. Fibroblasts will start to degrade the fibrin clot and replace this with a new extra cellular matrix (ECM) called granulation tissue. Granulation tissue consists of immature collagen (predominantly type III collagen), fibronectin and proteoglycans [53]. Granulation tissue helps in the differentiation and migration of cells, and supports the formation of blood vessels through endothelial cells (angiogenesis) [46]. Lastly, macrophages will secrete growth factors, cytokines, and matrixmetalloproteinases to aid the aforementioned cells and drive the differentiation of cells [46].

1.4.4 Tissue remodeling

The last phase of the wound healing response starts approximately 3 weeks after surgery and can last up to 1 year or longer [54]. Fibroblasts are the primary cell type responsible for tissue remodeling. Fibroblasts will replace the existing ECM with mature collagen fibers (predominantly collagen type I), increasing the tensile strength of the tissue [55]. Under the influence of transforming growth factor-β fibroblasts will transdifferentiate into myofibroblasts (characterized by the expression

of α-smooth muscle actin). Myofibroblasts will generate the contractile strength necessary for wound contracture [56]. When the wound healing response is complete, cells will undergo apoptosis or exit the site of injury, leaving solely fibrotic or scar tissue behind [57].

1.4.3 Mitomycin C

In order to reduce the postoperative fibrotic response, the antimetabolites MMC and 5-FU are currently used during and/or after surgery. MMC and 5-FU were introduced in the 1990s as an intraoperative treatment [58]. Due to the increased success rate associated with the use MMC, MMC became the gold standard antifibrotic therapy [59]. MMC is favored over 5-FU due to its increased potency [60-62]. However, the use of especially MMC is accompanied by vision threatening complications, such as bleb leaks, endophthalmitis, and corneal endothelial cell loss [63, 64]. MMC is nonselective in nature, it inhibits DNA synthesis and proliferation in all cells it encounters [58]. MMC is currently used as an intraoperative treatment (application within sub-Tenon's space) or as a postoperative treatment (bleb needling) [58, 59, 65, 66]. Postoperative treatment with MMC is needed in approximately 30-50% of cases, indicating that intraoperative treatment alone is insufficient to sufficiently inhibit the fibrotic response [58]. Within Europe, MMC is used off-label [67]. This results in unstandardized treatment strategies differing with each surgeon, leading to variable results across patients. The implementation of a novel treatment modality in the form of a drug delivery system might offer solutions towards improving standardization, and decreasing the toxicity associated with use of MMC.

The efficacy and toxicity of a drug is affected by the dosage, mechanism of action, and the route of administration [68, 69]. Lower drug concentrations that are still sufficiently antifibrotic might offer safer treatment regimens for MMC. Development of small drug eluting devices or a drug delivery system (DDS) might be suitable solutions. A DDS will release a drug at low concentrations near the surgical site for a sustained period. Through this mechanism, toxic drugs (such as MMC) are less likely to reach toxic levels within a tissue, while still reaching therapeutic antifibrotic levels over a sustained period. Currently, a wide range of antifibrotic therapies are being developed and tested [70]. However, most have not yet shown to be as effective as MMC.

1.5 The SEAMS project

The goal of the Smart, Easy and Accurate Minimally invasive glaucoma Surgery (SEAMS) project was to reduce the failure rate of bleb-forming glaucoma surgery by developing a novel miniature drainage device and DDS. The drainage device would

contain flow control properties to eliminate the risk of postoperative hypotony and have optimal material properties that reduce the fibrotic response *in vivo* and thereby postoperative bleb failure. Additionally, we aimed for a sustained release of MMC to reduce the fibrotic response, while maintaining a safe dosage within the eye, by developing a DDS.
All the work done during this project was performed under the framework of Chemelot Institute for Science and Technology (InSciTe), within a multidisciplinary collaboration between Maastricht University (UM), the University Eye Clinic of the Maastricht University Medical Center + (MUMC+), Eindhoven University of Technology (TU/e) and InnFocus Inc., a Santen company. This company previously developed a new bleb-forming drainage device called the PRESERFLO MicroShunt (previously known as the InnFocus MicroShunt).

1.6 Aims and outline of this thesis

The goal of this thesis is to provide a clear understanding of the development and preclinical testing of novel biomedical devices for use in bleb-forming glaucoma surgery, more specifically, a novel miniature glaucoma drainage device and a DDS loaded with MMC. These novel devices were tested at first *in vitro* (not part of this thesis) by our partners. Hereafter, optimized designs were implanted into a rabbit model of glaucoma surgery.

In **chapter 2** we reviewed current standards for GFS animal models and antifibrotic drugs that are currently in the phase of preclinical testing. While most drugs had a lower antifibrotic efficacy compared MMC, they also induced fewer side-effects compared to MMC. The preclinical testing of devices and/or drugs has been performed on several types of animal models including mice, rats, rabbits, dogs, and primates. Based on specific requirements (such as the size of the eye) and also considering ethics, we chose the rabbit model to continue our research. **Chapter 3** describes an *in vivo* study in which we compared state-of-the-art tonometers commonly used in animals (TonoPen, TonoLab, and TonoVet). We compared the reproducibility, reliability, and agreement of the different tonometers. Furthermore, we studied the effect of sedation on the IOP. From the tested tonometers, the TonoVet was chosen as it showed to be the most reliable tonometer to use within a rabbit model by multiple users. Additionally, sedation lowered the IOP, and we took this into consideration for our further experiments.
We aimed to study key cellular players within the fibrotic response after implantation of a SIBS microshunt in a rabbit model for maximally 40 days (**chapter 4**). We wanted to elucidate the interplay between, fibroblasts, myofibroblasts, macrophages, PMNs, and foreign body giant cells. Subsequently, a pilot study in which material enhancing surface topographies were tested *in vivo* for their antifibrotic efficacy is

presented in **chapter 5**. MMC has been used in glaucoma surgery for its antifibrotic properties since the 1990s. In **chapter 6,** we aimed to discuss the history, presence, and future use of MMC, outlining the importance of refinement and development of novel treatment modalities. Finally, **chapter 7** describes the development of two novel drug delivery systems *in vitro* and *in vivo* compared to the gold standard, one-time application of MMC. A general discussion is provided in **chapter 8,** and the impact of the research is outlined in **chapter 9**.

References

1. Tham, Y.C., et al., *Global prevalence of glaucoma and projections of glaucoma burden through 2040: a systematic review and meta-analysis.* Ophthalmology, 2014. **121**(11): p. 2081-90.
2. Conlon, R., H. Saheb, and Ahmed, II, *Glaucoma treatment trends: a review.* Can J Ophthalmol, 2017. **52**(1): p. 114-124.
3. Ophthalmology, A.A.o., *Fundamentals and Principles of Ophthalmology*. 2012.
4. Liu, H., et al., *Aqueous humor dynamics during the day and night in healthy mature volunteers.* Arch Ophthalmol, 2011. **129**(3): p. 269-75.
5. Buffault, J., et al., *The trabecular meshwork: Structure, function and clinical implications. A review of the literature.* J Fr Ophtalmol, 2020. **43**(7): p. e217-e230.
6. Johnson, M., J.W. McLaren, and D.R. Overby, *Unconventional aqueous humor outflow: A review.* Exp Eye Res, 2017. **158**: p. 94-111.
7. *The Advanced Glaucoma Intervention Study (AGIS): 7. The relationship between control of intraocular pressure and visual field deterioration.The AGIS Investigators.* Am J Ophthalmol, 2000. **130**(4): p. 429-40.
8. Hoon, M., et al., *Functional architecture of the retina: development and disease.* Prog Retin Eye Res, 2014. **42**: p. 44-84.
9. Conlon, R., H. Saheb, and I.I.K. Ahmed, *Glaucoma treatment trends: a review.* Canadian Journal of Ophthalmology, 2017. **52**(1): p. 114-124.
10. Sommer, A., et al., *Relationship Between Intraocular Pressure and Primary Open Angle Glaucoma Among White and Black Americans: The Baltimore Eye Survey.* Archives of Ophthalmology, 1991. **109**(8): p. 1090-1095.
11. McMonnies, C.W., *Glaucoma history and risk factors.* J Optom, 2017. **10**(2): p. 71-78.
12. Bar-David, L. and E.Z. Blumenthal, *Evolution of Glaucoma Surgery in the Last 25 Years.* Rambam Maimonides Med J, 2018. **9**(3).
13. Storgaard, L., et al., *Glaucoma Clinical Research: Trends in Treatment Strategies and Drug Development.* Front Med (Lausanne), 2021. **8**: p. 733080.
14. Weinreb, R.N., et al., *Oral Memantine for the Treatment of Glaucoma: Design and Results of 2 Randomized, Placebo-Controlled, Phase 3 Studies.* Ophthalmology, 2018. **125**(12): p. 1874-1885.
15. Scozzafava, A. and C.T. Supuran, *Glaucoma and the applications of carbonic anhydrase inhibitors.* Subcell Biochem, 2014. **75**: p. 349-59.
16. *European Glaucoma Society Terminology and Guidelines for Glaucoma, 5th Edition.* Br J Ophthalmol, 2021. **105**(Suppl 1): p. 1-169.
17. Okeke, C.O., et al., *Adherence with topical glaucoma medication monitored electronically the Travatan Dosing Aid study.* Ophthalmology, 2009. **116**(2): p. 191-9.
18. Kosoko, O., et al., *Risk factors for noncompliance with glaucoma follow-up visits in a residents' eye clinic.* Ophthalmology, 1998. **105**(11): p. 2105-11.
19. McVeigh, K.A. and G. Vakros, *The eye drop chart: a pilot study for improving administration of and compliance with topical treatments in glaucoma patients.* Clin Ophthalmol, 2015. **9**: p. 813-9.
20. Beckers, H.J., et al., *Adherence improvement in Dutch glaucoma patients: a randomized controlled trial.* Acta Ophthalmol, 2013. **91**(7): p. 610-8.
21. Beckers, H.J., et al., *Side effects of commonly used glaucoma medications: comparison of tolerability, chance of discontinuation, and patient satisfaction.* Graefes Arch Clin Exp Ophthalmol, 2008. **246**(10): p. 1485-90.
22. *The Glaucoma Laser Trial (GLT) and glaucoma laser trial follow-up study: 7. Results. Glaucoma Laser Trial Research Group.* Am J Ophthalmol, 1995. **120**(6): p. 718-31.
23. Samples, J.R., et al., *Laser Trabeculoplasty for Open-Angle Glaucoma: A Report by the American Academy of Ophthalmology.* Ophthalmology, 2011. **118**(11): p. 2296-2302.
24. McAlinden, C., *Selective laser trabeculoplasty (SLT) vs other treatment modalities for glaucoma: systematic review.* Eye (Lond), 2014. **28**(3): p. 249-58.
25. Latina, M.A. and J.A. Tumbocon, *Selective laser trabeculoplasty: a new treatment option for open angle glaucoma.* Curr Opin Ophthalmol, 2002. **13**(2): p. 94-6.
26. Lusthaus, J. and I. Goldberg, *Current management of glaucoma.* Medical Journal of Australia, 2019. **210**(4): p. 180-187.
27. Lin, S., D. Byles, and M. Smith, *Long-term outcome of mitomycin C-augmented needle revision of trabeculectomy blebs for late trabeculectomy failure.* Eye (Lond), 2018. **32**(12): p. 1893-1899.

28. Beckers, H.J., K.C. Kinders, and C.A. Webers, *Five-year results of trabeculectomy with mitomycin C.* Graefes Arch Clin Exp Ophthalmol, 2003. **241**(2): p. 106-10.
29. Alasbali, T., A.A. Alghamdi, and R. Khandekar, *Outcomes of Ahmed valve surgery for refractory glaucoma in Dhahran, Saudi Arabia.* Int J Ophthalmol, 2015. **8**(3): p. 560-4.
30. Gedde, S.J., et al., *Primary Open-Angle Glaucoma Suspect Preferred Practice Pattern®.* Ophthalmology, 2021. **128**(1): p. P151-P192.
31. Gillmann, K. and K. Mansouri, *Minimally Invasive Glaucoma Surgery: Where Is the Evidence?* Asia Pac J Ophthalmol (Phila), 2020. **9**(3): p. 203-214.
32. Pereira, I.C.F., et al., *Conventional glaucoma implants and the new MIGS devices: a comprehensive review of current options and future directions.* Eye (Lond), 2021. **35**(12): p. 3202-3221.
33. Green, W., J.T. Lind, and A. Sheybani, *Review of the Xen Gel Stent and InnFocus MicroShunt.* Curr Opin Ophthalmol, 2018. **29**(2): p. 162-170.
34. Riss, I., et al., *[One-year results on the safety and efficacy of the InnFocus MicroShunt depending on placement and concentration of mitomycin C].* J Fr Ophtalmol, 2015. **38**(9): p. 855-60.
35. Batlle, J.F., A. Corona, and R. Albuquerque, *Long-term Results of the PRESERFLO MicroShunt in Patients With Primary Open-angle Glaucoma From a Single-center Nonrandomized Study.* Journal of glaucoma, 2021. **30**(3): p. 281-286.
36. Scheres, L.M.J., et al., *XEN(®) Gel Stent compared to PRESERFLO™ MicroShunt implantation for primary open-angle glaucoma: two-year results.* Acta ophthalmologica, 2021. **99**(3): p. e433-e440.
37. Busch, T., et al., *Learning Curve and One-Year Outcome of XEN 45 Gel Stent Implantation in a Swedish Population.* Clinical ophthalmology (Auckland, N.Z.), 2020. **14**: p. 3719-3733.
38. Theilig, T., et al., *Comparing the efficacy of trabeculectomy and XEN gel microstent implantation for the treatment of primary open-angle glaucoma: a retrospective monocentric comparative cohort study.* Scientific reports, 2020. **10**(1): p. 19337-19337.
39. Quaranta, L., et al., *Efficacy and Safety of PreserFlo(®) MicroShunt After a Failed Trabeculectomy in Eyes with Primary Open-Angle Glaucoma: A Retrospective Study.* Advances in therapy, 2021. **38**(8): p. 4403-4412.
40. Chen, D.Z. and C.C.A. Sng, *Safety and Efficacy of Microinvasive Glaucoma Surgery.* J Ophthalmol, 2017. **2017**: p. 3182935.
41. Mokhles, P., et al., *Glaucoma blindness at the end of life.* Acta Ophthalmol, 2017. **95**(1): p. 10-11.
42. Henderson, N.C., F. Rieder, and T.A. Wynn, *Fibrosis: from mechanisms to medicines.* Nature, 2020. **587**(7835): p. 555-566.
43. Guo, S. and L.A. Dipietro, *Factors affecting wound healing.* J Dent Res, 2010. **89**(3): p. 219-29.
44. Reinke, J.M. and H. Sorg, *Wound repair and regeneration.* Eur Surg Res, 2012. **49**(1): p. 35-43.
45. Lockwood, A., S. Brocchini, and P.T. Khaw, *New developments in the pharmacological modulation of wound healing after glaucoma filtration surgery.* Current Opinion in Pharmacology, 2013. **13**(1): p. 65-71.
46. Wilkinson, H.N. and M.J. Hardman, *Wound healing: cellular mechanisms and pathological outcomes.* Open Biol, 2020. **10**(9): p. 200223.
47. Palta, S., R. Saroa, and A. Palta, *Overview of the coagulation system.* Indian J Anaesth, 2014. **58**(5): p. 515-23.
48. Golebiewska, E.M. and A.W. Poole, *Platelet secretion: From haemostasis to wound healing and beyond.* Blood Rev, 2015. **29**(3): p. 153-62.
49. Mann, K.G., *Factor VII-Activating Protease.* Circulation, 2003. **107**(5): p. 654-655.
50. Martin, P. and S.J. Leibovich, *Inflammatory cells during wound repair: the good, the bad and the ugly.* Trends in Cell Biology, 2005. **15**(11): p. 599-607.
51. Delavary, B.M., et al., *Macrophages in skin injury and repair.* Immunobiology, 2011. **216**(7): p. 753-762.
52. Shaw, T.J. and P. Martin, *Wound repair: a showcase for cell plasticity and migration.* Current Opinion in Cell Biology, 2016. **42**: p. 29-37.
53. *Extracellular Matrix Reorganization During Wound Healing and Its Impact on Abnormal Scarring.* Advances in Wound Care, 2015. **4**(3): p. 119-136.
54. Gonzalez, A.C., et al., *Wound healing - A literature review.* An Bras Dermatol, 2016. **91**(5): p. 614-620.

55. Diegelmann, R.F. and M.C. Evans, *Wound healing: an overview of acute, fibrotic and delayed healing.* FBL, 2004. **9**(1): p. 283-289.
56. Stadelmann, W.K., A.G. Digenis, and G.R. Tobin, *Physiology and healing dynamics of chronic cutaneous wounds.* Am J Surg, 1998. **176**(2A Suppl): p. 26s-38s.
57. *Immune Regulation of Skin Wound Healing: Mechanisms and Novel Therapeutic Targets*. Advances in Wound Care, 2018. **7**(7): p. 209-231.
58. Wolters, J.E.J., et al., *History, presence, and future of mitomycin C in glaucoma filtration surgery.* Curr Opin Ophthalmol, 2021. **32**(2): p. 148-159.
59. Schlunck, G., et al., *Conjunctival fibrosis following filtering glaucoma surgery.* Exp Eye Res, 2016. **142**: p. 76-82.
60. Seibold, L.K., M.B. Sherwood, and M.Y. Kahook, *Wound modulation after filtration surgery*. Surv Ophthalmol, 2012. **57**(6): p. 530-50.
61. Smith, S., P.A. D'Amore, and E.B. Dreyer, *Comparative toxicity of mitomycin C and 5-fluorouracil in vitro.* Am J Ophthalmol, 1994. **118**(3): p. 332-7.
62. Jampel, H.D., *Effect of brief exposure to mitomycin C on viability and proliferation of cultured human Tenon's capsule fibroblasts.* Ophthalmology, 1992. **99**(9): p. 1471-6.
63. Coppens, G. and P. Maudgal, *Corneal complications of intraoperative Mitomycin C in glaucoma surgery.* Bull Soc Belge Ophtalmol, 2010(314): p. 19-23.
64. Jongsareejit, B., et al., *Efficacy and complications after trabeculectomy with mitomycin C in normal-tension glaucoma.* Jpn J Ophthalmol, 2005. **49**(3): p. 223-7.
65. Hung, P., *Mitomycin-C in Glaucoma Filtering Surgery.* Asian Journal of OPHTHALMOLOGY and Asia-Pacific Journal of Ophthalmology, 2000. **2**.
66. Ghoneim, E., *Needle Revision with Antimetabolites in Bleb Failure.* J Clin Res Ophthalmol 2 (1): 007-009. DOI: 10.17352/2455, 2015. **1414**(007).
67. Bell, K., et al., *Learning from the past: Mitomycin C use in trabeculectomy and its application in bleb-forming minimally invasive glaucoma surgery.* Survey of Ophthalmology, 2021. **66**(1): p. 109-123.
68. Guengerich, F.P., *Mechanisms of drug toxicity and relevance to pharmaceutical development.* Drug Metab Pharmacokinet, 2011. **26**(1): p. 3-14.
69. Bertens, C.J.F., et al., *Topical drug delivery devices: A review.* Exp Eye Res, 2018. **168**: p. 149-160.
70. Akman, A., et al., *Suramin modulates wound healing of rabbit conjunctiva after trabeculectomy: comparison with mitomycin C.* Curr Eye Res, 2003. **26**(1): p. 37-43.

Chapter 2

Animal models and drug candidates for use in glaucoma filtration surgery: a systematic review

van Mechelen, R. J. S., Wolters, J. E.J., Bertens, C. J. F., Webers, C. A. B., van den Biggelaar, F. J. H. M., Gorgels, T. G. M. F., & Beckers, H. J. M. (2022). Animal models and drug candidates for use in glaucoma filtration surgery: A systematic review. Experimental eye research, 217, 108972

Abstract

Glaucoma, a degenerative disease of the optic nerve, is the leading cause of irreversible blindness worldwide. Currently, there is no curative treatment. The only proven treatment is lowering intraocular pressure (IOP), the most important risk factor. Glaucoma filtration surgery (GFS) can effectively lower IOP. However, approximately 10% of all surgeries fail yearly due to excessive wound healing, leading to fibrosis. GFS animal models are commonly used for the development of novel treatment modalities. The aim of the present review was to provide an overview of available animal models and antifibrotic drug candidates. MEDLINE and Embase were systematically searched. Manuscripts until September 1st 2021 were included. Studies that used animal models of GFS were included in this review. Additionally, the snowball method was used to identify other publications which had not been identified through the systematic search. In total two hundred and one articles were included in this manuscript. Small rodents (*e.g.*, mice and rats) are often used to study the fibrotic response after GFS and to test drug candidates. Due to their larger eyes, rabbits are better suited to develop medical devices. Novel drugs aim to inhibit specific pathways, *e.g.*, through the use of modulators, monoclonal antibodies, aqueous suppressants or gene therapy. Although most newly studied drugs offer a higher safety profile compared to antimetabolites, their efficacy is in most cases lower when compared to MMC. Future research should focus on refining current animal models (for example through the induction of glaucoma prior to undertaking GFS) and standardizing animal research to ensure a higher reproducibility and reliability across different research groups. Lastly, novel therapies need to be further optimized, *e.g.*, by conducting more research on the dosage, administration route, application frequency, the option of creating combination therapies, or the development of drug delivery systems for sustained release of antifibrotic medication.

2.1 Introduction

Glaucoma is an optic neuropathy in which degeneration of retinal ganglion cells (RGCs) and subsequently the optic nerve leads to progressive and irreversible visual field loss [1-3]. With a prevalence of 76 million patients in 2020 it is one of the leading causes of blindness worldwide, the number of patients is expected to increase to 112 million in 2040 [4, 5]. A major risk factor for glaucoma is increased intraocular pressure (IOP). Other risk factors include age, race, genetic background, and corneal thickness [3, 6-8]. The most common type of glaucoma is primary open angle glaucoma (POAG), in which the outflow of aqueous humor (AqH) from the eye is impaired, leading to increased IOP. Other forms of glaucoma include primary angle closure glaucoma and normal pressure glaucoma. Currently, there is no causative treatment for glaucoma. The only proven treatment is lowering IOP, the main risk factor [1-3]. Therefore, current therapies aim to reduce IOP to a target level that will prevent further visual field loss [2, 9]. Glaucoma is a chronic disease that requires monitoring (and possibly adjusting or intensifying treatment) throughout the patient's life [2]. Glaucoma treatment strategies have seen a rapid development over the years to keep up with the increasing prevalence of glaucoma. Many new topical medications (eye drops) have been developed since the 1990. Several types of glaucoma drainage devices (GDDs) were developed in the 2nd halve of the last century. However, trabeculectomy, a technique that is already decades old but has been refined over the years, still remains the gold standard for incisional surgery for primary open-angle glaucoma. However, as a second option, GDDs are gaining more and more popularity [10]. The second decade of the 2000s witnessed a growth in the development of minimally invasive glaucoma surgeries (MIGS) [11, 12]. Currently, treatment of glaucoma usually starts with topical medication to either decrease the production or increase the outflow of AqH, to decrease IOP. When insufficient to stop glaucoma progression or in case patients are intolerable to eye drops or do not adhere to the treatment regime, laser surgery can be performed. When the aforementioned treatments are insufficient to reach a sufficiently low target IOP, incisional glaucoma filtration surgery (GFS) is opted for [13, 14]. During the trabeculectomy an artificial passage route (or fistula) is created from the anterior chamber (AC) to the subconjunctival/sub Tenon's space, allowing AqH to flow out of the eye and form a reservoir or filtering "bleb" [2]. GDDs (*e.g.*, the frequently used Baerveldt and Ahmed glaucoma implants, or the recently introduced Paul glaucoma implant), typically consist out of a tube (placed through a needle tract into the AC) and an endplate (placed in the subconjunctival/sub-Tenon's space to form a bleb) to shunt AqH out of the eye. Although GFS is highly effective in reducing IOP, the outcome is often hampered by postoperative formation of fibrosis at the operation site, leading to scarring of the filtering bleb, due to an excessive wound healing response. Additional IOP-lowering medication or further surgery is often needed to control IOP. To reduce fibrosis of the bleb, intraoperative application of

antimetabolites such as mitomycin C (MMC) or 5-Fluorouracil (5-Fu) are now commonly used [15]. As a result, the efficacy of GFS to lower IOP increased by 50%. However, an increase in severe adverse events such as avascular blebs, bleb leakage, hypotony, or endophthalmitis has been observed due to the use of antimetabolites [16]. Despite these postoperative (possibly severe) complications, MMC is now routinely used in GFS. However, approximately 10% of GFS surgeries still fail due to the formation of fibrotic tissue in the subconjunctival space despite the use of antimetabolites [17]. Therefore, clinicians tend to withhold patients from surgery due to the considerable postoperative care and possible vision-threatening complications [2]. The recently introduced MIGS procedures were intended to fill the gap between topical medication or laser surgery, and GFS. [1, 2, 18-22]. These newer MIGS procedures claim a higher safety profile, shorter surgical time, faster recovery and require relatively simple instrumentation [2]. Although evidence on the outcomes of MIGS is still limited, studies have indicated that they may not be as effective in lowering IOP when compared to trabeculectomy or GDDs. MIGS that drain to the sub-Tenon's space lead to the formation of a filtering bleb, similar to common GFS procedures, and may, therefore, generate better IOP outcomes when compared to other (intraocular) MIGS techniques for which IOP cannot be lowered beyond the "floor" of episcleral venous pressure [23-29]. Nonetheless, some postoperative complications still occur, *e.g.*, hypotony, hyphema, and subconjunctival fibrosis [11, 27-30].

Despite the current treatment options for glaucoma (topical medication, laser surgery, MIGS, or GFS), It has been shown in recent studies that approximately ten percent of patients suffer from bilateral blindness at the end of their life due to glaucoma [31]. This underlines the importance and unmet need for the development of new treatment modalities that result in better IOP outcomes. Novel treatments with a comparable or higher efficacy as MMC but a higher safety profile may provide more predictable outcomes after surgery.

Cell culture models, organ culture models, *post mortem* eye models, and animal models are routinely used in the laboratory to (1) investigate the pathophysiology of the fibrotic response and (2) develop novel treatment modalities for GFS [3, 32]. When compared to human studies, animal models allow a more invasive approach (such as enucleation of eyes to perform histological evaluation), and progression can be tracked from the start of the disorder [3, 33]. Different types of animal models have been used during the search for new treatment modalities [34, 35]. GFS models are also useful to study new surgical or pharmaceutical strategies that reduce postoperative fibrosis after GFS or MIGS [36-39], or to study the pathophysiology of the wound healing response after GFS [34]. In the present review, we describe current GFS animal models and provide an overview of current developments in relation to innovative *in vivo* GFS treatments.

2.2 Methods

The Embase and MEDLINE databases were systematically searched to identify articles on GFS animal models or drug candidates, an advanced search was conducted using the keywords “glaucoma filtration surgery” or “GFS” and “animal” or “animals” and “fibrosis” or “wound healing”. Articles published until September 1st, 2021 were included. Figure 2-1 provides an overview of the complete search.

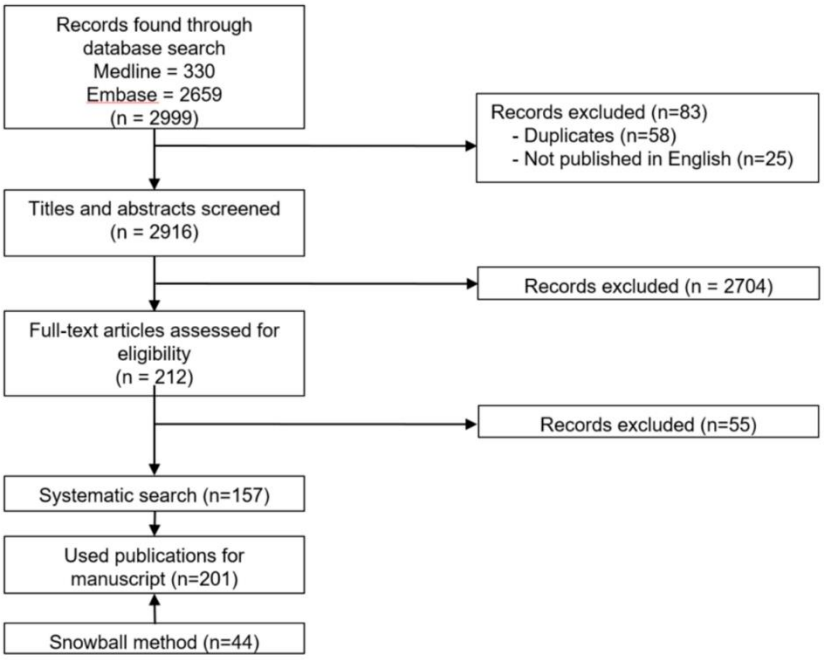

Figure 2-1: Systematic search and results of the records found through Medline and Embase. In total 157 manuscripts were found through the systematic search. An additional 44 manuscripts were added through the snowball method. Into a bleb through the implanted microshunt. In short, (1)

A total of 2999 articles were retrieved during the literature search. After removal of duplicates (n=58) and articles that were not available in English (n=25), 2916 articles remained. Two reviewers (R.J.S van Mechelen and J.E.J. Wolters) checked all titles and abstracts of the remaining articles and subsequently excluded articles that focused solely on glaucoma, *in vitro,* clinical research, or on implants unrelated to drug delivery systems (DDS), DDS matrices, MMC, or 5-FU. A total of 2704 papers were excluded. The full text of the remaining 212 articles were selected for further reading. After reading the manuscripts, 55 were excluded because they were not

accessible or had unclear results. Eventually, 157 were included in this review. Additionally, the snowball method was used to find additional articles that were not found with the initial search criteria: 44 articles were added. In total, 201 articles were included in the final review. All identified records were managed using Endnote X8.

2.3 Results

2.3.1 Glaucoma filtration surgery models

In table 2-1, a complete overview of GFS animal models is provided. In the following paragraphs, the table will be explained in more detail.

2.3.1.1 Mouse

Mice are commonly used as laboratory animals. Several surgical methods to induce a GFS mouse model currently exist. The first mouse model of subconjunctival wound healing was described in 1998 [40]. In this study, 25 µl of phosphate buffered saline (PBS) was injected into the subconjunctival space to create a blunt dissection of the conjunctiva [40]. Unfortunately, blebs were short lasting due to the absence of a fistula that ensured the flow of AqH into the bleb [40]. At postoperative day 14, no macroscopic differences were observed between eyes that received a subconjunctival injection of PBS and control eyes [40]. Although it is possible to study the subconjunctival wound healing response solely with this model [41], there are several disadvantages, *e.g.* the absence of AqH into the bleb and the limited surgical trauma. AqH contains several growth factors (*e.g.* vascular endothelial growth factor) that probably influence the wound healing response [42]. In addition, the flow of AqH together with the hydrostatic pressure have been implicated in the formation of fibrosis [42, 43]. In 2010, a new model was developed in which a fistula was created with a needle tract (a modified trabeculectomy) into the AC, allowing AqH to flow into a bleb [44]. Mice deficient of the SPARC (a protein involved in extracellular matrix production and organization) gene were used in this study to assess the effect of SPARC silencing on the formation of fibrosis after GFS. SPARC knock out mice had a bleb survival of 87.5% after 14 days, whereas in control wild type mice this was 0% [44]. Seet *et al.* [45] validated this model to assess the efficacy of antifibrotic medication. Episcleral application of the intended bleb location with a sponge soaked in MMC during surgery prolonged bleb survival to 28 days postoperatively in 75% of eyes, compared to the control group which had a postoperative bleb survival of 10% at 28 days [45]. In general mice models are cost effective, molecular tools are readily available, they are easy to house, and genetic models are readily available [44, 46]. However, the size of the eye limits the overall usage of the mice since implants routinely used in the clinic cannot be studied in mice. Additionally, the size of the eye requires a high surgical precision to reliably induce these models. Mice have been used for the assessment of novel antifibrotic therapies [47-50] and for studying the pathophysiology of subconjunctival wound healing [51-53].

2.3.1.2 Rat

The rat has been used as a model of ocular wound healing [54, 55]. In the rat model two types of GFS models have been induced as compared by Sherwood *et al.* [56] 1) A scleral fistula surgery (modified trabeculectomy) and 2) A cannula implantation, tube shunt surgery with a silicone tube implanted into the AC (comparable to a GDD) [56]. Sclerostomies made with a needle tract closed by day 3 and documenting any stage of bleb failure was difficult, whereas blebs with outflow through silicone tubes failed between 8 and 13 postoperative days [56]. Tube shunt surgeries mimic certain surgeries that are routinely used in human patients who undergo a shunt implantation into the AC [56]. Similar to mice, rats are a cost-effective model with molecular tools readily available, and housing of rats is relatively easy. Although the eye is more suited for different types of surgery on, a high surgical skill is still needed for perform reliable outcomes in GFS models. The rat model of GFS can be used to study the pathology of GFS failures [34, 57], to help find new antifibrotic drugs [35, 58, 59] and for the development of novel biomedical devices [60].

2.3.1.3 Rabbit

The rabbit is a well-established model for GFS [56, 61-63]. The rabbit is by far the most used animal model for GFS at the moment. Rabbits are known to have a strong subconjunctival fibrotic reaction [64-66]. Bleb failure in the rabbit occurs approximately within 10 to 14 days postoperatively when no antimetabolites are used [56, 65, 67]. Usage of antimetabolites such as MMC have shown to prolong bleb survival up to 40- 60 days [67, 68]. several types of GFS have been performed on the rabbit, including cannula implantation (22-gauge) [38, 61, 67, 69], implantation of long-tube glaucoma devices (*e.g.*, the Baerveldt and Ahmed glaucoma valve) [70-72], and several adaptations of trabeculectomy (including partial/full thickness scleral flaps and sclerostomies) [36, 65, 73, 74], and MIGS[75, 76]. Novel surgical interventions are, in the most part, translatable from the rabbit to clinical use. The rabbit is docile, has large ocular structures, and is ethically preferable compared to non-human primates [63, 77, 78]. The rabbit model can be used for the development of novel biomedical devices [75, 79, 80], new antifibrotic therapeutics [36, 38, 68, 81], assessing the effectiveness of surgical adaptations [39], and for studies involving the molecular mechanism regarding conjunctival fibrosis following GFS [82-84]. Unfortunately, molecular tools such as microarrays are not easily available, limiting their applicability for molecular research compared to mice and rats.

2.3.1.4 Other animals

Over the years, other animals have also been used to study GFS, including hamsters [85], canines [86-89] and non-human primates [90, 91]. In the case of canines and non-human primates, these animals have larger eyes than rabbits. However, high

costs, housing requirements, limited ease of handling, limited availability, and ethical concerns have contributed to the preference for using rabbits and rodents for research. Interestingly, veterinarians have also started to treat pet animals that have glaucoma with GFS, offering an unique way to study GFS procedures in animals [92]. Whereas mice and rats are mostly used in molecular research, hamsters have been used in research regarding the formation of angiotensin II (a hormone that affects blood pressure/IOP). It has been shown that hamsters, canines and non-human primates have chymase activity in the eye, which can lead to the activation of various cytokines through angiotensin II [85]. However, as with mice and rats, the size of the eye limits the usage of this animal model.

2.3.2 Novel treatments modalities for GFS

Yearly, approximately 10% of all GFS surgeries fail due to the formation of fibrosis and subsequent scarring of the filtering bleb [17]. Currently, the gold standard is the application of MMC or 5-FU during GFS. However, severe complications such as endophthalmitis, bleb leaks, and corneal endothelial cell loss are often observed after antimetabolites were used [93, 94]. These complications often arise due to the non-selective nature of MMC and 5-FU, causing toxic side effects. Therefore, there is a need for novel drugs that can inhibit fibrosis with less toxic side effects and with a higher predictable outcome [95]. In this review we compared drugs that were tested *in vivo* multiple times, as these drugs may be the most interesting for future studies, and provided an overview of current literature. Drugs that were tested *in vivo* only once were excluded. The following drugs were excluded Losartan [96], Silver nanoparticles [97], Lovastatin [98], Trastuzumab [99], SB 202190 [100], SB 431542 [101], Doxycycline [102], Y-27632 [103], Anti-PlGF antibody [50], TGF-beta antisense oligonucleotides [104], Connexin43 [105], α-lipoic acid [106], Dimethylenastron [107], Anti-TGF-beta 2 antibody [60, 108], Sonepcizumab [62], P605 peptide [109], Human RAD50 [110], Withaferin A [111], Everolimus [112], Minoxidil [113], Rosmarinic acid [114], Sunitinib [115], Aminoproprionitrile [116], S-nitrosoglutathione [117], Triamcinolone acetate [118], AMA0526 [119], Interferon alpha-2b [120], 10-hydroxycamptothecin [121], 5-hydroxytryptamine(1A) [122], DNA topoisomerase II [123], Monocyte chemoattractant protein-1 inhibitor [5], alofuginone [124], and Cytosine arabinoside [125], Forkhead domain inhibitory-6 [126].

Many experimental drugs that may be beneficial for preventing the formation of fibrosis are currently being investigated such as bevacizumab [38, 49, 66, 127-130], veronistat [73, 131], and short interfering RNA (siRNA) [37, 132] (see table 2-2 for an extensive overview).

Table 2-1: Overview of possible applications and limitations per animal species for use in GFS research.

Species	Surgical methods	Advantages	Disadvantages	Research applications
Mouse	- Subconjunctival blunt dissection [40] -Modified trabeculectomy (needle tract surgery) [44, 45]	- Cost effective - Molecular tools readily available [45] - Easy housing - Genetic models available [44, 46]	- Small eye	- Pathophysiology [51-53] - Antifibrotic drug development [47-50]
Rat	- Modified trabeculectomy (needle tract surgery) [56] - Tube shunt surgery [56]	- Cost effective - Molecular tools readily available - Easy housing	- Small eye	- Pathophysiology [34, 57, 169] - Antifibrotic drug development [35, 58, 59] - Biomedical device development [60]
Hamster	- Sclerocorneal surgery [85]	- Easy housing - Ease of handling	- Small eye	- Pathophysiology [85] - Antifibrotic drug development
Rabbit	- Several adaptations of trabeculectomy [36, 65, 73, 74] - Canula implantation [38, 61, 67, 69] - Glaucoma drainage device implantation [70-72] - MIGS [75, 76]	- Large eye [78] - Easy to handle	- Molecular tools not readily accessible [45]	- Surgical adaptations [39, 170, 171] - Antifibrotic drug development [36, 38, 81] - Biomedical device development [75, 79, 80] - Pathophysiology [64, 82-84, 172]
Canine	- Trabeculectomy [86-89]	- Large eye	- Molecular tools not readily available - Ethical concerns	- Surgical adaptations [173]

			- Housing requirements - Hard to handle - High costs - Limited availability	- Antifibrotic drug development - Biomedical device development [87, 88, 142] - Pathophysiology
Non-human primate	- Trabeculectomy [90, 91, 174]	- Large eye - Molecular tools available	- Ethical concerns - Housing requirements - Hard to handle - High costs - Limited availability	- Surgical adaptations - Antifibrotic drug development - Biomedical device development - Pathophysiology

Table 2-2: Overview of studied drugs *in vivo*. Treatment results, route of aministration, dosage, type of drug, and drug target are listed.

Drug	Results	Route of drug administration (Dosage)	Type of drug (target)
CLT-28643	- Inferior to 0.04% MMC [175] - Superior efficacy compared to MMC + more tolerable [47]	- Subconjunctival injection (100 µl 0.2%) and eye drops [175] - Subconjunctival injections and eye drops (1-10 ug) [47]	Monoclonal antibody (alpha5beta1-intergrin)
Ilomastat	- Similar bleb survival to MMC [68] - Less toxic to conjunctiva, sclera and cornea compared to MMC [176] - Reduced formation scar tissue [177]	- Subconjunctival injection (100 um) [68, 176, 177]	Moduclator (MMP inhibition)
Saratin	- Topical + 2 injections increased bleb survival (33.6 days), only topical no improvement, no adverse effects as seen with MMC visible [178] - Single injection prolonged bleb survival compared to BSS, multiple injections reduced infectiveness and caused short term eye inflammation [179]	- Topical application during surgery (5 mg/ml) and postoperative subconjunctival injections (0.1 ml solution) [178] - Single or multiple subconjunctival injections (0.1 ml of 5 mg/ml) [179]	Modulator (Inhibitor of platelet-collagen interaction)
Infliximab	- Similar to MMC on postoperative day 14 (time point of sacrifice) [134] - Less effective than MMC [180]	- 4x per day eye drops (10 mg/ml) for 14 days postoperative [134] - Topical application intraoperative (1-5mg in 0.1ml) [180]	Monoclonal antibody (TNF-α)
Rosiglitazone	- Prolonged bleb survival [181] - PHBV/rosiglitazone DDS is safe and prevents scar formation [182]	- Intraoperative topical application (50 mg/ml) [181] - Drug delivery system (0.5, 5 and 50 mg/ml) [182]	Modulator (nuclear Peroxisome proliferator-activated

			receptor-c agonist)
Bevacizumab	- Combined effect with MMC larger, inhibitory effect greater when used alone [38] - Bleb morphology features might be better than MMC alone. However unlikely to be as effective [127] - Synergistic effect with 5-FU [128] - Subconjunctival injection more effective compared to subconjunctival 5-FU and intravitreal bevacizumab [129] - Complimentary effect to MMC, can use less MMC to reach antifibrotic effect [49] - Use in mouse models of ocular pathologies [130] - Subconjunctival injections improve GFS outcome [66]	- Subconjunctival injection (1.25 mg/0.05 ml) [38] - Subconjucntival injection (0.1 ml of 25 mg/ml) [128] - Subconjunctival and intravitreal injections on several days (1.2 5mg/0.05 ml) [129] - Subconjunctival, intracameral and intravitreal injections [49] - Subconjunctival (1ul; 25ug) [130] - Multiple postoperative subconjunctival injections (1.25mg; 25mg/ml) [66]	Monoclonal antibody (VEGF A)
Octreotide	- Similar to MMC and corticosteroids [135] - Decreased presence fibroblasts and macrophages [183] - Reduction subconjunctival scarring in 2 weeks [184]	- Multiple subcutaneous injections [135] - Eye drops 3x per day (10 ug) [183] - Eye drops 3x per day (10 ug/ml) [184]	Modulator (Somatostatin analogue)
Plasminogen activator	- Significant decrease episcleral fibrosis, no toxicity or complications found [185] - Tissue plasminogen activator interferes with healing response and may promote bleb formation [186]	- Gel delivery vehicle (1 mg/ml) [185] - Intracameral (25ug) [186]	Modulator

Pirfenidone	- Effective alternative to MMC [124] - 0.5% pirfenidone eye drops improved bleb survival [187] - No difference between 1% and 0.5% pirfenidone. Decreases fibrosis with minimal side effects [188]	- Eye drops, 1 drop till 14 days post-surgery (0.5%) [124] - Eye drops 6x a day (0.1% or 0.5%) [187] - Eye drops 4x daily for 28 days (0.1% or 0.5%) [188]	Modulator
Homoharringtonine liposome	- Inhibits scar formation and promote formation of filtering bleb [189] - High dosage needed with significant elevation of side effects [190]	- Subconjunctival injection [189] - Subconjunctival injection (0.025% and 0.1%) [190]	
Sirolimus	- Sirolimus suppresses conjunctival scarring [115] - DDS with sirolimus inhibits inflammation, fibroblast proliferation and induces fibroblast-apoptosis. Safe and effective treatment strategy [191]	- Intraoperative sponges (30 ng/ml) [115] - Poly(lactic-co-glycolic acid) film (15.6mg per film) [191]	Modulator (inhibition of mammalian target or rapamycin)
Suramin	- Prolongs bleb survival comparable to MMC [95] - Broadly inhibits growth factors, highly effective, fewer side effects compared to MMC [192]	- Intraoperative sponges (250 mg/ml) [95] - Intraoperative sponges and 4x subconjunctival injection (10 – 333mg/ml) [192]	Modulator (antagonist receptor for heparin binding growth factors)
Paclitaxel	- Lipid nana emulsions with paclitaxel, intravenous less effective compared to subcutaneous injections or MMC but possible use as an adjuvant [193] - Pilot study showed paclitaxel in a hydrogel to be comparable to MMC with histology [136]	- Intravenous injections (4 mg/kg) or subconjunctival injections (1.5 mg; 300ul) [193] - Hydrogel (1 mg/ml) [136]	Antineoplastic

Cyclosporine	- A cyclosporine A Poly(lactic-co-glycolic acid) DDS, safe and effective to prevent scar formation [194] - Topical 2% cyclosporine may enhance GFS [195]	- DDS placed during surgery [194] - Topical [195]	
Valproic acid	- Reduced chemokine and cytokine levels *in vivo* [196] - Reduced collagen deposition and upregulated Smad6 [197]	- Subconjunctival injection (300ug/ml) [196] [197]	Genetic (histone deacetylase inhibitor)
Latanoprost	- Latanoprost upregulates MMP-3 and TIMP-2 *in vivo* [198] - May inhibit wound healing after GFS [199]	- Eye drops daily for 7 days (50ug/ml) [198] - Intraoperative treatment (25ul 0.005%)[199]	IOP lowering drug
Timolol	- Early treatment with aqueous suppressant decreased fibrotic response [200]	- Eye drops, 4 week treatment (0.5%) [200]	IOP lowering drug
Etoposide	- Taxol had a greater antiproliferative compared to etoposide and greater duration of release from polymer [90] - Release of etoposide was sufficient to reduce fibroblast proliferation for at least 12 days post-surgery [201]	- Subconjunctival implantation polyanhydride disk (1mg) [90] [201]	Modulator (topoisomerase II)
Veronistat	- Decrease in collagen deposition, fibroblast and myofibroblast presence. However, MMC treated animals showed an higher antifibrotic efficacy [73] - Co-treatment of a low dose of MMC (0.2 mg/ml) together with veronistat	- Subconjunctival injection (50uM) [73] - Intraoperative application sponges (350uM + co-treatment MMC) [131]	Genetic (histone deacetylase inhibitor)

	resulted in a similar outcome compared to a single high dose (0.4 mg/ml) MMC [131]		
Short interfering RNA - IκB kinase beta [132] - secreted protein acidic and rich in cysteine (SPARC) [37]	-Higher safety compared to MMC. However, less effective in elongating bleb survival [132] - Reduced collagen production and SPARC silencing [37]	- Subconjunctival injection, till 7 days post-surgery (50 nM) [132] - subconjunctival injection (5 ul) after surgery [37]	Genetic (RNA interference)
Adenoviral vectors - $P21^{waf1/cip1}$[137, 138] - $P27^{KIP1}$[202] - Connective tissue growth factor SiRNA [203]	- Effective in reducing fibrotic response, outflow facility was higher in eyes treated with MMC [137] - Comparable results to MMC, and less damage to surrounding tissue [138] - No difference seen between MMC and adenoviral vector treated animals at 28 days postoperative, no complications were noted [202] - Reduced fibrotic response after surgery [203]	- Intraoperative application with sponges [137, 138] - Subconjunctival injection [202, 203]	Genetic (gene therapy)

While all drugs aim to inhibit a particular pathway or protein related to fibrosis not all drugs do this to the same extent. Different types of drugs or drug targets are routinely studied *e.g.*, neoplastics or antimetabolites, monoclonal antibodies, modulators of specific pathways, IOP lowering drugs, and genetic therapies. The efficacy and toxicity of a drug is often affected by the dosage, route of administration and its application frequency [133]. Several administration routes have been studied, *e.g.* intraoperative application with sponges, topical application of eye drops, intracameral injections, intravitreal injections, and subconjunctival injections. Most of these drugs had a higher safety profile when compared to MMC, with less toxic side effects. However, in most cases, their efficacy was lacking or lower when directly compared to MMC. Some drugs such as Infliximab [134], CLT-28643 [47], octreotide [135], pirfenidone [124], suramin [95], paclitaxel [136], and the adenoviral vector $P21^{waf1/cip1}$ [137, 138] showed a comparable efficacy when compared to MMC. Depending on the dosage or duration of MMC application, contradicting results have been found across studies with the same drug. Alternatively, the drugs bevacizumab and veronistat have been used as a co-treatment for MMC, leading to lower dosages of MMC that could be safely used while still upholding a comparable efficacy compared to a higher dose of MMC [38, 49, 128, 131], Other synergistic effects between different types of drugs would be worthwhile to study to increase the efficacy and to reduce potential adverse events.

2.4 Discussion

There is an ongoing search for new treatment options that cure or minimize the onset of glaucoma. To accommodate the need for these treatments, *in vivo* models are invaluable tools in research. *In vivo* models are used for the development of novel treatments (*e.g.*, assessment of safety and efficacy), for pathophysiological studies regarding the fibrotic response, or for studying surgical adaptations to existing methods. Several animal species have been used for GFS models. All existing animal models eventually lead to postoperative failure due to the extensive wound healing response encountered in animals [34]. Small rodents such as mice, rats, and hamsters have also been used. Although small rodents are less costly, the smaller size of their eyes is a limitation to successfully perform operations that mimic those performed in humans.

Mice or rats will be best suited for the development of antifibrotic drugs and for studying the pathophysiology of subconjunctival fibrosis, because of the availability of molecular tools. Larger animals with ocular structures more similar to the human eye, such as rabbits, will be a better choice for the development of novel medical devices and for studying the effect of surgical adaptations to existing techniques.

To reduce adverse events related to the use of antimetabolites MMC or 5-FU, novel therapies are routinely developed and studied. Some drugs have shown promising results *in vivo*. However, further optimization of drug treatment in the form of dosage,

administration route, and application frequency is needed. Furthermore, the development of combination therapies [36, 48, 81, 131, 139, 140] drug releasing hydrogels [87, 88, 141-143], microspheres [144], or drug delivery systems based on other biodegradable polymers [145-148] could reduce toxic side effects while still reaching therapeutic efficacy.

2.5 Future directions

A preclinical animal trial is required to assess the efficacy and safety of novel treatments, before human trials can commence. Currently, research that involves GFS is focusing on the development of new drugs and/or medical devices that will reduce fibrosis, thereby reducing the possibility of postoperative failure. Unfortunately, high failure rates are encountered in drug development [184]. These failures are partly accountable for the translational failure of animal models towards humans [185]. To improve results, animal models should constantly be revised and optimized, both scientifically and ethically, for instance by creating suitable models that mimic the human pathology of a given disorder.

Glaucomatous eyes have a higher expression of growth factors in comparison to healthy eyes, probably leading to a higher fibrotic reaction after surgery [42, 186]. Therefore, an animal model in which glaucoma can be reliably induced before performing GFS could be beneficial for the preclinical validation of antifibrotic drugs or medical devices. Two distinct forms of glaucoma models exist, spontaneous (natural) and induced. Spontaneous models do not require surgical intervention to trigger RGC death. However, severity, time of onset, and comorbidities can vary among individual animals [7, 187], which can lead to an increased need for additional animals due to a higher variation [188]. Therefore, induced models might offer a more reliable method to create glaucomatous eyes in animals. In general, the rabbit is the most frequently used animal in GFS research. Intracameral injection of latex beads has been shown to successfully induce raised IOP in rabbits [189]. However, this raise in IOP is only temporary, possibly due to clearing of the latex beads from the AC. Repeated intracameral injections might be required to induce a long lasting increased IOP in rabbits [190]. Additionally, after GFS, beads might settle in front of the artificially created route (*e.g.*, a tube) leading to an unsatisfactory filtering bleb or they could induce a foreign body response, increasing the inflammatory state of the eye. A trabecular or post-trabecular intervention, such as alpha-chymotrypsin injection or episcleral vein cautery, might be better suited to induce glaucoma in cases where GFS is required. If successful, this could lead to a higher translation of treatments that are currently developed in GFS models.

Lastly, in animal research there is a high variation within an experimental setting. Standardization of methods could help in reducing this variation between different research groups. Many organizations and groups currently exist that create guidelines for reporting and planning of animal experiments such as the ARRIVE

guidelines, and the PREPARE guidelines [191, 192]. Additionally, the Association for Research in Vision and Ophthalmology (ARVO), has set up guidelines for the humane treatment, experimental design, and ethical use of animals in vision related animal research. The national center for the replacement, refinement & reduction of animals in research (NC3R) offers standard operating procedures on their website. Therefore, this type of institution might offer a way for researchers to make their SOPs easily available to other researchers.

Regarding to GFS research, several factors can influence the reliability and reproducibility of an experiment. Firstly, the type of animal model. An animal model should be based on its strengths and limitations. Secondly, primary and secondary read out parameters. Several parameters are of great value to assess *in vivo*, for example IOP, and bleb formation or morphology. A low postoperative IOP is an indicator for a successfully performed surgery. However, IOP is known to have a strong standard deviation within these animal models and differences over time can be minimal since no glaucoma is induced beforehand. Additionally, care should be taken when performing IOP measurements on sedated animals, IOP will be lower compared to awake animals [193]. Several types of analyses can be performed over a set period of time to assess bleb morphology or formation, in recent years more tools have become available to check the bleb morphology, for example, OCT has seen advances for its use to monitor the inner bleb structures in patients and have quantifiable parameters which could also be useful in animal research [194-196]. Several bleb grading scales currently exist and parameters of the bleb can be scored through these scales, such as, vascularity, bleb height, and bleb extent [197]. Often, grading bleb survival is based on the scoring of the bleb height and extent. Additional caution is warranted when interpreting results after subconjunctival injections of a drug without proper controls (*e.g.*, sham injections). If control experiments are omitted, wrong conclusions on bleb survival might be drawn. On a molecular or cellular level, histology is of great importance to study specific cell types and tissue interaction in the bleb [198, 199]. Tear fluid analysis (proteins, lipids, and metabolites) may also prove useful [200-202]. Tear samples can be used for transcriptomics, proteomics, or metabolomics studies. Lastly, time points for performing measurements or euthanizing animals should be based on the specific research question. For example, in studies involving antifibrotic drugs, measurements should be relatively frequent, *e.g.*, once every 3-5 days in the first 2-3 postoperative weeks, since bleb morphology changes especially within the first few weeks.

The search for new antifibrotic therapies will continue. The development of novel drugs or the testing of new treatment regimens will lead to constant improvements in the safety and efficacy of GFS. When tested *in vivo* and compared to the gold standard MMC treatment, novel drugs often have a lower efficacy. However, a higher safety profile is repeatedly seen, as mentioned in table 2-2. Therefore, further

refinement in relation to drug-dosage, the administration route of the drug, and its application frequency is needed. Additionally, combination therapies of several drugs could provide a higher efficacy and better safety since multiple fibrotic pathways could be inhibited while using a lower dose [36, 48, 81, 131, 175, 176]. Lastly, the development of drug delivery systems offers a way to administer a certain drug over a prolonged period of time without reaching toxic levels. Thus, toxic drugs (*e.g.*, MMC) might be able to reach nontoxic levels while still reaching an antifibrotic effect.

2.6 Conclusion

A large variety of animals have been used to study GFS. Small rodents like mice and rats are better suited to study the fibrotic response after GFS and to test drug candidates. Because of the similarities to the human eye, rabbit eyes are the most suitable *in vivo* alternative for the development of medical devices. Additionally, drug candidates could also be tested on rabbits. Nonetheless, detection techniques are less commonly available when compared to those of mice or rats. Additionally, standardization of animal research will increase the reliability and reproducibility of experiments across different research groups. Currently, novel drugs that inhibit specific pathways are routinely tested in animal models. Although these often offer a higher safety profile, MMC or 5-FU in most cases have a higher antifibrotic efficacy. Therefore, drug-dosage, administration route, application frequency, and potentially the development of combination therapies or drug delivery systems should be optimized for these novel drugs to increase their efficacy.

References

1. Mauro, A., et al., *A novel patient-oriented numerical procedure for glaucoma drainage devices*. Int J Numer Method Biomed Eng, 2018. **34**(12): p. e3141.
2. Bar-David, L. and E.Z. Blumenthal, *Evolution of Glaucoma Surgery in the Last 25 Years*. Rambam Maimonides Med J, 2018. **9**(3).
3. Guo, C., et al., *A murine glaucoma model induced by rapid in vivo photopolymerization of hyaluronic acid glycidyl methacrylate.* PLoS One, 2018. **13**(6): p. e0196529.
4. Tham, Y.C., et al., *Global prevalence of glaucoma and projections of glaucoma burden through 2040: a systematic review and meta-analysis.* Ophthalmology, 2014. **121**(11): p. 2081-90.
5. Chong, R.S., et al., *Inhibition of Monocyte Chemoattractant Protein 1 Prevents Conjunctival Fibrosis in an Experimental Model of Glaucoma Filtration Surgery.* Invest Ophthalmol Vis Sci, 2017. **58**(9): p. 3432-3439.
6. Biswas, S. and K.H. Wan, *Review of rodent hypertensive glaucoma models.* Acta Ophthalmol, 2018.
7. Chen, S. and X. Zhang, *The Rodent Model of Glaucoma and Its Implications.* Asia Pac J Ophthalmol (Phila), 2015. **4**(4): p. 236-41.
8. *European Glaucoma Society Terminology and Guidelines for Glaucoma, 4th Edition - Chapter 2: Classification and terminologySupported by the EGS Foundation: Part 1: Foreword; Introduction; Glossary; Chapter 2 Classification and Terminology.* Br J Ophthalmol, 2017. **101**(5): p. 73-127.
9. Toris, C.B., et al., *Making Basic Science Studies in Glaucoma More Clinically Relevant: The Need for a Consensus.* J Ocul Pharmacol Ther, 2017. **33**(7): p. 501-518.
10. Gedde, S.J., et al., *Primary Open-Angle Glaucoma Suspect Preferred Practice Pattern®.* Ophthalmology, 2021. **128**(1): p. P151-P192.
11. Gillmann, K. and K. Mansouri, *Minimally Invasive Glaucoma Surgery: Where Is the Evidence?* Asia Pac J Ophthalmol (Phila), 2020. **9**(3): p. 203-214.
12. Pereira, I.C.F., et al., *Conventional glaucoma implants and the new MIGS devices: a comprehensive review of current options and future directions.* Eye (Lond), 2021. **35**(12): p. 3202-3221.
13. *European Glaucoma Society Terminology and Guidelines for Glaucoma, 4th Edition - Chapter 3: Treatment principles and options Supported by the EGS Foundation: Part 1: Foreword; Introduction; Glossary; Chapter 3 Treatment principles and options.* Br J Ophthalmol, 2017. **101**(6): p. 130-195.
14. Dikopf, M.S., T.S. Vajaranant, and D.P. Edward, *Topical treatment of glaucoma: established and emerging pharmacology.* Expert Opin Pharmacother, 2017. **18**(9): p. 885-898.
15. Wolters, J.E.J., et al., *History, presence, and future of mitomycin C in glaucoma filtration surgery.* Curr Opin Ophthalmol, 2021. **32**(2): p. 148-159.
16. Gedde, S.J., *Results from the tube versus trabeculectomy study.* Middle East Afr J Ophthalmol, 2009. **16**(3): p. 107-11.
17. Beckers, H.J., K.C. Kinders, and C.A. Webers, *Five-year results of trabeculectomy with mitomycin C.* Graefes Arch Clin Exp Ophthalmol, 2003. **241**(2): p. 106-10.
18. Lee, R.M.H., et al., *Translating Minimally Invasive Glaucoma Surgery Devices*. Clin Transl Sci, 2020. **13**(1): p. 14-25.
19. Ansari, E., *An Update on Implants for Minimally Invasive Glaucoma Surgery (MIGS).* Ophthalmol Ther, 2017. **6**(2): p. 233-241.
20. Pillunat, L.E., et al., *Micro-invasive glaucoma surgery (MIGS): a review of surgical procedures using stents.* Clin Ophthalmol, 2017. **11**: p. 1583-1600.
21. Pereira, I.C.F., et al., *Conventional glaucoma implants and the new MIGS devices: a comprehensive review of current options and future directions*. Eye, 2021.
22. Ahmed, J.R.S.I.I.K., *Current developments in glaucoma surgery and MIGS*. New concepts in glaucoma - surgery series. 2020: Kugler publications. 300.
23. Green, W., J.T. Lind, and A. Sheybani, *Review of the Xen Gel Stent and InnFocus MicroShunt.* Curr Opin Ophthalmol, 2018. **29**(2): p. 162-170.
24. Riss, I., et al., *[One-year results on the safety and efficacy of the InnFocus MicroShunt depending on placement and concentration of mitomycin C].* J Fr Ophtalmol, 2015. **38**(9): p. 855-60.
25. Batlle, J.F., A. Corona, and R. Albuquerque, *Long-term Results of the PRESERFLO MicroShunt in Patients With Primary Open-angle Glaucoma From a Single-center Nonrandomized Study*. Journal of glaucoma, 2021. **30**(3): p. 281-286.

26. Scheres, L.M.J., et al., *XEN(®) Gel Stent compared to PRESERFLO™ MicroShunt implantation for primary open-angle glaucoma: two-year results.* Acta ophthalmologica, 2021. **99**(3): p. e433-e440.
27. Busch, T., et al., *Learning Curve and One-Year Outcome of XEN 45 Gel Stent Implantation in a Swedish Population.* Clinical ophthalmology (Auckland, N.Z.), 2020. **14**: p. 3719-3733.
28. Theilig, T., et al., *Comparing the efficacy of trabeculectomy and XEN gel microstent implantation for the treatment of primary open-angle glaucoma: a retrospective monocentric comparative cohort study.* Scientific reports, 2020. **10**(1): p. 19337-19337.
29. Quaranta, L., et al., *Efficacy and Safety of PreserFlo(®) MicroShunt After a Failed Trabeculectomy in Eyes with Primary Open-Angle Glaucoma: A Retrospective Study.* Advances in therapy, 2021. **38**(8): p. 4403-4412.
30. Chen, D.Z. and C.C.A. Sng, *Safety and Efficacy of Microinvasive Glaucoma Surgery.* J Ophthalmol, 2017. **2017**: p. 3182935.
31. Mokhles, P., et al., *Glaucoma blindness at the end of life.* Acta Ophthalmol, 2017. **95**(1): p. 10-11.
32. Weinreb, R.N. and J.D. Lindsey, *The importance of models in glaucoma research.* J Glaucoma, 2005. **14**(4): p. 302-4.
33. Gelatt, K.N., *Animal models for glaucoma.* Invest Ophthalmol Vis Sci, 1977. **16**(7): p. 592-6.
34. Esson, D.W., et al., *Microarray analysis of the failure of filtering blebs in a rat model of glaucoma filtering surgery.* Invest Ophthalmol Vis Sci, 2004. **45**(12): p. 4450-62.
35. Wang, L., et al., *Exogenous Tissue Inhibitor of Metalloproteinase-2 Affects Matrix Metalloproteinase-2 Expression in Conjunctival Filtering Blebs and Bleb Scarring in Rats.* Biomed Res Int, 2018. **2018**: p. 9365950.
36. Zuo, L., J. Zhang, and X. Xu, *Combined Application of Bevacizumab and Mitomycin C or Bevacizumab and 5-Fluorouracil in Experimental Glaucoma Filtration Surgery.* J Ophthalmol, 2018. **2018**: p. 8965709.
37. Seet, L.F., et al., *Targeted therapy for the post-operative conjunctiva: SPARC silencing reduces collagen deposition.* Br J Ophthalmol, 2018. **102**(10): p. 1460-1470.
38. Hilgert, C.R., et al., *Antiscarring effect of intraoperative bevacizumab in experimental glaucoma filtration surgery.* Arq Bras Oftalmol, 2018. **81**(4): p. 316-322.
39. Rodgers, C.D., et al., *The impact of conjunctival flap method and drainage cannula diameter on bleb survival in the rabbit model.* PLoS One, 2018. **13**(5): p. e0196968.
40. Reichel, M.B., et al., *New model of conjunctival scarring in the mouse eye.* Br J Ophthalmol, 1998. **82**(9): p. 1072-7.
41. Cordeiro, M.F., et al., *Transforming growth factor-beta1, -beta2, and -beta3 in vivo: effects on normal and mitomycin C-modulated conjunctival scarring.* Invest Ophthalmol Vis Sci, 1999. **40**(9): p. 1975-82.
42. Schlunck, G., et al., *Conjunctival fibrosis following filtering glaucoma surgery.* Exp Eye Res, 2016. **142**: p. 76-82.
43. Gardiner, B.S., et al., *Computational modeling of fluid flow and intra-ocular pressure following glaucoma surgery.* PLoS One, 2010. **5**(10).
44. Seet, L.F., et al., *SPARC deficiency results in improved surgical survival in a novel mouse model of glaucoma filtration surgery.* PLoS One, 2010. **5**(2): p. e9415.
45. Seet, L.F., et al., *Validation of the glaucoma filtration surgical mouse model for antifibrotic drug evaluation.* Mol Med, 2011. **17**(5-6): p. 557-67.
46. Yamanaka, O., et al., *Inhibition of p38MAP kinase suppresses fibrogenic reaction in conjunctiva in mice.* Mol Vis, 2007. **13**: p. 1730-9.
47. Van Bergen, T., et al., *Integrin alpha5beta1 Inhibition by CLT-28643 Reduces Postoperative Wound Healing in a Mouse Model of Glaucoma Filtration Surgery.* Invest Ophthalmol Vis Sci, 2016. **57**(14): p. 6428-6439.
48. Van Bergen, T., et al., *The Combination of PlGF Inhibition and MMC as a Novel Anti-Scarring Strategy for Glaucoma Filtration Surgery.* Invest Ophthalmol Vis Sci, 2016. **57**(10): p. 4347-55.
49. Van Bergen, T., et al., *Complementary effects of bevacizumab and MMC in the improvement of surgical outcome after glaucoma filtration surgery.* Acta Ophthalmol, 2015. **93**(7): p. 667-78.
50. Van Bergen, T., et al., *Inhibition of placental growth factor improves surgical outcome of glaucoma surgery.* J Cell Mol Med, 2013. **17**(12): p. 1632-43.
51. Seet, L.F., et al., *Novel insight into the inflammatory and cellular responses following experimental glaucoma surgery: a roadmap for inhibiting fibrosis.* Curr Mol Med, 2013. **13**(6): p. 911-28.

52. Seet, L.F., et al., *Upregulation of distinct collagen transcripts in post-surgery scar tissue: a study of conjunctival fibrosis.* Dis Model Mech, 2017. **10**(6): p. 751-760.
53. Adachi, K., et al., *Alteration of gene expression in mice after glaucoma filtration surgery.* Sci Rep, 2020. **10**(1): p. 15036.
54. Fini, M.E., M.T. Girard, and M. Matsubara, *Collagenolytic/gelatinolytic enzymes in corneal wound healing.* Acta Ophthalmol Suppl, 1992(202): p. 26-33.
55. WoldeMussie, E., et al., *Neuroprotective effect of memantine in different retinal injury models in rats.* J Glaucoma, 2002. **11**(6): p. 474-80.
56. Sherwood, M.B., et al., *A new model of glaucoma filtering surgery in the rat.* J Glaucoma, 2004. **13**(5): p. 407-12.
57. Lu, H., et al., *The effects of glaucoma filtering surgery on anterior chamber-associated immune deviation and contribution of lymphatic drainage in rats.* Eye (Lond), 2009. **23**(1): p. 215-21.
58. Liu, Y., et al., *Inhibition by a retinoic acid receptor gamma agonist of extracellular matrix remodeling mediated by human Tenon fibroblasts.* Mol Vis, 2015. **21**: p. 1368-77.
59. Sung, M.S., et al., *Trichostatin A Ameliorates Conjunctival Fibrosis in a Rat Trabeculectomy Model.* Invest Ophthalmol Vis Sci, 2018. **59**(7): p. 3115-3123.
60. Zhu, X., et al., *Evaluation of Chitosan/Aptamer Targeting TGF-beta Receptor II Thermo-Sensitive Gel for Scarring in Rat Glaucoma Filtration Surgery.* Invest Ophthalmol Vis Sci, 2015. **56**(9): p. 5465-76.
61. Cordeiro, M.F., et al., *Effect of varying the mitomycin-C treatment area in glaucoma filtration surgery in the rabbit.* Invest Ophthalmol Vis Sci, 1997. **38**(8): p. 1639-46.
62. Lukowski, Z.L., et al., *Prevention of ocular scarring after glaucoma filtering surgery using the monoclonal antibody LT1009 (Sonepcizumab) in a rabbit model.* J Glaucoma, 2013. **22**(2): p. 145-51.
63. Tsonis, P.A., *Animal models in eye research*, ed. P.A. Tsonis. 2008: Elsevier. 232.
64. Shima, I., et al., *Expression of matrix metalloproteinases in wound healing after glaucoma filtration surgery in rabbits.* Ophthalmic Res, 2007. **39**(6): p. 315-24.
65. Doyle, J.W., et al., *Intraoperative 5-fluorouracil for filtration surgery in the rabbit.* Invest Ophthalmol Vis Sci, 1993. **34**(12): p. 3313-9.
66. Memarzadeh, F., et al., *Postoperative use of bevacizumab as an antifibrotic agent in glaucoma filtration surgery in the rabbit.* Invest Ophthalmol Vis Sci, 2009. **50**(7): p. 3233-7.
67. SooHoo, J.R., et al., *Bleb morphology and histology in a rabbit model of glaucoma filtration surgery using Ozurdex(R) or mitomycin-C.* Mol Vis, 2012. **18**: p. 714-9.
68. Wong, T.T., A.L. Mead, and P.T. Khaw, *Prolonged antiscarring effects of ilomastat and MMC after experimental glaucoma filtration surgery.* Invest Ophthalmol Vis Sci, 2005. **46**(6): p. 2018-22.
69. Kim, J.L., et al., *Effect of Porcine Chondrocyte-Derived Extracellular Membrane (CDECM) on Postoperative Wound Healing in an Experimental Rabbit Model of Glaucoma Filtration Surgery.* Curr Eye Res, 2017. **42**(6): p. 897-907.
70. Lee, J.W., et al., *Tissue response to implanted Ahmed glaucoma valve with adjunctive amniotic membrane in rabbit eyes.* Ophthalmic Res, 2014. **51**(3): p. 129-39.
71. Prata, J.A., Jr., et al., *Effects of intraoperative mitomycin-C on the function of Baerveldt glaucoma drainage implants in rabbits.* J Glaucoma, 1996. **5**(1): p. 29-38.
72. Lloyd, M.A., et al., *Long-term histologic studies of the Baerveldt implant in a rabbit model.* J Glaucoma, 1996. **5**(5): p. 334-9.
73. Sharma, A., et al., *Epigenetic Modification Prevents Excessive Wound Healing and Scar Formation After Glaucoma Filtration Surgery.* Invest Ophthalmol Vis Sci, 2016. **57**(7): p. 3381-9.
74. Khaw, P.T., et al., *Effects of intraoperative 5-fluorouracil or mitomycin C on glaucoma filtration surgery in the rabbit.* Ophthalmology, 1993. **100**(3): p. 367-72.
75. Acosta, A.C., et al., *A newly designed glaucoma drainage implant made of poly(styrene-b-isobutylene-b-styrene): biocompatibility and function in normal rabbit eyes.* Arch Ophthalmol, 2006. **124**(12): p. 1742-9.
76. Grierson, I., et al., *A Novel Schlemm's Canal Scaffold: Histologic Observations.* J Glaucoma, 2015. **24**(6): p. 460-8.
77. Gwon, A., *The rabbit in IOL/Cataract surgery*. Animal models in eye research, ed. P.A. Tsonis. Vol. 1. 2009: Elsevier. 215.
78. Zernii, E.Y., et al., *Rabbit Models of Ocular Diseases: New Relevance for Classical Approaches.* CNS Neurol Disord Drug Targets, 2016. **15**(3): p. 267-91.

79. Villamarin, A., et al., *In vivo testing of a novel adjustable glaucoma drainage device.* Invest Ophthalmol Vis Sci, 2014. **55**(11): p. 7520-4.
80. Desai, A.R., et al., *Co-delivery of timolol and hyaluronic acid from semi-circular ring-implanted contact lenses for the treatment of glaucoma: in vitro and in vivo evaluation.* Biomater Sci, 2018. **6**(6): p. 1580-1591.
81. Sherwood, M.B., *A sequential, multiple-treatment, targeted approach to reduce wound healing and failure of glaucoma filtration surgery in a rabbit model (an American Ophthalmological Society thesis).* Trans Am Ophthalmol Soc, 2006. **104**: p. 478-92.
82. Van Bergen, T., et al., *The role of LOX and LOXL2 in scar formation after glaucoma surgery.* Invest Ophthalmol Vis Sci, 2013. **54**(8): p. 5788-96.
83. Ji, H., et al., *The Effect of Dry Eye Disease on Scar Formation in Rabbit Glaucoma Filtration Surgery.* Int J Mol Sci, 2017. **18**(6).
84. Esson, D.W., et al., *Expression of connective tissue growth factor after glaucoma filtration surgery in a rabbit model.* Invest Ophthalmol Vis Sci, 2004. **45**(2): p. 485-91.
85. Sakaguchi, H., et al., *Chymase and angiotensin converting enzyme activities in a hamster model of glaucoma filtering surgery.* Curr Eye Res, 2002. **24**(5): p. 325-31.
86. Kiremitci-Gumusderelioglu, M., M. Gokce, and R.F. Akata, *A novel MMC-loaded pHEMA drainage device for the treatment of glaucoma: in vitro and in vivo studies.* J Biomater Sci Polym Ed, 1996. **7**(10): p. 857-69.
87. Kojima, S., et al., *Effects of Gelatin Hydrogel Loading Mitomycin C on Conjunctival Scarring in a Canine Filtration Surgery Model.* Invest Ophthalmol Vis Sci, 2015. **56**(4): p. 2601-5.
88. Kojima, S., et al., *Effects of gelatin hydrogel containing chymase inhibitor on scarring in a canine filtration surgery model.* Invest Ophthalmol Vis Sci, 2011. **52**(10): p. 7672-80.
89. Shute, T.S., et al., *Biocompatibility of a Novel Microfistula Implant in Nonprimate Mammals for the Surgical Treatment of Glaucoma.* Invest Ophthalmol Vis Sci, 2016. **57**(8): p. 3594-600.
90. Jampel, H.D., et al., *Glaucoma filtration surgery in nonhuman primates using taxol and etoposide in polyanhydride carriers.* Invest Ophthalmol Vis Sci, 1993. **34**(11): p. 3076-83.
91. Okada, K., et al., *Effects of mitomycin C on the expression of chymase and mast cells in the conjunctival scar of a monkey trabeculectomy model.* Mol Vis, 2009. **15**: p. 2029-36.
92. Park, K.H., et al., *Ahmed glaucoma valve implantation with Ologen((R)) Collagen Matrix for the surgical treatment of feline glaucoma.* Vet Ophthalmol, 2018. **21**(1): p. 96-100.
93. Coppens, G. and P. Maudgal, *Corneal complications of intraoperative Mitomycin C in glaucoma surgery.* Bull Soc Belge Ophtalmol, 2010(314): p. 19-23.
94. Jongsareejit, B., et al., *Efficacy and complications after trabeculectomy with mitomycin C in normal-tension glaucoma.* Jpn J Ophthalmol, 2005. **49**(3): p. 223-7.
95. Akman, A., et al., *Suramin modulates wound healing of rabbit conjunctiva after trabeculectomy: comparison with mitomycin C.* Curr Eye Res, 2003. **26**(1): p. 37-43.
96. Shi, H., et al., *Losartan Attenuates Scar Formation in Filtering Bleb After Trabeculectomy.* Invest Ophthalmol Vis Sci, 2017. **58**(3): p. 1478-1486.
97. Butler, M.R., et al., *Topical silver nanoparticles result in improved bleb function by increasing filtration and reducing fibrosis in a rabbit model of filtration surgery.* Invest Ophthalmol Vis Sci, 2013. **54**(7): p. 4982-90.
98. Park, J.H., C. Yoo, and Y.Y. Kim, *Effect of Lovastatin on Wound-Healing Modulation After Glaucoma Filtration Surgery in a Rabbit Model.* Invest Ophthalmol Vis Sci, 2016. **57**(4): p. 1871-7.
99. Turgut, B., et al., *Impact of trastuzumab on wound healing in experimental glaucoma surgery.* Clin Exp Ophthalmol, 2015. **43**(1): p. 67-76.
100. Nassar, K., et al., *A p38 MAPK inhibitor improves outcome after glaucoma filtration surgery.* J Glaucoma, 2015. **24**(2): p. 165-78.
101. Xiao, Y.Q., et al., *SB-431542 inhibition of scar formation after filtration surgery and its potential mechanism.* Invest Ophthalmol Vis Sci, 2009. **50**(4): p. 1698-706.
102. Sen, E., et al., *Effect of doxycycline on postoperative scarring after trabeculectomy in an experimental rabbit model.* J Ocul Pharmacol Ther, 2010. **26**(5): p. 399-406.
103. Honjo, M., et al., *Potential role of Rho-associated protein kinase inhibitor Y-27632 in glaucoma filtration surgery.* Invest Ophthalmol Vis Sci, 2007. **48**(12): p. 5549-57.
104. Cordeiro, M.F., et al., *Novel antisense oligonucleotides targeting TGF-beta inhibit in vivo scarring and improve surgical outcome.* Gene Ther, 2003. **10**(1): p. 59-71.
105. Deva, N.C., et al., *Connexin43 modulation inhibits scarring in a rabbit eye glaucoma trabeculectomy model.* Inflammation, 2012. **35**(4): p. 1276-86.

106. Ekinci, M., et al., *Reduction of conjunctival fibrosis after trabeculectomy using topical alpha-lipoic acid in rabbit eyes.* J Glaucoma, 2014. **23**(6): p. 372-9.
107. Luke, J., et al., *The effect of adjuvant dimethylenastron, a mitotic Kinesin Eg5 inhibitor, in experimental glaucoma filtration surgery.* Curr Eye Res, 2010. **35**(12): p. 1090-8.
108. Mead, A.L., et al., *Evaluation of anti-TGF-beta2 antibody as a new postoperative anti-scarring agent in glaucoma surgery.* Invest Ophthalmol Vis Sci, 2003. **44**(8): p. 3394-401.
109. Avila, M., et al., *GGRGDSPCA peptide: a new antiscarring agent on glaucoma filtration surgery.* Ophthalmic Surg Lasers, 2001. **32**(2): p. 134-9.
110. Yoon, K.C., et al., *Effect of human RAD50 gene therapy on glaucoma filtering surgery in rabbit eye.* Curr Eye Res, 2004. **28**(3): p. 181-7.
111. Bargagna-Mohan, P., et al., *Withaferin A effectively targets soluble vimentin in the glaucoma filtration surgical model of fibrosis.* PLoS One, 2013. **8**(5): p. e63881.
112. Cinik, R., et al., *The Effect of Everolimus on Scar Formation in Glaucoma Filtering Surgery in a Rabbit Model.* Curr Eye Res, 2016. **41**(11): p. 1438-1446.
113. Sharir, M., *Topical minoxidil for glaucoma filtration surgery in the rabbit.* Exp Eye Res, 1994. **59**(6): p. 707-14.
114. Ferreira Jde, L., et al., *Rosmarinic Acid Suppresses Subconjunctival Neovascularization in Experimental Glaucoma Surgery.* Curr Eye Res, 2015. **40**(11): p. 1134-40.
115. Eren, K., et al., *The Suppression of Wound Healing Response with Sirolimus and Sunitinib Following Experimental Trabeculectomy in a Rabbit Model.* Curr Eye Res, 2016. **41**(3): p. 367-76.
116. Fourman, S., *Effects of aminoproprionitrile on glaucoma filter blebs in rabbits.* Ophthalmic Surg, 1988. **19**(9): p. 649-52.
117. Tannous, M., et al., *S-nitrosoglutathione photolysis as a novel therapy for antifibrosis in filtration surgery.* Invest Ophthalmol Vis Sci, 2000. **41**(3): p. 749-55.
118. Rangel, H., et al., *Healing modulation in glaucoma surgery after application of subconjunctival triamcinolone acetate alone or combined with mitomycin C: an experimetal study.* Rev Col Bras Cir, 2018. **45**(4): p. e1861.
119. Van de Velde, S., et al., *Rho kinase inhibitor AMA0526 improves surgical outcome in a rabbit model of glaucoma filtration surgery.* Prog Brain Res, 2015. **220**: p. 283-97.
120. Xiong, X., et al., *[A study of interferon alpha-2b as an accessory drug after glaucoma filtration surgery].* Zhonghua Yan Ke Za Zhi, 1999. **35**(1): p. 52-4, 5.
121. Xia, D., et al., *Effect of 10-hydroxycamptothecin on functional bleb following antiglaucomatous filtering surgery.* Chinese Journal of Experimental Ophthalmology, 2014. **32**: p. 131-136.
122. Osborne, N.N., et al., *5-Hydroxytryptamine1A agonists: potential use in glaucoma. Evidence from animal studies.* Eye (Lond), 2000. **14 (Pt 3B)**: p. 454-63.
123. Yamamoto, K., et al., *The DNA topoisomerase II inhibitor amsacrine as a novel candidate adjuvant in a model of glaucoma filtration surgery.* Scientific Reports, 2019. **9**(1): p. 19288.
124. Kasar, K., et al., *The effect of halofuginone and pirfenidone on wound healing in experimental glaucoma filtration surgery.* J Fr Ophtalmol, 2021. **44**(3): p. 340-349.
125. Al-Aswad, L.A., M. Huang, and P.A. Netland, *Inhibition of Tenon's fibroblast proliferation and enhancement of filtration surgery in rabbits with cytosine arabinoside.* J Ocul Pharmacol Ther, 1999. **15**(1): p. 41-9.
126. Lan, C., et al., *Forkhead domain inhibitory-6 attenuates subconjunctival fibrosis in rabbit model with trabeculectomy.* Exp Eye Res, 2021. **210**: p. 108725.
127. Mathew, R. and K. Barton, *Anti--vascular endothelial growth factor therapy in glaucoma filtration surgery.* Am J Ophthalmol, 2011. **152**(1): p. 10-15 e2.
128. How, A., et al., *Combined treatment with bevacizumab and 5-fluorouracil attenuates the postoperative scarring response after experimental glaucoma filtration surgery.* Invest Ophthalmol Vis Sci, 2010. **51**(2): p. 928-32.
129. Ozgonul, C., T. Mumcuoglu, and A. Gunal, *The effect of bevacizumab on wound healing modulation in an experimental trabeculectomy model.* Curr Eye Res, 2014. **39**(5): p. 451-9.
130. Hollanders, K., et al., *Bevacizumab revisited: its use in different mouse models of ocular pathologies.* Curr Eye Res, 2015. **40**(6): p. 611-21.
131. Kim, T.H., et al., *Co-treatment of suberoylanilide hydroxamic acid and mitomycin-C induces the apoptosis of rabbit tenon's capsule fibroblast and improves the outcome of glaucoma filtration surgery.* Curr Eye Res, 2008. **33**(3): p. 237-45.
132. Ye, H., et al., *Cationic nano-copolymers mediated IKKbeta targeting siRNA to modulate wound healing in a monkey model of glaucoma filtration surgery.* Mol Vis, 2010. **16**: p. 2502-10.

133. Bertens, C.J.F., et al., *Topical drug delivery devices: A review.* Exp Eye Res, 2018. **168**: p. 149-160.
134. Turgut, B., et al., *Topical infliximab for the suppression of wound healing following experimental glaucoma filtration surgery.* Drug Des Devel Ther, 2014. **8**: p. 421-9.
135. Akyol, N., et al., *Effects of systemic octreotide, local mytomycine-C and local corticosteroids on wound-healing reaction after glaucoma surgery.* Int Ophthalmol, 2001. **24**(5): p. 235-41.
136. Koz, O.G., et al., *The effect of paclitaxel on conjunctival wound healing: a pilot study.* J Glaucoma, 2007. **16**(7): p. 610-5.
137. Perkins, T.W., et al., *Adenovirus-mediated gene therapy using human p21WAF-1/Cip-1 to prevent wound healing in a rabbit model of glaucoma filtration surgery.* Arch Ophthalmol, 2002. **120**(7): p. 941-9.
138. Heatley, G., et al., *Gene therapy using p21WAF-1/Cip-1 to modulate wound healing after glaucoma trabeculectomy surgery in a primate model of ocular hypertension.* Gene Ther, 2004. **11**(12): p. 949-55.
139. Nakamura-Shibasaki, M., et al., *Matrix metalloproteinase and cytokine expression in Tenon fibroblasts during scar formation after glaucoma filtration or implant surgery in rats.* Cell Biochem Funct, 2013. **31**(6): p. 482-8.
140. Duan, X., Z. He, and X. Zhang, *A comparative study of the effects of ab externo superpulse carbon dioxide laser-assisted trabeculectomy with conventional trabeculectomy in rabbits.* Photomed Laser Surg, 2010. **28**(1): p. 109-13.
141. Gong, R., et al., *A Comparison of Subconjunctival Wound Healing between Different Methods of Dissecting Subconjunctival Tissues.* Ophthalmic Res, 2021. **64**(1): p. 99-107.
142. Grisanti, S., et al., *Decorin modulates wound healing in experimental glaucoma filtration surgery: a pilot study.* Invest Ophthalmol Vis Sci, 2005. **46**(1): p. 191-6.
143. Maggio, F. and D. Bras, *Surgical Treatment of Canine Glaucoma: Filtering and End-Stage Glaucoma Procedures.* Vet Clin North Am Small Anim Pract, 2015. **45**(6): p. 1261-82, vi-vii.
144. Maeda, M., et al., *Effects of Gelatin Hydrogel Containing Anti-Transforming Growth Factor-beta Antibody in a Canine Filtration Surgery Model.* Int J Mol Sci, 2017. **18**(5).
145. Desjardins, D.C., et al., *Wound healing after filtering surgery in owl monkeys.* Arch Ophthalmol, 1986. **104**(12): p. 1835-9.
146. Schultheiss, M., et al., *alpha5beta1-Integrin inhibitor (CLT-28643) effective in rabbit trabeculectomy model.* Acta Ophthalmol, 2017. **95**(1): p. e1-e9.
147. Suh, W., K.E. Han, and J.R. Han, *Safety of Using Matrix Metalloproteinase Inhibitor in Experimental Glaucoma Filtration Surgery.* J Korean Med Sci, 2017. **32**(4): p. 666-671.
148. Wong, T.T., A.L. Mead, and P.T. Khaw, *Matrix metalloproteinase inhibition modulates postoperative scarring after experimental glaucoma filtration surgery.* Invest Ophthalmol Vis Sci, 2003. **44**(3): p. 1097-103.
149. Min, J., et al., *Prevention of ocular scarring post glaucoma filtration surgery using the inflammatory cell and platelet binding modulator saratin in a rabbit model.* PLoS One, 2012. **7**(4): p. e35627.
150. Min, J., et al., *Comparison of single versus multiple injections of the protein saratin for prolonging bleb survival in a rabbit model.* Invest Ophthalmol Vis Sci, 2012. **53**(12): p. 7625-30.
151. Nikita, E., et al., *A Pilot Study on Ocular Safety and Efficacy of Infliximab as an Antifibrotic Agent After Experimental Glaucoma Filtration Surgery.* Ophthalmol Ther, 2017. **6**(2): p. 323-334.
152. Zhang, F., et al., *Rosiglitazone Treatment Prevents Postoperative Fibrosis in a Rabbit Model of Glaucoma Filtration Surgery.* Invest Ophthalmol Vis Sci, 2019. **60**(7): p. 2743-2752.
153. Zhang, F., et al., *Effects of rosiglitazone/PHBV drug delivery system on postoperative fibrosis in rabbit glaucoma filtration surgery model.* Drug Deliv, 2019. **26**(1): p. 812-819.
154. Demir, T., et al., *Effects of octreotide acetate and amniotic membrane on wound healing in experimental glaucoma surgery.* Doc Ophthalmol, 2003. **107**(2): p. 87-92.
155. Arslan, S., et al., *Modulation of postoperative scarring with tacrolimus and octreotide in experimental glaucoma filtration surgery.* Curr Eye Res, 2012. **37**(3): p. 228-33.
156. Strauss, G.H., et al., *Subconjunctival high dose plasminogen activator in rabbit filtration surgery.* J Ocul Pharmacol, 1991. **7**(1): p. 9-19.
157. Fourman, S. and K. Vaid, *Effects of tissue plasminogen activator on glaucoma filter blebs in rabbits.* Ophthalmic Surg, 1989. **20**(9): p. 663-7.
158. Zhong, H., et al., *Evaluation of pirfenidone as a new postoperative antiscarring agent in experimental glaucoma surgery.* Invest Ophthalmol Vis Sci, 2011. **52**(6): p. 3136-42.

159. Westermeyer, H.D., et al., *Safety and efficacy of topically applied 0.5% and 1% pirfenidone in a canine model of subconjunctival fibrosis.* Vet Ophthalmol, 2019. **22**(4): p. 502-509.
160. Peng, D., et al., *An experimental study on homoharringtonine liposome and glaucoma filtration surgery.* Yan Ke Xue Bao, 1999. **15**(1): p. 51-4, 50.
161. Xu, Y., et al., *[Effects of homoharringtonine liposomes and homoharringtonine solution on glaucoma filtration surgery in rabbits].* Zhonghua Yan Ke Za Zhi, 1998. **34**(4): p. 304-7, 21.
162. Yan, Z.C., et al., *Anti-proliferation effects of Sirolimus sustained delivery film in rabbit glaucoma filtration surgery.* Mol Vis, 2011. **17**: p. 2495-506.
163. Mietz, H., et al., *Suramin inhibits wound healing following filtering procedures for glaucoma.* Br J Ophthalmol, 1998. **82**(7): p. 816-20.
164. Occhiutto, M.L., et al., *Paclitaxel Associated With Lipid Nanoparticles as a New Antiscarring Agent in Experimental Glaucoma Surgery.* Invest Ophthalmol Vis Sci, 2016. **57**(3): p. 971-8.
165. Dai, Z., et al., *Development of a novel CsA-PLGA drug delivery system based on a glaucoma drainage device for the prevention of postoperative fibrosis.* Mater Sci Eng C Mater Biol Appl, 2016. **66**: p. 206-214.
166. Park, K.H., D.M. Kim, and D.H. Youn, *Topical cyclosporine and glaucoma drainage implant surgery in rabbits*. Ophthalmic Surg Lasers, 1996. **27**(6): p. 452-8.
167. Seet, L.F., et al., *Valproic acid exerts specific cellular and molecular anti-inflammatory effects in post-operative conjunctiva.* J Mol Med (Berl), 2019. **97**(1): p. 63-75.
168. Seet, L.F., et al., *Valproic acid suppresses collagen by selective regulation of Smads in conjunctival fibrosis.* J Mol Med (Berl), 2016. **94**(3): p. 321-34.
169. Mietz, H., et al., *Latanoprost stimulates secretion of matrix metalloproteinases in tenon fibroblasts both in vitro and in vivo.* Invest Ophthalmol Vis Sci, 2003. **44**(12): p. 5182-8.
170. Wu, K.Y., et al., *Novel usage of intraocular pressure-lowering drugs as wound-healing inhibitors after trabeculectomy with cell culture and animal models.* Kaohsiung J Med Sci, 2013. **29**(7): p. 353-61.
171. Jung, K.I., J.E. Woo, and C.K. Park, *Effects of aqueous suppressants and prostaglandin analogues on early wound healing after glaucoma implant surgery.* Sci Rep, 2019. **9**(1): p. 5251.
172. Uppal, P., et al., *Pharmacokinetics of etoposide delivery by a bioerodible drug carrier implanted at glaucoma surgery.* J Ocul Pharmacol, 1994. **10**(2): p. 471-9.
173. Yang, J.G., et al., *Adenovirus-mediated delivery of p27(KIP1) to prevent wound healing after experimental glaucoma filtration surgery.* Acta Pharmacol Sin, 2009. **30**(4): p. 413-23.
174. Lim, D.H., T.E. Kim, and C. Kee, *Evaluation of Adenovirus-Mediated Down-Regulation of Connective Tissue Growth Factor on Postoperative Wound Healing After Experimental Glaucoma Surgery.* Curr Eye Res, 2016. **41**(7): p. 951-6.
175. Martorana, G.M., et al., *Sequential Therapy with Saratin, Bevacizumab and Ilomastat to Prolong Bleb Function following Glaucoma Filtration Surgery in a Rabbit Model.* PLoS One, 2015. **10**(9): p. e0138054.
176. Andres-Guerrero, V., et al., *The Effect of a Triple Combination of Bevacizumab, Sodium Hyaluronate and a Collagen Matrix Implant in a Trabeculectomy Animal Model.* Pharmaceutics, 2021. **13**(6).
177. Liang, L., et al., *Prevention of filtering surgery failure by subconjunctival injection of a novel peptide hydrogel into rabbit eyes.* Biomed Mater, 2010. **5**(4): p. 045008.
178. Han, Q., et al., *Effects of bevacizumab loaded PEG-PCL-PEG hydrogel intracameral application on intraocular pressure after glaucoma filtration surgery*. J Mater Sci Mater Med, 2015. **26**(8): p. 225.
179. Kimura, H., et al., *Injectable microspheres with controlled drug release for glaucoma filtering surgery.* Invest Ophthalmol Vis Sci, 1992. **33**(12): p. 3436-41.
180. Paula, J.S., et al., *Bevacizumab-loaded polyurethane subconjunctival implants: effects on experimental glaucoma filtration surgery.* J Ocul Pharmacol Ther, 2013. **29**(6): p. 566-73.
181. Du, L.Q., et al., *Effect of poly(DL-lactide-co-glycolide) on scar formation after glaucoma filtration surgery.* Chin Med J (Engl), 2013. **126**(23): p. 4528-35.
182. Swann, F.B., et al., *Effect of 2 Novel Sustained-release Drug Release Systems on Bleb Fibrosis: An In Vivo Trabeculectomy Study in a Rabbit Model.* J Glaucoma, 2019. **28**(6): p. 512-518.
183. Ang, M., et al., *Evaluation of sustained release of PLC-loaded prednisolone acetate microfilm on postoperative inflammation in an experimental model of glaucoma filtration surgery.* Curr Eye Res, 2011. **36**(12): p. 1123-8.

184. Pound, P. and M. Ritskes-Hoitinga, *Is it possible to overcome issues of external validity in preclinical animal research? Why most animal models are bound to fail.* J Transl Med, 2018. **16**(1): p. 304.
185. Ferri, N., et al., *Drug attrition during pre-clinical and clinical development: understanding and managing drug-induced cardiotoxicity.* Pharmacol Ther, 2013. **138**(3): p. 470-84.
186. Kaeslin, M.A., et al., *Changes to the Aqueous Humor Proteome during Glaucoma.* PLoS One, 2016. **11**(10): p. e0165314.
187. Agarwal, R. and P. Agarwal, *Rodent models of glaucoma and their applicability for drug discovery.* Expert Opin Drug Discov, 2017. **12**(3): p. 261-270.
188. Turner, A.J., et al., *DBA/2J mouse model for experimental glaucoma: pitfalls and problems.* Clin Exp Ophthalmol, 2017. **45**(9): p. 911-922.
189. Ngumah, Q.C., S.D. Buchthal, and R.F. Dacheux, *Longitudinal non-invasive proton NMR spectroscopy measurement of vitreous lactate in a rabbit model of ocular hypertension.* Exp Eye Res, 2006. **83**(2): p. 390-400.
190. Morgan, J.E. and J.R. Tribble, *Microbead models in glaucoma.* Exp Eye Res, 2015. **141**: p. 9-14.
191. Kilkenny, C., et al., *Animal research: reporting in vivo experiments: the ARRIVE guidelines.* J Gene Med, 2010. **12**(7): p. 561-3.
192. Smith, A.J., et al., *PREPARE: guidelines for planning animal research and testing.* Lab Anim, 2018. **52**(2): p. 135-141.
193. Bertens, C.J.F., et al., *Repeatability, reproducibility, and agreement of three tonometers for measuring intraocular pressure in rabbits.* Sci Rep, 2021. **11**(1): p. 19217.
194. Seo, J.H., et al., *Evaluation of Functional Filtering Bleb Using Optical Coherence Tomography Angiography.* Transl Vis Sci Technol, 2019. **8**(3): p. 14.
195. Cantor, L.B., et al., *Morphologic classification of filtering blebs after glaucoma filtration surgery: the Indiana Bleb Appearance Grading Scale.* J Glaucoma, 2003. **12**(3): p. 266-71.
196. Wells, A.P., et al., *A pilot study of a system for grading of drainage blebs after glaucoma surgery.* J Glaucoma, 2004. **13**(6): p. 454-60.
197. Wells, A.P., et al., *Comparison of two clinical Bleb grading systems.* Ophthalmology, 2006. **113**(1): p. 77-83.
198. Laing, A.E., et al., *Evaluation of bleb characteristics after implantation of the EX-PRESS™ glaucoma filtration device.* Mol Vis, 2012. **18**: p. 10-3.
199. Filippopoulos, T., et al., *Correlation of filtration bleb morphology with histology.* Int Ophthalmol Clin, 2009. **49**(1): p. 71-82.
200. Azkargorta, M., et al., *Human tear proteomics and peptidomics in ophthalmology: Toward the translation of proteomic biomarkers into clinical practice.* J Proteomics, 2017. **150**: p. 359-367.
201. von Thun Und Hohenstein-Blaul, N., S. Funke, and F.H. Grus, *Tears as a source of biomarkers for ocular and systemic diseases.* Exp Eye Res, 2013. **117**: p. 126-37.
202. You, J., et al., *Tear fluid protein biomarkers.* Adv Clin Chem, 2013. **62**: p. 151-96.

Chapter 3

Repeatability, reproducibility, and agreement of three tonometers for measuring intraocular pressure in rabbits

*Bertens, C. J. F., *van Mechelen, R. J. S., Berendschot, T. T. J. M., Gijs, M., Wolters, J. E. J., Gorgels, T. G. M. F., Nuijts, R. M. M. A., & Beckers, H. J. M. (2021). Repeatability, reproducibility, and agreement of three tonometers for measuring intraocular pressure in rabbits. Scientific reports, 11(1), 19217. * shared co-author.

Abstract

The aim of this study was to evaluate repeatability, reproducibility, and agreement of three commonly used tonometers in animal research (TonoLab, TonoVet, and TonoPEN AVIA) in a cohort of 24 rabbits. Additionally, the impact of sedation on IOP was investigated in 21 New Zealand White rabbits with the TonoVet tonometer.

Repeatability was determined using the coefficient of variation (CoV) for two observers. For the TonoLab (6.55%) and TonoVet (6.38%) the CoV was lower than for the TonoPEN AVIA (10.88%). The reproducibility was highest for the TonoVet (0.2±3.3mmHg), followed by the TonoLab (0±12.89mmHg) and lowest for the TonoPEN AVIA (-1.48±10.3mmHg). The TonoLab and TonoVet showed the highest agreement ($r=0.85$, $R^2=0.73$). After sedation, a significant IOP reduction (often >25%) was observed.

Our results show that among the three tonometers tested, the TonoVet tonometer is best for use in rabbits while the TonoLab should be avoided. The impact of sedation on IOP was substantial and should be taken into account during experimentation.

3.1 Introduction

Increased intraocular pressure (IOP) and fluctuations in IOP are important characteristics of glaucoma. Repeatable and reproducible objective measurement of IOP are of great importance for disease management. Animal models are routinely used to study underlying pathophysiology and are used in the development of new glaucoma therapies. For example, in glaucoma animal models the anterior chamber of the eye can be injected with microbeads to block the outflow of aqueous humor (AH), thus increasing IOP [1-3].

IOP in animal experiments can be measured by manometry or tonometry. Although manometry is the most accurate method, it is invasive and requires trained personnel along with expensive and specialized equipment. Tonometry is an indirect non-invasive measuring method that can be divided into three different subcategories: indentation, applanation, and rebound tonometry. Indentation (also known as impression) tonometry uses a plunger to measure the depth of corneal indentation, as used in the Schiøtz tonometer [4]. In applanation tonometry, the force needed to flatten the cornea is used to calculate IOP. This method is routinely used in regular clinical care, where Goldmann applanation tonometry (GAT) is the gold standard [5, 6]. Rebound tonometry determines the IOP via induction of a current generated by the rebound effect of a small probe onto the cornea. The use of rebound tonometry (*e.g.* iCare tonometers) is gaining popularity in the clinic, especially for children and non-cooperative patients, as the tonometers are handheld devices and no topical anesthesia is required for the procedure [7].

In animal research, the most commonly used tonometers are the TonoLab (intended for mice and rats), TonoVet (intended for dogs, cats, and horses) and TonoPEN (intended for all animals) (Table 3-1). Although none of these tonometers have been specifically designed for rabbits and there may be substantial differences between the devices, they are commonly used on rabbits for research purposes.

Therefore, we wanted to investigate which tonometer is most suitable for research with rabbits. The TonoLab and TonoVet are both rebound tonometers, whereas the TonoPEN is an applanation tonometer. However, it is unknown which tonometer has the best repeatability and reproducibility when used by multiple observers. Biomechanical factors may also affect IOP readings, such as corneal thickness and stiffness [8-10], mental stress [11-14], circadian rhythm [15, 16], and the type of (*e.g.* general) anesthesia or sedation [17-21]. The use of sedatives is common practice in animal studies and clinical procedures [22], but the effect of injectable sedatives on IOP has not been fully characterized. Furthermore, different absolute IOP values are commonly observed when various tonometers are compared. Hence, the aim of this study was to compare the repeatability, reproducibility and agreement of the TonoLab, TonoVet, and TonoPEN AVIA tonometers, together with investigating the

effect of the injectable sedative medetomidine (an α2 adrenergic agonist) on rabbit IOP.

3.2 Materials and methods

3.2.1 Animals and animal Care

Animal procedures were conducted according to the Association for Research in Vision and Ophthalmology (ARVO) Statement for the Use of Animals in Ophthalmic and Visual Research, the Animal Research: Reporting of *In Vivo* Experiments (ARRIVE) 2.0 guidelines [89], and the Guidelines of the Central Laboratory Animal Facility of Maastricht University. All protocols were approved by the Central Authority for Scientific Procedures on Animals (CCD, Den Haag, NL) and were in accordance with the European Guidelines (2010/63/EU) (Approved Dutch license number: AVD107002017829 and AVD1070020197464).

New Zealand White (NZW) rabbits (2.0 kg – 2.5 kg, males and females) (Envigo (Horst, NL and Bicester, UK) and Charles River (Ecully, FR)) were group housed (maximum 7 animals per cage, males and females separated), and maintained under controlled conditions of temperature and humidity on a 12h:12h light-dark cycle. The rabbits had *ad libitum* access to water and 100g dried chow per animal and all had a two-week acclimatization period before the start of the experiments. All rabbits were normotensive. At the end of the experiment the rabbits were euthanized with an overdose of pentobarbital sodium, 200 mg/kg (Euthasol 20, Produlab Pharma B.V., NL), intravenously injected.

3.2.2 Animals

24 NZW rabbits were used (12 males) for the IOP part of the study (AVD107002017829), whereas 21 NZW rabbits (10 males) were used for the sedation part (AVD1070020197464). The rabbits were trained for one week to get used to the restrainer and the IOP measurements. At the start of each experiment, the rabbits were intra muscularly (IM) sedated using medetomidine (0.5 mg/kg) (Sedator, A.S.T. Farma B.V., Oudewater, NL). Prior to the TonoPEN AVIA measurement, the eye was topically anesthetized with 0.4% Oxybuprocaine hydrochloride solution (MINIMS, Bausch & Lomb Pharma, Brussels, BE). After the measurements, the animals were recovered using 1 mg/kg i.m. atipamezole (Antisedan, ORION pharma, Mechelen, BE). For both studies, the left eye of the rabbits was used.

Table 3-1. Literature overview of the use of different tonometers in animal research. CCT= central corneal thickness, IOP=intraocular pressure.

Animals	ICare TonoLab	ICare TonoVet (Plus)	Reichert TonoPEN (XL, VET, or AVIA)
Frogs	- Determination of reference IOP [23, 24]	- Determination of reference IOP [23-25]	- Determination of reference IOP [25]
Turtles	- Tonometer validation [26]	- Tonometer validation [26, 27]	
Mice	- Effect of general anesthesia on IOP [28] - Tonometer validation [29, 30] - Glaucoma research [31, 32] - Effect of CCT on IOP [33]		- Tonometer validation [30, 34] - Glaucoma research [31]
Chinchillas	- Tonometer validation [35]	- Tonometer validation [35] - Determination of reference IOP [36]	- Tonometer validation [35]
Rats	- Tonometer validation [29, 30, 37-39] - Effect of general anesthesia on IOP [37]		- Tonometer validation [30, 34, 39-41] - Effect of general anesthetics on IOP [42, 43] - Circadian variation [44]
Guinea pigs			- Determination of reference IOP [45] - Effect of topical drugs on IOP [46]
Ferrets			- Determination of reference IOP [47]
Hedgehogs		- Determine prevalence of ocular diseases [48]	- Determine reference IOP [49]
Rabbits		- Tonometer validation [50-54] - Effect of topical drugs on IOP [55]	- Tonometer validation [6, 50, 51, 53, 54, 56] - Effect of topical drugs on IOP [46, 57-59]
Dogs		- Effect of CCT on IOP [60]	- Effect of CCT on IOP [60]

		- Tonometer validation [61-63] - Glaucoma research [64, 65]	- Tonometer validation [61, 62] - Glaucoma research [64, 65] - Effect of topical drugs on IOP [66] - Effect of age on the IOP [67]
Cats		- Glaucoma research [65, 68] - Tonometer validation [69] - Effect of general anesthetics on IOP [70] - Effect of topical drugs on IOP [55]	- Glaucoma research [65] - Tonometer validation [69]
Birds		- Tonometer validation [71, 72] - Determination of reference IOP [73-77]	- Tonometer validation [71] - Determination of reference IOP [73, 74]
Cows		- Determination of reference IOP [78]	
Horses and donkeys		- Determination of reference IOP [79] - Effect of endurance training on IOP [80]	- Determination of reference IOP [79]
Pigs		- Tonometer validation [81]	- Tonometer validation [81]
Alpaca's		- Determination of reference IOP [82]	- Determination of reference IOP [82]
Goats and sheep		- Determination of reference IOP [83]	
Non-human primates		- Tonometer validation [84, 85] - Determination of reference IOP [86]	- Tonometer validation [85] - Determination of reference IOP [86] - Effect of general anesthetics on IOP [87] - Glaucoma research [88]

3.2.3 Tonometers

IOP was measured using the iCare TonoLab (iCare Finland Oy, Vantaa, FI) (in rat setting) (Fig. 3-1a), followed by the iCare TonoVet (iCare Finland Oy, Vantaa, FI) (in dog/cat setting) (Fig.3-1b) and finally, Reichert TonoPEN AVIA (AMETEK Inc., Unterschleißheim, DE). An Ocu-Film tip-cover was used for the TonoPEN AVIA (Fig. 3-1c). The TonoPEN AVIA was used last, due to the potential effect of topical anesthesia on the TonoVET and TonoLab [90].

3.2.4 Repeatability, reproducibility, and agreement of three tonometers

To investigate the repeatability of IOP measurements, defined as the ability of the observer to produce similar results time after time, all measurements were performed in triplicate [91]. The average of six readings is reported by the tonometer. According to the manufacturer's instructions, IOP measurements with a repetition deviation ≥1.0 mmHg (TonoLab and TonoVet) or a repetition confidence lower than 90% (TonoPEN AVIA) were discarded and the measurements were then repeated. The TonoLab, TonoVet, and TonoPEN AVIA had a detection limit of 7-60 mmHg, 10-60 mmHg, and 5-55 mmHg, respectively. Measurements were performed at baseline, 4 hours, 8 hours, 24 hours, 4 days, 7 days, 14 days, 21 days, and 28 days. N equals the number of animals times the number of time points.

Reproducibility (also known as interobserver reproducibility) was defined as the ability to produce the same results for IOP measurements of identical samples under the same conditions by two different observers. Agreement (also known as intraobserver reproducibility) was defined as the ability of one observer to produce the same results of IOP in identical samples using different tonometers.

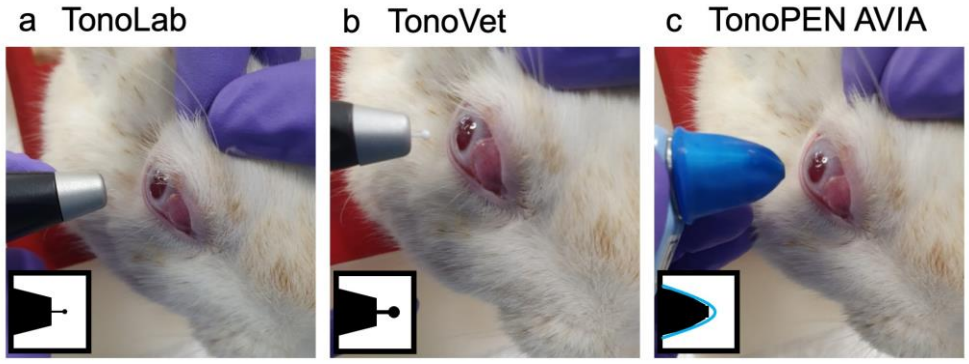

Figure 3-1. Measuring IOP in a rabbit using different tonometers. (a) TonoLab (rebound tonometer), (b) TonoVet (rebound tonometer), (c) TonoPEN AVIA with a single-use blue Ocu-Film tip-cover (applanation tonometer).

3.2.5 Effect of sedation on IOP

IOP was measured using the TonoVet tonometer before (awake) and after sedation. The TonoVet was selected based on the results obtained in paragraph 2.2. First, the IOP of the left eye was measured sixfold. Rabbits were then IM sedated with medetomidine (0.5 mg/kg). Within 15 minutes after induction of sedation, the IOP of the left eye was measured again sixfold. Measurements were performed 1, 5, 7, 11, 15, 25, and 40 days after acclimatization.

3.2.6 Sample size and statistical analysis

Sample size was determined using Meads resource equation [92]. IOP measurements were performed as part of another study [93], hence the deviation in animal groups. All observed data were paired data between the two observers. Values were presented as mean IOP ± standard deviation (SD) for observer 1, observer 2, and both. To examine repeatability, IOP measurements were evaluated by coefficient of variation (CoV) as a normalized SD, as shown in;

$$CoV = \frac{SD}{Mean} x\ 100\ (\%)$$

A smaller CoV means better repeatability. A CoV< 10% was indicative of good repeatability and a CoV< 5% of very high repeatability [94]. The CoV was calculated per measurement with the average providing a mean CoV.

Reproducibility was visualized by plotting mean values of observer 1 over observer 2 and calculating a linear regression line with 95% confidence interval (CI). Pearson's correlation analysis was applied between both observers, followed by Bland and Altman analysis [95, 96]. The Bland and Altman analysis compares the difference of the measurements versus the mean. Agreement of the different tonometers was also visualized through this method.

In calculating the influence of sedation, a two-way repeated measures ANOVA test was performed with Bonferroni correction for multiple testing to compare sedated to awake situations. In addition, the repeatability of measurements in sedated animals were plotted as Bland and Altman plots, including the difference between the measurement and mean along with the percentage of equality (agreement, lower is better) between the values and mean.

Tests were performed using GraphPad Prism version 9 (GraphPad Software inc., San Diego, CA, USA).

3.3 Results

3.3.1 Repeatability

An overview of the IOP results for all three tonometers, performed by both observers, is shown in Table 3-2. Mean IOP measured by the TonoLab was approximately three times higher for both observers compared to the TonoVet and TonoPEN AVIA. Both observers showed good repeatability (CoV < 10%) by using the TonoLab and TonoVet, while TonoPEN AVIA use resulted in poorer repeatability.

The repeatability of IOP measurements for each tonometer and for each observer was visualized in a Bland and Altman plot, showing the difference between the individual values and the mean for repeated measurements (Fig. 3-2). The smallest deviation was observed for the TonoVet by both observers (1.34 and 1.65 for observer 1 and observer 2, respectively, Fig. 3-2b and e, dashed lines). The TonoLab showed a deviation of 4.17 and 4.81 for observer 1 and observer 2, respectively (Fig. 3-2a and d). Observer 1 showed a lower deviation than observer 2 when using the TonoPEN AVIA (2.76 vs 5.50) (Fig. 3-2c and f). This higher deviation of observer 2 could be caused by the increased scattering in higher IOP values.

When plotted over time (Fig. 3-3a and d), the repeatability of the TonoLab remained stable for both observers. For the TonoVet (Fig. 3-3b and d), the repeatability of observer 1 was improved over time (measurement 1-300 showed good repeatability (CoV < 10%) while measurement 301-400 showed very high repeatability (CoV < 5%)).This trend was similar for observer 2. Furthermore, during the earlier IOP measurements with the TonoPEN AVIA, more values were outside the 95% confidence interval (limit of agreement) for observer 2 (see Fig. 3-3c, and this correlated with the higher CoV% for measurement 1-100 (see Fig. 3-3d)). In addition, CoV% of IOP measurements from observer 2 decreased from 18.25% (measurement 1-100) to 8.28% (measurement 401-500) (Fig. 3-3d) indicating a learning curve when using the TonoPEN AVIA (observable by the funnel structure in Fig. 3-3c).

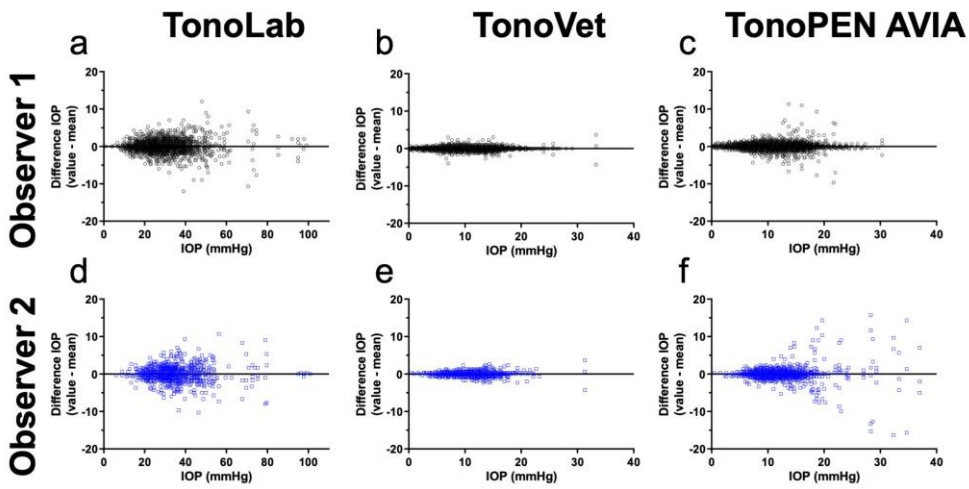

Figure 3-2. Repeatability of IOP measurements in tonometers (TonoLab (a and d), TonoVet (b and e), and TonoPEN AVIA (c and f)) for both observers. Difference per measurement (y-axis) is plotted over the mean IOP (x-axis). Dotted lines represent 1.96 times the SD (95% confidence interval).

Table 3-2. Summary of IOP results of both observers. Measurements performed in triplicate, IOP expressed in mmHg. Coefficient of variation (CoV), standard deviation (SD), percentile (PCTL).

		TonoLab	**TonoVet**	**TonoPEN AVIA**
Observer 1	**n**	166	94	164
	Mean IOP (SD)	37.00 (14.84)	11.41 (3.98)	11.76 (3.73)
	Median IOP (25% PCTL -75% PCTL)	34.00 (26.92-44.25)	11.00 (9.00 – 12.75)	11.67 (10.00 – 13.33)
	CoV%	6.55	6.38	10.88
Observer 2	**n**	166	94	164
	Mean IOP (SD)	37.00 (14.24)	11.38 (3.71)	13.24 (5.78)
	Median IOP (25% PCTL -75% PCTL)	34.83 (27.92 – 44.00)	10.67 (9.33 – 13.08)	12.00 (10.00 – 14.25)
	CoV%	7.04	7.08	14.78

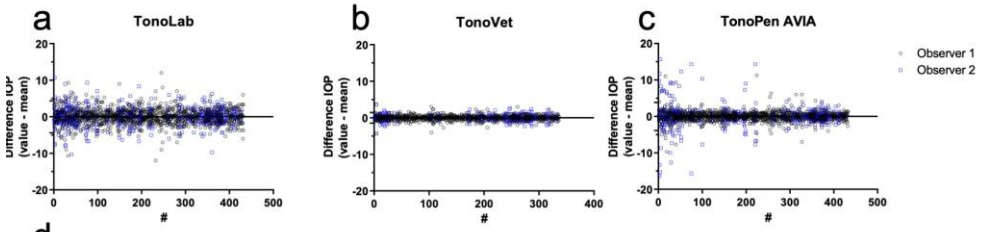

d

	TonoLab		TonoVet		TonoPEN AVIA	
	Observer 1	Observer 2	Observer 1	Observer 2	Observer 1	Observer 2
CoV% (1-100)	6.07	6.80	6.48	6.97	12.09	18.25
CoV% (101-200)	7.71	7.33	7.43	8.23	10.33	13.67
CoV% (201-300)	7.63	8.49	5.73	6.69	10.69	14.57
CoV% (301-400)	6.51	7.05	4.64	7.88	10.02	9.62
CoV% (401-500)	8.06	6.36	na	na	7.26	8.28

Figure 3-3. Repeatability of IOP measurements plotted over time. Intra-observer difference in IOP for the (a) TonoLab, (b) TonoVet, and (c) TonoPEN AVIA. (a-c) Dotted lines represent 1.96 times the SD (95% confidence interval (CI)). (d) Table summarizing the coefficient of variation (CoV) per range of measurements (per 100). Measurement #1 is the first measurement taken with the device, whereas #400 is the 400th measurement. na; not applicable.

3.3.2 Reproducibility

Figure 3-4 shows the reproducibility of the different tonometers of each observer. The TonoLab and TonoVet displayed a very strong correlation between observers ($r=0.90$, $p<0.0001$, $R^2=0.8$, for both Fig. 3-4a and Fig. 3-4b, respectively), while the TonoPEN AVIA showed a moderate correlation ($r=0.45$, $p<0.0001$, $R^2=0.2$ (Fig. 3-4c)).

Both observers obtained similar results with the TonoLab (a bias of 0.0 with a deviation of ± 12.89 (Fig. 3-4d)). IOP values measured by observer 2 were on average 0.2 mmHg lower than those measured by observer 1 using the TonoVet, (a bias of 0.2 with a deviation of ± 3.3 (Fig. 3-4e)). Furthermore, IOP values measured by observer 1 were on average 1.48 mmHg lower than those measured by observer 2 with the TonoPEN AVIA (bias of -1.48 with a deviation of ± 10.3 (Fig. 3-4f)). The negative bias was mainly caused by the large difference between both observers in the higher IOP values, as shown by the linear regression line ($R^2=0.20$) in the plot.

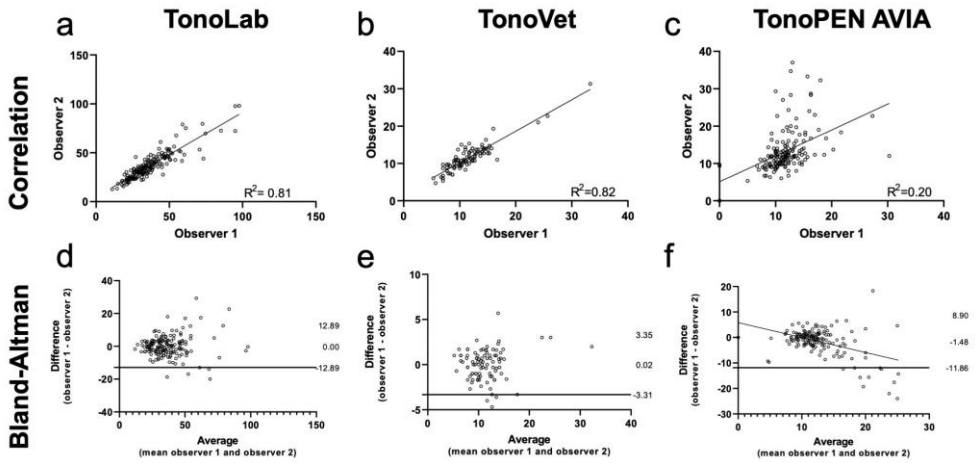

Figure 3-4. Reproducibility of different tonometers. a, b and c show scatter plots with linear regressions (dashed lines is the 95% confidence interval (CI)).d, e and f show a Bland and Altman plot expressing the difference of measurements by the observers plotted over the mean of the observers.

3.3.3. Agreement between different tonometers

Agreement between the different tonometers was assessed by combining data of observer 1 and 2 (Fig. 3-5). Data for the individual observers is shown in Fig. S1. A strong correlation was observed between the TonoLab and TonoVet ($r=0.85$, $p<0.0001$, $R^2=0.73$, Fig. 3-5a). A moderate correlation was found for the comparison of the TonoPEN AVIA with the TonoVet, and the TonoLab with TonoPEN AVIA ($r=0.53$, $p<0.0001$, $R^2=0.29$, Fig. 3-5d and $r=0.58$, $p<0.0001$, $R^2=0.33$, Fig 3-5c, respectively). Due to the learning curve of observer 2 for the TonoPEN AVIA, a lower correlation and linear regression were obtained when compared to observer 1 (Fig. S1b, c, e, and f). A moderate correlation was found for the comparison of the TonoPEN AVIA with the TonoVet for observer 1, whereas this was low for observer 2 ($r=0.60$, $p<0.0001$, $R^2=0.36$, Fig. S1b and $r=0.35$, $p<0.0001$, $R^2=0.12$, Fig. S1e, respectively). A similar pattern was observed when comparing the TonoLab with TonoPEN AVIA for observer 1 and observer 2 ($r=0.63$, $p<0.0001$, $R^2=0.40$, Fig. S1d and $r=0.40$, $p<0.0001$, $R^2=0.16$, Fig. S1f, respectively).

After plotting the difference between the tonometers, the TonoLab showed on average 22.7 ± 20.9 mmHg higher IOP values than the TonoVet (Fig. 3-5d). This difference was caused by the higher absolute IOP values of the TonoLab compared to the TonoVet, additionally confirmed by the linear regression line ($R^2=0.92$).

The TonoVet and TonoPEN AVIA were more in agreement with a bias of 0.45 (the TonoVet provided a slightly higher IOP value than the TonoPEN AVIA) with a deviation of ± 6.5 (Fig. 3-5e). The TonoLab and TonoPEN AVIA showed a negative

trend when differences were plotted against the mean values (R^2=0.80, Fig. 3-5f). Similar to the comparison with the TonoVet, a bias of -24.6 ± 24.2 mmHg was observed between the TonoLab and the TonoPEN AVIA, due to the high absolute values measured by the TonoLab. The findings were in line with individual differences between tonometers (Fig. S1g-l).

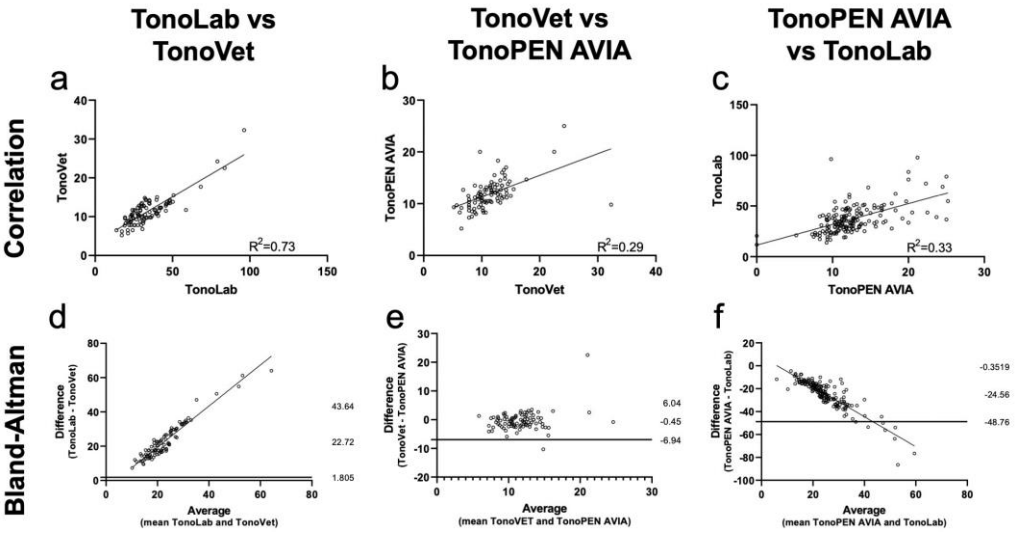

Figure 3-5. Agreement between tonometers. a, b and c show a scatter plot with linear regression (dashed lines is the 95% confidence interval (CI)). d, e and f show a Bland and Altman plot expressing the difference of measurements by the tonometers plotted over the mean values of the tonometers.

3.3.4. Effect of sedation on IOP

Figure 3-6a shows IOP over time in awake and sedated animals, measured with the TonoVet by observer 2. A two-way repeated measures ANOVA showed a significant difference between awake and sedated IOP measurement on all days, (Table 3-3, Fig. 3-6a) except for day 40 ($p>0.9999$). For day 0 until day 25, the IOP of sedated animals was about 25% lower than of awake animals, while on day 40 this difference was only about 2% (Fig. 3-6d). The repeatability of the measurement was not affected by sedation, as shown in the Bland and Altman plots (Fig. 3-6b and c).

Table 3-3. Results of the two-way repeated measures ANOVA with Bonferroni correction, N=21. CI, confidence interval;

	Mean awake	*Mean sedated*	*Mean diff.*	*SE of diff.*	95% CI of diff.	*P Value*
Day 0	11.13	8.03	3.09	0.45	1.80 to 4.39	**<0.0001**
Day 1	10.61	6.43	4.18	0.31	3.31 to 5.04	**<0.0001**
Day 5	10.80	8.30	2.50	0.34	1.55 to 3.45	**<0.0001**
Day 7	11.48	8.33	3.15	0.40	2.04 to 4.26	**<0.0001**
Day 11	9.65	8.13	1.52	0.37	0.48 to 2.55	**0.0007**
Day 15	9.90	8.32	1.58	0.29	0.77 to 2.40	**<0.0001**
Day 25	10.43	7.73	2.70	0.33	1.78 to 3.62	**<0.0001**
Day 40	9.78	9.58	0.20	0.48	-1.14 to 1.54	>0.9999

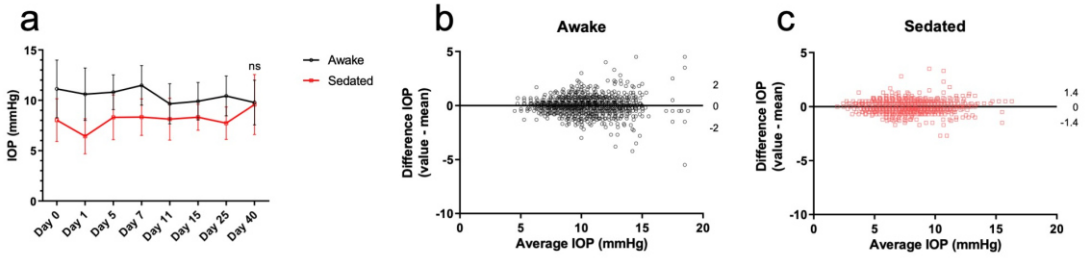

d

Day 0	Day 1	Day 5	Day 7	Day 11	Day 15	Day 25	Day 40
27.80%	39.38%	23.15%	27.43%	15.72%	15.99%	25.88%	2.04%

Figure 3-6. Effect of sedation on IOP. Measurements taken by the same observer using the TonoVet. (a) IOP over time in both awake and sedated rabbits. (d) Percentage difference in IOP between awake and sedated rabbits. (b and c) Bland and Altman plot from the awake and sedated rabbits. Dotted lines show 1.96 times the SD (95% confidence interval). ns; not significant.

3.4 Discussion

In this study, we calculated the reproducibility, repeatability and agreement of three different tonometers (the TonoLab, the TonoVet and the TonoPEN AVIA) in a cohort of normotensive NZW rabbits, alongside the effect of sedation on IOP measurements.

Our results showed higher absolute IOP values when using the TonoLab compared to the TonoVet and the TonoPEN AVIA. Since the TonoLab is designed for use in mice and rats, the thicker cornea of the rabbit probably affected the readings of this device [97, 98]. The TonoVet showed the highest repeatability (CoV of 6.38%), followed by the TonoLab and TonoPen AVIA (CoV of 6.55% and 10.88%, respectively). Furthermore, the repeatability was acceptable (defined as CoV<10%) [94] for the TonoVet and TonoLab and the measurements were in line with previous reports that found a CoV of 6.50% and 10.30% for the TonoVet and TonoPEN XL (an older version of the TonoPEN AVIA), respectively [53].

Applanation tonometry is known to be sensitive to the technique used as well as the force applied [6], while rebound tonometers can be easier to use. The ease of use for the TonoVet and TonoLab was comparable between the two, both allowing probes to be easily installed and correct usage of the device to be learned quickly. However, the TonoPEN AVIA showed to have a steeper learning curve. Applying the tip-cover of the TonoPEN AVIA may also introduce additional errors. Results showed that (for the TonoPEN AVIA in particular) extremely high IOP values (above 20 mmHg) are prone to larger error, in line with previous studies [51, 54]. The highest correlation with regard to reproducibility was found with the two rebound tonometers, TonoLab and TonoVet, with a lower reproducibility of the TonoPEN AVIA. A possible explanation for this might be that using the TonoPEN AVIA is more difficult.

On agreement between the different tonometers, the TonoLab and TonoVet showed a strong correlation ($r=0.85$, $R^2=0.73$, $p<0.0001$), in line with our expectations as both measure the IOP via rebound tonometry. When comparing the TonoPEN AVIA with the TonoVet, and the TonoLab with the TonoPEN AVIA, a more moderate agreement correlation was found ($r=0.53$, $p<0.0001$, and $r=0.58$, $p<0.0001$, respectively). Pereira *et al.* showed a correlation of $r=0.60$ ($R^2=0.36$) between the TonoVet and the TonoPEN AVIA in a cohort of 76 rabbit eyes [51], in line with our findings. Ma *et al.* compared the TonoVet to the TonoPEN XL in rabbits. They found a high linear regression ($R^2=0.98$) between both tonometers, but correlation was not tested separately [53].

Recently, Gloe *et al.* examined the TonoVet Plus (a novel version of the TonoVet that has a rabbit setting, released after the onset of this study), TonoVet, TonoPEN Vet, and TonoPEN AVIA on *post-mortem* rabbit eyes. Their results showed a high linear regression of the tonometers when compared to manometry, the TonoVet Plus

(R^2=0.99), the TonoVet (R^2=0.98), the TonoPEN Vet (R^2=0.92), and the TonoPEN AVIA (R^2=0.92). However, no correlation between the tonometers was done. Their findings indicate that all tonometers tend to underestimate IOP when compared to manometry [54].

In the present study, the TonoVet and TonoPEN AVIA showed the highest agreement; however, the correlation is moderate due to the different working mechanisms of the tonometers (rebound versus applanation). The TonoLab and TonoVet demonstrated the best correlation, however their agreement was lower because the measurements of the TonoLab showed a much higher IOP than the TonoVet. Since the probe size of the TonoLab is specifically designed for use in small rodents, the system is not calibrated for the thick corneas of rabbits [35]. The average central corneal thickness (CCT) has been reported to be 105 μm for mice and 130 μm for rats [35]. The average CCT of New Zealand White rabbits is 407±20 μm [99], 3 to 4 times thicker than the reported values in rodents. The rabbit's greater corneal thickness is likely responsible for inaccurate IOP values obtained with the TonoLab. Although we did not measure CCT in every animal and could therefore not correct for CCT differences, they were all New Zealand White rabbits from the same age, and differences in CCT were therefore likely to be limited . Additionally, all animals were measured with all three devices and the aim was to observe the differences between those devices .

Overall, the TonoVet was the best tonometer in terms of repeatability, reproducibility, and agreement and it was the most consistent tonometer in comparison to the TonoPEN AVIA and TonoLab. The TonoVet showed the highest agreement and strongest correlation to the other tonometers. The correlation between the TonoLab and TonoPEN AVIA was found to be moderate, presumably from them being different mechanisms of measurement, similar to the TonoPEN AVIA and the TonoVet having a moderate correlation.

The effect of the selective alpha 2-adrenoceptor agonist medetomidine on IOP was examined using the TonoVet. Our results indicated a ~25% reduction in IOP after IM sedation. In dogs, no reduction of IOP has been observed using a similar dose of 0.5mg/kg medetomidine IM [100]. In rabbits, medetomidine has also topically been instilled [18, 19]. Two studies found that a dose of 25μg medetomidine reduced the IOP of the contralateral eye in 30 minutes by ~50%, while the treated eye was not affected [18, 19]. This effect has also been observed in dogs [101].

In contrast to other time points in our study, no difference in IOP between awake and sedated animals was observed at day 40. This might have been caused by elevated mental stress levels in the rabbits, caused by euthanasia of animals performed in the same room, an effect also observed in dogs [101]. Levels of mental stress were not assessed during the study but did not affect the repeatability and reproducibility of the measurements.

Because IOP fluctuates over short periods of time, similar to fluctuations in heart rate during the day [15], any tonometer that records a near-instantaneous measurement of IOP is taking a sample from the IOP cycle causing measurements to only provide an estimation of the IOP at one time point. Variables such as fluctuating blood pressure, pulse, respiration, and anxiety could also account for discrepancies in IOP, along with the mental stress of repeated measures [102].

3.5 Conclusion

Of the three tonometers tested, TonoVet was the most favorable as it showed the smallest inter- and intra-observer variations, without a learning curve. The TonoLab showed three-fold higher IOP values compared to the TonoVet, making it unsuitable for determining rabbit IOP. Additionally, when IM sedation is required in future experiments, it should be taken into account that it significantly reduces the IOP of rabbits (often by more than 25%).

References

1. Dang, Y., et al., *Intraocular pressure elevation precedes a phagocytosis decline in a model of pigmentary glaucoma.* F1000Res, 2018. **7**: p. 174.
2. Yang, Q., et al., *Microbead-induced ocular hypertensive mouse model for screening and testing of aqueous production suppressants for glaucoma.* Invest Ophthalmol Vis Sci, 2012. **53**(7): p. 3733-41.
3. Mukai, R., et al., *Mouse model of ocular hypertension with retinal ganglion cell degeneration.* PLoS One, 2019. **14**(1): p. e0208713.
4. Alguire, P.C., *Tonometry*, in *Clinical Methods: The History, Physical, and Laboratory Examinations*, rd, et al., Editors. 1990: Boston.
5. Pearce, J.G. and T. Maddess, *The Clinical Interpretation of Changes in Intraocular Pressure Measurements Using Goldmann Applanation Tonometry: A Review.* J Glaucoma, 2019. **28**(4): p. 302-306.
6. Lim, K.S., et al., *Accuracy of intraocular pressure measurements in new zealand white rabbits.* Invest Ophthalmol Vis Sci, 2005. **46**(7): p. 2419-23.
7. Davies, L.N., et al., *Clinical evaluation of rebound tonometer.* Acta Ophthalmol Scand, 2006. **84**(2): p. 206-9.
8. Whitacre, M.M., R.A. Stein, and K. Hassanein, *The effect of corneal thickness on applanation tonometry.* Am J Ophthalmol, 1993. **115**(5): p. 592-6.
9. Ko, Y.C., C.J. Liu, and W.M. Hsu, *Varying effects of corneal thickness on intraocular pressure measurements with different tonometers.* Eye (Lond), 2005. **19**(3): p. 327-32.
10. Ehlers, N., T. Bramsen, and S. Sperling, *Applanation tonometry and central corneal thickness.* Acta Ophthalmol (Copenh), 1975. **53**(1): p. 34-43.
11. Turner, D.C., et al., *Acute Stress Increases Intraocular Pressure in Nonhuman Primates.* Ophthalmol Glaucoma, 2019. **2**(4): p. 210-214.
12. Gillmann, K., K. Hoskens, and K. Mansouri, *Acute emotional stress as a trigger for intraocular pressure elevation in Glaucoma.* BMC Ophthalmol, 2019. **19**(1): p. 69.
13. Jimenez, R. and J. Vera, *Effect of examination stress on intraocular pressure in university students.* Appl Ergon, 2018. **67**: p. 252-258.
14. Dada, T., et al., *Mindfulness Meditation Reduces Intraocular Pressure, Lowers Stress Biomarkers and Modulates Gene Expression in Glaucoma: A Randomized Controlled Trial.* J Glaucoma, 2018. **27**(12): p. 1061-1067.
15. Rowland, J.M., D.E. Potter, and R.J. Reiter, *Circadian rhythm in intraocular pressure: a rabbit model.* Curr Eye Res, 1981. **1**(3): p. 169-73.
16. Li, R. and J.H. Liu, *Telemetric monitoring of 24 h intraocular pressure in conscious and freely moving C57BL/6J and CBA/CaJ mice.* Mol Vis, 2008. **14**: p. 745-9.
17. Dear, G.D., et al., *Anaesthesia and intra-ocular pressure in young children. A study of three different techniques of anaesthesia.* Anaesthesia, 1987. **42**(3): p. 259-65.
18. Potter, D.E. and M.J. Ogidigben, *Medetomidine-induced alterations of intraocular pressure and contraction of the nictitating membrane.* Invest Ophthalmol Vis Sci, 1991. **32**(10): p. 2799-805.
19. Ogidigben, M.J. and D.E. Potter, *Comparative effects of alpha-2 and DA-2 agonists on intraocular pressure in pigmented and nonpigmented rabbits.* J Ocul Pharmacol, 1993. **9**(3): p. 187-99.
20. Kelly, D.J. and S.M. Farrell, *Physiology and Role of Intraocular Pressure in Contemporary Anesthesia.* Anesth Analg, 2018. **126**(5): p. 1551-1562.
21. Basaran, B., A.A. Yilbas, and Z. Gultekin, *Effect of interscalene block on intraocular pressure and ocular perfusion pressure.* BMC Anesthesiol, 2017. **17**(1): p. 144.
22. Jasien, J.V., C.A. Girkin, and J.C. Downs, *Effect of Anesthesia on Intraocular Pressure Measured With Continuous Wireless Telemetry in Nonhuman Primates.* Invest Ophthalmol Vis Sci, 2019. **60**(12): p. 3830-3834.
23. Hausmann, J.C., et al., *Measuring Intraocular Pressure in White's Tree Frogs (Litoria Caerulea) by Rebound Tonometry: Comparing Device, Time of Day, and Manual Versus Chemical Restraint Methods.* J Zoo Wildl Med, 2017. **48**(2): p. 413-419.
24. Lewin, A.C., J.C. Hausmann, and P.E. Miller, *Intraocular Pressure and Examination Findings in Three Species of Central and South American Tree Frogs (Cruziohyla Craspedopus, Cruziohyla Calcarifer, and Anotheca Spinosa).* J Zoo Wildl Med, 2017. **48**(3): p. 688-693.

25. Cannizzo, S.A., G.A. Lewbart, and H.D. Westermeyer, *Intraocular pressure in American Bullfrogs (Rana catesbeiana) measured with rebound and applanation tonometry.* Vet Ophthalmol, 2017. **20**(6): p. 526-532.
26. Delgado, C., et al., *Evaluation of rebound tonometry in red-eared slider turtles (Trachemys scripta elegans).* Vet Ophthalmol, 2014. **17**(4): p. 261-7.
27. Rajaei, S., et al., *Measurement of Intraocular Pressure Using Tonovet(R) in European Pond Turtle (Emys Orbicularis).* J Zoo Wildl Med, 2015. **46**(2): p. 421-2.
28. Qiu, Y., H. Yang, and B. Lei, *Effects of three commonly used anesthetics on intraocular pressure in mouse.* Curr Eye Res, 2014. **39**(4): p. 365-9.
29. Wang, W.H., et al., *Noninvasive measurement of rodent intraocular pressure with a rebound tonometer.* Invest Ophthalmol Vis Sci, 2005. **46**(12): p. 4617-21.
30. Saeki, T., et al., *The efficacy of TonoLab in detecting physiological and pharmacological changes of mouse intraocular pressure--comparison with TonoPen and microneedle manometery.* Curr Eye Res, 2008. **33**(3): p. 247-52.
31. Pease, M.E., J.C. Hammond, and H.A. Quigley, *Manometric calibration and comparison of TonoLab and TonoPen tonometers in rats with experimental glaucoma and in normal mice.* J Glaucoma, 2006. **15**(6): p. 512-9.
32. Pease, M.E., et al., *Calibration of the TonoLab tonometer in mice with spontaneous or experimental glaucoma.* Invest Ophthalmol Vis Sci, 2011. **52**(2): p. 858-64.
33. Chatterjee, A., et al., *Central corneal thickness does not correlate with TonoLab-measured IOP in several mouse strains with single transgenic mutations of matricellular proteins.* Exp Eye Res, 2013. **115**: p. 106-12.
34. Reitsamer, H.A., et al., *Tonopen measurement of intraocular pressure in mice.* Exp Eye Res, 2004. **78**(4): p. 799-804.
35. Snyder, K.C., et al., *Tonometer validation and intraocular pressure reference values in the normal chinchilla (Chinchilla lanigera).* Vet Ophthalmol, 2018. **21**(1): p. 4-9.
36. Muller, K., D.A. Mauler, and J.C. Eule, *Reference values for selected ophthalmic diagnostic tests and clinical characteristics of chinchilla eyes (Chinchilla lanigera).* Vet Ophthalmol, 2010. **13 Suppl**: p. 29-34.
37. Liu, L.F., C.K. Huang, and M.Z. Zhang, *Reliability of Tonolab measurements in rats.* Int J Ophthalmol, 2014. **7**(6): p. 930-4.
38. Lee, E.J., et al., *Assessing intraocular pressure by rebound tonometer in rats with an air-filled anterior chamber.* Jpn J Ophthalmol, 2008. **52**(6): p. 500-503.
39. Morrison, J.C., et al., *Reliability and sensitivity of the TonoLab rebound tonometer in awake Brown Norway rats.* Invest Ophthalmol Vis Sci, 2009. **50**(6): p. 2802-8.
40. Moore, C.G., S.T. Milne, and J.C. Morrison, *Noninvasive measurement of rat intraocular pressure with the Tono-Pen.* Invest Ophthalmol Vis Sci, 1993. **34**(2): p. 363-9.
41. Goldblum, D., et al., *Non-invasive determination of intraocular pressure in the rat eye. Comparison of an electronic tonometer (TonoPen), and a rebound (impact probe) tonometer.* Graefes Arch Clin Exp Ophthalmol, 2002. **240**(11): p. 942-6.
42. Jia, L., et al., *Effect of general anesthetics on IOP in rats with experimental aqueous outflow obstruction.* Invest Ophthalmol Vis Sci, 2000. **41**(11): p. 3415-9.
43. Moore, C.G., et al., *Long-term non-invasive measurement of intraocular pressure in the rat eye.* Curr Eye Res, 1995. **14**(8): p. 711-7.
44. Moore, C.G., E.C. Johnson, and J.C. Morrison, *Circadian rhythm of intraocular pressure in the rat.* Curr Eye Res, 1996. **15**(2): p. 185-91.
45. Williams, D. and A. Sullivan, *Ocular disease in the guinea pig (Cavia porcellus): a survey of 1000 animals.* Vet Ophthalmol, 2010. **13 Suppl**: p. 54-62.
46. Tammewar, A.M., et al., *Intraocular properties of an alkoxyalkyl derivative of cyclic 9-(S)-(3-hydroxyl-2-phosphonomehoxypropyl) adenine, an intravitreally injectable anti-HCMV drug in rabbit and guinea pig.* J Ocul Pharmacol Ther, 2007. **23**(5): p. 433-44.
47. Montiani-Ferreira, F., B.C. Mattos, and H.H. Russ, *Reference values for selected ophthalmic diagnostic tests of the ferret (Mustela putorius furo).* Vet Ophthalmol, 2006. **9**(4): p. 209-13.
48. Williams, D., N. Adeyeye, and E. Visser, *Ophthalmological abnormalities in wild European hedgehogs (Erinaceus europaeus): a survey of 300 animals.* Open Vet J, 2017. **7**(3): p. 261-267.
49. Ghaffari, M.S., et al., *Intraocular pressure and Schirmer tear test results in clinically normal Long-Eared Hedgehogs (Hemiechinus auritus): reference values.* Vet Ophthalmol, 2012. **15**(3): p. 206-9.

50. Kalesnykas, G. and H. Uusitalo, *Comparison of simultaneous readings of intraocular pressure in rabbits using Perkins handheld, Tono-Pen XL, and TonoVet tonometers.* Graefes Arch Clin Exp Ophthalmol, 2007. **245**(5): p. 761-2.
51. Pereira, F.Q., et al., *Comparison of a rebound and an applanation tonometer for measuring intraocular pressure in normal rabbits.* Vet Ophthalmol, 2011. **14**(5): p. 321-6.
52. Zhang, H., et al., *Validation of rebound tonometry for intraocular pressure measurement in the rabbit.* Exp Eye Res, 2014. **121**: p. 86-93.
53. Ma, D., et al., *Repeatability, reproducibility and agreement of intraocular pressure measurement in rabbits by the TonoVet and Tono-Pen.* Sci Rep, 2016. **6**: p. 35187.
54. Gloe, S., et al., *Validation of the Icare((R)) TONOVET plus rebound tonometer in normal rabbit eyes.* Exp Eye Res, 2019. **185**: p. 107698.
55. Kovalcuka, L. and M. Nikolajenko, *Changes in intraocular pressure, horizontal pupil diameter, and tear production during the use of topical 1% cyclopentolate in cats and rabbits.* Open Vet J, 2020. **10**(1): p. 59-67.
56. Taskiran Comez, A., et al., *Relationship between raised intraocular pressure and ischemia-modified albumin in serum and humor aqueous: a pilot study in rabbits.* Int J Ophthalmol, 2014. **7**(3): p. 421-5.
57. Zagon, I.S., et al., *Topical application of naltrexone facilitates reepithelialization of the cornea in diabetic rabbits.* Brain Res Bull, 2010. **81**(2-3): p. 248-55.
58. Goldblum, D., J.G. Garweg, and M. Bohnke, *Topical rivastigmine, a selective acetylcholinesterase inhibitor, lowers intraocular pressure in rabbits.* J Ocul Pharmacol Ther, 2000. **16**(1): p. 29-35.
59. Fleischhauer, J.C., et al., *Topical ocular instillation of nitric oxide synthase inhibitors and intraocular pressure in rabbits.* Klin Monbl Augenheilkd, 2001. **218**(5): p. 351-3.
60. Park, Y.W., et al., *Effect of central corneal thickness on intraocular pressure with the rebound tonometer and the applanation tonometer in normal dogs.* Vet Ophthalmol, 2011. **14**(3): p. 169-73.
61. Nagata, N., M. Yuki, and T. Hasegawa, *In vitro and in vivo comparison of applanation tonometry and rebound tonometry in dogs.* J Vet Med Sci, 2011. **73**(12): p. 1585-9.
62. Ahn, J.T., et al., *Accuracy of intraocular pressure measurements in dogs using two different tonometers and plano therapeutic soft contact lenses.* Vet Ophthalmol, 2012. **15 Suppl 1**: p. 83-8.
63. de Oliveira, J.K., F. Montiani-Ferreira, and D.L. Williams, *The influence of the tonometer position on canine intraocular pressure measurements using the Tonovet((R)) rebound tonometer.* Open Vet J, 2018. **8**(1): p. 68-76.
64. Slack, J.M., J. Stiles, and G.E. Moore, *Comparison of a rebound tonometer with an applanation tonometer in dogs with glaucoma.* Vet Rec, 2012. **171**(15): p. 373.
65. von Spiessen, L., et al., *Clinical comparison of the TonoVet((R)) rebound tonometer and the Tono-Pen Vet((R)) applanation tonometer in dogs and cats with ocular disease: glaucoma or corneal pathology.* Vet Ophthalmol, 2015. **18**(1): p. 20-7.
66. Taylor, N.R., et al., *Variation in intraocular pressure following application of tropicamide in three different dog breeds.* Vet Ophthalmol, 2007. **10 Suppl 1**: p. 8-11.
67. Mughannam, A.J., C.S. Cook, and C.L. Fritz, *Change in intraocular pressure during maturation in Labrador Retriever dogs.* Vet Ophthalmol, 2004. **7**(2): p. 87-9.
68. Adelman, S., et al., *The post-natal development of intraocular pressure in normal domestic cats (Felis catus) and in feline congenital glaucoma.* Exp Eye Res, 2018. **166**: p. 70-73.
69. Rusanen, E., et al., *Evaluation of a rebound tonometer (Tonovet) in clinically normal cat eyes.* Vet Ophthalmol, 2010. **13**(1): p. 31-6.
70. Rodrigues, B.E., et al., *Intraocular pressure and pupil diameter in healthy cats anesthetized with isoflurane and pre-medicated with isolated acepromazine or in combination with tramadol. .* Arquivo Brasileiro de Medicina Veterinária e Zootecnia, 2021. **73**(03): p. 631-638.
71. Jeong, M.B., et al., *Comparison of the rebound tonometer (TonoVet) with the applanation tonometer (TonoPen XL) in normal Eurasian Eagle owls (Bubo bubo).* Vet Ophthalmol, 2007. **10**(6): p. 376-9.
72. Reuter, A., et al., *Accuracy and reproducibility of the TonoVet rebound tonometer in birds of prey.* Vet Ophthalmol, 2010. **13 Suppl**: p. 80-5.
73. Harris, M.C., et al., *Ophthalmic examination findings in a colony of Screech owls (Megascops asio).* Vet Ophthalmol, 2008. **11**(3): p. 186-92.
74. Meekins, J.M., et al., *Ophthalmic Diagnostic Tests and Ocular Findings in a Flock of Captive American Flamingos (Phoenicopterus ruber ruber).* J Avian Med Surg, 2015. **29**(2): p. 95-105.

75. Ansari Mood, M., et al., *Measurement of tear production and intraocular pressure in ducks and geese.* Vet Ophthalmol, 2017. **20**(1): p. 53-57.
76. Kovalcuka, L., D. Boiko, and D.L. Williams, *Tear production and intraocular pressure values in clinically normal eyes of whooper swans (Cygnus cygnus).* Open Vet J, 2018. **8**(3): p. 335-339.
77. Ansari Mood, M., et al., *Measurement of Intraocular Pressure in the Domestic Pigeon (Columbia Livia).* J Zoo Wildl Med, 2016. **47**(3): p. 935-938.
78. Tofflemire, K.L., et al., *Schirmer tear test I and rebound tonometry findings in healthy calves.* Vet Ophthalmol, 2015. **18**(2): p. 147-51.
79. Hibbs, C.D., P.M. Barrett, and D.D. Dees, *Intraocular pressure reference intervals in eyes of clinically normal miniature donkeys (Equus africanus asinus).* Vet Ophthalmol, 2019. **22**(1): p. 24-30.
80. Allbaugh, R.A., et al., *Intraocular pressure changes in equine athletes during endurance competitions.* Vet Ophthalmol, 2014. **17 Suppl 1**: p. 154-9.
81. Lewin, A.C. and P.E. Miller, *Calibration of the TonoVet and Tono-Pen Vet tonometers in the porcine eye.* Vet Ophthalmol, 2017. **20**(6): p. 571-573.
82. McDonald, J.E., et al., *Comparison of intraocular pressure measurements using rebound (TonoVet((R))) and applanation (TonoPen-XL((R))) tonometry in clinically normal alpacas (Vicugna pacos).* Vet Ophthalmol, 2017. **20**(2): p. 155-159.
83. Peche, N. and J.C. Eule, *Intraocular pressure measurements in cattle, sheep, and goats with 2 different types of tonometers.* Can J Vet Res, 2018. **82**(3): p. 208-215.
84. Yu, W., et al., *Evaluation of monkey intraocular pressure by rebound tonometer.* Mol Vis, 2009. **15**: p. 2196-201.
85. McAllister, F., R. Harwerth, and N. Patel, *Assessing the True Intraocular Pressure in the Non-human Primate.* Optom Vis Sci, 2018. **95**(2): p. 113-119.
86. Dubicanac, M., et al., *Intraocular pressure in the smallest primate aging model: the gray mouse lemur.* Vet Ophthalmol, 2018. **21**(3): p. 319-327.
87. Kim, J., et al., *IOP change undergoing anesthesia in rhesus macaques (Macaca mulatta) with laser-induced ocular hypertension.* J Vet Med Sci, 2012. **74**(10): p. 1359-61.
88. Ollivier, F.J., et al., *Time-specific intraocular pressure curves in Rhesus macaques (Macaca mulatta) with laser-induced ocular hypertension.* Vet Ophthalmol, 2004. **7**(1): p. 23-7.
89. Percie du Sert, N., et al., *The ARRIVE guidelines 2.0: Updated guidelines for reporting animal research.* BMC Vet Res, 2020. **16**(1): p. 242.
90. Baudouin, C. and P. Gastaud, *Influence of topical anesthesia on tonometric values of intraocular pressure.* Ophthalmologica, 1994. **208**(6): p. 309-13.
91. British Standards Institution., *Accuracy (trueness and precision) of measurement methods and results: basic methods for the determination of repeatability and reproducibility of a standard measurement method.* ISO 5725 part 2, 1994.
92. Charan, J. and N.D. Kantharia, *How to calculate sample size in animal studies?* J Pharmacol Pharmacother, 2013. **4**(4): p. 303-6.
93. Bertens, C.J.F., et al., *Pharmacokinetics and efficacy of a ketorolac-loaded ocular coil in New Zealand white rabbits.* Drug Deliv, 2021. **28**(1): p. 400-407.
94. Fujimura, F., et al., *Repeatability and reproducibility of measurements using a NT-530P noncontact tono/pachymeter and correlation of central corneal thickness with intraocular pressure.* Biomed Res Int, 2013. **2013**: p. 370592.
95. Bland, J.M. and D.G. Altman, *Statistical methods for assessing agreement between two methods of clinical measurement.* Lancet, 1986. **1**(8476): p. 307-10.
96. Bland, J.M. and D.G. Altman, *Comparing methods of measurement: why plotting difference against standard method is misleading.* Lancet, 1995. **346**(8982): p. 1085-7.
97. Yildiz, A. and T. Yasar, *Comparison of Goldmann applanation, non-contact, dynamic contour and tonopen tonometry measurements in healthy and glaucomatous eyes, and effect of central corneal thickness on the measurement results.* Med Glas (Zenica), 2018. **15**(2): p. 152-157.
98. Doughty, M.J., et al., *Central corneal thickness in European (white) individuals, especially children and the elderly, and assessment of its possible importance in clinical measures of intra-ocular pressure.* Ophthalmic Physiol Opt, 2002. **22**(6): p. 491-504.
99. Chan, T., S. Payor, and B.A. Holden, *Corneal thickness profiles in rabbits using an ultrasonic pachometer.* Invest Ophthalmol Vis Sci, 1983. **24**(10): p. 1408-10.
100. Kanda, T., et al., *Effects of medetomidine and xylazine on intraocular pressure and pupil size in healthy Beagle dogs.* Vet Anaesth Analg, 2015. **42**(6): p. 623-8.
101. Verbruggen, A.M., et al., *The effect of intravenous medetomidine on pupil size and intraocular pressure in normotensive dogs.* Vet Q, 2000. **22**(3): p. 179-80.

102. Whitacre, M.M. and R. Stein, *Sources of error with use of Goldmann-type tonometers.* Surv Ophthalmol, 1993. **38**(1): p. 1-30.

Chapter 4

Wound Healing Response After Bleb-Forming Glaucoma Surgery With a SIBS Microshunt in Rabbits

van Mechelen, R. J. S., Wolters, J. E. J., Herfs, M., Bertens, C. J. F., Gijbels, M., Pinchuk, L., Gorgels, T. G. M. F., & Beckers, H. J. M. (2022). Wound Healing Response After Bleb-Forming Glaucoma Surgery With a SIBS Microshunt in Rabbits. Translational vision science & technology, 11(8), 29.

Abstract

The PRESERFLO MicroShunt is an innovative implant for the surgical treatment of glaucoma. Although effective, surgeries still fail due to fibrosis. This study was conducted to gain insight into the histological aspects of the fibrotic response and find potential targets to reduce postoperative fibrosis. Fifteen New-Zealand White rabbits were implanted with a microshunt and followed up for 40 days. Animals were euthanized at postoperative day (POD) 1, 5, and 40 to collect eyes for histological evaluation. Bleb formation and ocular health were assessed by slit lamp bio-microscopy (SL) and optical coherence tomography (OCT). IOP was measured using rebound tonometry. Blebs failed after approximately 2 weeks based on bleb survival and IOP measurements. No severe complications were observed with OCT and SL. Histology revealed a wide variety of cells, in the bleb and around the microshunt including polymorphonuclear leucocytes (PMNs), myofibroblasts, and foreign body giant cells, at different PODs.
Current antifibrotic therapies aim to inhibit myofibroblasts. However, a wide variety of cells are involved in the fibrotic response. Future research focusing on these cells could offer novel methods in reducing the fibrotic response after glaucoma surgery. For example, by developing novel antifibrotic drugs, methods for sustained delivery of medications, or augmenting material properties.

4.1 Introduction

Glaucoma is classified as a degenerative optic neuropathy in which retinal ganglion cell loss and subsequent loss of optic nerve fibers lead to irreversible and progressive visual field loss [1, 2]. Untreated, the disease may lead to severe visual impairment and blindness. Currently, glaucoma is the leading cause of irreversible blindness worldwide. It is estimated that approximately 112 million patients will suffer from glaucoma in 2040 [3]. The primary risk factor is increased intraocular pressure (IOP). Currently, no causative treatment exists for glaucoma. The only proven treatment is lowering IOP to a target level that is sufficiently low to halt progression of the disease. Patients are primarily treated with medications (usually eye drops), and/or laser surgery to reduce IOP to "normal" limits (10-21 mmHg) [4-6]. Although highly effective, bleb forming glaucoma surgery is often postponed as a last resort treatment due to vision threatening complications [1]. During glaucoma filtration surgery (GFS), IOP is lowered by creating a transscleral outflow channel through which aqueous humor (AqH) flows out of the eye into the subconjunctival/sub-Tenon's space. With this procedure, a small fluid-filled blister is formed, which is referred to as a filtering bleb [1, 7]. However, approximately 10% of all bleb based surgeries fail each year due to excessive wound healing and the formation of fibrosis [8]. Fibrosis limits the outflow of AqH by scarring of the bleb leading to inadequate IOP reduction [7]. Overall, fibrosis is considered as an overreaching wound healing response, with myofibroblasts persistently present in the wound [7]. To reduce the fibrotic response, the anti-metabolites mitomycin-C (MMC) or 5-fluoracil (5-FU) are often used, either as a one-time application during surgery or as one, or several, injections into the bleb after surgery [9]. Unfortunately, use of anti-metabolites may be accompanied by complications such as endophthalmitis, corneal endothelial cell loss, avascular filtering blebs, hypotony, thinning of the conjunctiva, and bleb leaks [10]. To improve the safety of glaucoma surgery, new and less invasive bleb-forming glaucoma surgeries were introduced and commercialized over the last decade. One of these is the PRESERFLO MicroShunt, which is made from an innovative material, poly (styrene-block-isobutylene-block-styrene) (SIBS). *In vivo* research has previously shown that SIBS induces less encapsulation and activation of myofibroblasts when compared to silicone. Additionally, flow was still visible after 1 year of follow up [11]. Clinical studies have shown that the overall success rate of the PRESERFLO MicroShunt is 70% after approximately 1 year [12, 13]. Although effective in reducing IOP, surgeries may still fail due to the formation of fibrosis, even with the additional usage of MMC [14, 15]. Patients will often require additional IOP-lowering medications or surgeries to reach the desired low IOP level.

To find potential targets to further improve surgical outcomes, we wanted to investigate the wound healing response after placement of a SIBS microshunt, on a

histological level. For this purpose, we implanted rabbits with a SIBS microshunt and followed the histological response for up to 40 days. The SIBS microshunts that were used in our study are closely similar to the commercially available PRESERFLO MicroShunt.

4.2 Materials and methods

4.2.1 Animals

All animal procedures were approved by the Central Authority for Scientific Procedures on Animals (CCD, Den Haag, NL), were approved by the local ethical committee, and were in accordance with the European Directive for animal experiments (2010/63/EU) (Approved Dutch license number: AVD1070020197464). They also complied with the Association for Research in Vision and Ophthalmology (ARVO) statement for the use of animals in ophthalmic and vision research and the Animal Research: Reporting of *In Vivo* Experiments (ARRIVE) 2.0 guidelines. Fifteen normotensive New Zealand white rabbits (Charles River, FR) were used, with an approximate age of 12 weeks, weighing 2.5 to 3 kg. Both male and female rabbits were used. The Rabbits were maintained under controlled conditions of temperature and humidity on a 12h:12h light-dark cycle. The rabbits had ad libitum access to water and food (100 gr of dried chow per rabbit per day and unlimited access to hay). Before the start of the experiment, animals had a two-week acclimatization period. A randomized complete block design was used to allocate animals to groups, and animals were euthanized at POD 1, 5, and 40 (n=5 per group) with an overdose of pentobarbital sodium, 200 mg/kg (Euthasol 20, Produlab Pharma B.V., NL) intravenously injected.

4.2.2 Surgical procedure

In total, 15 animals were randomly assigned to be implanted with the PRESERFLO MicroShunt (Figure 4-1) (InnFocus Inc, a Santen company, Miami Florida, USA). Animals were surgically anesthetized by injecting 30 mg/kg ketamine and 0.25 mg/kg medetomidine (Sedator, A.S.T. Farma B.V., Oudewater, NL) intramuscularly (IM). Additionally, inhalation anesthetics were provided if needed (0.5 to 1% isoflurane). In all rabbits, the right eye was used for implantation. All surgeries were performed by a single surgeon (R.M). Local analgesia was provided in the form of 0.4% oxybuprocaine hydrochloride drops (MINIMS, Bausch & Lomb Pharma, Brussels, BE). The surgical area was exposed with a speculum. A fornix-based conjunctival flap was created with Westcott tenotomy scissors, after which a 1 mm wide and 1 mm deep scleral pocket was formed, 3 mm posterior to the limbus. Through the scleral pocket, a needle tract was made with a 25G needle into the anterior chamber. The microshunt was then implanted through the needle tract. The fins were wedged

firmly into the scleral pocket. Afterwards, flow was checked by massaging the eye until a droplet of aqueous formed at the distal end of the microshunt. Lastly, the conjunctiva and Tenon's capsule were sutured with a Vicryl 9-0 suture (Ethicon LLC, Puerto Rico, USA). After completion of the surgery, the rabbit received an IM injection of 0.5 mg/kg atipamezole (Antisedan, ORION pharma, Mechelen, BE) to accelerate recovery. Animals were treated with 1% chloramphenicol ointment BID for 5 days and received a subcutaneous injection of buprenorphine (0.05 mg/kg Bupaq Multidose, Richter Pharma AG, Wels, AT) up until POD 1 twice a day, if needed analgesia was extended.

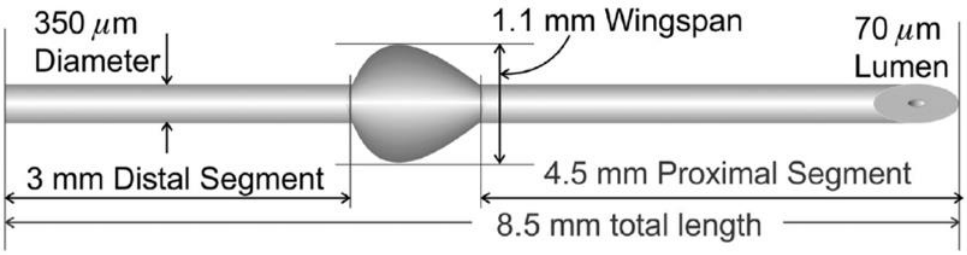

Figure 4-1: Schematic representation of the PRESERFLO MicroShunt. The image was used with permission from InnFocus Inc. a Santen company.

4.2.3 *In vivo* measurements

Rabbits were sedated using 0.40 mg/kg medetomidine IM. Afterwards, rabbits were examined using IOP measurements with the iCare® TonoVet (iCare Finland Oy, Vantaa, FI). Slit lamp bio-microscopy (SL) examinations (Haag-Streit BI 900, Haag-Streit, Köniz, CH), optical coherence tomography (OCT, Heidelberg Engineering SL-OCT mounted on a Haag-Streit BD 900 SL, Heidelberg Engineering GmbH, Heidelberg, DE), and bleb images were taken using a photo camera (Canon EOS 4000D, Canon, Tokio, JP). One week before surgery, baseline recordings were taken for each rabbit. The follow up examinations were performed on POD 1, 5, 7, 11, 15, 25, and 40. When a bleb appeared to be flat, the eye was gently massaged, if the bleb remained flat after massage, the bleb was categorized as failed.

4.2.4 Light microscopy and staining

Bromodeoxyuridine (BrdU, 30 mg/kg, Abcam, Cambridge UK) was injected intravenously twice, one day before sacrifice. Animals were euthanized using 200 mg/kg pentobarbital sodium (Euthasol 20, Produlab Pharma B.V., NL). After euthanasia, both eyes were dissected and fixed in 4% paraformaldehyde (PFA) for 2 days (PFA was refreshed once a day), after fixation, eyes were dehydrated and embedded in paraffin blocks. Sections were cut with a thickness of 4 µm and were stained with Hematoxylin & Eosin (H&E), mouse-anti-alpha-smooth muscle actin (α-

SMA) (ThermoFisher scientific, US, MA5-11547, 1:500) and sheep-anti-BrdU (Novus biologicals, US, NB500-235, 1:2500). In the case of anti-α-SMA and anti-BrdU, slides were blocked using 3% hydrogen peroxidase and 10% donkey serum (Abcam, UK, ab7475). A secondary antibody (donkey-anti-mouse, Jackson immunoresearch, UK, 715-065-151, 1:2000) and donkey-anti-sheep (LSBio, US, LS-C61150, 1:3000) with a biotin label was used to detect the primary antibody. Lastly, an ABC kit (Vector laboratories, US, PK6100) was used to enhance the biotin label for staining and Novared (Vector laboratories, US, SK-4800) was used to stain the slides. Histological slides were assessed and semi-qualitatively scored by two blinded observers, as a control the contralateral eyes were used (from the same time point as the experimental eye). Percentages of cells were graded by looking at high magnification fields and estimating the number of cells present per field. PMNs (multilobed and in rabbits they have heterophilic cytoplasmic granules because they are heterophils [16]) and macrophages were identified based on nuclear morphology, cytoplasm color, and nuclear cytoplasmic ratio (see Figure 4-2). Photographs were taken using a confocal scanning microscope (BX-51, Olympus, JP).

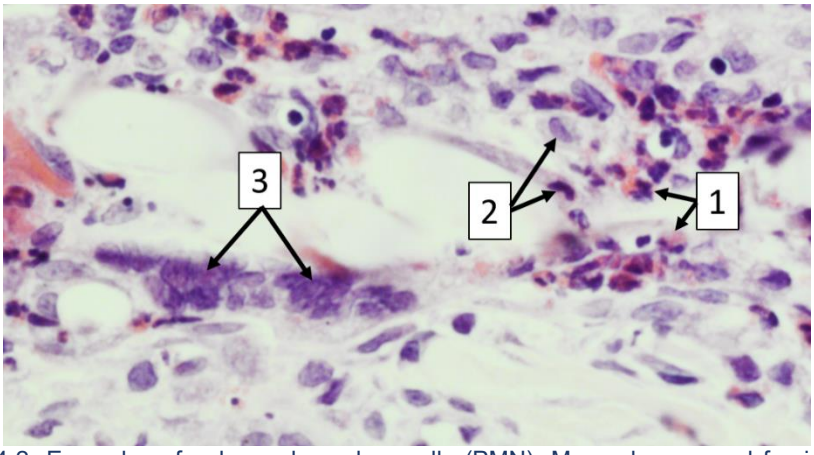

Figure 4-2: Examples of polymorphonuclear cells (PMN), Macrophages, and foreign body giant cells (FBGC). (1) PMNs are distinguishable due to their multilobed nucleus and eosinophilic cytoplasm. (2) Macrophages have a basophilic cytoplasm and a bean-shaped or ovoid nucleus. (3) FBGC are large clusters of fused macrophages. The image was taken at a 400X magnification.

4.2.5 Statistical analysis

A two-way ANOVA with Šidák post hoc comparisons was used to compare the IOP between groups. A Kaplan-Meier survival curve was created to plot the bleb survival. GraphPad Prism version 9.3.1 (GraphPad Software inc. La Jolla, US).

4.3 Results

4.3.1 Bleb morphology

A detailed overview of the bleb morphology is provided in Figure 4-3 After surgery, blebs were well visible with increased signs of vascularization and redness that subsided around POD 7. All blebs appeared flat at POD 15. In some animals, at POD 40, the curvature of the microshunt could be seen through the conjunctiva due to contraction of the tissue (see Figure 4-3A). Bleb analysis (see Figure 4-3B showed that all blebs failed within approximately 2 weeks postoperative, on average blebs failed within 10.2 ± 2.99 days. No severe adverse events were noted. In several cases, corneal edema was visible with the OCT after surgery, which reduced to normal within 2-3 days (data not shown).

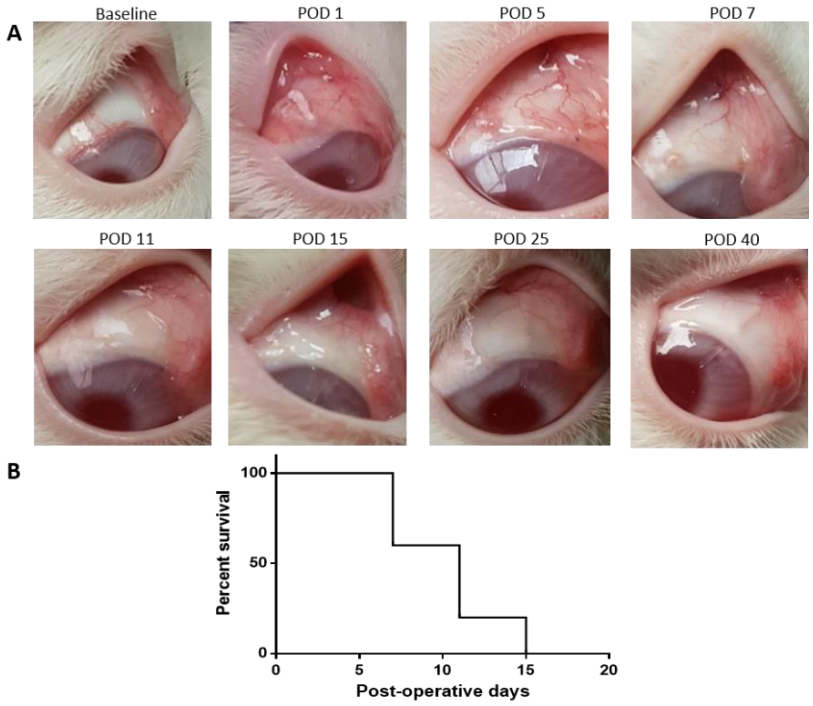

Figure 4-3: Overview of bleb morphology after microshunt implantation. (A) Baseline images showed a healthy eye without any signs of inflammation. After implantation, vascularization increased and a filtering bleb was visible. At POD 7 the bleb began to decline in height becoming non-distinguishable at POD 15. At POD 25 the microshunt became visible through the conjunctiva, indicating that the tissue was being pulled back towards the sclera. At POD 40, signs of inflammation were no longer visible. (B) Bleb survival (n=5), within 15 days postoperative, all blebs appeared flat.

4.3.2 Intraocular pressure

After surgery the IOP decreased, indicating a successful implantation and working filtering bleb. Although no significant differences were found between groups, a trend was observed showing that the IOP initially decreased at POD 1 and gradually increased again until POD 11 (see figure 4-4A). At POD 11 the IOP of both the operated and healthy control eyes are largely similar. Interestingly the IOP remained below baseline throughout the entire experiment (figure 4-4B).

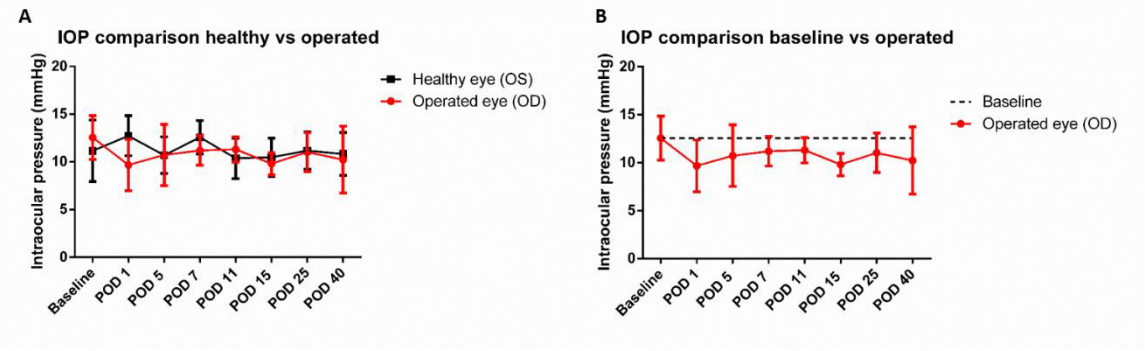

Figure 4-4: Intraocular pressure (IOP) measurements (n=5). IOP measurements were performed on baseline, postoperative day (POD) 1, 5, 7, 11, 15, 25, and 40. (A) Compared to the healthy eye, The IOP reduced after surgery. A lower IOP was observed until POD 11. Afterwards, no large differences between the healthy eye and operated eye were found. (B) The IOP remained below baseline (dotted line). No significant differences were found.

4.3.3 Histology

To assess the fibrotic response after implantation of the microshunt, several staining's were performed. The H&E (Figure 4-5) stain revealed a high infiltration of PMNs at POD 1 (see Figure 4-6A). The total amount of PMNs decreased at POD 5 and more macrophages were present as compared to PMNs at this time point (Figure 4-6B). By POD 40, the infiltration of inflammatory cells was drastically decreased. Nevertheless, a low amount of PMNs and macrophages were still present at POD 40, whereas more macrophages were present compared to PMNs (Figure 4-6C). Increased neovascularization and vessel swelling was noted on POD 5 (Figure 4-5C). Interestingly, a thickening of the conjunctival wall was evident at POD 1 and 5 (Figure 4-5D), increasing to a cellular thickness of approximately 3-4 cell layers compared to healthy controls which had a cellular thickness of 1. A capsule surrounding the shunt was visible at POD 40. Some foreign body giant cells (FBGCs) were noted sporadically around the shunt at POD 40 (Figure 4-6E). Nonetheless, an open space between the conjunctival wall and the collagen deposition was still visible at POD 40.

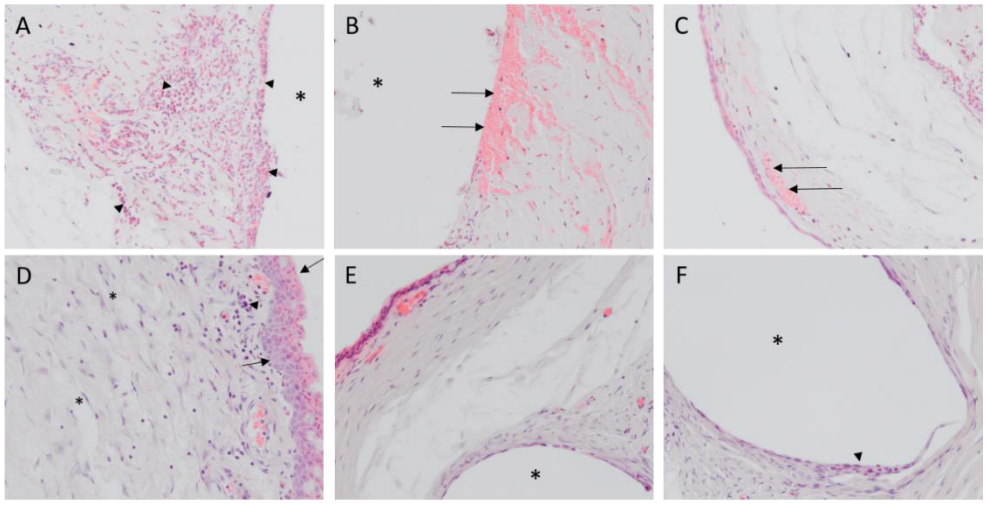

Figure 4-5: Hematoxylin & eosin (H&E) stain at postoperative day (POD) 1, 5 and 40. (A) At POD 1 a high number of polymorphonuclear leucocytes (PMNs) (see arrowhead) have infiltrated the bleb area. (B) Red blood cells around the implantation site were clearly visible (arrows). (C) Some vessel swelling was visible around the conjunctiva (arrows). (D) POD 5 revealed significant granulation tissue in the bleb with many fibroblasts (asterisk for examples) and macrophages (arrowhead for example) present. Additionally, an increased thickness of the conjunctiva was noted at this time point (arrows). (E) At POD 40 less inflammatory cells resided in the bleb. However, a low number of macrophages and PMNs were sporadically observed. The bleb wall has been contracted and granulation tissue has been replaced. (F) Although minimal, some foreign body giant cells are visible around the SIBS microshunt (arrowheads). * = Position SIBS microshunt. All images were taken at 200x magnification.

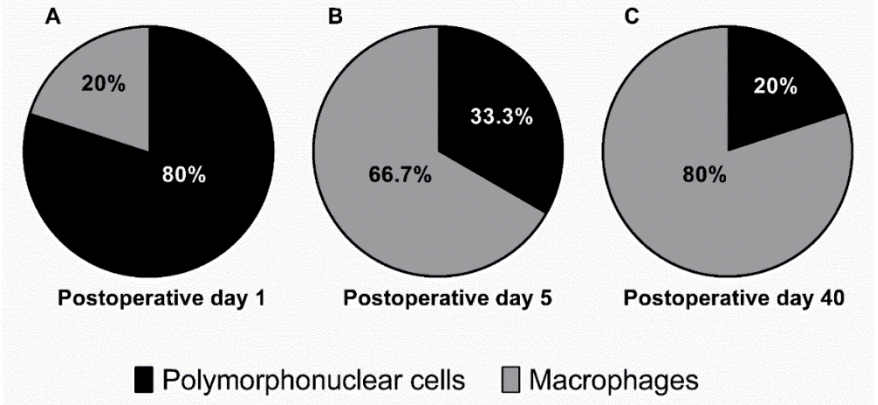

Figure 4-6: Grading of leukocytes present per postoperative day (POD) in percentages. (A) On POD 1 an increased amount of polymorphonuclear leucocytes (PMNs) was present (80%), indicating acute inflammation. (B) A shift in PMNs (33.3%) and macrophages (66.7%) were observed at POD 5. (C) At POD 40 a relatively high number of macrophages were still present in the bleb (80%) indicating a chronic inflammatory state.

No myofibroblasts were present at POD 1 (Figure 4-7A and 4-7B). At POD 5 a limited amount of staining was evident at the conjunctiva (Figure 4-8C and 4-8D). The α-SMA stain revealed a large amount of myofibroblasts present around the conjunctival wall at POD 40 (Figure 4-7E). Although myofibroblasts were also visible throughout the filtering bleb and around the shunt (Figure 4-7F), they were mainly concentrated at the bleb wall.

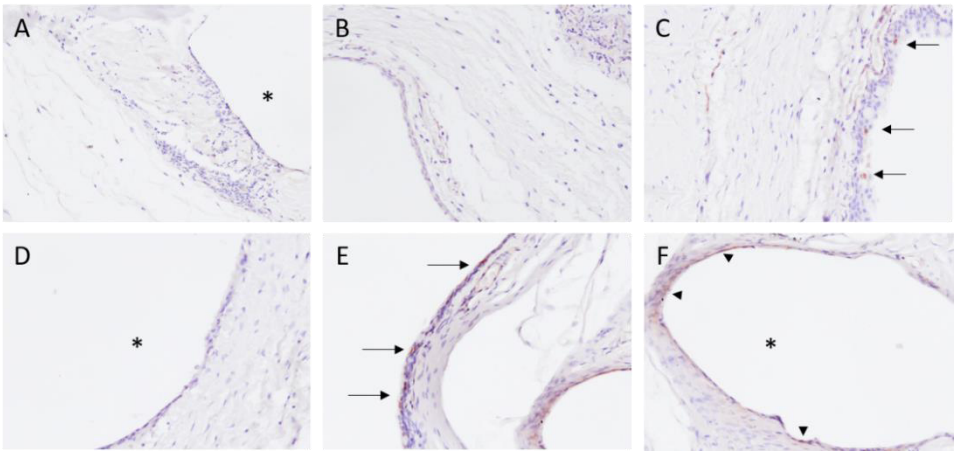

Figure 4-7: Representative images of the alpha-smooth muscle actin (alpha-SMA). (A and B) No alpha-SMA was present at postoperative day (POD) 1 (C) a limited amount of staining was visible at POD 5 in the conjunctiva (see arrows). (D) No Alpha-SMA was present around the SIBS microshunt (E) Alpha-SMA was mainly stained in the conjunctival wall at POD 40 indicating a strong presence of activated myofibroblasts at this time point (arrows). (F) Some staining was evident around the SIBS microshunt at POD 40 (red arrowheads). * = Position SIBS microshunt. All images were taken at 200x magnification.

The BrdU staining showed some proliferating cells in the conjunctiva at POD 1 (Figure 4-8A). At POD 5 a high amount of proliferation was seen at the conjunctiva (see Figure 4-8B). Additionally, a high amount of neovascularization, as was previously noted with the H&E, was seen (data not shown). Furthermore, a limited amount of proliferation was seen around the microshunt (figure 4-8C). At POD 40 a low amount of proliferation was noted in the conjunctiva. However, around the microshunt an increased proliferation was seen compared to POD 5 (Figure 4-8D).

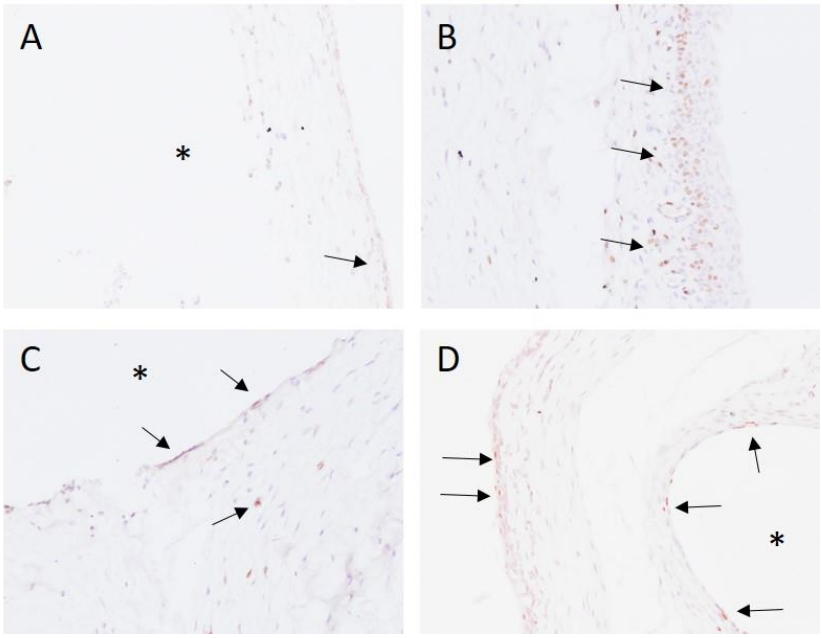

Figure 4-8: Bromodeoxyuridine (BrdU) staining. (A) At postoperative day (POD) 1, a limited amount of proliferation was noted in the conjunctiva (see arrow), no proliferation was seen around the implant site. (B) An increased proliferation was visible around the conjunctiva. Additionally, the conjunctival layer is increased at POD 5. (C) A limited amount of proliferation was visible around the implant site at POD 5. (D) POD 40 revealed a relatively low proliferation in the conjunctiva. However, around the implant site more proliferating cells were visible. * = Position SIBS microshunt. Images were taken with a 200X magnification.

4.4 Discussion

Despite current advances in the development of surgical techniques, new devices, materials, and anti-fibrotic therapies [11, 17-25], fibrosis is still a critical determinant for success after glaucoma surgery [8]. To obtain more knowledge regarding the fibrotic response, normotensive New-Zeeland White rabbits were implanted were implanted with a PRESERFLO MicroShunt. Previous research, where rabbits were implanted with SIBS microshunts, showed that bleb survival was extended up to 1 year, with limited signs of myofibroblasts and fibrosis [11]. Although we did not find results as favorable regarding bleb survival, we did see a relatively low response of myofibroblasts, comparable to the previous study of Acosta *et al*. However, we did find FBGCs, macrophages and PMNs surrounding the microshunt. With regard to bleb survival, similar results were found when compared to other studies, with bleb failure occurring around 2 weeks without the additional use of MMC or other anti-fibrotic agents [26-28]. IOP results showed a similar trend as bleb survival, although no significant differences were found when compared to the healthy control eye. IOP

decreased at POD 1 and gradually started to increase again until POD 11. No large differences were observed between the control and operated eye after POD 11. Interestingly, the average IOP remained lower than the average IOP at baseline, suggesting that a residual amount of AqH might still flow into the bleb. Unfortunately, IOP is known to be an unclear outcome parameter with regard to GFS in animals. IOP deviations are often small within this type of animal model, as normotensive animals without glaucoma are used [29, 30].

Histology showed an increased amount of red blood cells around the surgical site, PMNs were visible in high numbers in the bleb at POD 1. In general, PMNs are attracted due to damage associated molecular patterns, leakage of plasma proteins, and chemokines released from thrombocytes or red blood cells [16, 31]. At POD 5, increased neovascularization, macrophage presence, and proliferation was noted. Although fibroblasts were clearly present, no high amounts of myofibroblasts were observed at POD 5. It was also observed that the bleb was further contracted at POD 40 as compared to the previous time points. At POD 40 a small capsule was visible around the SIBS shunt, with low amounts of myofibroblasts, fibroblasts, macrophages, and foreign body giant cells surrounding the implant. Additionally, in the bleb area myofibroblasts were seen. Although in our histology specimens an open space was still visible inside the bleb, this is most likely an artefact caused by the manipulation of tissue during enucleation and processing of the eye.

As mentioned, inflammatory cells were present in high amounts at POD 1 (PMNs) and POD 5 (macrophages). Interestingly, in fetal wounds, wounds tend to heal without the formation of fibrotic tissue, which is thought to be attributable to the limited inflammatory response and reduced neutrophil and macrophage infiltration [32]. Therefore, ameliorating or reducing PMNs infiltration might offer a mechanism to reduce the fibrotic response, especially for glaucoma patients who have a predisposition for an increased inflammatory response due to the influx of AqH, which contains growth factors such as transforming growth factor- β (TGF-β) and vascular endothelial growth factor [33-35]. Recently, it was shown that inhibition of monocyte chemoattractant protein-1 (MCP-1) resulted in increased bleb survival and a downregulation of pro fibrotic genes. MCP-1 is known as one of the primary proteins secreted by monocytes/macrophages to attract additional macrophages [36]. Therefore, inhibition of pro-inflammatory cytokines or chemoattractants could offer a potential target for the downregulation of the wound healing response in the bleb. These experiments suggest that a chronic state of inflammation is reached at POD 40, with still some PMNs and macrophages present in the healed bleb area which can predispose the tissue to an increased fibrotic response in the event a second surgery (due to failure of the first surgery) is performed. Future research could try to elucidate which type of macrophages are present within the bleb at this time. the presence of anti-inflammatory or alternatively activated (M2) macrophages

is needed to resolve inflammation and start the tissue remodeling [37]. However, a persisted presence of these type of macrophages can predisposes tissue to the formation of fibrosis [38]. By altering or skewing the polarization state of macrophages to a more favorable state, *e.g.* reducing the number of anti-inflammatory macrophages, the fibrotic response could be reduced.

An increased amount of proliferation was noted at POD 5 in the conjunctival wall and inside the bleb, most likely due to neovascularization and fibroblast proliferation. Additionally, thickening of the conjunctival wall was noted. Epithelial cells are in a constant state of renewal, where new cells are being formed and older cells undergo apoptosis. However, potentially due to the increase of growth factors, such as TGF-β, it is likely that an increased proliferation is seen in these epithelial cells, increasing the thickness of the conjunctival wall. The increased presence of epithelial cells could also induce a different process called epithelial mesenchymal transition (EMT). During EMT, epithelial cells, under the influence of TGF-β, transdifferentiate into mesenchymal stem cells and afterwards into fibroblasts [39]. Additionally, a study by Potenta *et. al* showed that endothelial cells in the microvasculature can undergo a similar process known as endothelial mesenchymal transition (EndMT) [40]. Future research is required to confirm if conjunctival epithelial cells can also undergo EMT. If so, reducing EMT and EndMT might offer a potential therapeutic approach to alter the fibrotic response after glaucoma surgery. Further, if reducing EMT and EndMT is effective, perhaps a new line of anti-fibrotic agents could be developed such as bone morphogenic protein-7 which has been shown to reverse TGF-β induced EMT [41]. Currently, MMC is used during bleb-forming glaucoma surgery to reduce the fibrotic response [9]. It is thought that MMC reduces the resident fibroblast response and reduces the number of fibroblasts that can transdifferentiate into myofibroblasts. As we observed in our study, myofibroblasts were predominantly present at POD 40 during the tissue remodeling phase. Myofibroblasts create the contractile forces required to contract a wound [42]. Thus, it can be hypothesized that MMC, while still hampering the fibrotic response by inhibiting the proliferation and transdifferentiation of resident fibroblasts, could also have an effect (either direct or indirect) on infiltrating cells such as PMNs, and macrophages, since these are present early in the wound healing response.

Novel methods to inhibit the formation of fibrosis would need to be safer than and as effective as MMC. Several approaches could be of interest for future research. Firstly, anti-fibrotic therapies could be improved. Current novel anti-fibrotic therapies, although often safer *in vivo,* do not outperform MMC [30]. Novel targets (as earlier described in this section) could be studied to find alternatives. Secondly, augmenting material properties could be beneficial. Implants innately induce a foreign body response, inducing encapsulation of the device/implant within the tissue. Our study shows that, while limited, a SIBS microshunt also triggers a foreign body response.

Several ways exist to change the material properties *e.g.* chemical modifications [43], coatings [44], plasma treatment [45], and alterations to surface topographical features [46-48]. Surface topographies have received a lot of attention over the years in the medical field due to their ability to skew the reaction that cells have towards a material. For example, recent *in vitro* findings show that surface topographies can skew macrophage response into a pro- or anti-inflammatory reaction [49]. Moreover, surface topographies on breast implants have shown to be able to skew the encapsulation process *in vivo* [50]. One study with large glaucoma implants such as the Ahmed glaucoma valves showed that a rough surface can increase the encapsulation of an implant, potentially caused by an increased adhesion of fibroblasts on to a rough surface or due to micro-movements of Tenon's capsule and conjunctiva on the surface of the implant [46]. It remains unclear which type of surface topographies can offer a more reliable outcome for glaucoma implants. Lastly, the addition of a drug delivery system (DDS) for sustained medication could reduce the fibrotic response, since low dosages of a drug can be released over an extended period of time. However, the type of drug, exact dosage, time of release, and material for the DDS are currently unclear and more research is needed.

4.5 Conclusion

We observed that after implantation of a SIBS microshunt in rabbits, a wide variety of cells are present during wound healing, such as monocytes/macrophages, PMNs, FBGCs, and epithelial cells. These cells offer new topics for future research to find novel methods to reduce the fibrotic response *in vivo*, for example by developing novel antifibrotic drugs, novel methods for sustained drug delivery, or augmenting material properties.

References

1. Bar-David, L. and E.Z. Blumenthal, *Evolution of Glaucoma Surgery in the Last 25 Years*. Rambam Maimonides Med J, 2018. **9**(3).
2. Mauro, A., et al., *A novel patient-oriented numerical procedure for glaucoma drainage devices*. Int J Numer Method Biomed Eng, 2018. **34**(12): p. e3141.
3. Tham, Y.C., et al., *Global prevalence of glaucoma and projections of glaucoma burden through 2040: a systematic review and meta-analysis.* Ophthalmology, 2014. **121**(11): p. 2081-90.
4. Lee, R.M.H., et al., *Translating Minimally Invasive Glaucoma Surgery Devices*. Clin Transl Sci, 2020. **13**(1): p. 14-25.
5. *European Glaucoma Society Terminology and Guidelines for Glaucoma, 4th Edition - Chapter 3: Treatment principles and options Supported by the EGS Foundation: Part 1: Foreword; Introduction; Glossary; Chapter 3 Treatment principles and options.* Br J Ophthalmol, 2017. **101**(6): p. 130-195.
6. Dikopf, M.S., T.S. Vajaranant, and D.P. Edward, *Topical treatment of glaucoma: established and emerging pharmacology.* Expert Opin Pharmacother, 2017. **18**(9): p. 885-898.
7. Schlunck, G., et al., *Conjunctival fibrosis following filtering glaucoma surgery.* Exp Eye Res, 2016. **142**: p. 76-82.
8. Beckers, H.J., K.C. Kinders, and C.A. Webers, *Five-year results of trabeculectomy with mitomycin C.* Graefes Arch Clin Exp Ophthalmol, 2003. **241**(2): p. 106-10.
9. Wolters, J.E.J., et al., *History, presence, and future of mitomycin C in glaucoma filtration surgery.* Curr Opin Ophthalmol, 2021. **32**(2): p. 148-159.
10. L, J.L., L. Hall, and J. Liu, *Improving Glaucoma Surgical Outcomes with Adjunct Tools.* J Curr Glaucoma Pract, 2018. **12**(1): p. 19-28.
11. Acosta, A.C., et al., *A newly designed glaucoma drainage implant made of poly(styrene-b-isobutylene-b-styrene): biocompatibility and function in normal rabbit eyes.* Arch Ophthalmol, 2006. **124**(12): p. 1742-9.
12. Ibarz Barberá, M., et al., *Efficacy and Safety of the Preserflo Microshunt ® with Mytomicin C for the Treatment of Open Angle Glaucoma.* J Glaucoma, 2022.
13. Beckers, H.J.M., et al., *Safety and Effectiveness of the PRESERFLO® MicroShunt in Primary Open-Angle Glaucoma: Results from a 2-Year Multicenter Study.* Ophthalmology Glaucoma, 2022. **5**(2): p. 195-209.
14. Batlle, J.F., A. Corona, and R. Albuquerque, *Long-term Results of the PRESERFLO MicroShunt in Patients With Primary Open-angle Glaucoma From a Single-center Nonrandomized Study.* J Glaucoma, 2021. **30**(3): p. 281-286.
15. Scheres, L.M.J., et al., *XEN(®) Gel Stent compared to PRESERFLO™ MicroShunt implantation for primary open-angle glaucoma: two-year results.* Acta Ophthalmol, 2021. **99**(3): p. e433-e440.
16. Qian, L.W., et al., *Exacerbated and prolonged inflammation impairs wound healing and increases scarring.* Wound Repair Regen, 2016. **24**(1): p. 26-34.
17. Pereira, I.C.F., et al., *Conventional glaucoma implants and the new MIGS devices: a comprehensive review of current options and future directions.* Eye, 2021.
18. Rodgers, C.D., et al., *The impact of conjunctival flap method and drainage cannula diameter on bleb survival in the rabbit model.* PLoS One, 2018. **13**(5): p. e0196968.
19. Duan, X., Z. He, and X. Zhang, *A comparative study of the effects of ab externo superpulse carbon dioxide laser-assisted trabeculectomy with conventional trabeculectomy in rabbits.* Photomed Laser Surg, 2010. **28**(1): p. 109-13.
20. Gong, R., et al., *A Comparison of Subconjunctival Wound Healing between Different Methods of Dissecting Subconjunctival Tissues.* Ophthalmic Res, 2021. **64**(1): p. 99-107.
21. Sherwood, M.B., *A sequential, multiple-treatment, targeted approach to reduce wound healing and failure of glaucoma filtration surgery in a rabbit model (an American Ophthalmological Society thesis).* Trans Am Ophthalmol Soc, 2006. **104**: p. 478-92.
22. Hilgert, C.R., et al., *Antiscarring effect of intraoperative bevacizumab in experimental glaucoma filtration surgery.* Arq Bras Oftalmol, 2018. **81**(4): p. 316-322.
23. Zuo, L., J. Zhang, and X. Xu, *Combined Application of Bevacizumab and Mitomycin C or Bevacizumab and 5-Fluorouracil in Experimental Glaucoma Filtration Surgery.* J Ophthalmol, 2018. **2018**: p. 8965709.
24. Villamarin, A., et al., *In vivo testing of a novel adjustable glaucoma drainage device*. Invest Ophthalmol Vis Sci, 2014. **55**(11): p. 7520-4.

25. Desai, A.R., et al., *Co-delivery of timolol and hyaluronic acid from semi-circular ring-implanted contact lenses for the treatment of glaucoma: in vitro and in vivo evaluation.* Biomater Sci, 2018. **6**(6): p. 1580-1591.
26. Sherwood, M.B., et al., *A new model of glaucoma filtering surgery in the rat.* J Glaucoma, 2004. **13**(5): p. 407-12.
27. SooHoo, J.R., et al., *Bleb morphology and histology in a rabbit model of glaucoma filtration surgery using Ozurdex(R) or mitomycin-C.* Mol Vis, 2012. **18**: p. 714-9.
28. Doyle, J.W., et al., *Intraoperative 5-fluorouracil for filtration surgery in the rabbit.* Invest Ophthalmol Vis Sci, 1993. **34**(12): p. 3313-9.
29. Bertens, C.J.F., et al., *Repeatability, reproducibility, and agreement of three tonometers for measuring intraocular pressure in rabbits.* Sci Rep, 2021. **11**(1): p. 19217.
30. van Mechelen, R.J.S., et al., *Animal models and drug candidates for use in glaucoma filtration surgery: A systematic review.* Exp Eye Res, 2022. **217**: p. 108972.
31. Pober, J.S. and W.C. Sessa, *Inflammation and the blood microvascular system.* Cold Spring Harb Perspect Biol, 2014. **7**(1): p. a016345.
32. Satish, L. and S. Kathju, *Cellular and Molecular Characteristics of Scarless versus Fibrotic Wound Healing.* Dermatol Res Pract, 2010. **2010**: p. 790234.
33. Takai, Y., M. Tanito, and A. Ohira, *Multiplex Cytokine Analysis of Aqueous Humor in Eyes with Primary Open-Angle Glaucoma, Exfoliation Glaucoma, and Cataract.* Investigative Ophthalmology & Visual Science, 2012. **53**(1): p. 241-247.
34. Park, H.-Y.L., J.H. Kim, and C.K. Park, *Lysyl Oxidase-Like 2 Level and Glaucoma Surgical Outcomes.* Investigative Ophthalmology & Visual Science, 2014. **55**(5): p. 3337-3343.
35. Li, Z., et al., *Inhibition of Vascular Endothelial Growth Factor Reduces Scar Formation after Glaucoma Filtration Surgery.* Investigative Ophthalmology & Visual Science, 2009. **50**(11): p. 5217-5225.
36. Chong, R.S., et al., *Inhibition of Monocyte Chemoattractant Protein 1 Prevents Conjunctival Fibrosis in an Experimental Model of Glaucoma Filtration Surgery.* Invest Ophthalmol Vis Sci, 2017. **58**(9): p. 3432-3439.
37. Lis-López, L., et al., *Is the Macrophage Phenotype Determinant for Fibrosis Development?* Biomedicines, 2021. **9**(12).
38. Vernon, M.A., K.J. Mylonas, and J. Hughes, *Macrophages and renal fibrosis.* Semin Nephrol, 2010. **30**(3): p. 302-17.
39. Kalluri, R. and R.A. Weinberg, *The basics of epithelial-mesenchymal transition.* J Clin Invest, 2009. **119**(6): p. 1420-8.
40. Potenta, S., E. Zeisberg, and R. Kalluri, *The role of endothelial-to-mesenchymal transition in cancer progression.* Br J Cancer, 2008. **99**(9): p. 1375-9.
41. Song, Y., et al., *Overexpression of BMP-7 reverses TGF-β1-induced epithelial-mesenchymal transition by attenuating the Wnt3/β-catenin and TGF-β1/Smad2/3 signaling pathways in HK-2 cells.* Mol Med Rep, 2020. **21**(2): p. 833-841.
42. Yamanaka, O., et al., *Pathobiology of wound healing after glaucoma filtration surgery.* BMC Ophthalmol, 2015. **15 Suppl 1**: p. 157.
43. Castel, N., et al., *Polyurethane-coated breast implants revisited: a 30-year follow-up.* Arch Plast Surg, 2015. **42**(2): p. 186-93.
44. Xu, H., et al., *Hydrogel-coated ventricular catheters for high-risk patients receiving ventricular peritoneum shunt.* Medicine (Baltimore), 2016. **95**(29): p. e4252.
45. Barnea, Y., et al., *Plasma Activation of a Breast Implant Shell in Conjunction With Antibacterial Irrigants Enhances Antibacterial Activity.* Aesthet Surg J, 2018. **38**(11): p. 1188-1196.
46. Choritz, L., et al., *Surface topographies of glaucoma drainage devices and their influence on human tenon fibroblast adhesion.* Invest Ophthalmol Vis Sci, 2010. **51**(8): p. 4047-53.
47. Hulshof, F.F.B., et al., *Mining for osteogenic surface topographies: In silico design to in vivo osseo-integration.* Biomaterials, 2017. **137**: p. 49-60.
48. Doloff, J.C., et al., *The surface topography of silicone breast implants mediates the foreign body response in mice, rabbits and humans.* Nature Biomedical Engineering, 2021. **5**(10): p. 1115-1130.
49. Vassey, M.J., et al., *Immune Modulation by Design: Using Topography to Control Human Monocyte Attachment and Macrophage Differentiation.* Adv Sci (Weinh), 2020. **7**(11): p. 1903392.
50. Doloff, J.C., et al., *The surface topography of silicone breast implants mediates the foreign body response in mice, rabbits and humans.* Nat Biomed Eng, 2021. **5**(10): p. 1115-1130.

Chapter 5

The influence of design modifications and microstructured surface Topographies on bleb survival after glaucoma tube shunt implantation

van Mechelen, R. J. S., Sudarsanam, P., Bertens, C. J. F.,
Tas, M. O., Gijbels, M. J. J., Pinchuk, L., de Boer, J., & Beckers, H. J. M. (2023). The Influence of Design Modifications and Microstructured Surface Topographies on Bleb Survival after Glaucoma Tube Shunt Implantation. Advanced biology.

Abstract

Lowering intraocular pressure (IOP) by placement of a glaucoma shunt is an effective treatment for glaucoma. However, fibrosis of the outflow site can hamper surgical outcome. In this study, the antifibrotic effect of adding an endplate (with or without microstructured surface topographies) to a microshunt made of poly(styrene-block-isobutylene-block-styrene) (SIBS) was investigated. New Zealand white rabbits were implanted with a control implant (without endplate) and modified implants. Afterwards, bleb morphology and IOP was recorded for 30 days. After killing of the animals, eyes were collected for histology.

Addition of an endplate extended bleb survival, Topo-990 had the longest recorded bleb-survival time. Histology revealed that the addition of an endplate increased the presence of myofibroblasts, macrophages, polymorphonuclear cells and foreign body giant cells compared to the control. However, an increased capsule thickness and inflammatory response was observed in the groups with surface topographies.

The addition of an endplate resulted in prolonged bleb survival, demonstrating that engineering of the shape of glaucoma implants could prolong bleb functionality. Future research should further elaborate the effect of surface topographies on long-term bleb survival, since an increased presence of pro-fibrotic cells and increased capsule thickness was observed compared to the control.

5.1 Introduction

Glaucoma is a degenerative optic neuropathy characterized by progressive visual field loss [1]. The most important risk factor is elevated intraocular pressure (IOP), which needs to be lowered to a target IOP that is low enough to prevent further vision loss. Surgical treatment is mostly undertaken after medication or laser therapy have failed to reach the desired IOP.

Implantation of a glaucoma drainage device (GDD) is a highly effective surgical treatment. A GDD drains aqueous humor (AqH) from the anterior chamber of the eye into the subconjunctival space, forming a filtering bleb (see figure 5-1). Although highly effective, an overreaching wound healing response leads to fibrosis at the outflow site. As a result, scarring of the filtering bleb occurs, limiting AqH outflow and subsequently elevation of IOP [2-5]. Throughout the years, several types of GDDs have been developed with different designs and materials [6]. Currently, the most commonly used GDDs consist of a silicone tube and an endplate made from silicone or polypropylene (*e.g.* Molteno, Baerveldt, Ahmed) [6]. During the last decade, new, less invasive bleb-forming implants from new materials have been developed, which may be safer than the conventional ones. A promising material is poly(styrene-block-isobutylene-block-styrene) ("SIBS"). SIBS is a biocompatible biostable thermoplastic elastomer [7, 8]. Previous research with SIBS microshunts showed that SIBS induced less fibrosis when compared to silicone shunts in rabbit eyes. After 3 months, less collagen IV and α-smooth muscle actin (α-SMA) was observed around a SIBS tube as compared to a silicone tube [7]. A SIBS microshunt (the PRESERFLO® MicroShunt) has been successfully introduced in the clinic. However, after placement of this microshunt, subconjunctival fibrosis is still observed which may hamper the desired reduction of IOP [2, 4, 5]. Theoretically, the bleb survival can be improved by addition of an endplate to the SIBS tube [9, 10], or by reduction of the fibrotic response by *e.g.* plasma treatment [11], coatings [12, 13], or the addition of surface topographical features [14-20]. The benefit of micro- or nano scaled surface topographies has been widely studied within the medical field. Specific surface topographies can exert influence on the cell migration, adhesion, alignment, proliferation, encapsulation process, and cellular morphology through a process called mechanotransduction [14-20]. Moreover, micron scaled surface topographies have been recently shown to modulate the activation of macrophages and fibroblasts *in vitro*, potentially capable of limiting the encapsulation process *in vivo* [21]. In the case of glaucoma implants, it remains unknown which type of microstructured surface topographies can improve the success rate of glaucoma surgery. In the present study, we engineered a SIBS microshunt with an endplate, 5 mm in diameter. The endplate had either a smooth surface or a surface with microstructured surface topographies to direct cell adherence, proliferation,

differentiation, and gene expression. Surface topographies were selected based on previous experiments and *in vitro* screening results. Three topographies were selected for this study. Firstly, topography Topo-1008 showed the lowest proliferative response of fibroblasts *in vitro*, which correlated with previous work performed by Vasilevich *et al.* on mesenchymal stem cells [22]. Secondly, Topo-990 was chosen based on a previous study, performed by a collaborating research group, where Topo-990 showed a high cell attachment with increased M2 macrophage polarization [14]. Lastly, Topo-1594 was selected based on an *in vivo* study in mice (unpublished data, currently under review), this study showed that topo-1594 induced a low capsule formation and less foreign body giant cell formation. We hypothesized that by the addition of microstructured surface topographies that have an anti-fibrotic effect we can skew the fibrotic response into a more favourable state resulting in prolonged bleb survival and optimal bleb formation. *In vivo* bleb formation, and bleb survival were studied through *in vivo* measurements. Histology was used to assess the cellular effect of the endplate and cell modulating surface topographies.

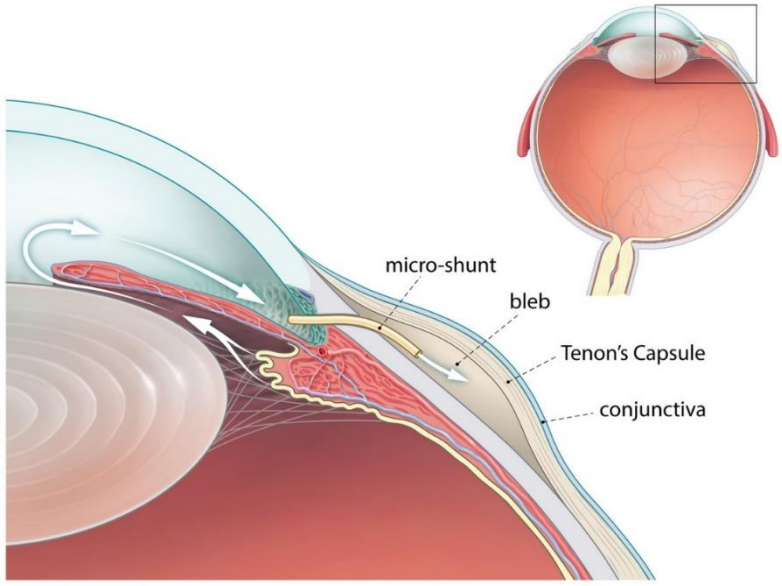

Figure 5-1: Schematic overview of aqueous humor flow after implantation of a microshunt. Fluid flows from the ciliary body via the posterior chamber into the anterior chamber through the tube into a bleb, the bleb consists out of the so-called Tenon's capsule and conjunctiva.

5.2 Materials and methods

5.2.1 Animals

All animal procedures were in accordance with the European Directive for animal experiments (2010/63/EU) (Approved Dutch license number: AVD1070020197464. The Central Authority for Scientific Procedures on Animals (CCD, Den Haag, NL), and the local ethical committee approved all animal procedures. Additionally, they complied with the Association for Research in Vision and Ophthalmology (ARVO) statement for the use of animals in ophthalmic and vision research and the Animal Research: Reporting of *In Vivo* Experiments (ARRIVE) 2.0 guidelines [23].
Fifteen normotensive New Zealand white rabbits (Charles River, FR) were used (n=3 per group), with an approximate age of 12 weeks, weighing 2.5 to 3 kg, both male and female. The rabbits were maintained under controlled conditions of temperature and humidity on a 12h:12h light-dark cycle, with *ad libitum* access to water and food. Before the start of the experiment, the animals were acclimatized for two weeks. Prior to surgery, researchers were blinded. A randomized complete block design was used to allocate animals to different groups. After data collection and analysis, researchers were unblinded. Rabbits were euthanized at postoperative day (POD) 30 with an overdose of pentobarbital sodium, 200 mg/kg (Euthasol 20, Produlab Pharma B.V., NL) intravenously administrated.

5.2.2 Production of modified microshunts

Three specific surface topographies were selected, Topo-990 [14], 1008 *(*unpublished *in vitro* research) and, 1594. SIBS sheets with a thickness of 250 µm either with or without topographies were produced by hot embossing these SIBS sheets between custom made molds, all topographies, irrespective of design, had a height of 10 µm. A biopsy punch with a diameter of 5 mm was used to punch out circular discs from micropatterned SIBS sheets. Afterwards, a surgical blade was used to cut discs into semi-circles. In a fumehood one mL of toluene was drop-casted on a hydrophilic surface, then the inner cross-section of the semi-circles were dipped in toluene for 1 second. Quickly after, the semi-circles were solvent-welded against the distal end of the microshunt, forming an endplate. The position was held for approximately 30 seconds to allow toluene to evaporate and strengthen adhesion. The modified microshunts were placed into an oven at 65 °C for 60 minutes to evaporate any remaining toluene. Lastly, channel flow was tested by injecting milli-Q (pure H_2O) into the anterior part of the shunt, to ensure no channels were collapsed due to the toluene solvent binding. See figure 5-2 for the design and different topographies included in this study.

5.2.3 Scanning electron microscopy

Implants were assessed by scanning electron microscopy (SEM). Samples were first placed on conductive carbon paper and then coated with 5 nm of gold using the JEOL JFC-1300 Auto Fine coater (Peabody, MA, USA). Images were taken with a JEOL-6010LV SEM (Peabody, MA, USA) under vacuum.

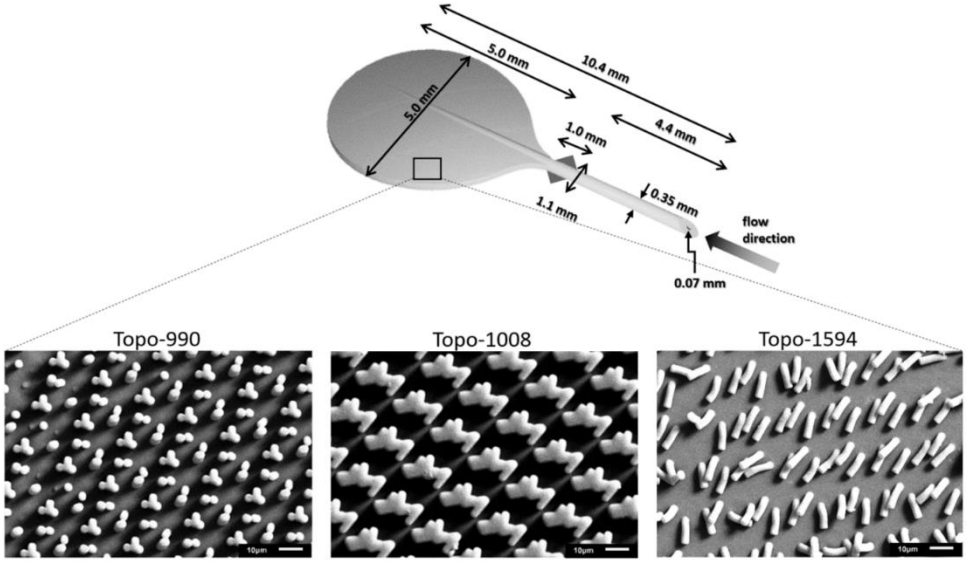

Figure 5-2: Overview of the design of the modified microshunts: an endplate with either a smooth surface or specific topography (Topo-990, 1008, or 1594) was attached to the posterior end of the microshunt. Scale bar is 10 µm.

5.2.4 Surgical procedure

In total, 15 animals were randomly assigned to be implanted with a control SIBS microshunt (InnFocus Santen, Miami Florida, USA) or a microshunt with endplate (either smooth or with a topography). The surgical procedure was comparable to previous experiments [24]. In short, the right eye was implanted, at all times and all surgeries were performed by a single surgeon (RM). Local analgesia was provided in the form of 0.4% oxybuprocaine hydrochloride drops (MINIMS, Bausch & Lomb Pharma, Brussels, BE). A fornix-based conjunctival flap was dissected with Westcott tenotomy scissors, after which a 1 mm wide and 1 mm deep scleral pocket was formed with a knife, 3 mm posterior to the limbus. Afterwards, the shunt was placed posteriorly into the conjunctival pouch. Through the scleral pocket, a needle tract was made with a 25G needle into the anterior chamber. The microshunt was then inserted through the pocket and needle tract. The fins were wedged firmly into the

scleral pocket. Flow was checked by massaging the eye until a droplet of aqueous formed at the distal end of the microshunt. Lastly, the conjunctiva and Tenon's capsule were sutured closed with a Vicryl 9-0 suture (Ethicon LLC, Puerto Rico, USA). Animals were treated with 1% chloramphenicol ointment twice daily, for 5 days and received a subcutaneous injection of buprenorphine (0.05 mg/kg Bupaq Multidose, Richter Pharma AG, Wels, AT) up until POD 1 twice daily, if needed analgesia was extended.

2.5 *In vivo* measurements

Rabbits were sedated using 0.40 mg/kg medetomidine IM. Slit lamp (SL) examinations (Haag-Streit BI 900, Haag-Streit, Köniz, CH), and bleb images were taken using a photo camera (Canon EOS 4000D, Canon, Tokio, JP). IOP measurements were performed with the iCare® TonoVet (iCare Finland Oy, Vantaa, FI). One week prior to surgery, IOP baseline measurements were obtained for each rabbit. Follow-up examinations were performed on POD 1, 4, 7, 14, 21, and 30. Blebs were graded based on redness, and vascularization. To assess the bleb survival, bleb height, and bleb extent where examined. Additionally, when a bleb appeared flat, the eye was gently massaged, if the bleb remained flat after massage, the bleb was categorized as failed.

5.2.6 Patency test

Fluorescein was injected into the anterior chamber to visualize fluid flow into the bleb. Rabbits were sedated with 5 mg/kg ketamine and 0.20 mg/kg medetomidine IM. After complete sedation the anterior chamber of the eye was entered using a 30G needle, approximately 0.1 ml of fluorescein was injected into the anterior chamber. After 10 seconds, the needle was carefully retracted from the anterior chamber and fluid was allowed to flow out of the eye to resolve increased IOP due to the injection. The slit-lamp was turned on blue dichroic excitation (460 to 493 nm). Lastly, the slit-lamp was aligned with the bleb to visualize patency of the shunt. The patency test was performed at POD 7, 14, 21, and 28.

5.2.7 Light microscopy and staining

Bromodeoxyuridine (BrdU, 30 mg/kg, product no. ab142567, Abcam, Cambridge UK) was injected intravenously twice, one day before sacrifice. Animals were euthanized using 200 mg/kg pentobarbital sodium (Euthasol 20, Produlab Pharma B.V., NL). After euthanasia, the eyes were dissected and fixed in 4% paraformaldehyde (PFA) for 2 days (PFA was refreshed once a day), and after fixation, eyes were dehydrated and embedded in paraffin blocks. Sections were cut with a thickness of 4 µm and were stained with Hematoxylin & Eosin (H&E), mouse-

anti-alpha-smooth muscle actin (α-SMA) (ThermoFisher scientific, US, MA5-11547, 1:500) and sheep-anti-BrdU (Novus biologicals, US, NB500-235, 1:2500). In the case of anti-α-SMA and anti-BrdU, slides were blocked using 3% hydrogen peroxidase and 10% donkey serum (Abcam, UK, ab7475). A secondary antibody (donkey-anti-mouse, Jackson immunoresearch, UK, 715-065-151, 1:2000 and donkey-anti-sheep (LSBio, US, LS-C61150, 1:3000) with a biotin label was used to detect the primary antibody. Lastly, an ABC kit (Vector laboratories, US, PK6100) was used to enhance the biotin label for staining and Novared (Vector laboratories, US, SK-4800) was used to stain the slides. Histological slides were assessed and semi-qualitatively scored by two blinded observers, after which photographs were taken using a confocal scanning microscope (BX-51, Olympus, JP), as performed previously [24]. Bleb height and capsule thickness were quantified using the CellSens Entry software from Olympus (Olympus, JP). The bleb was measured on 3 locations in the bleb per section. Two sections were used per rabbit to quantify the measurement.

5.2.8 Statistical analysis

GraphPad Prism version 6.01 was used (GraphPad Software inc. La Jolla, US) to analyse the data. A one-way ANOVA and two-way ANOVA with Tukey post hoc comparisons were used to compare the results between groups (n=3 per group), data is represented as mean ± standard deviation (SD)

.

5.3 Results

5.3.1 Clinical signs

All animals experienced mild ocular discomfort postoperatively until POD 7, such as squeezing of the eye, conjunctival redness and ocular discharge. In figure 5-3, images of bleb formation and morphology are shown per group. Animals showed comparable findings with regard to inflammation and vascularization on macroscopic level. Vascularization increased after surgery until POD 4 and started to decrease at POD 7. Animals with Topo-1594 showed signs of less bleb vascularization. However, when scored, this did not reach statistical significance

5.3.2 Bleb survival and patency

The mean bleb survival of all groups is plotted in figure 5-4A. Topo-990 (30 ± 0 days) showed the highest bleb survival compared to other groups; control (12 ± 3 days), smooth (22 ± 7 days) and Topo-1008 (22 ± 7 days) and Topo-1594 (19 ± 8 days), due to the experimental set-up a maximum follow up time of 30 days was chosen. Therefore, the total bleb survival time of Topo-990 is underrepresented in the data. A significant difference was observed between the control and the Topo-990 group

(P=0.0487), however, no significant differences were found between the other groups. The patency of the microshunt is plotted in figure 5-4B. Although, no significant differences were found between groups, the control group and Topo-1594 had a lower patency in comparison with other groups. On average, the control and Topo-1594 demonstrated a patency of 21 days. Comparatively, the smooth, Topo-990 and, Topo-1008 demonstrated a patency of 28 days. At POD 30, several animals (2/3, 2/3, 2/3, and 1/3 in the smooth, Topo-990, Topo-1008, and Topo-1594 groups respectively) developed a locally formed bleb around the circumference of the endplate (see figure 5-5A for an example). Despite adhesion of tissue onto the endplate, a fluid filled bleb was still visible. SEM analysis of the implants revealed the presence of rough edges around the endplate of the implant (figure 5-5B). Additionally, macrophages and foreign body giant cells were noted around the rim of the implant after a stain with H&E (figure 5-5C).

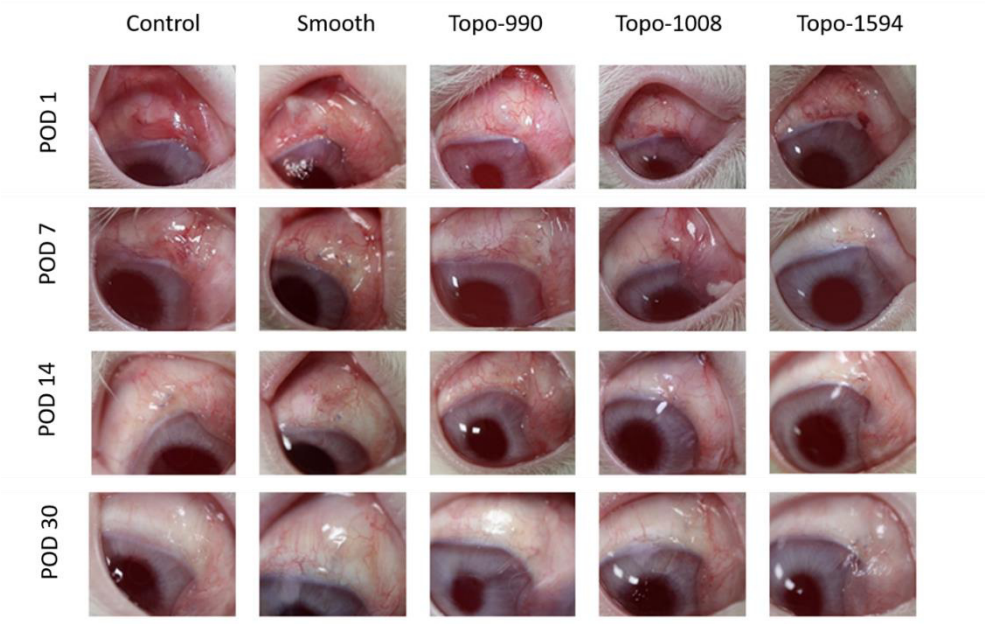

Figure 5-3: Macroscopic evaluation of the bleb formation. Photographic images were created on all follow up time points from POD 1 until POD 30. The control group showed a normal wound healing response, with a flat bleb visible at POD 14. Blebs with a modified implant lasted longer, and were in some cases visible up until POD 30. No severe clinical adverse events were noted. Although, Topo-1594 groups showed less signs of vascularization (inflammation) compared to the other groups no significant difference was found when scored

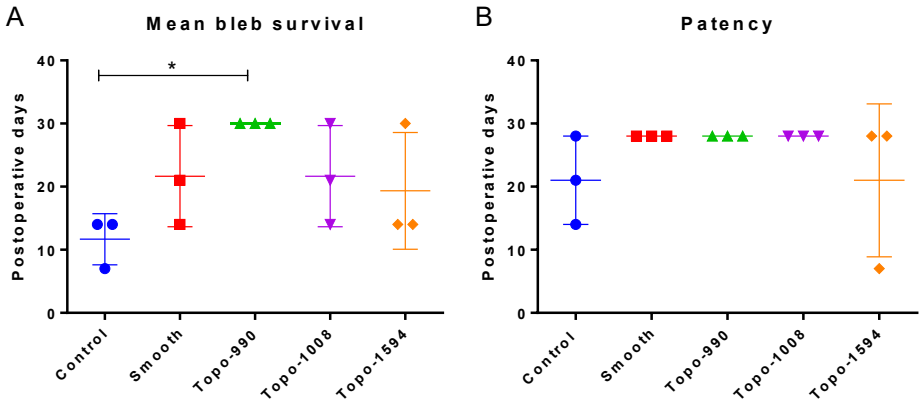

Figure 5-4: Mean bleb survival and patency after implantation of the SIBS microshunt and modified microshunts. (A) The Topo-990 group had the highest bleb survival, a significant difference compared to the control group was found. (B) Although the control and Topo-1594 had the lowest patency, no significant differences were found between groups when compared. * = P value < 0.05. A one-way ANOVA with Tukey post-hoc comparisons was used to find potentially significant differences (n=3 per group)

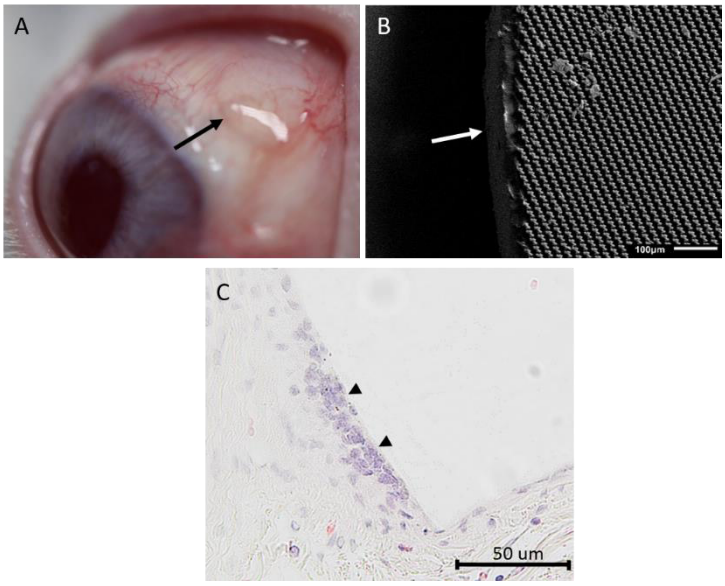

Figure 5-5: Overview of implant adhesion at a macroscopic and microscopic viewpoint. (A) Macroscopically a localized bleb (arrow) developed surrounding the rim of the implant. (B) SEM images of the implants showed that the sides were relatively rough, with some “sharp” edges at the rim of the endplate of the modified microshunts (see arrow). (C) When stained with an H&E stain, large amounts of macrophages and foreign body giant cells were seen at the edges of the endplate (arrowhead).

5.3.3 Intraocular pressure measurements

IOP was decreased in most groups post-surgery, indicating a successful implantation (see figure 5-6). Looking at figure 5-6 at POD 1, the IOP in the operated eye (OD) was reduced from baseline, for the control (∆2.94 mmHg), smooth (∆4.72 mmHg), Topo-1008 (∆1.22 mmHg) and Topo-1594 (∆3.55 mmHg) groups. The Topo-990 group did not show an initial decrease. However, at POD 4, IOP decreased (∆1.72 mmHg) compared to baseline. The IOP of the operated eye (OD) remained lower compared to the control eye (OS) for approximately 21, 14, 14, 4, and 21 days for the control, smooth, Topo-990, Topo-1008, and Topo-1594, respectively. No significant differences were found between groups.

5.3.4 Bleb morphology

The control group showed low inflammation with limited amounts of PMNs, macrophages, and fibroblasts present in the bleb area near the conjunctiva. All groups with a modified microshunts showed increased signs of inflammation when evaluated microscopically (see figure 5-7A and B). No clear differences between individual groups of animals with modified microshunts were noted in regard to inflammation. Collagen fibres in the blebs of the control group were relatively contracted and a dense structure, limited signs of oedema were visible. Collagen fibres with a modified implant showed more oedema (less tightly arranged collagen fibres) (see figure 5-7C and 8D). When measured, the total bleb height of the control, smooth, Topo-990, Topo-1008, and Topo-1594 had a bleb height of 411 ± 109 µm, 520 ± 239 µm, 675 ± 279 µm, 521 ± 181 µm, and 416 ± 123 µm, respectively. However, the differences in bleb height were not found to be significant 8E.

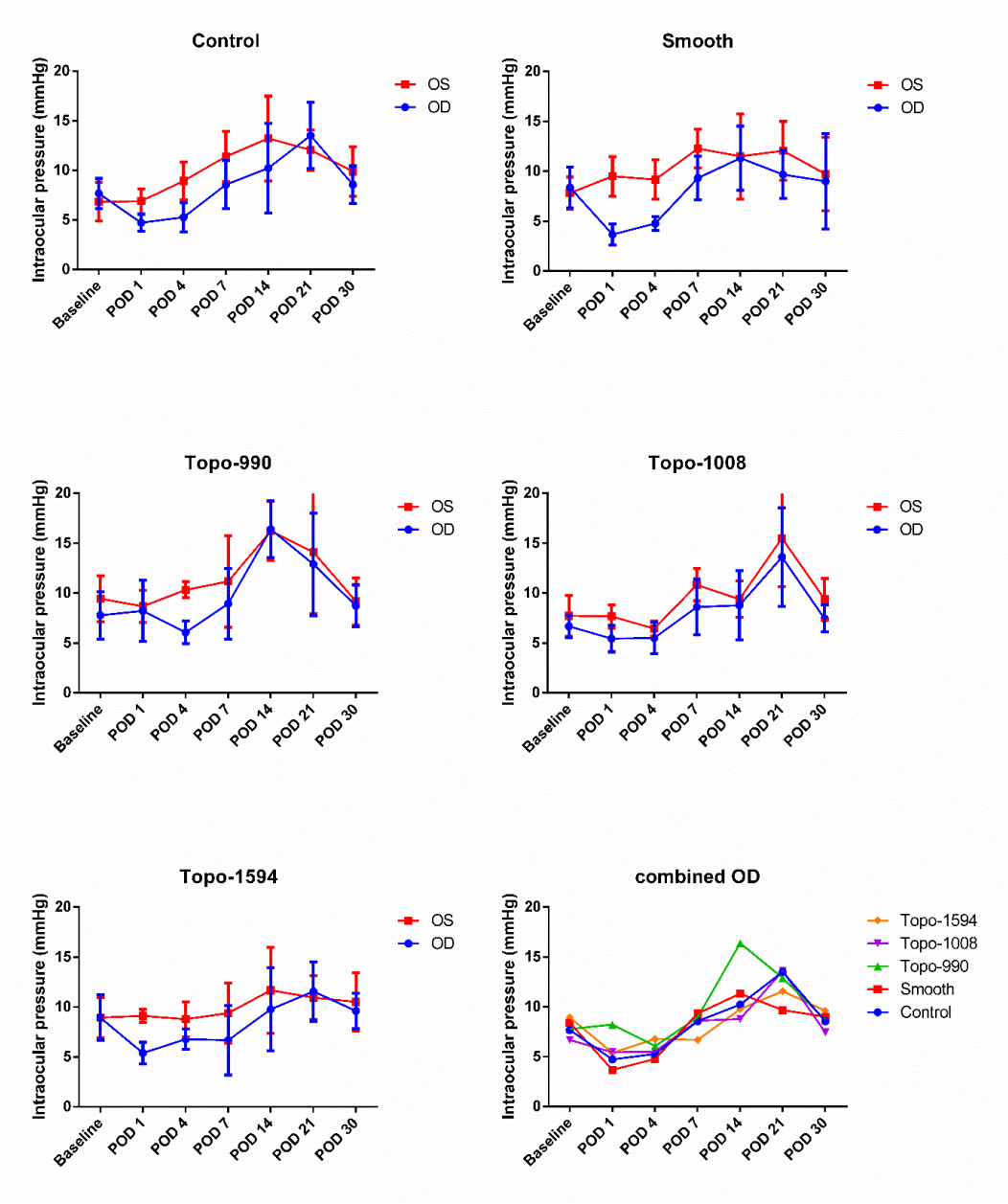

Figure 5-6: Intraocular pressure (IOP) measurement after implantation of the SIBS microshunt and modified microshunts with endplate attached. After surgery, an initial decrease in IOP is visible (OD eye) in most groups instead of the Topo-1008 group. IOP remained lowered up until POD 14-21 where all IOP's where similar to the unoperated eye (OS). No statistical differences were observed at all time points (n=3 for all groups).

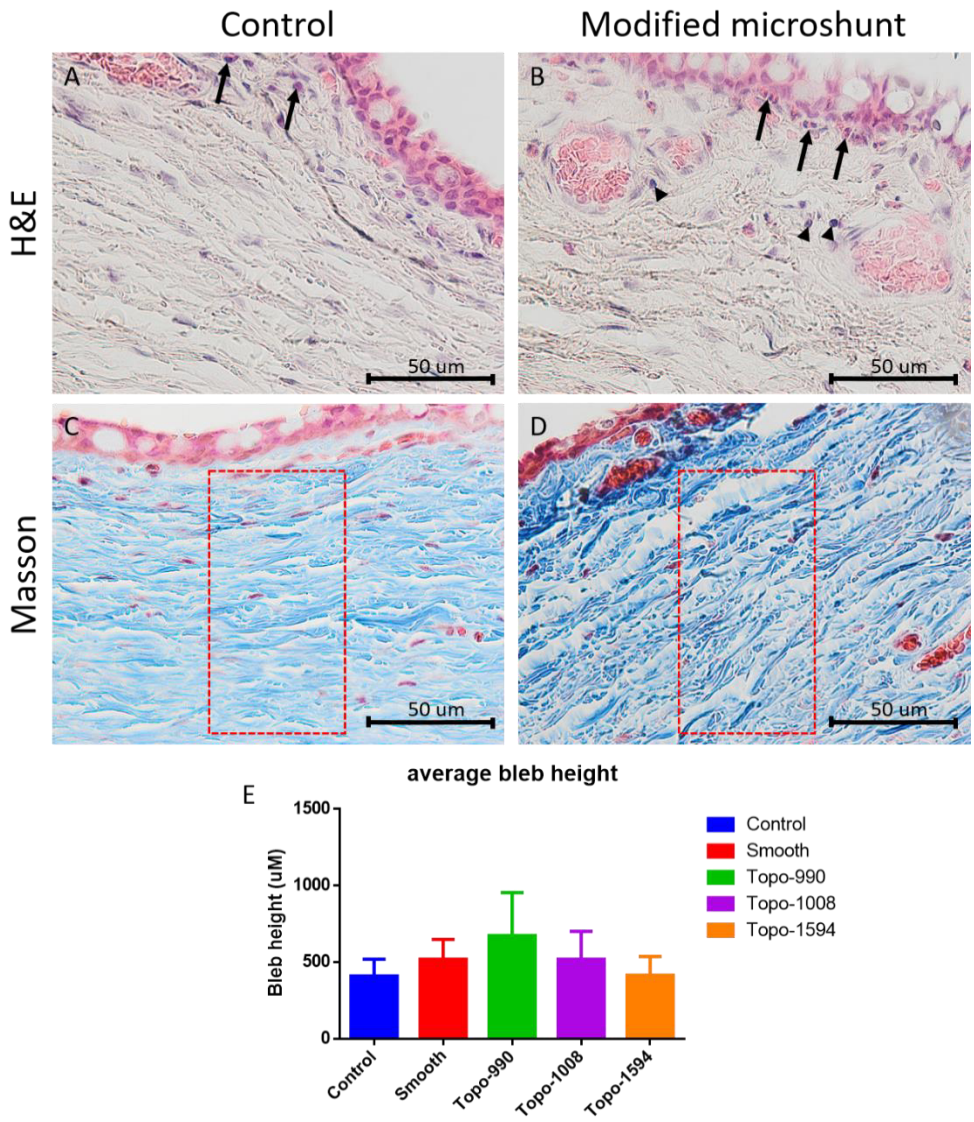

Figure 5-7: Overview of bleb morphology. The blebs of control animals (A) showed well healed bleb, with limited signs of inflammation (see arrows). An increased amount of polymorphonuclear cells (arrows) and macrophages (arrowhead) were visible within the bleb of animals with a modified microshunt (B). Collagen fibers were found to be more tightly arranged within the control group (C) when compared to animals that received a modified microshunt (D) (indicated with the red outline). A one-way ANOVA with Tukey post-hoc comparisons was used to find potentially significant differences (n=3 per group). No significant difference was observed in regard to the average bleb height (E).

5.3.5 Foreign body response and capsule formation around implant.

A tightly arranged fibrous collagen capsule with increased vascularization formed around the implants. The capsule consisted out of a dense network of fibroblasts and inflammatory cells such as, polymorphonuclear cells (PMNs), macrophages and foreign body giant cells which were observed in the capsule of all groups. However, compared to the control, we observed an increase of inflammatory cells and myofibroblasts in the capsule of groups that were implanted with the modified microshunts with endplates. Capsule thickness was significantly increased in the topography groups in comparison to the control and smooth implant. A smaller capsule formed on the control and smooth implant, which was significantly smaller compared to Topo-990, Topo-1008, and Topo 1594 (see figure 5-8), on average the capsule thickness was, 25 ± 13 µm, 39 ± 10 µm, 83 ± 16 µm, 65 ± 19 µm, and 81 ± 8 µm for the control, smooth, Topo-990, Topo-1008, and Topo-1594, respectively. No significant differences were found between the control and smooth implant. Macrophages as well as PMNs, foreign body giant cells and fibroblasts were observed surrounding the individual topographies on each plate (figure 5-8H). Some proliferation was also noted within the capsule of the implants and on the sides of the implant (data not shown). However, no differences regarding extent of proliferation was observed within these groups.

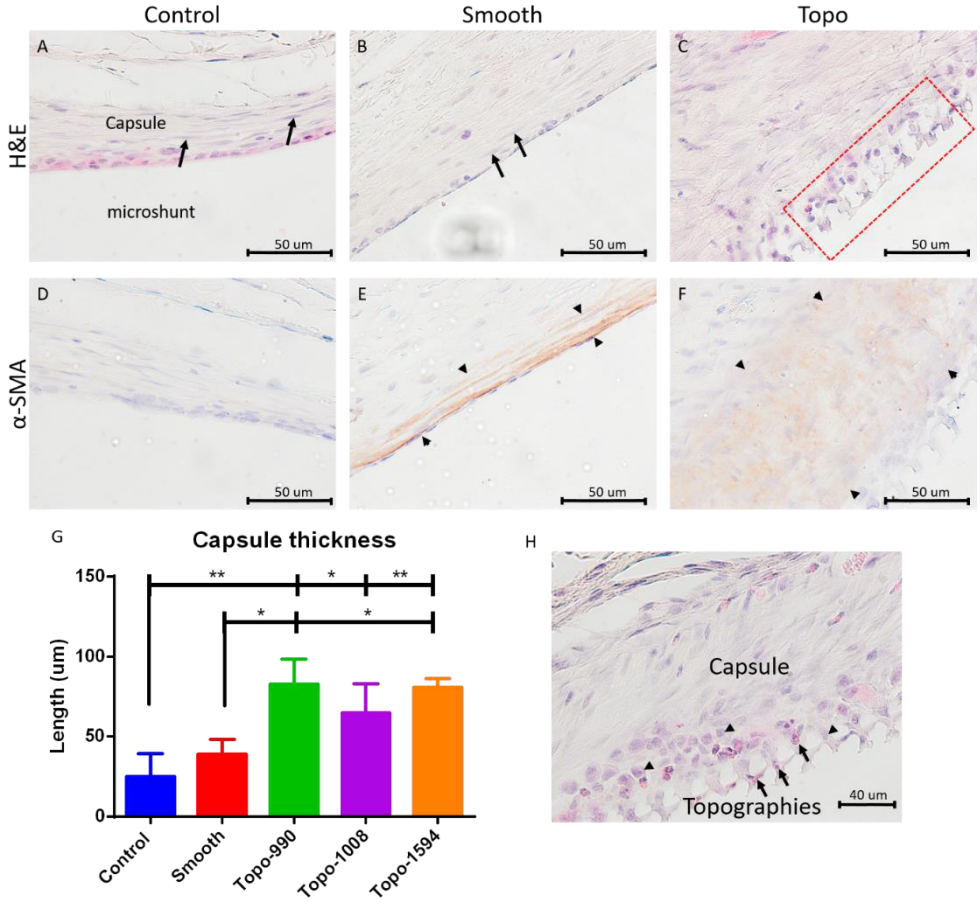

Figure 5-8: Capsule morphology after an H&E and α-SMA stain. The capsule of animals with a control implant or a smooth surface (A and B) showed low signs of inflammatory cells, fibroblasts were observed within the capsule (arrows). The capsule of animals with a topography (C) showed increased signs of inflammation, more polymorphonuclear cells and macrophages were seen surrounding the topography (red outline). After staining with an α-SMA stain control animals had no to limited myofibroblasts present in the capsule (D) increased presence of myofibroblasts was observed in the smooth group (E) and, increasingly, in the topo groups (see arrowheads) (F). Total capsule thickness was found to increase after implantation of a modified microshunt with topographies (G). (H) Enlargement of red outline of figure 5-8C, macrophages (arrowhead), polymorphonuclear cells (arrow) and fibroblasts (*) were observed near and between the topographies. * = $P<0.05$, ** = $P<0.005$. A one-way ANOVA with Tukey post-hoc comparisons was used to find potentially significant differences (n=3 per group).

5.4 Discussion

Two research questions were addressed during this pilot study: First, can cell modulating surface topographies in an orthotropic environment induce a cellular response and thus, increase bleb survival? And second, can the addition of an endplate on the outlet of a SIBS microshunt (comparable to a larger endplate in other GDDs) increase bleb survival? Topographies were selected based on previous experience and performed research [14, 22]. After surgery, fluid filled blebs were visible in all groups. Blebs in the control animals failed within 2 weeks, which is comparable to other literature after bleb forming surgery without the use of anti-fibrotic medication [24-26]. Addition of the 5 mm disc (smooth group) endplate extended bleb survival up until 3 weeks postoperative. Topo-990 showed the longest bleb survival (30 days) where blebs remained visible up until the day of euthanization (POD 30). These observations suggest that future experiments should be conducted for a longer period of time to better understand the significance of cellular modulating topographies in the eye model. An increased amount of PMNs, macrophages, fibroblasts, and slight increase of capsule thickness was observed in the smooth group compared to the control. Encapsulation of the implant was significantly increased in all groups with a surface topography. This finding is comparable to what Wilcox and Kadri found, they showed a correlation between implant size and encapsulation, when size of the implant increased an increased encapsulation was observed, facilitated by the increased mechanical stress due to the increased outflow of AqH. Indicating that capsular tension and collagen deposition increases with size [27]. Choritz *et al.* hypothesized that a smooth surface resulted in less encapsulation and fibrosis. In their study, cells were seeded on 4 different implants made out of either silicone or polypropylene. A high correlation between surface roughness and adhesion of fibroblasts was found [18]. Surface topographies increase the total surface area of an implant, which could increase the foreign body response and, therefore, increase encapsulation. Although the surface topographies that were used in this study were magnitudes smaller compared to the study of Choritz *et al.*, they could still serve as points of contact for different cell types and thereby increase encapsulation. A recent study on surface roughness in breast implants showed that an average roughness of 4 µm provoked the lowest amount of inflammation and foreign body response [20]. Thus, our topographies might have been too large (10 µm). Anti-adhesive surface topographies have been validated *in* vitro and have been shown to reduce adhesion of fibroblasts and macrophages *in vitro* [21]. However, *in vivo* research is still required to elucidate the effect of these topographies in more detail. A localized bleb formed in most animals with a modified microshunt, potentially caused by adherence of the tissue onto the rim of the implant. Smoothing or rounding of edges (or edges with anti-fibrotic topographies) could result in less

adhesion of tissue onto the rim the implant. Although we did not see any adverse side effects during our study, thinning of the conjunctiva or even bleb leakage could occur as a result of high bleb pressure when capsule integrity has not matured enough to withstand high pressure or tension for a prolonged period of time [27]. Longer follow up times in eyes with actual glaucoma (higher baseline IOP) are therefore warranted to ensure safety of the current design. IOP results are inconclusive, no clear differences between groups were found, which may be attributed to the animals not having glaucoma and the small number of animals used in the study [28].

Topographies that can increase fluid permeability around the encapsulated microshunt (*e.g.* by having a higher amount of type III collagen compared to type I) might help to lower IOP by increasing the permeability of the capsule thereby allowing more AqH to leave the bleb. A functioning filtering bleb is in a constant equilibrium between flow of AqH into and out from the bleb. Similarly, topographies that hamper the production of collagen type I, *e.g.* by ameliorating fibroblast or pro-fibrotic macrophage response, could reduce encapsulation of the implant and increase permeability, again lowering IOP.

5.5 Conclusion

This study shows that the addition of a 5 mm diameter endplate on the distal end of a SIBS microshunt extends bleb survival. The incorporation of surface topographies onto the endplate suggests that bleb survival and functionality can be increased. However, due to the increased capsule thickness and presence of pro-fibrotic cells further research is warranted. Longer duration studies with a higher power need to be conducted to validate the effects of surface topographies on bleb survival and fibrosis.

References

1. Lee, R.M.H., et al., *Translating Minimally Invasive Glaucoma Surgery Devices.* Clin Transl Sci, 2020. **13**(1): p. 14-25.
2. Scheres, L.M.J., et al., *XEN(®) Gel Stent compared to PRESERFLO™ MicroShunt implantation for primary open-angle glaucoma: two-year results.* Acta Ophthalmol, 2021. **99**(3): p. e433-e440.
3. Schlunck, G., et al., *Conjunctival fibrosis following filtering glaucoma surgery.* Exp Eye Res, 2016. **142**: p. 76-82.
4. Batlle, J.F., A. Corona, and R. Albuquerque, *Long-term Results of the PRESERFLO MicroShunt in Patients With Primary Open-angle Glaucoma From a Single-center Nonrandomized Study.* J Glaucoma, 2021. **30**(3): p. 281-286.
5. Fellman, R.L., et al., *American Glaucoma Society Position Paper: Microinvasive Glaucoma Surgery.* Ophthalmol Glaucoma, 2020. **3**(1): p. 1-6.
6. Pereira, I.C.F., et al., *Conventional glaucoma implants and the new MIGS devices: a comprehensive review of current options and future directions.* Eye (Lond), 2021. **35**(12): p. 3202-3221.
7. Acosta, A.C., et al., *A newly designed glaucoma drainage implant made of poly(styrene-b-isobutylene-b-styrene): biocompatibility and function in normal rabbit eyes.* Arch Ophthalmol, 2006. **124**(12): p. 1742-9.
8. Pinchuk, L., et al., *Medical applications of poly(styrene-block-isobutylene-block-styrene) ("SIBS").* Biomaterials, 2008. **29**(4): p. 448-60.
9. Minckler, D.S., et al., *Experimental studies of aqueous filtration using the Molteno implant.* Trans Am Ophthalmol Soc, 1987. **85**: p. 368-92.
10. Britt, M.T., et al., *Randomized clinical trial of the 350-mm2 versus the 500-mm2 Baerveldt implant: longer term results: Is bigger better?11Dr. Baerveldt has a financial interest in the Baerveldt glaucoma implant; the other authors have no proprietary interest in any of the materials used in this study.* Ophthalmology, 1999. **106**(12): p. 2312-2318.
11. Barnea, Y., et al., *Plasma Activation of a Breast Implant Shell in Conjunction With Antibacterial Irrigants Enhances Antibacterial Activity.* Aesthet Surg J, 2018. **38**(11): p. 1188-1196.
12. Xu, H., et al., *Hydrogel-coated ventricular catheters for high-risk patients receiving ventricular peritoneum shunt.* Medicine (Baltimore), 2016. **95**(29): p. e4252.
13. Castel, N., et al., *Polyurethane-coated breast implants revisited: a 30-year follow-up.* Arch Plast Surg, 2015. **42**(2): p. 186-93.
14. Vassey, M.J., et al., *Immune Modulation by Design: Using Topography to Control Human Monocyte Attachment and Macrophage Differentiation.* Adv Sci (Weinh), 2020. **7**(11): p. 1903392.
15. Franco, D., et al., *Control of initial endothelial spreading by topographic activation of focal adhesion kinase.* Soft Matter, 2011. **7**(16): p. 7313-7324.
16. Potthoff, E., et al., *Toward a rational design of surface textures promoting endothelialization.* Nano Lett, 2014. **14**(2): p. 1069-79.
17. Ferrari, A., et al., *Neuronal polarity selection by topography-induced focal adhesion control.* Biomaterials, 2010. **31**(17): p. 4682-94.
18. Choritz, L., et al., *Surface topographies of glaucoma drainage devices and their influence on human tenon fibroblast adhesion.* Invest Ophthalmol Vis Sci, 2010. **51**(8): p. 4047-53.
19. Hulshof, F.F.B., et al., *Mining for osteogenic surface topographies: In silico design to in vivo osseo-integration.* Biomaterials, 2017. **137**: p. 49-60.
20. Doloff, J.C., et al., *The surface topography of silicone breast implants mediates the foreign body response in mice, rabbits and humans.* Nature Biomedical Engineering, 2021. **5**(10): p. 1115-1130.
21. Robotti, F., et al., *A micron-scale surface topography design reducing cell adhesion to implanted materials.* Scientific Reports, 2018. **8**(1): p. 10887.
22. Vasilevich, A.S., et al., *On the correlation between material-induced cell shape and phenotypical response of human mesenchymal stem cells.* Scientific Reports, 2020. **10**(1): p. 18988.
23. Percie du Sert, N., et al., *The ARRIVE guidelines 2.0: Updated guidelines for reporting animal research.* Br J Pharmacol, 2020. **177**(16): p. 3617-3624.
24. van Mechelen, R.J.S., et al., *Wound Healing Response After Bleb-Forming Glaucoma Surgery With a SIBS Microshunt in Rabbits.* Transl Vis Sci Technol, 2022. **11**(8): p. 29.

25. SooHoo, J.R., et al., *Bleb morphology and histology in a rabbit model of glaucoma filtration surgery using Ozurdex® or mitomycin-C*. Mol Vis, 2012. **18**: p. 714-9.
26. Doyle, J.W., et al., *Intraoperative 5-fluorouracil for filtration surgery in the rabbit.* Invest Ophthalmol Vis Sci, 1993. **34**(12): p. 3313-9.
27. Wilcox, M. and O.A. Kadri, *Force and geometry determine structure and function of glaucoma filtration capsules.* Ophthalmologica, 2007. **221**(4): p. 238-43.
28. Bertens, C.J.F., et al., *Repeatability, reproducibility, and agreement of three tonometers for measuring intraocular pressure in rabbits.* Sci Rep, 2021. **11**(1): p. 19217.

Chapter 6

History, presence, and future of mitomycin C in glaucoma filtration surgery

*Wolters, J. E. J., *van Mechelen, R. J. S., Al Majidi, R., Pinchuk, L., Webers, C. A. B., Beckers, H. J. M., & Gorgels, T. G. M. F. (2021). History, presence, and future of mitomycin C in glaucoma filtration surgery. Current opinion in ophthalmology, 32(2), 148–159. * shared co-author

Abstract

Mitomycin C (MMC) is an alkylating agent with extraordinary ability to crosslink DNA, preventing DNA synthesis. By this virtue, MMC is an important antitumor drug. In addition, MMC has become the gold standard medication for glaucoma filtration surgery (GFS). This eye surgery creates a passage for drainage of aqueous humor (AqH) out of the eye into the sub-Tenon's space with the aim of lowering the intraocular pressure. A major cause of failure of this operation is fibrosis and scarring in the sub-Tenon's space, which will restrict AqH outflow. Intraoperative application of MMC during GFS has increased GFS success rate, presumably mainly by reducing fibrosis after GFS. However, still 10% of glaucoma surgeries fail within the first year. In this review, we evaluate risks and benefits of MMC as an adjuvant for GFS. In addition, we discuss possible improvements of its use by adjusting dose and method of administration. One way of improving GFS outcome is to prolong MMC delivery by using a drug delivery system.

6.1 Introduction

Glaucoma is the leading cause of irreversible blindness worldwide [1-3]. By 2020, the prevalence of glaucoma is estimated to be around 80 million people worldwide [4]. High intraocular pressure (IOP) is one of the most important risk factors of glaucoma [5-7]. All current glaucoma treatment modalities aim at lowering IOP, initially with eye drops and/or laser treatment [1, 8]. If these treatments do not have the desired effect, a surgical intervention can be performed, the so-called glaucoma filtration surgery (GFS) [1, 8-10]. GFS is the last resort treatment option for glaucoma patients [7, 11]. Current standard GFS techniques (*e.g.* trabeculectomy or long-tube glaucoma implant/shunt) have been practiced for several decades [3, 6] and are the most effective treatments to achieve sustained IOP reduction [9]. During GFS, an artificial passage (*e.g.* by placing a shunt) [2, 9, 12] is created for drainage of aqueous humor (AqH) from the anterior chamber into the space under the conjunctiva and Tenon's capsule, forming a filtering bleb. This procedure will increase outflow of AqH and reduce IOP. GFS requires a substantial follow-up care and does not always lead to a permanent IOP reduction [13]. An important complication is the development of fibrosis (scarring) of the filtering bleb [4, 14-16], which often reduces the outflow of AqH through the operatively created drainage passage; as a consequence, IOP will rise again [9]. This phenomenon of IOP rise after GFS is classified as a GFS-failure and most patients need to restart their medication and/or undergo a revision or new surgery procedure.

The introduction of mitomycin C (MMC) administration to augment the outcome of trabeculectomy in the early 1990s resulted in improved long-term IOP control [17], presumably by its antifibrotic action [12]. Currently, intraoperative MMC administration in the sub-Tenon's space with a sponge soaked in MMC is the gold standard antifibrotic treatment in GFS [8, 9]. Additionally, the use and application of MMC in ophthalmology, especially in glaucoma procedures, has been increasing in recent years, because of its modulatory effects on wound healing [18]. Unfortunately, MMC administration does not completely prevent failures of current GFS procedures. In order to reduce the number of failures, new so-called minimally invasive glaucoma surgical (MIGS) devices and procedures have been developed and have been made available for several years [19-21]. These MIGS devices are less stressful for patients [19-21], but unfortunately also not always successful [22]. There are currently three general types of MIGS devices (implants) that shunt from the anterior chamber to, 1) Schlemm's Canal (iStent®, Hydrus®), 2) the supraciliary space (new devices in development) and 3) to a bleb formed under the conjunctiva and Tenon's capsule, (Allergan XEN-gel stent® and the Santen PRESERFLO™ MicroShunt) which emulates GFS [21]. Importantly, MMC administration still remains

necessary in GFS-based subconjunctival-based MIGS for suppressing the fibrotic reaction. Recent results show that a substantial proportion of MIGS placed in the sub-Tenon's space, augmented with MMC, still show an increase in IOP within the first year, too often leading to failure [23]. Overall, we conclude that despite the development of new GFS methods the administration of MMC is still required. A more important concern is that failure rates of the new MIGS methods with onetime intra-operative MMC administration remain relatively high.

The aim of this literature review is to evaluate the risks and benefits of MMC as an adjuvant for GFS. In addition, we discuss possible improvements of MMC use. The question is whether MMC is here to stay, is it time to adjust its way of application or is it time to find a new drug and medication regimen?

6.2 Use of MMC IN GLAUCOMA FILTRATION SURGERY

6.2.1 Physical and chemical properties of MMC

Mitomycin C (MMC) was isolated from the broth of the *Streptomyces caespitosus* in Japan in 1954 [8, 17, 18, 24-27]. MMC is isolated as blue violet crystals [26]. The molecular weight of MMC ($C_{15}H_{18}N_4O_5$) is 334,33 Daltons. MMC is readily soluble in water (0.5 mg/mL) and organic solvents [26, 28]. The melting point is 360°C [29]. MMC solutions, in 0.9% saline, are stable for at least 6 hours at 37°C [30].

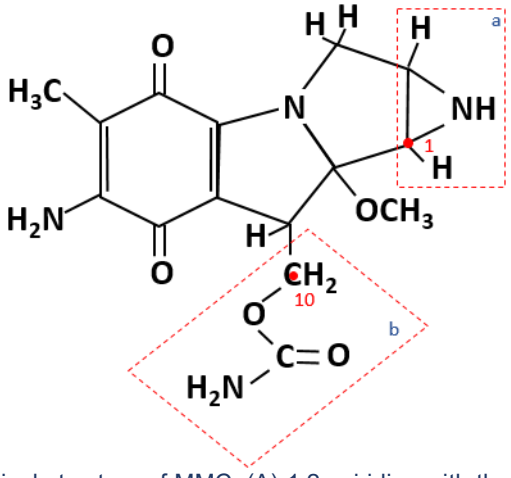

Figure 6-1: Chemical structure of MMC. (A) 1,2 aziridine with the first alkylating reactivity at the C1 position (see red dot), (B) 10-carbamate group with a second alkylating center at the C10 position (see red dot).

6.2.2 Reactive properties of MMC

MMC is an alkylation agent targeting DNA, RNA, proteins, and lipids. Interestingly, MMC was postulated to have two alkylating centers, the 1,2-aziridine (C1 position) and 10-carbamate group (C10 position) (Figure 6-1) [27]. As an example, the chemical reaction (reductive alkylation) with DNA is illustrated in Figure 6-2, adapted from Verweij and Pinedo [26].

The interaction of DNA with MMC results in the alkylation of multiple DNA guanine residues [31]. The clinically used antitumor agent MMC alkylates DNA upon reductive activation and forms in this process six covalent DNA adducts [27]. First, a one- or two-electron reduction (Figure 6-2A to Figure 6-2B) occurs under anaerobic conditions, followed by a spontaneous loss of methanol that leads to the formation of an unstable reactive intermediate (Figure 6-2B to Figure 6-2C). Thereafter, rearrangement of the reactive intermediate (Figure 6-2C) will be followed by a nucleophilic addition of DNA which results in a mono-alkylated product (Figure 6-2D). Intramolecular displacement of the carbamate group would then result in the cross-linked adduct (Figure 6-2E to Figure 6-2F).
Overall, DNA alkylation by MMC will block DNA synthesis and consequently inhibit cell proliferation [8, 31]. In addition, several of the formed DNA adducts are capable of inducing cell death in cancer cells since they can alkylate and cross-link DNA (for review see: [27]).
Activation of MMC within the cell is influenced by several factors. Firstly, it is known that MMC is activated by enzymatic reduction within the cell, a process mediated by cytochrome P-450 reductase and that occurs most effectively in a hypoxic environment [24, 26]. Secondly, it has been noted that MMC activation is also nicotinamide adenine dinucleotide phosphate (NADPH)-dependent [29]. Thirdly, it is known that MMC activates the PI3K/Akt signaling pathway in a p53-dependant manner [27, 32]. Activation of MMC will result in alkylation/crosslinking of DNA as shown in Figure 6-2.

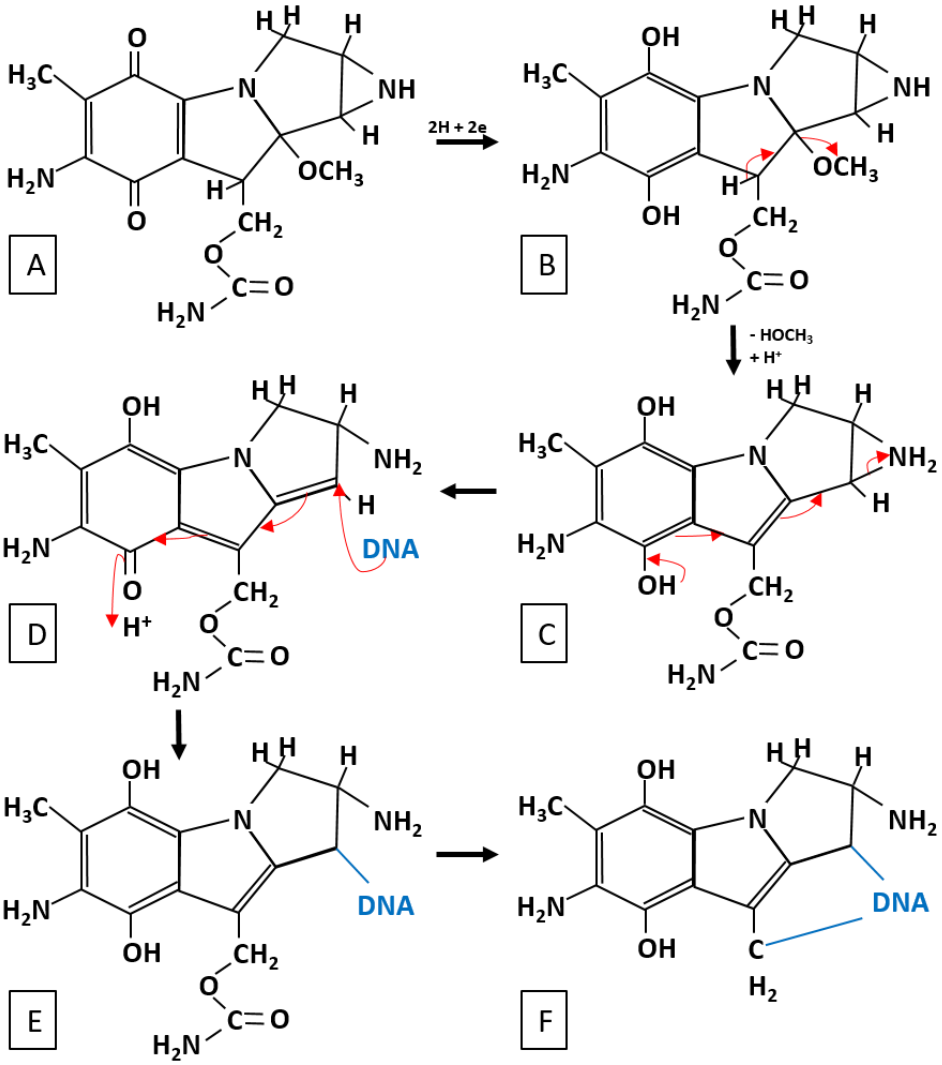

Figure 6-2: Reductive activation and DNA alkylation of MMC, adapted from Verweij and Pinedo [26]. (A) MMC, (B) intermediate of MMC, (C) unstable reactive intermediate of MMC, (D) quinone methide (has a high alkylating reactivity at the C1 position, (E) MMC-DNA adduct (with a second alkylating center at C10), (F) MMC cross-linked DNA adduct.

In addition, it has been shown that MMC crosslinks the complementary strands of the DNA double helix especially in CpG-sites [25, 26]. Furthermore, activated MMC is most effective in the late G1- and S- phases of the cell cycle [17, 18, 26], but is not essentially cell cycle specific [17]. Because MMC is relatively nonspecific and reacts with cells in every phase in the cell cycle, it causes cytotoxicity by lipid peroxidation and by damage to DNA and protein [33].
MMC is not only known as an alkylating agent [24, 32], but also as an antibiotic [34], cross-linking reagent [35], and a nucleic acid synthesis inhibitor [36]. Besides the specific inhibition of DNA synthesis due to alkylation, inhibition of RNA and protein synthesis seem to be non-specific manifestations of MMC cell toxicity [26, 29]. The use of MMC as an anti-cancer agent or as an antifibrotic/anti-adhesion agent relies on exactly the same molecular mechanism of action, namely the formation of covalent adducts of MMC with DNA [31].

6.2.3 Common applications of MMC

By virtue of the actions as described above, MMC is used as an antitumor, antibiotic, anti-proliferative, antifibrotic, and immunosuppressive agent. The antitumor MMC has shown clinical activity in a number of cancers, including stomach cancer, breast cancer, and cervical cancer [26, 37, 38]. Furthermore, MMC is known to have immunosuppressive properties and has been shown *in vitro* to inhibit B-cell, T-cell, and macrophage proliferation and impair antigen presentation, as well as the secretion of interferon gamma (IFN-γ), tumor necrosis factor alpha (TNF-α), and interleukin (IL)-2 [36]. Despite these properties it is not often used as an immunosuppressive agent in the clinic. Its use in ophthalmology has been increasing in recent years, because of its modulatory effects on wound healing (anti-proliferative, antifibrotic) [18]. In this application, MMC leads to an almost complete inhibition of fibroblast proliferation [24] and therefore a significant reduction of fibrosis [39].

6.2.4 GFS and cause of failures

Increased IOP can be caused by a myriad of factors contributing to either overproduction of aqueous humor (AqH) by the ciliary body or increased resistance in the AqH outflow paths from the anterior chamber [2]. Conventional outflow from the anterior chamber is through the trabecular meshwork into Schlemm's Canal, subsequently to the collector channels and then into the venous plexus in the sclera [2]. The secondary outflow path is into the supraciliary space and then into the venous plexus in the sclera [2]. If any of these paths are of high resistance, the IOP will become high. GFS reduces IOP by increasing the outflow of AqH out of the anterior chamber through an artificial passage that bypasses the trabecular meshwork, Schlemm's Canal, the collector channels and the venous plexus (*e.g.* by

trabeculectomy or by placing a tube shunt) [6, 9, 11]. AqH is directed into the space under the conjunctiva and Tenon's capsule, the sub-Tenon's space, forming a filtering bleb [6, 9, 11]. Outflow from the bleb can be through the conjunctiva into the tear film or into the episcleral veins, whichever is of lower resistance [40]. The success of GFS is threatened by fibrosis of the filtering bleb, which progressively limits AqH outflow from the anterior chamber into the filtering bleb. Therefore, during GFS, surgeons use a onetime MMC administration intraoperatively within the wound bed to inhibit the postoperative formation of fibrotic and scar tissue [16]. This usually works very well in the first postoperative period. Unfortunately, despite this onetime intraoperative MMC treatment during GFS, fibrosis (scarring) occurs postoperatively and results in 5-10% failure rate every year [23]. Fibrosis, while being a part of the normal wound healing, will have the negative effect of blocking the artificial passage (for example by closing the flap or distal tube end) postoperatively [9, 15, 16]. This will result in a rise in IOP, requiring restart of glaucoma medications, an intervention (*e.g.* laser suture lysis, needling) or reoperation.

Wound healing and scarring is a complex process that consists of a series of events, including hemostasis (phase 1), inflammation (phase 2), proliferation (phase 3), and remodeling (phase 4) after surgical tissue trauma [4, 9, 15, 16]. In more detail, the surgery starts with inducing a tissue trauma with at least some release of blood cells and plasma proteins, or hemostasis (phase 1), which will trigger a localized inflammatory response (phase 2). During the inflammation phase the innate immune system will be activated and inflammatory cytokines will be released. In the early inflammation phase, platelet activation provides a rich source of mediators (such as platelet-derived growth factor (PDGF), vascular endothelial growth factor alpha (VEGF-A), and transforming growth factor beta type 1 (TGF-β1)). These factors enhance the recruitment of macrophages which also release different growth factors, such as transforming growth factors alpha and beta (TGF-α, TGF-β), PDGF, and fibroblast growth factor (FGF). Thereafter, 1 to 3 days after surgery, the proliferation phase (phase 3) ensues with propagation and invading of fibroblasts (this is driven for example by PDGF). Herein, transdifferentiation of fibroblasts into myofibroblasts will be induced by the growth factor TGF-β. Finally, this will enhance the expression of extracellular matrix (ECM) proteins to strengthen the ECM (phase 4).

This normal, naturally occurring wound healing reaction can produce an adverse result in GFS when scar tissue is generated in the filtering bleb, more specifically if this scar tissue encloses the ostium and scleral flap after trabeculectomy, or the distal end of the tube implant in MIGS procedure, limiting AqH outflow and resorption.

6.2.5 Introduction of MMC in GFS and its regulation

To prevent fibrosis, MMC is applied in conjunction with GFS. In 1983, Chen *et al.* [41] were the first to describe the efficacy of MMC treatment in enhancing bleb

survival following trabeculectomy in eyes with a high risk of failure [24, 41]. The introduction of MMC treatment in trabeculectomy surgeries has improved the long-term IOP control through delayed wound healing resulting from inhibition of fibroblast proliferation [17]. Chen *et al.* [42] originally reported in 1990 that application of a MMC solution at a concentration of 0.2 to 0.4 mg/ml for 5 minutes is adequate, and poses little risk of severe complications such as ocular hypotony [24, 42]. However, they also suggested that 0.2 mg/ml for 5 minutes may be the safest effective dose [42]. Later, in 1995, Hung *et al.* [43] investigated the use of MMC by a subconjunctival injection prior to trabeculectomy in patients with refractory glaucoma [24, 43]. In 2004, a survey of British ophthalmology consultants reported that 82% of the surgeons used antimetabolites (apart from MMC also 5-fluorouracil (5-FU) is used) during trabeculectomy [24, 44]. Finally, MMC was reported as the most commonly used antimetabolite among American Glaucoma Society members in 2008 [24, 45].

Legislation of MMC-usage is different in each country. Mitosol® (mitomycin for solution, 0.2 mg/vial, Kit for Ophthalmic Use) [46] and Mitozytrex [47] are the only FDA approved ophthalmic formulations of MMC [24]. These are not allowed in Europe, where traditionally MMC is used off-label for ophthalmic purposes, and is freshly prepared by the hospital pharmacist prior to the scheduled surgery.

6.2.6 MMC administration during GFS and its results

During GFS, MMC solution is administered to the eye, at the location of the planned filtering bleb. It is known to be highly bioavailable for the target tissue [18, 28]. The MMC is mostly applicated by inserting a sponge soaked in a concentration of 0.1 - 0.5 mg/mL MMC underneath a conjunctival/Tenon's flap onto the sclera, for 1-5 minutes [48]. For example, a sponge soaked in 0.2 mg/mL MMC for 2-3 minutes is the standard intraoperative treatment in for example many European sites (also at the University Eye Clinic Maastricht). Clinical studies have observed that most tissues become saturated with MMC after an intraoperative treatment of 1 minute [24]. Furthermore, IOP levels in patients after GFS were similar between the conditions where MMC was used for 2 or for 5 minutes [24]. In addition, sometimes MMC is also administered postoperatively by 0.1 mL subconjunctival injections of a 0.02 mg/mL solution (needling procedure) [48].

Xi *et al.* [49] reported that MMC is the most effective and popular anti proliferative drug for GFS, especially in eyes with high risk of failure. Intraoperative MMC treatment is effective in 90% of the GFSs whereby the created outflow pathway is open (meaning: MMC was able to inhibit the formation of fibrotic tissue after TE and MIGS, which otherwise would close/block the outflow of AqH from the anterior chamber through the ostium (or MIGS shunt) into the filtering bleb) and the IOP remains in the normal-ranges (<15 mmHg for trabeculectomy).

6.2.7 Mechanistic aspects of MMC-treatment in GFS

MMC can function in GFS due to the alkylating effect of the drug [24, 26, 32]. Thereby, it inhibits cell proliferation/differentiation (*e.g.* fibroblasts into myofibroblasts) (phase 3 of the wound healing process), kills cells (phase 1-3 of the wound healing process), and inhibits induction of inflammation (phase 2 of the wound healing process) [8, 18, 24, 31, 33, 36, 39]. A direct effect of MMC on the differentiation into M1-macrophages (pro-inflammatory; TNF-α) and M2-macrophages (anti-inflammatory; IL-10 and CD163) type macrophages has not been studied yet. Most interestingly, MMC represents the most efficacious antifibrotic agent that is used as intraoperative treatment to attenuate the formation of fibrosis after trabeculectomy and to prolong the bleb survival [50]. Furthermore, fibroblasts of the Tenon's capsule are critical to the production of new extracellular matrix (such as collagen and glycosaminoglycans) in response to surgery [51, 52]. Intra-operative MMC treatment inhibits the proliferation of these fibroblasts of Tenon's capsule [51, 53, 54].

In general, MMC inhibits processes in wound healing such as collagen synthesis, fibroblast migration and fibroblast proliferation (myofibroblast formation) [51, 52, 55]. Therefore, the artificial drainage passage will not be blocked by fibrotic tissue and AqH can freely flow out of the anterior chamber, which leads to an IOP reduction.

6.2.8 Failure of MMC-treatment

Overall, ten percent of the GFSs fail within the first year and this is mostly caused by the formation of fibrotic tissue in/under the filtering bleb [56]. Clearly then, the current medication regimen is not fully effective in preventing fibrosis after GFS. Possible explanations of the failures could be: 1. MMC treatment is too short to prevent the formation of fibrotic tissue, 2. presence of pro-fibrotic agents in the AqH, 3. variation between patients, 4. toxic side effects of MMC treatment (see paragraph 2.8.1 until paragraph 2.8.4, respectively). Finally, fifthly, it may be that MMC is not the optimal GFS medication after all (see paragraph 2.9).

6.2.8.1 MMC treatment is too short

The first reason for a GFS failure could be that the intraoperative MMC treatment is not sustained long enough to prevent fibrosis, considering for example that phase 3 of the wound healing process normally occurs after 5-7 days. There are several indications that the current onetime administration (within safe limits of concentration and duration) may not provide sustained levels of MMC. Firstly, MMC has a relatively short half-life of plasma distribution (2-10 minutes) [26]. Secondly, MMC has a relatively short biological half-life (8-48 minutes) [36]. Thirdly, MMC has a relatively rapid elimination time (25-90 minutes) [26, 47]. Finally, the intraoperative MMC

treatment and the corresponding rinsing techniques during GFS can result in quite variable local tissue levels of MMC; it may also vary considerably among surgeons [8]. In conclusion, MMC is rapidly cleared, has a fast half-life time, and the level of MMC present in the eye can differ between each GFS. All of these factors can contribute to why some patients fail after GFS and others do not. Off course, also variation between patients (see paragraph 2.8.3), will contribute to this.

6.2.8.2 Presence of pro-fibrotic agents in the AqH

Secondly, the tissue of the filtering bleb is continuously exposed to AqH drained from the anterior chamber. This contact normally does not occur, since AqH drains directly into Schlemm's canal and is carried away by the circulation. Multiple studies have shown that AqH of glaucoma patients contains a number of inflammatory cytokines, including IL-6 [57], IL-8 [57-59], TNF-α [60], serum amyloid A (SAA) [59] and the growth factor TGF-β1 [59, 61] [62-65]. Expression changes of the ocular inflammatory cytokines (including TNF-α, IL-8, and SAA) and the growth factor TGF-β1 in AqH, are known to play a role in IOP elevations in patients with primary open angle glaucoma (POAG) [63]. These inflammatory cytokines and growth factors influence the wound healing response (namely, stimulating inflammation (phase 2) and proliferation (phase 3)), as described in paragraph 2.4. TGF-β is known to induce the transdifferentiation of fibroblasts into myofibroblasts [4, 9, 15, 16]. In conclusion, the continuous exposure of the filtering bleb to "glaucomatous" AqH that contains increased inflammatory cytokines and TGF-β1 will lead to a continuation of inflammation, proliferation, and finally fibrosis of the wound healing process and could therefore be one of the reasons why some patients will develop fibrotic tissue in such a manner that it will block the AqH outflow. This mechanism also could account for the fact that failure still occurs in cases long after GFS.

6.2.8.3 Variation between patients

Thirdly, it is questionable whether the intraoperative MMC-treatment is equally effective in each individual, since MMC effectivity is p53- [32], pH- [18, 24], and [O_2]- [26] dependent. Cheng *et al.* clearly showed that MMC deactivates Akt, which is known as a key player in cellular processes (such as glucose metabolism, apoptosis, cell proliferation, transcription and cell migration), in a p53-dependent way, since Akt levels were only inhibited by MMC in MCF-7 (p53-proficient) cells and not in K562 (p53-deficient) cells [32]. Furthermore, Mudhol *et al.* [18] and Velpandian *et al.* [66] reported that MMC is inactivated in acidic solutions (pH of 6) and is mostly active at neutral pH (pH of 7). Most interestingly, in 1984, Coles & Jaros [67] reported that ocular surface pH shifted during the day and also differs between individuals. In addition, Verweij & Pinedo [26] reported that MMC is mainly active under anaerobic circumstances (low O_2 values, hypoxia). Most likely, this MMC activity under hypoxic

conditions is an important reason why MMC is effective in killing cancer cells, since it is generally known that cancer cells survive under hypoxic conditions [68, 69]. In addition, as mentioned in paragraph 2.8.1, the intraoperative MMC treatment and the washing techniques can differ between surgeries, which lead to different levels of MMC in the eye between individual surgeries [8]. Finally, patients differ also in fibrosis propensity due to for example differences in age, ethnicity, pre-medication and genetic differences [16]. In conclusion, the inter-individual variability between patients regarding dose and activation of MMC as well as variations in the fibrosis process itself may result in variation in extent and timing of fibrosis and thus of failures between patients.

6.2.8.4 Toxic side effects

Fourthly, MMC treatment has several side effects. It is known that MMC is toxic to cells (*e.g.* hepatotoxicity) [36]. Systemic MMC treatment has several known side effects such as delayed myelosuppression, thrombocytopenia, leucocytopenia and anemia [26, 37]. Ocular use of MMC can lead to a variety of ocular complications mostly related to the typical thin-walled MMC filtering blebs, including blebitis, endophthalmitis, corneal epithelial defects, and hypotony with accompanying vision loss [10, 18, 33, 49]. In conclusion, some failures may result from toxic side effects of MMC. Furthermore, the mechanism of action of MMC is relatively harsh and unspecific, which means that it will also kill and inhibit cell growth of cells that would have a beneficial effect (such as the sub-conjunctival blood- and lymph-vessels that can transport/absorb the AqH of the filtering bleb).

6.2.9 Improvements of GFS medication regime

Clearly then, the current GFS medication regime is not fully effective in all patients. Roughly two different approaches have been taken to improve the success rate.

The first approach is to repeat or extend the duration of the administration of the currently used antifibrotic drugs. In fact, in case of failure or threat of failure, needle revisions (*i.e.*, subconjunctival fibrotic strands are cut with a needle and an antifibrotic drug is applied again by subconjunctival injection) are often performed in the clinic. If necessary, this treatment can be repeated at various time points, sometimes long after surgery. For these needle revisions mostly 5-FU has been used, but also MMC needle revisions are performed, for example after a trabeculectomy and XEN gel stent surgeries [70-82]. Some examples of 5-FU and MMC needle revisions are shown in table 6-1.

Table 6-1: Usage of antimetabolites across different types of procedures.

Surgery type	Species	Intra-operative treatment	Needle revisions	Success rate
Trabeculectomy [76]	Human	MMC 0,4 mg/ml, 1-2 minutes	- 5-FU, 0.1 ml (50mg/ml) - MMC, 0.1 ml (0.2 mg/ml)	- 5-FU → 34.3% (after 12 months) - MMC → 57,5% (after 12 months)
Trabeculectomy [77]	Human	-	MMC, 0.1 ml (80 µg/ml)	76%
Trabeculectomy [75]	Human	-	MMC, 0.15-0.2 ml (0.02%)	40.3% (after 3 years)
Trabeculectomy [70]	Human	-	- 5-FU, 0.1 ml (50 mg/ml) - MMC, 0.1 ml (0.2 mg/ml)	- 5-FU → 47% - MMC → 80%
Trabeculectomy [78]	Human	-	MMC, 0.2 ml (0.3 mg/ml)	84.6%
Trabeculectomy [71]	Primates	MMC 0.27 mg/ml, 4 minutes	MMC, 0.4 mg/ml	-
XEN140 [82]	Human	-	5-FU and MMC in 32% of cases	-
XEN140 [81]	Human	-	5-FU and MMC in 43% of cases	-
XEN63 [82]	Human	-	5-FU and MMC in 32% of cases	-
XEN45 [79]	Human	MMC	None	-
XEN45 [72]	Human	MMC	5-FU and MMC in 2.4% of cases	-
XEN45 [80]	Human	MMC	5-FU and MMC in 43.2% of cases	-
XEN45 [74]	Human	MMC	5-FU and MMC in 32.3% of cases	-
XEN45 [73]	Human	MMC	5-FU and MMC in 30.7% of cases	-

It shows that needle revisions, with MMC or 5-FU of failing filter blebs after trabeculectomy, are successful [70, 71, 75-78]. Furthermore, it shows that a needle revision with MMC is more effective than a needle revision with 5-FU [70, 76]. Needle revisions, with 5-FU or MMC, are needed in 30-50% of all the XEN gel stent surgery cases [72-74, 79-82].

The positive results of repeated administration of MMC suggest that the onetime intraoperative application of MMC is too short to curtail fibrosis in the long term. It may be better to present antifibrotic drugs by a drug delivery system (DDS) for sustained drug delivery. This sustained delivery may result in a longer and better (better controlled in dose and duration) MMC treatment than the current onetime intra-operative MMC treatment [13, 83, 84]. In this manner the antifibrotic drugs are present throughout the whole wound healing process (see paragraph 2.8.1). Furthermore, a DDS with continuous delivery of MMC over a long time, may be more efficacious since fibroblasts and/or tissue are continuously exposed to AqH which contains inflammatory cytokines and an important growth factor for the inducement of the wound healing processes (see paragraph 2.8.2). Due to the long-term postoperative scar formation time, which lasts at least for over two weeks [85], a DDS that can maintain an effective drug concentration for an appropriate period of time to regulate postoperative proliferation and maintain bleb filtering with fewer complications is desirable [49]. Multiple sustained drug delivery systems (DDSs) have been developed in the last years. Many of these studies with the DDSs were performed within the eye of humans and/or animals. Examples of interesting DDSs are listed in table 6-2: 1) a non-biodegradable poly(2-hydroxyethyl methacrylate) (P(HEMA))-MMC device [86, 87], 2) cyclodextrin polymers loaded with MMC [83], 3) a biodegradable poly(lactic-co-glycolic acid) (PLGA) system with 5-FU with and without MMC [87, 88], 4) a cross-linked hyaluronan (HA) hydrogel that contained MMC [31, 89], 5) a thermo-sensitive hydrogel from poly(trimethylene carbonate)15-F127-poly(trimethylene carbonate)15 (PTMC15-F127-PTMC15) loaded with MMC [49], 6) a thermosensitive hydrogel from MitoGel loaded with MMC [90, 91], 7) MMC encapsulated in LDLr targeting drug delivery system (LDL-MMC-chitosan nanoparticles) [33], 8) thin films of two different polymers, Poly(3-hydroxybutyrate) (P(3HB)) and Poly(4-hydroxybutyrate) (P(4HB)), containing MMC or paclitaxel (PTX) were attached to silicone-tubes [92], 9) lipidated prodrug of mitomycin C (MLP) on the membrane of a pegylated liposome formulation (PL-MLP), also known as Promitil [93], 10) polycaprolactone (PCL) implants that achieve zero-order release of a proprietary ocular hypotensive agent (DE-117) [94], 11) a PLGA system loaded with cyclosporine A (CsA) [95], and 12) encapsulation of bevacuzimab in the core of electrospun fibers [96].

Table 6-2: Overview of developed drug delivery systems.

Device	Material	Type	Degradable	Drug	Concentration	Release period	*In vitro* or *in vivo* validation
non-biodegradable poly(2-hydroxyethyl methacrylate) (P(HEMA))-mitomycin C [86]	P(HEMA)	gel	No	MMC	- 0.17, 0.35, 0.8 mg MMC per gram gel - 6.5 ug	in vitro over 1 to 2 weeks (80% after 4 days)	*in vitro* and *in vivo*
non-biodegradable poly(2-hydroxyethyl methacrylate) (P(HEMA))-mitomycin C [87]	P(HEMA)	Disk	No	MMC	- 6.5 ug	-	*in vitro* and *in vivo*
cyclodextrin polymers with MMC [83]	cyclodextrin polymers	Gel	Not tested (possibly long-term degradability)	MMC	0.4 ug/ml (IC50)	100 h	*in vitro*
biodegradable poly(lactic-co-glycolic acid) (PLGA) system with 5-fluorouracil (5-FU) with and without MMC [87]	PLGA	Film	Yes	MMC	0. 65 µg		*in vitro* and *in vivo*
biodegradable poly(lactic-co-glycolic acid) (PLGA) system with 5-fluorouracil (5-FU)	PLGA	Film	Yes	MMC	1 and 5 µg	2) 20% after 8 days (1 ug) and 30% after 1 day (5 ug)	*In vitro*

with and without MMC [88]							
biodegradable poly(lactic-co-glycolicacid) (PLGA), burst of mitomycin C (MMC) release followed by a slow release of 5-fluorouracil (5-FU) [88]	PLGA	Film	Yes	5-FU	0.1, 0.4, and 2 mg	0.03 mg after 20 days (0.1 mg) and 0.24 mg after 20 days (0.4 mg) en 1.5 mg after 30 days (2.0 mg)	*In vitro*
cross-linked hyaluronan (HA) hydrogel with MMC [31]	HA	Hydrogel	Yes	MMC	0.5% and 2% of total film weight	70% after 4 days (thereafter no release anymore)	*in vitro* and *in vivo*
crosslinked hyaluronan (HA) hydrogels that contained covalently-bound MMC [89]		Gel			0.31%, 0.625% and 1.25% of total film weight		*in vitro* and *in vivo*
biodegradable thermo-sensitive hydrogel from poly(trimethylene carbonate)15-F127-poly(trimethylenecarbonate)15 (PTMC15-F127-	PTMC15-F127-PTMC15	Hydrogel	Yes	MMC	0.1mg/ml	80% after 15 days	*in vitro* and *in vivo*

PTMC15) was designed and evaluated as an injectable implant. Loaded with MMC [49]							
A novel sustained release formulation of MMC based on RTGel, a proprietary thermosensitive hydrogel technology [90,91]	MitoGel (thermosensitive hydrogel)	Hydrogel	/	MMC	- 2 mg/ml and 4 mg/ml [90] - 2 mg/ml (14mg), 4mg/ml (28mg), and 8 mg/ml (56mg) [91]		*In vivo*
MMC encapsulated in LDLr targeting drug delivery system [33]	LDL-MMC-chitosan nanoparticles (targeted)	Nanoparticles in HA film	Yes	MMC	-	60 hour	-
Poly(3-hydroxybutyrate) (P(3HB)), containing the drugs mitomycin C (MMC) or paclitaxel (PTX) [92]	P(3HB)	Film	Yes	- MMC - PTX	- 69ug MMC of the 460ug - 213ug PTX of the 1418ug	- 3-4 days MMC release (80%) - 25 PTX days release (1%)	*in vitro* and *in vivo*
Poly(4-hydroxybutyrate) (P(4HB)), containing the drugs mitomycin C (MMC) or paclitaxel (PTX) [92]	P(4HB)		Yes	- MMC - PTX	- 63 ug MMC of the 420ug - 112 ug PTX of the 747ug	- 3-4 days MMC release (80%) - 25 PTX days release (14%)	*in vitro* and *in vivo*

Lipidated prodrug of mitomycin C (MLP) on the membrane of a pegylated liposome formulation (PL-MLP), also known as Promitil [93]	Membrane of a pegylated liposome formulation (PL-MLP), also known as Promitil	Liposome	Not tested (likely Yes)	MLP (MMC)	5 mg/mL	-	*in vitro*
polycaprolactone (PCL) implants with a proprietary ocular hypotensive agent (DE-117) [94	PCL	Film	Yes	DE-117	-	180 days a constant release of 0.5 ug/day	*in vitro* and *in vivo*
poly(lactic-co-glycolic acid) (PLGA) comprising cyclosporine A (CsA) [95]	PLGA	Coating / film	Yes	CsA	6 mg	80% after 100 days, the best and highest release are found after the first 10 days	*in vitro* and *in vivo*
Electrospun fibers were prepared with bevacizumab encapsulated in the core, surrounded by a poly-e-caprolactone sheath. {96}	Electrospun fibers surrounden by a poly-e-caprolactone sheath	Fibers reservoir	Not tested (unlikely that polymer would undergo complete degradation)	Bevacuzimab	24 ug bevacizumab in 1 mg of fibers	60% after 20 days	*in vitro*

No DDS for sustained delivery of antifibrotic drugs is currently FDA approved. One DDS of MMC, namely PL-MLP (see also in table 6-2) is now being tested in clinical trials.

The second approach to improve GFS outcome in the long term is to develop other (classes of) GFS medication [4, 15, 16]. This option will not be discussed in detail in this review. Multiple drugs have been tested in the last years, often aiming to influence the wound healing after GFS in a more specific and physiological manner (*e.g.* by targeting TGF-β) rather that the unspecific treatment with MMC. This research has extensively been reviewed by Li *et al.* [14], Schlunck *et al.* [9], Yu-Wai-Man & Khaw [4], and Friedlander [97]. These new GFS drugs may avoid several of the side effects of MMC (see paragraph 2.8.4) and maybe also the individual variability between patients (see paragraph 2.8.3). In the future, medication may be personalized taking account of individual differences in fibrosis [98].

6.3 Conclusion

Glaucoma filtration surgery (GFS) is currently the last resort treatment to stop or limit vision loss in patients that suffer from glaucoma. A major complication, which frequently causes failure of GFS, is the formation of fibrosis in the filtering bleb. The antifibrotic drug Mitomycin C (MMC), given as an adjuvant during GFS, has significantly increased GFS success rates. MMC is also used in GFS surgery with the novel minimally invasive glaucoma surgical (MIGS) devices.

While MMC certainly improved GFS success rates, still roughly 10% of bleb-based MIGS surgeries with a onetime MMC application fail within the first year, mostly because of fibrosis in the filtering bleb. To further reduce GFS failure rate, we roughly have two options: either we improve the MMC application or we switch to new drugs. Treatment of GFS failures with repeated injections of MMC shows positive results. This suggests that prolonged presence of MMC may control fibrosis over a longer period of time. Drug delivery systems for sustained release of MMC are currently being developed and these will show if this hypothesis is true. If not, we need to implement new approaches and drugs to create a suitable GFS wound healing, which will further increase GFS success rate.

References

1. Mansouri, K., F.A. Medeiros, and R.N. Weinreb, *Global rates of glaucoma surgery.* Graefes Arch Clin Exp Ophthalmol, 2013. **251**(11): p. 2609-15.
2. Braunger, B.M., R. Fuchshofer, and E.R. Tamm, *The aqueous humor outflow pathways in glaucoma: A unifying concept of disease mechanisms and causative treatment.* Eur J Pharm Biopharm, 2015. **95**(Pt B): p. 173-81.
3. Weinreb, R.N., T. Aung, and F.A. Medeiros, *The pathophysiology and treatment of glaucoma: a review.* Jama, 2014. **311**(18): p. 1901-11.
4. Yu-Wai-Man, C. and P.T. Khaw, *Developing novel antifibrotic therapeutics to modulate post-surgical wound healing in glaucoma: big potential for small molecules.* Expert Rev Ophthalmol, 2015. **10**(1): p. 65-76.
5. Lang, G.K., *Ophthalmology: A Pocket Textbook Atlas, 2nd edition.* Clinical and Experimental Optometry, 2008. **91**(1): p. 126-126.
6. Jonas, J.B., et al., *Glaucoma.* Lancet, 2017. **390**(10108): p. 2183-2193.
7. King, A., A. Azuara-Blanco, and A. Tuulonen, *Glaucoma.* Bmj, 2013. **346**: p. f3518.
8. Hung, P., *Mitomycin-C in Glaucoma Filtering Surgery.* Asian Journal of OPHTHALMOLOGY and Asia-Pacific Journal of Ophthalmology, 2000. **2**.
9. Schlunck, G., et al., *Conjunctival fibrosis following filtering glaucoma surgery.* Exp Eye Res, 2016. **142**: p. 76-82.
10. Martorana, G.M., et al., *Sequential Therapy with Saratin, Bevacizumab and Ilomastat to Prolong Bleb Function following Glaucoma Filtration Surgery in a Rabbit Model.* PLoS One, 2015. **10**(9): p. e0138054.
11. Mantravadi., A.V. and N. Vadhar, *Glaucoma.* Primary Care: Clinics in Office Practice, 2015. **42**(3): p. 437-449.
12. Chang, M.R., Q. Cheng, and D.A. Lee, *Basic science and clinical aspects of wound healing in glaucoma filtering surgery.* J Ocul Pharmacol Ther, 1998. **14**(1): p. 75-95.
13. Patel, S. and L.R. Pasquale, *Glaucoma drainage devices: a review of the past, present, and future.* Semin Ophthalmol, 2010. **25**(5-6): p. 265-70.
14. Li, X., et al., *Drugs and Targets in Fibrosis.* Front Pharmacol, 2017. **8**: p. 855.
15. Lockwood, A., S. Brocchini, and P.T. Khaw, *New developments in the pharmacological modulation of wound healing after glaucoma filtration surgery.* Curr Opin Pharmacol, 2013. **13**(1): p. 65-71.
16. Seibold, L.K., M.B. Sherwood, and M.Y. Kahook, *Wound modulation after filtration surgery.* Surv Ophthalmol, 2012. **57**(6): p. 530-50.
17. Mearza, A.A. and I.M. Aslanides, *Uses and complications of mitomycin C in ophthalmology.* Expert Opin Drug Saf, 2007. **6**(1): p. 27-32.
18. Mudhol, R., N. Zingade, and R. Mudhol, *Mitomycin C in ophthalmology.* Journal of the Scientific Society, 2012. **39**(1): p. 4-6.
19. Bar-David, L. and E.Z. Blumenthal, *Evolution of Glaucoma Surgery in the Last 25 Years.* Rambam Maimonides Med J, 2018. **9**(3).
20. Lavia, C., et al., *Minimally-invasive glaucoma surgeries (MIGS) for open angle glaucoma: A systematic review and meta-analysis.* PLoS One, 2017. **12**(8): p. e0183142.
21. Ansari, E., *An Update on Implants for Minimally Invasive Glaucoma Surgery (MIGS).* Ophthalmol Ther, 2017. **6**(2): p. 233-241.
22. Saheb, H. and Ahmed, II, *Micro-invasive glaucoma surgery: current perspectives and future directions.* Curr Opin Ophthalmol, 2012. **23**(2): p. 96-104.
23. Batlle, J.F., et al., *Three-Year Follow-up of a Novel Aqueous Humor MicroShunt.* J Glaucoma, 2016. **25**(2): p. e58-65.
24. Al Habash, A., et al., *A review of the efficacy of mitomycin C in glaucoma filtration surgery.* Clin Ophthalmol, 2015. **9**: p. 1945-51.
25. Tomasz, M., *Mitomycin C: small, fast and deadly (but very selective).* Chem Biol, 1995. **2**(9): p. 575-9.
26. Verweij, J. and H.M. Pinedo, *Mitomycin C: mechanism of action, usefulness and limitations.* Anticancer Drugs, 1990. **1**(1): p. 5-13.
27. Bargonetti, J., E. Champeil, and M. Tomasz, *Differential toxicity of DNA adducts of mitomycin C.* J Nucleic Acids, 2010. **2010**.
28. Fang, Y.P., P.Y. Hu, and Y.B. Huang, *Diminishing the side effect of mitomycin C by using pH-sensitive liposomes: in vitro characterization and in vivo pharmacokinetics.* Drug Des Devel Ther, 2018. **12**: p. 159-169.

29. Crooke, S.T. and W.T. Bradner, *Mitomycin C: a review.* Cancer Treatment Reviews, 1976. **3**(3): p. 121-139.
30. Myers, A.L., et al., *Solubilization and Stability of Mitomycin C Solutions Prepared for Intravesical Administration.* Drugs in R&D, 2017. **17**(2): p. 297-304.
31. Li, H., et al., *Synthesis and biological evaluation of a cross-linked hyaluronan-mitomycin C hydrogel.* Biomacromolecules, 2004. **5**(3): p. 895-902.
32. Cheng, S.Y., et al., *Involvement of Akt in Mitomycin C and Its Analog Triggered Cytotoxicity in MCF-7 and K562 cancer cells.* Chem Biol Drug Des, 2018.
33. Shao, T., X. Li, and J. Ge, *Target drug delivery system as a new scarring modulation after glaucoma filtration surgery.* Diagn Pathol, 2011. **6**: p. 64.
34. *Mitomycin*. Drug created on June 13, 2005 07:24 / Updated on October 28, 2018 07:22 [cited 2018 30 October]; Available from: https://www.drugbank.ca/drugs/DB00305.
35. Hoorn, C.M., et al., *Toxicity of mitomycin C toward cultured pulmonary artery endothelium.* Toxicol Appl Pharmacol, 1995. **130**(1): p. 87-94.
36. *National Center for Biotechnology Information. PubChem Compound Database; CID=5746, https://pubchem.ncbi.nlm.nih.gov/compound/5746 (accessed Oct. 30, 2018).*
37. Bradner, W.T., *Mitomycin C: a clinical update.* Cancer Treat Rev, 2001. **27**(1): p. 35-50.
38. den Hartigh, J., et al., *Pharmacokinetics of mitomycin C in humans.* Cancer Res, 1983. **43**(10): p. 5017-21.
39. Kersey, J.P. and A.J. Vivian, *Mitomycin and amniotic membrane: a new method of reducing adhesions and fibrosis in strabismus surgery.* Strabismus, 2008. **16**(3): p. 116-8.
40. Sadruddin, O., et al., *Ab externo implantation of the MicroShunt, a poly (styrene-block-isobutylene-block-styrene) surgical device for the treatment of primary open-angle glaucoma: a review.* Eye and vision (London, England), 2019. **6**: p. 36-36.
41. CW., C., *Enhanced intraocular pressure controlling effectiveness of trabeculectomy by local application of mitomycine-C.* Trans Asia-Pacific Acad Ophthalmol. , 1983(9): p. 172-173.
42. Chen, C.W., et al., *Trabeculectomy with simultaneous topical application of mitomycin-C in refractory glaucoma.* J Ocul Pharmacol, 1990. **6**(3): p. 175-82.
43. Hung, P.T., et al., *Preoperative mitomycin-C subconjunctival injection and glaucoma filtering surgery.* J Ocul Pharmacol Ther, 1995. **11**(3): p. 233-41.
44. Siriwardena, D., et al., *National survey of antimetabolite use in glaucoma surgery in the United Kingdom.* Br J Ophthalmol, 2004. **88**(7): p. 873-6.
45. Desai, M.A., et al., *Practice preferences for glaucoma surgery: a survey of the American Glaucoma Society in 2008.* Ophthalmic Surg Lasers Imaging, 2011. **42**(3): p. 202-8.
46. *Mitomycin solution (Mitosol) for glaucoma surgery.* Med Lett Drugs Ther, 2013. **55**(1412): p. 24.
47. *FDA approves extra safe chemotherapy drug.* Expert Rev Anticancer Ther, 2002. **2**(6): p. 618-9.
48. *European Glaucoma Society Terminology and Guidelines for Glaucoma, 4th Edition - Chapter 3: Treatment principles and options
Supported by the EGS Foundation.* British Journal of Ophthalmology, 2017. **101**(6): p. 130.
49. Xi, L., et al., *Evaluation of an injectable thermosensitive hydrogel as drug delivery implant for ocular glaucoma surgery.* PLoS One, 2014. **9**(6): p. e100632.
50. Razeghinejad, M.R., S.J. Fudemberg, and G.L. Spaeth, *The changing conceptual basis of trabeculectomy: a review of past and current surgical techniques.* Surv Ophthalmol, 2012. **57**(1): p. 1-25.
51. Beatty, S., et al., *Trabeculectomy augmented with mitomycin C application under the scleral flap.* Br J Ophthalmol, 1998. **82**(4): p. 397-403.
52. Costa, V.P., et al., *Wound healing modulation in glaucoma filtration surgery.* Ophthalmic Surg, 1993. **24**(3): p. 152-70.
53. Jampel, H.D., *Effect of brief exposure to mitomycin C on viability and proliferation of cultured human Tenon's capsule fibroblasts.* Ophthalmology, 1992. **99**(9): p. 1471-6.
54. Yamamoto, T., et al., *Effects of 5-fluorouracil and mitomycin C on cultured rabbit subconjunctival fibroblasts.* Ophthalmology, 1990. **97**(9): p. 1204-10.
55. Smith, S., P.A. D'Amore, and E.B. Dreyer, *Comparative toxicity of mitomycin C and 5-fluorouracil in vitro.* Am J Ophthalmol, 1994. **118**(3): p. 332-7.
56. Mokhles, P., et al., *A Systematic Review of End-of-Life Visual Impairment in Open-Angle Glaucoma: An Epidemiological Autopsy.* J Glaucoma, 2016. **25**(7): p. 623-8.
57. Zenkel, M., et al., *Proinflammatory cytokines are involved in the initiation of the abnormal matrix process in pseudoexfoliation syndrome/glaucoma.* Am J Pathol, 2010. **176**(6): p. 2868-79.

58. Kuchtey, J., et al., *Multiplex cytokine analysis reveals elevated concentration of interleukin-8 in glaucomatous aqueous humor.* Invest Ophthalmol Vis Sci, 2010. **51**(12): p. 6441-7.
59. Takai, Y., M. Tanito, and A. Ohira, *Multiplex cytokine analysis of aqueous humor in eyes with primary open-angle glaucoma, exfoliation glaucoma, and cataract.* Invest Ophthalmol Vis Sci, 2012. **53**(1): p. 241-7.
60. Sawada, H., et al., *Tumor necrosis factor-alpha concentrations in the aqueous humor of patients with glaucoma.* Invest Ophthalmol Vis Sci, 2010. **51**(2): p. 903-6.
61. Picht, G., et al., *Transforming growth factor beta 2 levels in the aqueous humor in different types of glaucoma and the relation to filtering bleb development.* Graefes Arch Clin Exp Ophthalmol, 2001. **239**(3): p. 199-207.
62. Huang, W., et al., *Inflammation-related cytokines of aqueous humor in acute primary angle-closure eyes.* Invest Ophthalmol Vis Sci, 2014. **55**(2): p. 1088-94.
63. Khalef, N., et al., *Levels of cytokines in the aqueous humor of eyes with primary open angle glaucoma, pseudoexfoliation glaucoma and cataract.* Electronic Physician, 2017. **9**(2): p. 3833-3837.
64. Zheng, Y., et al., *Age-related pro-inflammatory and pro-angiogenic changes in human aqueous humor.* International Journal of Ophthalmology, 2018. **11**(2): p. 196-200.
65. Chua, J., et al., *Expression profile of inflammatory cytokines in aqueous from glaucomatous eyes.* Mol Vis, 2012. **18**: p. 431-8.
66. Velpandian, T., et al., *Evaluation of the stability of extemporaneously prepared ophthalmic formulation of mitomycin C.* J Ocul Pharmacol Ther, 2005. **21**(3): p. 217-22.
67. Coles, W.H. and P.A. Jaros, *Dynamics of ocular surface pH.* Br J Ophthalmol, 1984. **68**(8): p. 549-52.
68. Yttersian Sletta, K., et al., *Oxygen-dependent regulation of tumor growth and metastasis in human breast cancer xenografts.* PloS one, 2017. **12**(8): p. e0183254-e0183254.
69. Brown, J.M., *The Hypoxic Cell.* Cancer Research, 1999. **59**(23): p. 5863.
70. Anand, N. and A. Khan, *Long-term outcomes of needle revision of trabeculectomy blebs with mitomycin C and 5-fluorouracil: a comparative safety and efficacy report.* J Glaucoma, 2009. **18**(7): p. 513-20.
71. Bair, J.S. and C.W. Chen, *Trabeculectomy with multiple applications of mitomycin-C in monkeys with experimental glaucoma.* J Ocul Pharmacol Ther, 1997. **13**(2): p. 115-28.
72. De Gregorio, A., et al., *Minimally invasive combined glaucoma and cataract surgery: clinical results of the smallest ab interno gel stent.* Int Ophthalmol, 2018. **38**(3): p. 1129-1134.
73. Galal, A., et al., *XEN Glaucoma Implant with Mitomycin C 1-Year Follow-Up: Result and Complications.* J Ophthalmol, 2017. **2017**: p. 5457246.
74. Grover, D.S., et al., *Performance and Safety of a New Ab Interno Gelatin Stent in Refractory Glaucoma at 12 Months.* Am J Ophthalmol, 2017. **183**: p. 25-36.
75. Lin, S., D. Byles, and M. Smith, *Long-term outcome of mitomycin C-augmented needle revision of trabeculectomy blebs for late trabeculectomy failure.* Eye (Lond), 2018.
76. Liu, W., et al., *Comparison of Subconjunctival Mitomycin C and 5-Fluorouracil Injection for Needle Revision of Early Failed Trabeculectomy Blebs.* J Ophthalmol, 2016. **2016**: p. 3762674.
77. Maestrini, H.A., et al., *Late needling of flat filtering blebs with adjunctive mitomycin C: efficacy and safety for the corneal endothelium.* Ophthalmology, 2011. **118**(4): p. 755-62.
78. Pathak-Ray, V. and N. Choudhari, *Rescue of failing or failed trabeculectomy blebs with slit-lamp needling and adjunctive mitomycin C in Indian eyes.* Indian J Ophthalmol, 2018. **66**(1): p. 71-76.
79. Perez-Torregrosa, V.T., et al., *Combined phacoemulsification and XEN45 surgery from a temporal approach and 2 incisions.* Arch Soc Esp Oftalmol, 2016. **91**(9): p. 415-21.
80. Schlenker, M.B., et al., *Efficacy, Safety, and Risk Factors for Failure of Standalone Ab Interno Gelatin Microstent Implantation versus Standalone Trabeculectomy.* Ophthalmology, 2017. **124**(11): p. 1579-1588.
81. Sheybani, A., H.B. Dick, and Ahmed, II, *Early Clinical Results of a Novel Ab Interno Gel Stent for the Surgical Treatment of Open-angle Glaucoma.* J Glaucoma, 2016. **25**(7): p. e691-6.
82. Sheybani, A., et al., *Phacoemulsification combined with a new ab interno gel stent to treat open-angle glaucoma: Pilot study.* Journal of Cataract & Refractive Surgery, 2015. **41**(9): p. 1905-1909.
83. Merritt, S.R., G. Velasquez, and H.A. von Recum, *Adjustable release of mitomycin C for inhibition of scar tissue formation after filtration surgery.* Exp Eye Res, 2013. **116**: p. 9-16.

84. Schmidt, W., et al., *New concepts for glaucoma implants--controlled aqueous humor drainage, encapsulation prevention and local drug delivery.* Curr Pharm Biotechnol, 2013. **14**(1): p. 98-111.
85. Hollo, G., *Wound healing and glaucoma surgery: modulating the scarring process with conventional antimetabolites and new molecules.* Dev Ophthalmol, 2012. **50**: p. 79-89.
86. Sahiner, N., et al., *Creation of a drug-coated glaucoma drainage device using polymer technology: in vitro and in vivo studies.* Arch Ophthalmol, 2009. **127**(4): p. 448-53.
87. Schoenberg, E.D., et al., *Effect of Two Novel Sustained-Release Drug Delivery Systems on Bleb Fibrosis: An In Vivo Glaucoma Drainage Device Study in a Rabbit Model.* Transl Vis Sci Technol, 2015. **4**(3): p. 4.
88. Ponnusamy, T., et al., *A novel antiproliferative drug coating for glaucoma drainage devices.* J Glaucoma, 2014. **23**(8): p. 526-34.
89. Liu, Y., et al., *Crosslinked hyaluronan hydrogels containing mitomycin C reduce postoperative abdominal adhesions.* Fertil Steril, 2005. **83 Suppl 1**: p. 1275-83.
90. Donin, N.M., et al., *Sustained-release Formulation of Mitomycin C to the Upper Urinary Tract Using a Thermosensitive Polymer: A Preclinical Study.* Urology, 2017. **99**: p. 270-277.
91. Donin, N.M., et al., *Serial retrograde instillations of sustained release formulation of mitomycin C to the upper urinary tract of the Yorkshire swine using a thermosensitive polymer: Safety and feasibility.* Urol Oncol, 2017. **35**(5): p. 272-278.
92. Hovakimyan, M., et al., *Development of an Experimental Drug Eluting Suprachoroidal Microstent as Glaucoma Drainage Device.* Transl Vis Sci Technol, 2015. **4**(3): p. 14.
93. Wei, X., et al., *Characterization of Pegylated Liposomal Mitomycin C Lipid-Based Prodrug (Promitil) by High Sensitivity Differential Scanning Calorimetry and Cryogenic Transmission Electron Microscopy.* Mol Pharm, 2017. **14**(12): p. 4339-4345.
94. Kim, J., et al., *Biocompatibility and Pharmacokinetic Analysis of an Intracameral Polycaprolactone Drug Delivery Implant for Glaucoma.* Invest Ophthalmol Vis Sci, 2016. **57**(10): p. 4341-6.
95. Dai, Z., et al., *Development of a novel CsA-PLGA drug delivery system based on a glaucoma drainage device for the prevention of postoperative fibrosis.* Mater Sci Eng C Mater Biol Appl, 2016. **66**: p. 206-214.
96. Angkawinitwong, U., et al., *Electrospun formulations of bevacizumab for sustained release in the eye.* Acta Biomater, 2017. **64**: p. 126-136.
97. Friedlander, M., *Fibrosis and diseases of the eye.* J Clin Invest, 2007. **117**(3): p. 576-86.
98. Yu-Wai-Man, C. and P.T. Khaw, *Personalized Medicine in Ocular Fibrosis: Myth or Future Biomarkers.* Advances in wound care, 2016. **5**(9): p. 390-402.

Chapter 7

A degradable sustained-release drug delivery system for bleb-forming glaucoma surgery

van Mechelen, R. J. S., Wolters, J. E. J., Fredrich, S., Bertens, C. J. F., Gijbels, M. J. J., Schenning, A. P. H. J., Pinchuk, L., Gorgels, T. G. M. F., & Beckers, H. J. M. (2023). A Degradable Sustained-Release Drug Delivery System for Bleb-Forming Glaucoma Surgery. Macromolecular bioscience.

Abstract

Fibrosis of the filtering bleb is one of the main causes of failure after bleb-forming glaucoma surgery. Intraoperative application of mitomycin C (MMC) is the current gold standard to reduce the fibrotic response. However, MMC is cytotoxic and one-time application is often insufficient. A sustained-release drug delivery system (DDS), loaded with MMC, might be less cytotoxic and equally or more effective. Two degradable (polycaprolactone (PCL) and polylactic-co-glycolic acid (PLGA)) MMC-loaded DDSs were developed. Release kinetics were first assessed *in vitro* followed by rabbit implants in conjunction with the PRESERFLO® MicroShunt. As a control, the MicroShunt was implanted with adjunctive use of a MMC solution. Rabbits were euthanized at postoperative day (POD) 28 and 90.

The PLGA and PCL DDSs released (on average) 99% and 75% of MMC, respectively. All groups showed functioning blebs until POD 90. Rabbits implanted with a DDS showed more inflammation with avascular thin-walled blebs when compared to the control. However, collagen was more loosely arranged. The PLGA DDS showed less inflammation, less foreign body response (FBR) and more complete degradation at POD 90 when compared to the PCL DDS. Further optimization with regard to dosage is required to reduce side effects to the conjunctiva.

7.1 Introduction

Glaucoma filtration surgery (GFS) is an effective treatment to significantly reduce intraocular pressure (IOP) in patients with uncontrolled glaucoma. Conventional methods are trabeculectomy and (long)-tube glaucoma drainage device implantation. Recently, new, and less invasive bleb-forming surgeries have also become available. However, bleb-forming surgery still often fails due to an excessive wound healing response, leading to fibrosis and subsequently hampered outflow of aqueous humor. Fibrosis of the filtering bleb is therefore one of the main causes of failure after bleb-forming glaucoma surgery. Approximately 10% of surgeries fail annually[1]. The antimetabolites mitomycin C (MMC) and 5-fluorouracil (5-FU) were introduced in the 1980s to reduce the fibrotic response [2-4]. Trabeculectomy performed intraoperatively with MMC is currently the gold standard for antifibrotic therapy [5] as MMC was found to be more potent than 5-FU [6-8]. Unfortunately, the use of MMC has also been correlated with an increase in vision-threatening complications such as bleb leaks, corneal endothelial cell loss, and endophthalmitis [9, 10]. These effects are caused by the aselective cytotoxic effect of MMC. It inhibits DNA synthesis and proliferation in all cells by crosslinking its DNA [2]. During GFS, MMC is administered either intraoperatively by application of sponges soaked in MMC (ranging from 0.2 – 0.4 mg/mL) into the sub-Tenon's space or postoperatively by injecting MMC into the bleb (0.1 mL of 0.02 mg/mL MMC) [2, 5, 11, 12]. MMC is now also used in conjunction with new, less invasive bleb-forming procedures (XEN-gel stent and PRESERFLO® Microshunt). An additional postoperative treatment with MMC or 5-FU, by injection or needling of the filtering bleb, is needed in approximately 30-50% of cases after XEN-gel stent implantation, indicating that the intraoperative treatment alone is insufficient in inhibiting the fibrotic response [2]. Alvarado *et al*. explored the use of serial postoperative injections with the antimetabolite 5-FU over a period of 6 weeks after implantation of an Ahmed glaucoma valve, whereafter an increased success rate was observed [13]. However, patient discomfort, and risks associated with serial injections makes this an undesirable treatment option. Novel drugs are routinely tested *in vivo*. Even though these novel drugs often showed to be safer compared to the established MMC and 5-FU, a lower antifibrotic effect is often seen [14]. Recently, drug delivery systems (DDS(s)) have seen an emerging role in the biomedical industry. A continuous-release DDS, loaded with MMC, could reduce postoperative cytotoxic effects of MMC while still maintaining efficacy due to lower concentrations of applied MMC towards the tissue. Several materials have already been used for the development of drug delivery systems, as shown in a recent review [2].

The research presented herein focuses on the development of a DDS that can be introduced within bleb-forming glaucoma surgery to limit the development of fibrosis.

We hypothesized that a DDS design must meet several criteria. It should adapt to the curvature of the eye to be comfortable to the patient, be easy to handle during surgery, release MMC for at least 30 days to inhibit the fibrotic response, and degrade *in situ* so as to minimize the long-term foreign body response (FBR) [5]. Polycaprolactone (PCL) and poly(lactic-co-glycolic acid) (PLGA) are often used as drug eluting carriers [2]. PCL is a hydrophobic, slowly degrading (2-3 years) polymer which is completely metabolized by the body and is highly permeable to many drugs [15, 16]. PLGA degrades into glycolic acid and lactic acid through hydrolysis. It degrades faster than PCL, and the degradation can be controlled by altering the ratio of lactic acid versus glycolic acid monomers in combination with the polymer chain length [17-20].
Several DDS designs, all with a disc shape (3 mm in diameter), were manufactured with different percentages of MMC either dissolved or crystalized into the carrier matrix (see figure 7-1 for an overview of designs). Prototypes based on a sprayed fiber network were developed and tested in rabbits to evaluate the safety and efficacy compared to the gold standard treatment (one-time intraoperative treatment with sponges soaked in MMC) [2].

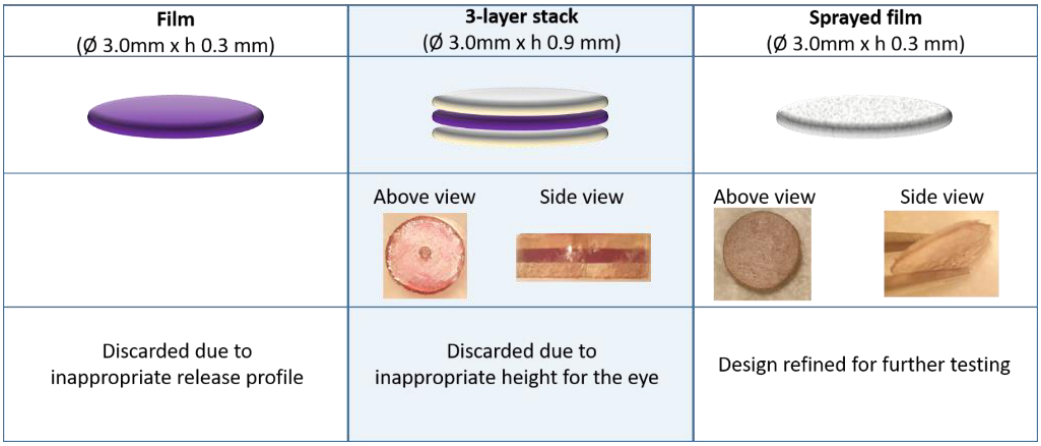

Figure 7-1: Overview of different design prototypes.

7.2 Methods

7.2.1 Calculation of MMC concentrations used in the clinic

To approximate the release of MMC during the intraoperative application of sponges, LASIK shields (7302, Synga Medical, NL) soaked with an MMC solution (0.2 mg/ml, prepared by the pharmacy of Maastricht University Medical Center+) were collected from two patients after 3-minute exposure in bleb-forming glaucoma surgery. The collected LASIK shields were centrifuged to collect the remainder of the MMC solution after application. Additionally, two LASIK shields were used as controls to determine the total volume a LASIK shield could absorb (~81.5 µL). Collected volumes were measured by reverse pipetting and MMC concentrations were calculated based on the used 0.2 mg/ml solution.

7.2.2 Production of drug delivery systems

A soft and loose fibrous meshwork of polymer with MMC (further called a "meshwork") was produced using a spraying process. Two polymer solutions were made containing 3% MMC, with either PCL (440744, Sigma Aldrich) or PLGA (M2320, TCI chemicals). The PCL solution was made by dissolving 400 mg of PCL in 12.5 mL dichloromethane (DCM) and 2.5 mL pentane, followed by the addition of 12 mg MMC. The PLGA solution was made by dissolving 400 mg of the resomer RG756S (719927, Sigma Aldrich) and 130 mg RG753H (769819, Sigma Aldrich) (a 3:1 ratio for RG756S:RG753H) in 4 mL DCM. Then, 130 µL ethyl lactate and 800 µL pentane was added to the solution. Thereafter, 15 mg MMC was added to the polymer solution. The polymer solutions were then loaded into a spray gun. A meshwork with a diameter of 10 cm was sprayed (keeping a distance between spray gun and target of approximately 20 cm, a gas pressure of 1 bar nitrogen, and an angle of roughly 45° towards the side wall of the target). Afterwards, the meshwork was placed in a vacuum oven overnight at 40 °C. Next, 3 mm diameter discs were cut out by using a 3 mm hole punch (see figure 7-2 for an SEM image of a DDS). On average, a DDS was loaded with 35 µg of MMC. Before use, they were sterilized using ethylene oxide and afterwards placed under vacuum to assure all ethylene oxide was evaporated.

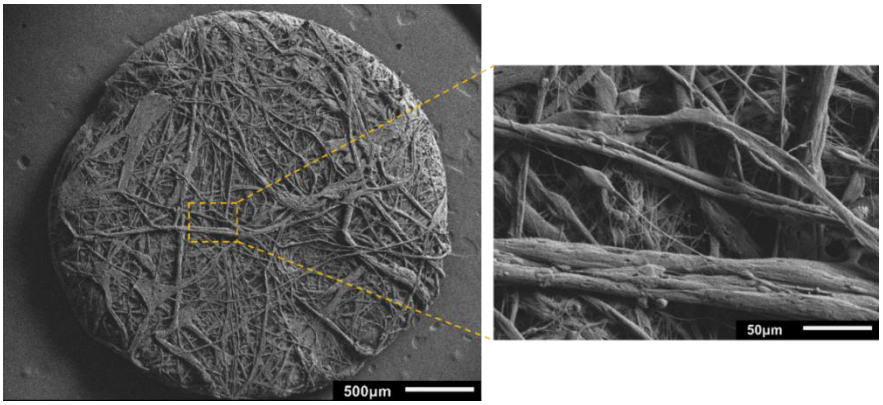

Figure 7-2: SEM photograph of a polycaprolactone drug delivery system (PCL DDS), the overall design is comparable to the PLGA DDS.

7.2.3 *In vitro* release kinetics

All *in vitro* release studies used an elution buffer of 1x PBS (pH 7.4). Each DDS (n = 3) was placed separately in a well of a 12-wells plate (untreated wells plate, VWR, Amsterdam, NL) with 1.5 mL elution buffer. The 12-wells plate was then placed on an orbital shaker at 120 rpm in a 37°C incubator. For each sampling time point, the elution buffer was collected and replaced with fresh buffer. The collected samples were stored at -80°C. At the day of HPLC measurement, samples were thawed and diluted 1:5 in methanol. Concentration of the diluted MMC sample was measured using high performance liquid chromatography (HPLC; 1260 Infinity Quaternary LC System, Agilent Technologies, Santa Clara, CA, USA). A C8 reverse-phase column (Symmetry C8, 100A 5 Um, 4.6 mm x 250 mm; Waters) was used with a gradient of mobile phase A:B (83.5:16.5 in 25 minutes) with an isocratic delivery at 0.9 mL/min. The mobile phase A contained 25 mM sodium phosphate (pH 5.4 adjusted with 1 N sodium hydroxide) in deionized water and mobile phase B was 50% HPLC-grade methanol (VWR, Pennsylvania, USA) with 50% HPLC-grade acetonitrile (VWR, Pennsylvania, USA). Detection was done via absorbance at a wavelength of 365 nm. The area under the curve of the MMC-peaks was analyzed using the OpenLab HPLC-software (Agilent Technologies). The unknown concentration of the samples of each time-point was calculated by using a standard curve of MMC (0-2400 µM) in each HPLC-run. The release rate at each time point was calculated by dividing the amount of drug collected by the duration between two time points. The cumulative release was calculated by summing the release of each time-point. The release was also plotted as a percentage by dividing the cumulative value of a specific time-point by the amount of drug loaded in each DDS at the start of the experiment. MMC had a retention time of 19.3 min, a limit of detection (LOD) of 1.3 ng, and a limit of quantification (LOQ) of 5.64 ng/mL

7.2.4 Animals

Rabbits were used as the animal model in this study as they have large eyes (comparable to human eyes), and are ideal for the development of biomedical devices related to bleb-forming glaucoma surgery [14, 21]. All animal procedures were conducted in accordance with the European Directive for animal experiments (2010/63/EU) (Approved Dutch license number: AVD1070020197464). The Central Authority for Scientific Procedures on Animals (CCD, Den Haag, NL), and the local ethical committee approved all animal procedures. Additionally, the license complied with the Association for Research in Vision and Ophthalmology (ARVO) statement for the use of animals in ophthalmic and vision research and the Animal Research: Reporting of *In Vivo* Experiments (ARRIVE) 2.0 guidelines [17].

Based on a power calculation, 5 animals were required per group. In total 30 New Zealand White Rabbits (Charles River, FR) were used (n=5 per group, 6 groups sacrificed at either postoperative day (POD) 28 or POD 90), with an approximate age of 12 weeks, weighing 2.5 to 3 kg, both male and female, normotensive. The rabbits were maintained under controlled conditions of temperature and humidity on a 12h:12h light-dark cycle, with *ad libitum* access to water and food. Before the start of the experiment, animals received a two-week acclimatization period. A randomized complete block design was used to allocate animals to different groups. Rabbits were killed at postoperative day (POD) 30 with an overdose of pentobarbital sodium, 200 mg/kg (Euthasol 20, Produlab Pharma B.V., NL) administered intravenously.

7.2.5 Surgical procedure

Thirty rabbits were randomly assigned to be implanted with either a PRESERFLO® MicroShunt in combination with a PCL DDS or a PLGA DDS, or a control group with a microshunt treated intraoperatively with a single dose of conventional MMC (0.4 mg/mL applied for 3 minutes). The surgical procedure control group was comparable to previous experiments in which a microshunt was implanted into the rabbit's eye [21]. In brief, following anesthesia, the surgical area was exposed with a speculum. A deep and wide conjunctival flap was formed with Westcott tenotomy scissors. A 1 mm wide and 1 mm deep scleral pocket was then formed with a knife, 3 mm posterior to the limbus. In the case of the control rabbits, a LASIK sponge soaked in 0.4 mg/mL MMC was placed into the subconjunctival flap for 3 minutes, then removed and the flap flushed with 0.9% NaCl. The microshunt was then implanted and checked for flow in the same manner as described in previous experiments [21]. In the sample populations, a DDS formed from either PCL or PLGA was placed next to the distal part of the microshunt and sutured onto the sclera with a nylon 8-0 suture (Ethicon LLC, Puerto Rico, USA). The conjunctiva and Tenon's capsule were closed with a Vicryl 9-0 suture (Ethicon LLC, Puerto Rico, USA). Recovery of the rabbits began

by injecting intramuscularly (IM) 0.5 mg/kg of atipamezole (Antisedan, ORION pharma, Mechelen, BE). A 1% chloramphenicol (Ceva sante animale B.V., Southern-Holland, NL) ointment was applied topically twice daily for 5 days. Additionally, rabbits received a subcutaneous injection of 0.05 mg/kg buprenorphine (Bupaq Multidose, Richter Pharma AG, Wels, AT) twice daily, up until POD 1, analgesia was extended when necessary.

7.2.6 *In vivo* measurements

Rabbits were sedated using 0.40 mg/kg medetomidine IM. IOP was measured with the iCare® TonoVet tonometer (iCare Finland Oy, Vantaa, FI). Slit lamp (SL) examinations (Haag-Streit BI 900, Haag-Streit, Köniz, CH), and bleb photographs were taken using a camera (canon EOS 4000D, Canon, Tokyo, JP). One week before surgery, IOP baseline measurements were obtained for each rabbit. Follow-up examinations were performed on POD 3, 7, 14, 21, 28, 42, 56, 80, and 90. Blebs were graded based on redness, vascularization, bleb height, and bleb extent. In case of a flat bleb, the eye was gently massaged, if the bleb remained flat after massage, it was categorized as failed.

7.2.7 Patency test

Fluorescein was injected into the anterior chamber to visualize fluid flow into the bleb. Rabbits were sedated with 5 mg/kg ketamine (Alfasan, Utrecht, NL) and 0.20 mg/kg medetomidine (Sedator, A.S.T. Farma B.V., Oudewater, NL) IM. After complete sedation the anterior chamber of the eye was entered using a 30G needle, approximately 0.1 mL of fluorescein (RVG 10165, Bausch + Lomb Ireland Limited, Dublin, IE) was injected into the anterior chamber. After 10 seconds, the needle was carefully retracted from the anterior chamber and fluid was allowed to dissipate from the eye to resolve increased IOP from the injection. The SL was set to blue dichroic excitation (460 to 493 nm). Lastly, the SL was aligned with the bleb to visualize patency of the shunt. The patency test was performed at POD 88.

7.2.8 Light microscopy and staining

Rabbits were euthanized using 200 mg/kg pentobarbital sodium (Euthasol 20, Produlab Pharma B.V., NL). The eyes were subsequently dissected and fixed in 4% paraformaldehyde (PFA) for 2 days (PFA was refreshed once a day). After fixation, eyes were dehydrated and embedded in paraffin blocks. Sections were cut with a thickness of 4 µm and were stained with Hematoxylin & Eosin (H&E) or mouse-anti-alpha-smooth muscle actin (α-SMA) (ThermoFisher scientific, US, MA5-11547, 1:500). With regard to anti-α-SMA, slides were blocked using 3% hydrogen

peroxidase and 10% donkey serum (Abcam, UK, ab7475). A secondary antibody (donkey-anti-mouse, Jackson immunoresearch, UK, 715-065-151, 1:2000 with a biotin label was used to detect the primary antibody. Lastly, an ABC kit (Vector laboratories, US, PK6100) was used to enhance the biotin label for staining, and Novared (Vector laboratories, US, SK-4800) was used to stain the slides. Histological slides were assessed and semi-qualitatively scored by two blinded observers, after which photographs were taken with a confocal scanning microscope (BX-51, Olympus, JP).

7.2.9 Statistics

GraphPad Prism version 6.01 was used (GraphPad Software inc. La Jolla, US) to analyze the data. A one-way ANOVA and two-way ANOVA with Tukey post hoc comparisons were used to compare the results between groups. Data is represented as mean ± standard deviation (SD).

7.3 Results

7.3.1 Applied concentrations of MMC during bleb-forming glaucoma surgery

To estimate the release of MMC during routine surgery in the clinic, LASIK shields were collected from 2 patients after being applied in the subconjunctival pocket for 3 minutes. It was determined that these LASIK shields released approximately 26, and 43 µL of MMC solution into the bleb. Thus, a total of 10.8 µg and 8 µg was released from the LASIK shields, respectively (based on a solution with a concentration of 0.2 mg/mL MMC in which the shields were soaked before applying them to the surgical site). Our aim was to develop a DDS with a concentration that would not exceed this concentration with its initial burst release.

7.3.2 *In vitro* release kinetics drug delivery systems

Each DDS were loaded with 35 µg of MMC. Upon dissolving unused DDSs and measuring total MMC concentrations, it was found that less MMC was available for drug release. On average 28.4 µg, and 23.0 µg of MMC was available for release in the PCL and PLGA DDS, respectively. The drug release study showed a sustained release of MMC in PBS for both DDSs. At 90 days the PCL DDS had released a total of 21.4 µg MMC (~75% of total loaded) and the PLGA DDS had released a total of 22.8 µg MMC (~99% of total loaded) (see figure 7-3A and 3B). A burst release was observed in the first 8 hours for both prototypes (Figure 7-3C). The PCL and PLGA DDS each released approximately 2.28 µg/mL and 1.42 µg/mL MMC, respectively, in the first hour. This slowly decreased to 0.17 µg/mL/hour MMC for the PCL DDS and to 0.25 µg/mL/hour MMC for the PLGA DDS after 8 hours, respectively. At day 50 until 56, a secondary burst release of MMC from the PLGA DDS was observed, potentially caused by degradation of the PLGA matrix.

Visually, the PLGA DDS increased in size (swelling of matrix) and the characteristic purple color of MMC decreased in intensity over time (less MMC crystals present in matrix) (Figure 7-3D).

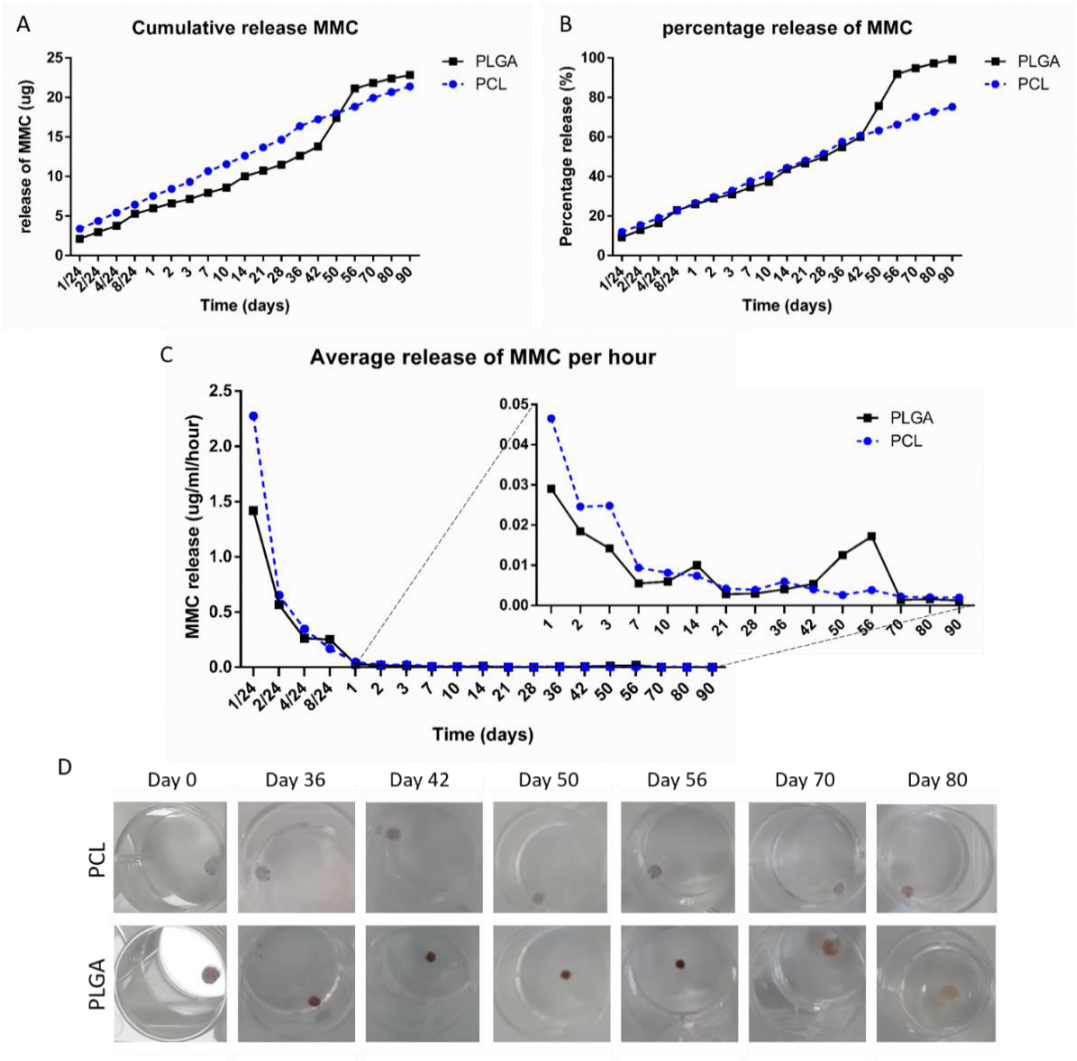

Figure 7-3: Degradation and release kinetics of a PLGA and PCL DDS (n=3 per group). (A) Cumulative release of MMC for both DDSs. (B) Average release of MMC in percentages compared to the average total of MMC available per DDS. (C) Average release kinetics of MMC per hour. (D) Photographs of the DDSs suspended in PBS up until day 80.

7.3.3 Bleb formation *in vivo*

Figure 7-4A shows the bleb formation in the rabbit's eye up to POD 90. At POD 3, increased vascularization and redness of the eye was observed in the control group, which decreased around POD 7, especially in the area where MMC was applied (see red outline in Figure 7-4A). At POD 28, the blebs appeared completely healed with a low amount of vascularization, blebs filled with aqueous humor (AqH) were clearly visible. After implantation with a DDS (both the PCL and PLGA DDS) a decreased vascularization and redness was noted around the area of the DDS (see figure 7-4A). Afterwards, rabbits implanted with a PCL DDS developed thin-walled blebs in 3 out of 5 rabbits around POD 14-21. Although 2 rabbits regained a thicker bleb wall within 28-42 days postoperative, in one rabbit the thin-walled bleb remained until POD 90. A similar thin-walled bleb was visible in the rabbits implanted with a PLGA DDS. In total, 3 out of 5 rabbits developed a thin-walled bleb between POD 7 and 14, however, these thin-walled blebs improved in thickness between POD 42 and 56. A thick dome shaped bleb was evident in the PLGA group in 2 out of 5 rabbits. Figures 7-4B and 4C show the bleb survival and the bleb survival on average. The control, PCL, and PLGA group respectively showed an average bleb survival of 81.2, 82.2, and 79.2 postoperative days (see Figure 7-3C). No significant differences were found between groups. No side effects were observed following the implantation of a DDS next to the distal end of the microshunt. All microshunts maintained their position in the AC without migrating posteriorly (Figure 7-5). Bleb function was assessed via the patency test. Three out of five control rabbits, 2 out of 5 rabbits implanted with a PCL DDS, and 4 out of 5 rabbits implanted with a PLGA DDS showed functioning blebs. A *post mortem* explantation of the DDS in one animal per group was performed to inspect degradation of the implants. Findings from these explantations showed a capsule surrounding each DDS at both POD 28 and 90. At POD 28, both DDSs remained intact. However, at POD 90 the PCL DDS was completely intact while only small fragments of the PLGA DDS were found (see online manuscript).

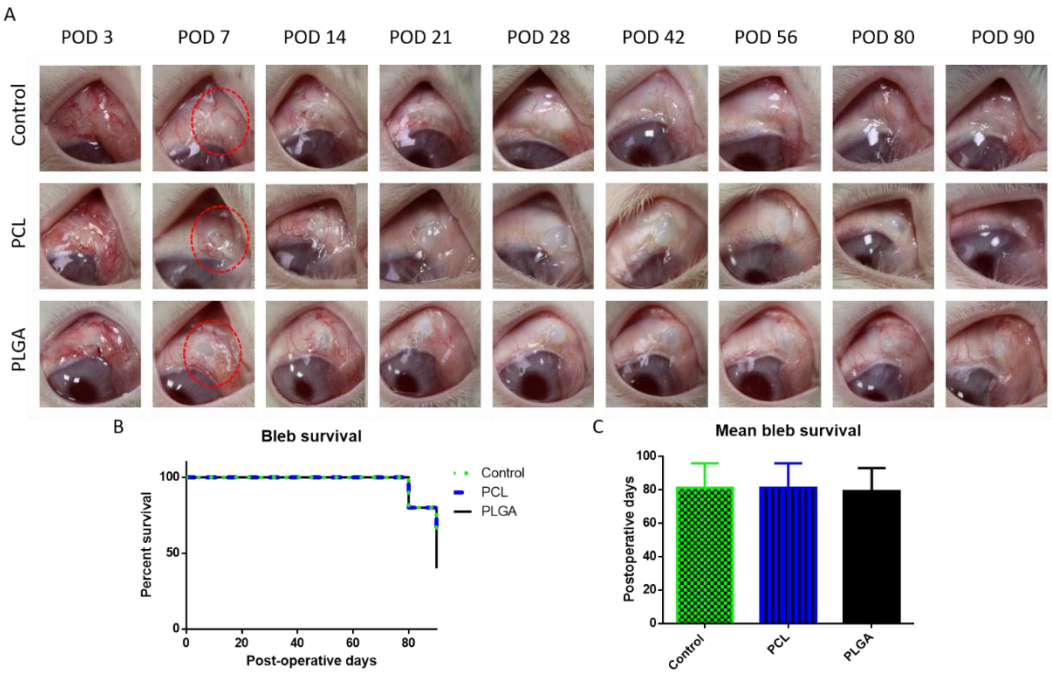

Figure 7-4: Macroscopic evaluation of bleb formation after implantation of a microshunt with either intraoperative treatment of 0.4 mg/mL MMC (control), or with implantation of a DDS (PCL or PLGA). (A) At postoperative day (POD) 3, an increased vascularization and redness was observed in all groups, which was visibly reduced around the site of MMC application at POD 7 (red outline). Thin-walled blebs developed in the groups with a DDS. However, in most cases, these were fully healed by POD 56. (B) Percentage of survival over the complete postoperative period is given within a Kaplan Meijer survival curve, survival was comparable between groups, bleb failure started around POD 80 in all groups. (C) On average, the bleb survival was comparable between all groups, control (81.2 ±13.18), PCL (81.2 ±13.18), and PLGA (79.2 ±12.43). No significant differences were found.

7.3.4 IOP measurements

We found an initial drop in IOP of 2.6 ± 0.2 mmHg, 3.9 ± 1.7 mmHg, and 1.0 ± 0.3 mmHg for the control, PCL, and PLGA group, respectively. Although no significant differences between groups were observed, a trend towards lower IOP was seen in the PCL group, potentially indicating an increased flow of AqH into the bleb (see figure 7-6).

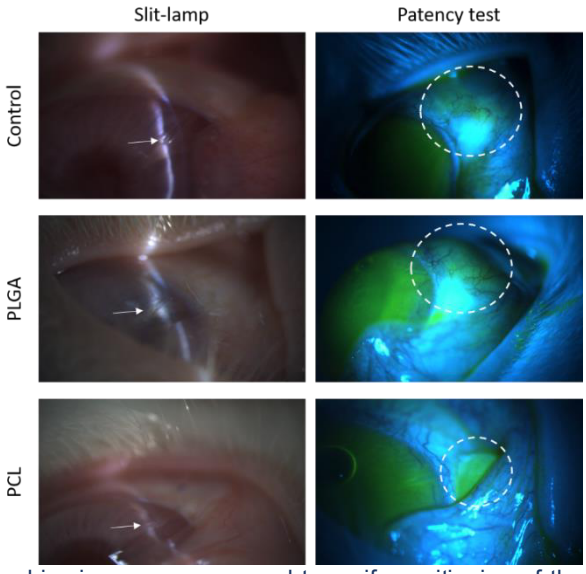

Figure 7-5: Slit-lamp biomicroscopy was used to verify positioning of the microshunt in the anterior chamber (white arrows). Additionally, the patency test was used to confirm functioning of a bleb. When a green fluorescence was noted inside the bleb (white outline), fluorescein is able to flow from the anterior chamber into the bleb.

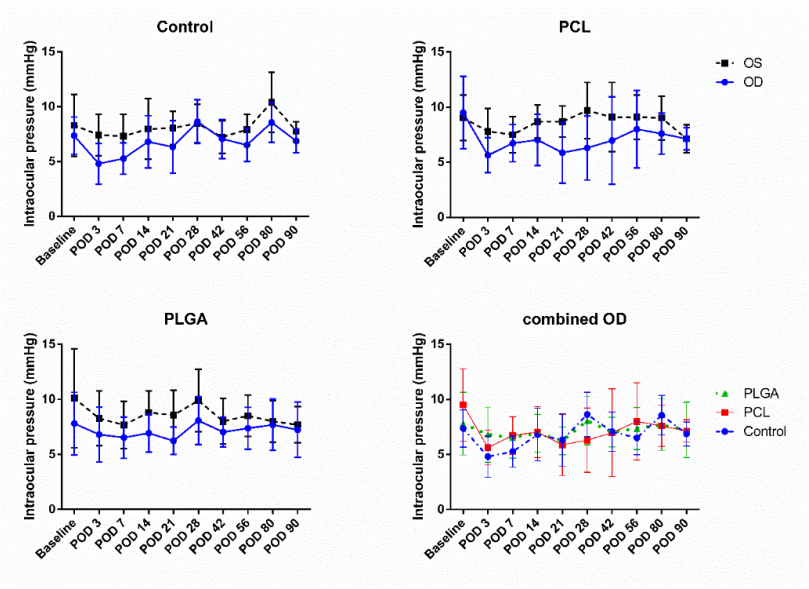

Figure 7-6: Intraocular pressure (IOP) measurements. While an initial decrease in IOP is visible (experimental eye (OD)) in all groups. No significant differences were observed between groups (n=5 per group).

7.3.5 Histology

Blebs were easily visible in the explanted rabbit's eyes. Control rabbits treated with MMC showed an edematous bleb with limited inflammation and few fibroblasts. A large dome shaped edematous bleb filled with relatively sparse collagen fibres was visible in both groups implanted with a DDS (figure 7-7). Although not significant, the bleb height was found to be increased at POD 28 and POD 90 for both the PLGA and PCL DDS compared to the control group. At POD 28, an average bleb height of 766 ± 177 µm, 1143 ± 885 µm, 1428 ± 708 µm was found for the control, PLGA, and PCL DDS, respectively. Furthermore, at POD 90 the bleb height increased further up to 810 ± 245 µm, 1488 ± 72 µm, and 1707 ± 402 µm for the control, PLGA, and PCL DDS, respectively (Figure 7-8). At POD 28, increased inflammation and neovascularization was noted in the PCL and PLGA DDS groups compared to the control. A higher inflammation was observed in the PLGA group compared to the PCL group. Interestingly, the inflammation of the PLGA group decreased at POD 90 while the inflammation in the PCL group was higher at this time point.

The DDSs were clearly encapsulated at POD 28, a high presence of fibroblasts, macrophages and PMNs were noted. Within the PLGA DDS a severe inflammation and FBR was observed at POD 28, which subsided at POD 90 where a mild inflammation and FBR was observed. Additionally, degradation of the PLGA DDS was noted at this time point. In contrast, for the PCL DDS a mild inflammation and FBR was found at POD 28 which was increased severely at POD 90 (see figure 7-9).

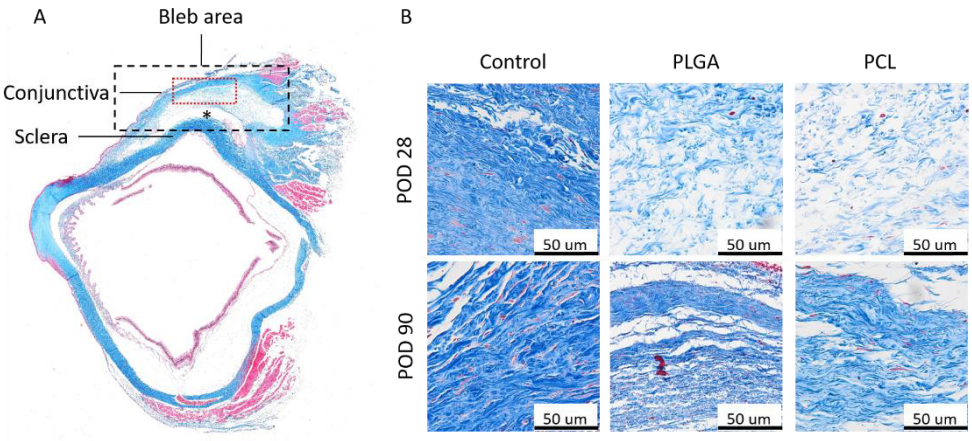

Figure 7-7: Collagen deposition inside the bleb area (black outline) with a Masson's trichrome stain. (A) Overview image of an eye implanted with a DDS (position indicated with an asterisk). (B) Within the bleb area collagen deposition was compared between the control, PLGA, and PCL group. At 28 days, the control already had a thick collagen layer in the bleb. However, some pockets were still visible where AqH could flow through. Comparatively, in the PLGA and PCL group, a loose collagen layer was visible (more edema). At POD 90 the collagen was comparable to 28 days in the control group. The collagen for the PLGA and PCL group appeared more matured and less loose collagen layers were visible. Microscopic images (figures B) were taken with a 400x magnification, scale bar represents 50 µm.

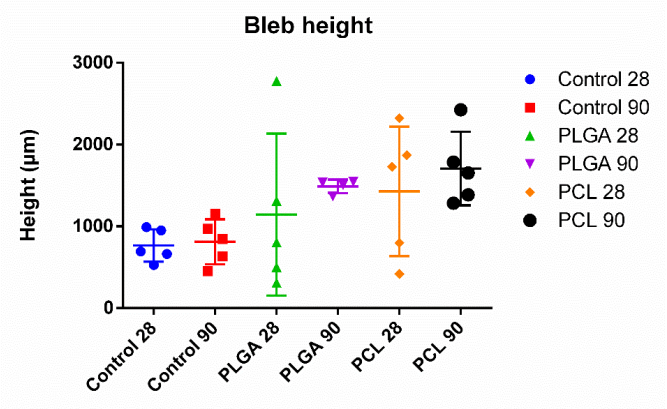

Figure 7-8: Average bleb height per group (n=5). The control group showed no major differences between POD 28 and 90. The PLGA DDS showed a variation among individual rabbits at POD 28. At POD 90 blebs appeared more synchronous between rabbits with an average bleb height of 1488 µm. The PCL DDS showed comparable results to the PLGA DDS with a high variation at POD 28 and a smaller variation at POD 90.

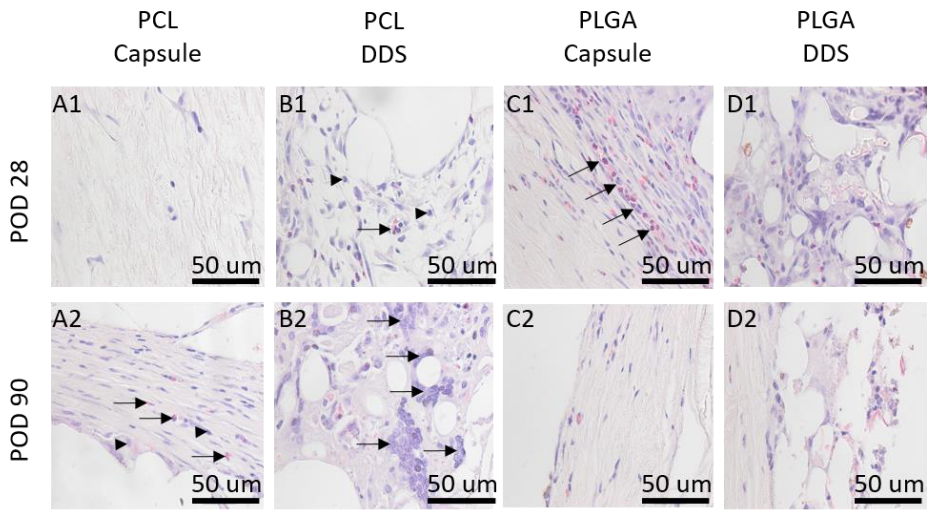

Figure 7-9: Tissue response of the DDS capsule and cellular response within the DDS meshwork at POD 28 and POD 90. (A) The PCL capsule showed limited signs of inflammation at POD 28. At POD 90, an increase in cells was visible in the capsule, predominantly fibroblasts, polymorphonuclear cells (PMNs) (arrow), and macrophages (arrowhead). (B) At POD 28, an influx of macrophages (arrowheads) and some PMNs (arrow) were visible within the DDS. Afterwards, at POD 90, a strong foreign body response was noticeable, foreign body giant cells (FBGCs) (see arrows) were easily visible within the meshwork of the DDS. Additionally, macrophages and some PMNs were still noticeable. (C) The capsule of the PLGA implant showed an increased inflammatory response compared to the PCL DDS. A strong presence of PMNs (arrows) and macrophages (arrowhead) was noted at POD 28. However, at POD 90, the inflammatory response was lowered, with only limited signs of PMNs and macrophages throughout the capsule. (D) A strong foreign body response was observed at POD 28. FBGCs along with PMNs, and macrophages were easily visible throughout the meshwork. At POD 90, the foreign body response subsided, only a limited amount of FBGCs were still visible. However, PMNs and macrophages were still found within the DDS meshwork. The scale bar represents 50 µm.

7.4 Discussion

We designed two degradable DDSs for use in bleb-forming glaucoma surgery and evaluated them both *in vitro* and *in vivo*. The DDS should be easy to handle during implantation, have a soft texture, adapt to the curvature of the eye, and have a sustained release of MMC. Rabbits were euthanized at day 28 and day 90 (these time points are commonly used [22]) and the histology surrounding the devices were investigated and compared.

In vitro results showed that the available amount of active MMC in each DDS was lower than the intended amount, suggesting that MMC potentially degraded during preparation of the DDSs [23]. Upon reconstitution, MMC solutions (protected against

light, and stored at 25˚C) were found to be stable after 8 hours. However, after 96 hours, approximately 20% of the initial MMC was degraded [24].

In vitro release kinetics for the PLGA DDS showed a release of MMC for approximately 90 days (99% was released by day 90). Due to termination of the experiment at 90 days, it is unclear if the PCL DDS (75% release at day 90) would have ultimately released all of the loaded MMC or if some of the MMC had degraded over time.

Bleb survival was comparable in all groups. Rabbits implanted with a DDS showed, macroscopically, a reduced vascularization at the location of the DDS, indicating the release and saturation of tissue with MMC. No serious adverse events such as corneal damage, scleral melt, or bleb leakage were observed. However, during follow up, a thin-walled avascular bleb developed in some rabbits implanted with a DDS between POD 7 and 21. Thin-walled blebs could have been caused by a high release of MMC, resulting in a local cytotoxic effect and thinning of the conjunctiva. Although the conjunctiva restored and thickened over time, blebs seemed to become increasingly high and encapsulated. Discomfort in the form of diplopia or bleb dysesthesia might follow due to the enlarged bleb wall pressing down on the eye. Therefore, a lower MMC concentration might be desired for future studies. Additionally, the use of 5-FU might lead to less cytotoxic side effects as it is known that 5-FU has less complication rates compared to MMC [25]. Future research should compare a sham DDS procedure to DDSs loaded with lower and higher concentrations of MMC to determine the optimum dose of MMC.

Although not significant, an increased bleb height trended in the rabbits implanted with a DDS as compared to the controls. As a larger area of the conjunctival flap was treated with MMC in the control group, the blebs tended to be more diffuse and lower than those with the DDS. The elution of MMC from the DDS to a smaller area could have led to the more elevated bleb as the MMC would be more concentrated in this area and the pressure from the aqueous humor accumulation more concentrated. However, it is unclear whether this higher more focal bleb is desired or not.

Swann *et al.* created two different PLGA based DDSs loaded with MMC called ElutiGlass [26]. They compared a slow releasing (23 to 30 days) and a fast releasing (5 to 7 days) DDS. They found that the slow releasing DDS had the strongest antifibrotic effect compared to the fast-releasing DDS and compared to the control. However, in their study control animals were treated with MMC for 45 seconds, compared to the present study, where rabbits were treated for 3 minutes intraoperatively with MMC [26]. The difference in treatment time could have contributed to the increased efficacy seen with the ElutiGlass compared to the DDSs developed in this study. Normally, a minimum of 1 minute application time is adhered to, to saturate the tissue with MMC [27]. Thus, an application time under 1 minute might not be representative to current practice.

From the present study it is unclear up to what time point both DDSs would degrade. Upon explantation at POD 28, both DDSs groups were completely intact, while at POD 90 only small fragments of the PLGA DDS remained and an intact PCL DDS was extracted. *In vitro* testing showed comparable results. Matrix swelling and some degradation (probably due to hydrolysis) was visible at day 90 for the PLGA DDS.
A strong FBR with a high number of macrophages and foreign body giant cells were observed at POD 28 for the PLGA DDS and at POD 90 for the PCL DDS. During the FBR, a unique interface between the surface of the implant and the cell membrane develops. As frustrated phagocytosis ensues, macrophages and foreign body giant cells will start to release high amounts of reactive oxygen species, enzymes, and acids (pH as low as 4 can develop due to phagolysosomes) [28]. This fibrotic reaction can have a negative effect on the wound healing response in the bleb, potentially skewing the wound healing response further into a fibrotic state [28]. Therefore, it is desirable to implant a DDS with a fast degradation rate to limit duration of the FBR.
MMC has been used in the clinic since the 1980s [3, 4]. In the United States, MMC has been approved to use intraoperatively, the approved formulation is sold as Mitosol® [4]. However, within most jurisdictions (*e.g.* , Europe and Australia), the use of MMC is still off label and unstandardized. This can lead to unreliable results concerning efficacy and safety after bleb-forming glaucoma surgery. The use of a single implantable DDS during bleb-forming glaucoma surgery will help to standardize the treatment to prevent postoperative formation of fibrosis.

7.5 Conclusion

MMC is currently often used in the clinic to limit the fibrotic response after bleb-forming glaucoma surgery. Despite its toxicity, and unstandardized method, it is still considered the gold standard worldwide. This study set out to develop a degradable sustained-release DDS loaded with MMC to replace the current gold standard treatment. By implementation of a DDS, postoperative outcomes should become more predictable, reducing vision threatening side effects associated with the current use of MMC. Additionally, ophthalmologists might be more inclined to use a DDS with a glaucoma shunt for early surgical intervention. From the two DDSs studied, the PLGA DDS showed the most promising results. At POD 90 the PLGA DDS demonstrated a 99% release of MMC *in vitro*, showed a high degradation speed with only fragments remaining *in vivo*, and induced a limited FBR compared to the PCL DDS. However, some toxicity towards the conjunctiva was noted in the early postoperative period after implantation of a DDS. Further optimization is required to minimize side effects causing thin-walled blebs, to enhance healthy bleb development, for example by lowering the total dosage, or providing a lower initial release of MMC.

References

1. Beckers, H.J., K.C. Kinders, and C.A. Webers, *Five-year results of trabeculectomy with mitomycin C.* Graefes Arch Clin Exp Ophthalmol, 2003. **241**(2): p. 106-10.
2. Wolters, J.E.J., et al., *History, presence, and future of mitomycin C in glaucoma filtration surgery.* Curr Opin Ophthalmol, 2021. **32**(2): p. 148-159.
3. Maheshwari, D., et al., *Intraoperative injection versus sponge-applied mitomycin C during trabeculectomy: One-year study.* Indian Journal of Ophthalmology, 2020. **68**(4): p. 615-619.
4. Bell, K., et al., *Learning from the past: Mitomycin C use in trabeculectomy and its application in bleb-forming minimally invasive glaucoma surgery.* Survey of Ophthalmology, 2021. **66**(1): p. 109-123.
5. Schlunck, G., et al., *Conjunctival fibrosis following filtering glaucoma surgery.* Exp Eye Res, 2016. **142**: p. 76-82.
6. Seibold, L.K., M.B. Sherwood, and M.Y. Kahook, *Wound modulation after filtration surgery.* Surv Ophthalmol, 2012. **57**(6): p. 530-50.
7. Smith, S., P.A. D'Amore, and E.B. Dreyer, *Comparative toxicity of mitomycin C and 5-fluorouracil in vitro.* Am J Ophthalmol, 1994. **118**(3): p. 332-7.
8. Jampel, H.D., *Effect of brief exposure to mitomycin C on viability and proliferation of cultured human Tenon's capsule fibroblasts.* Ophthalmology, 1992. **99**(9): p. 1471-6.
9. Coppens, G. and P. Maudgal, *Corneal complications of intraoperative Mitomycin C in glaucoma surgery.* Bull Soc Belge Ophtalmol, 2010. **314**: p. 19-23.
10. Jongsareejit, B., et al., *Efficacy and complications after trabeculectomy with mitomycin C in normal-tension glaucoma.* Japanese journal of ophthalmology, 2005. **49**(3): p. 223-227.
11. Hung, P., *Mitomycin-C in Glaucoma Filtering Surgery.* Asian Journal of OPHTHALMOLOGY and Asia-Pacific Journal of Ophthalmology, 2000. **2**.
12. Ghoneim, E., *Needle Revision with Antimetabolites in Bleb Failure.* J Clin Res Ophthalmol 2 (1): 007-009. DOI: 10.17352/2455, 2015. **1414**(007).
13. Alvarado, J.A., et al., *Ahmed Valve Implantation with Adjunctive Mitomycin C and 5-Fluorouracil: Long-term Outcomes.* American Journal of Ophthalmology, 2008. **146**(2): p. 276-284.e2.
14. van Mechelen, R.J.S., et al., *Animal models and drug candidates for use in glaucoma filtration surgery: A systematic review.* Exp Eye Res, 2022. **217**: p. 108972.
15. Kim, J., et al., *Fabrication and Characterization of Bioresorbable Drug-coated Porous Scaffolds for Vascular Tissue Engineering.* Materials (Basel), 2019. **12**(9).
16. Espinoza, S.M., et al., *Poly-ε-caprolactone (PCL), a promising polymer for pharmaceutical and biomedical applications: Focus on nanomedicine in cancer.* International Journal of Polymeric Materials and Polymeric Biomaterials, 2020. **69**(2): p. 85-126.
17. Kapoor, D.N., et al., *PLGA: a unique polymer for drug delivery.* Ther Deliv, 2015. **6**(1): p. 41-58.
18. Makadia, H.K. and S.J. Siegel, *Poly Lactic-co-Glycolic Acid (PLGA) as Biodegradable Controlled Drug Delivery Carrier.* Polymers (Basel), 2011. **3**(3): p. 1377-1397.
19. Mir, M., N. Ahmed, and A.U. Rehman, *Recent applications of PLGA based nanostructures in drug delivery.* Colloids Surf B Biointerfaces, 2017. **159**: p. 217-231.
20. Xu, Y., et al., *Polymer degradation and drug delivery in PLGA-based drug-polymer applications: A review of experiments and theories.* J Biomed Mater Res B Appl Biomater, 2017. **105**(6): p. 1692-1716.
21. van Mechelen, R.J.S., et al., *Wound Healing Response After Bleb-Forming Glaucoma Surgery With a SIBS Microshunt in Rabbits.* Transl Vis Sci Technol, 2022. **11**(8): p. 29.
22. Schwartz, R.S., et al., *Drug-eluting stents in preclinical studies: updated consensus recommendations for preclinical evaluation.* Circ Cardiovasc Interv, 2008. **1**(2): p. 143-53.
23. Kinast, R.M., et al., *The Degradation of Mitomycin C Under Various Storage Methods.* Journal of Glaucoma, 2016. **25**(6): p. 477-481.
24. Briot, T., et al., *Stability of Reconstituted and Diluted Mitomycin C Solutions in Polypropylene Syringes and Glass Vials.* Pharmaceutical Technology in Hospital Pharmacy, 2016. **1**(2): p. 83-89.
25. Chen, X., et al., *Safety and Efficacy of Bleb Needling with Antimetabolite after Trabeculectomy Failure in Glaucoma Patients: A Systemic Review and Meta-Analysis.* Journal of Ophthalmology, 2020. **2020**.

26. Swann, F.B., et al., *Effect of 2 Novel Sustained-release Drug Release Systems on Bleb Fibrosis: An In Vivo Trabeculectomy Study in a Rabbit Model.* J Glaucoma, 2019. **28**(6): p. 512-518.
27. Al Habash, A., et al., *A review of the efficacy of mitomycin C in glaucoma filtration surgery.* Clin Ophthalmol, 2015. **9**: p. 1945-51.
28. Anderson, J.M., A. Rodriguez, and D.T. Chang, *Foreign body reaction to biomaterials.* Semin Immunol, 2008. **20**(2): p. 86-100.

Chapter 8

General discussion

8. General discussion

Glaucoma has a high burden on the quality of life of a patient. A decrease in quality of life is already observed in early stages of the disease as it affects daily features of a patient's life, such as walking and reading [1]. As vision worsens, patients experience a high psychological burden due to fear of blindness, depression, and social withdrawal caused by impaired vision [2]. Currently, there are several treatment strategies, documented in guidelines in a step-up protocol that usually starts with medication (often eye drops) and/or laser therapy, and possibly followed by incisional glaucoma filtration surgery, to reduce progression of glaucomatous field loss [3]. Each treatment aims to reduce intraocular pressure (IOP). During bleb-forming glaucoma surgery, the outflow of aqueous humor (AqH) is increased by bypassing the trabecular meshwork and thereby reducing IOP. This can be accomplished by tube-shunt surgery or a trabeculectomy (currently still considered the gold standard) [3]. However, the success rate of bleb-forming glaucoma surgery is often hampered by the formation of fibrotic tissue within the bleb. The introduction of the antimetabolite mitomycin C (MMC) in bleb-forming glaucoma surgery (several decades ago) resulted in an increased success rate [4, 5]. However, its use has also been associated with possibly severe vision threatening complications [6-14]. Despite the usage of MMC, bleb-forming glaucoma surgeries still tend to fail. Annually, approximately 10% of surgeries fail due to fibrosis, and reoperation is reported to be needed in 29%, 9%, and 11.5% of patients after a trabeculectomy, tube-shunt surgery, and microshunt implantation, respectively [15-18]. Therefore, novel treatment modalities are continuously sought after to reduce postoperative failure rates.

During this project we set out to develop novel biomedical devices and methods for use in bleb-forming glaucoma surgery. The work presented in this dissertation was divided into three sub-goals. Firstly, validation of an animal model for glaucoma surgery research. Secondly, development of a novel glaucoma drainage device. Lastly, development of a sustained drug delivery system loaded with MMC.

8.1 Glaucoma surgery animal models

Animal models are invaluable tools within research. They have been used to study novel treatments and the underlying molecular mechanisms regarding the fibrotic response in bleb-forming glaucoma surgery. However, the translation from animal (model) to human can be burdensome, and high failure rates in treatments are encountered [19, 20]. In **Chapter 2**, a systematic review was conducted to provide an outline of the use of animal models within glaucoma surgery research. A multitude of animals have been used for glaucoma surgery research. This systematic review

showed that small rodents and rabbits are the preferred animal models to use for this purpose.
Small rodents (such as mice and rats) are preferred to study the fibrotic response after bleb-forming glaucoma surgery and to test drug candidates, because of the availability of molecular tools. Unfortunately, the size of their eye limits the use of these animals. On the other hand, rabbits have large eyes, making them ideal for testing novel medical devices. Nonetheless, a downside of currently used glaucoma surgery animal models is that they do not mimic the complete human pathology. Recent research has shown that the AqH of glaucoma patients contains a higher number of several growth factors and cytokines, *e.g.*, transforming growth factor-β, and tissue necrosis factor-α. These proteins may contribute to the fibrotic response after surgery [5, 21]. Therefore, translation of GFS animal models might benefit from the induction of glaucoma beforehand. A few examples to induce glaucoma are intracameral injection of beads or microspheres, episcleral vein cauterization, or laser photocoagulation [22-24]. When successfully optimized, a higher translation of treatments from animal to patient might be observed.

Standardization of animal models and protocols within research is key to minimize variation across animal research worldwide. Several guidelines have already been prepared and made available for researchers, such as the ARRIVE and the PREPARE guidelines for the reporting and preparation of an animal experiment [25, 26]. Furthermore, the national center for the replacement, refinement and reduction of animals in research (NC3R) has standard operating procedures freely available on their website [27]. However, further standardization within animal research is required to increase reproducibility and reliability across different research groups worldwide. One example is the use of tonometers within animal research. A variety of tonometers are available to measure IOP in animals. **In chapter 3**, the reproducibility, repeatability, and agreement of three tonometers that are routinely used within animal research, were compared. From the tested tonometers, the TonoVet showed the smallest inter- and intra-observer variations in rabbits and had no learning curve. Furthermore, a ~25% reduction in IOP was found after rabbits were sedated with medetomidine. Unfortunately, since no glaucoma was induced in the currently used animal models, IOP variations were limited (including this present study). Therefore, IOP alone is an unreliable readout parameter to monitor fibrosis and bleb survival in an animal model of glaucoma surgery in which no glaucoma (increased IOP) has been induced [28, 29].

8.2 Microshunt development

Glaucoma implants drain AqH from the anterior chamber into a bleb to relieve pressure inside of the eye. Over the years, several types of materials have been

used to develop glaucoma implants [30]. Conventional long-tube glaucoma implants all have a silicone tube (the part entering the anterior chamber of the eye), and an endplate usually made of silicone (Baerveldt) or polypropylene/polypropylene (some Ahmed or Molteno models) [30]. The PRESERFLO® MicroShunt was developed by InnFocus Inc., now a Santen company. It is made from poly(styrene-block-isobutylene-block-styrene) (SIBS). SIBS is a biocompatible thermoplastic elastomeric material, which induces less fibrosis compared to silicone [31]. However, even with the use of MMC, bleb fibrosis still occurs in patients [32, 33]. Although the PRESERFLO® MicroShunt induces less cases of hypotony and requires less postoperative intervention, *Baker et al.* showed in a recent head-to-head comparison that it unfortunately still has a lower success rate, higher IOP outcome, and higher postoperative medication burden compared to the conventional trabeculectomy [34]. In our current project, we set out to develop a novel SIBS-based microshunt that induces less fibrosis, by looking for different implant designs.

To validate our rabbit model and find potential therapeutic targets related to bleb fibrosis after implantation with a SIBS-based microshunt, rabbits were implanted with a PRESERFLO® MicroShunt **(chapter 4)**. Blebs were macroscopically visible up until postoperative week 2, which was comparable to literature [35-37]. Histologically, an influx of a high variety of cells such as monocytes/macrophages, polymorphonuclear cells (PMNs), FBGCs, fibroblasts, and myofibroblasts were observed around the MicroShunt and within the bleb. Additionally, increased proliferation of epithelial cells was found. Based on these results, inhibition of the inflammatory response and the downregulation of fibroblasts can offer novel therapeutic avenues to downregulate both the fibrotic response and foreign body response towards a SIBS-based implant.

Within this dissertation, several methods to extend bleb survival were evaluated. First, the use of tissue modifying/stimulating surface topographies **(chapter 5)**. Surface topographies have been shown to augment cellular response towards a material *in vitro* [38]. Therefore, we hypothesized that the implementation of antifibrotic surface topographies could help in reducing the fibrotic response towards a material and thereby reduce bleb failure *in vivo*. Unfortunately, due to COVID-19 regulations, *in vitro* research was delayed. Therefore, instead of performing an *in vitro* screening with SIBS to select viable surface topographies, literature, and prior experience with surface topographies on different materials such as polypropylene and silicone were used to select three viable surface topographies to implement onto a SIBS microshunt. Surface topographies were incorporated on a modified PRESERFLO® MicroShunt to which an endplate was added and compared to the standard PRESERFLO® MicroShunt (without endplate). As a control, a modified PRESERFLO® MicroShunt with a smooth surface endplate was used.

The addition of an endplate onto the SIBS microshunt resulted in extended bleb survival. Blebs remained visible until approximately week 3 postoperatively. Furthermore, one topography (Topo-990) showed the longest bleb survival; blebs remained visible until the day of euthanization (day 30). However, due to the low sample size (n=3) it cannot yet offer definite proof whether this is caused by the surface topography. The addition of an endplate with a smooth surface induced an increased amount of PMNs, macrophages, fibroblasts, and slight increase of bleb capsule thickness compared to the standard PRESERFLO® MicroShunt. This might be caused by the increased size of the implant [39]. Surface topographies induced an even higher influx of inflammatory cells and increased bleb capsule thickness compared to a smooth surface. Therefore, it seems that encapsulation and fibrosis can increase when improper surface topographies are used on an implant. Possibly due to the increase of the total surface area and roughness of an implant [39, 40].
From the three surface topographies tested, it remains unclear whether the addition of a surface topography will be beneficial for bleb-forming glaucoma surgery. An endplate with a smooth surface induced less inflammation and encapsulation compared to the tested surface topographies. Additionally, a smooth surface extended bleb survival when compared to the current PRESERFLO® MicroShunt without endplate. *In vitro* selection of viable surface topographies with SIBS is necessary to further select viable topographies for future use. This research is now undertaken by our current consortium (beyond the scope of this thesis).

8.4 Antifibrotic therapies

Since the introduction of MMC in the 1980s, it became the gold standard antifibrotic medication to use in bleb-forming glaucoma surgery. Despite being highly effective, use of MMC for bleb-forming glaucoma surgery is in most parts of the world, with exception of the United States of America, off-label. The FDA-approved formulation of MMC in the USA is Mitosol [41]. Usage of MMC decreased the failure rate of bleb-forming glaucoma surgery to approximately 10% within the first postoperative year, but MMC also has known toxic side effects [15, 42, 43] Therefore, novel antifibrotic drugs that can offer a higher safety profile compared to MMC, and have a comparable, or preferably higher, antifibrotic efficacy are sought after to improve the success rate of bleb-forming glaucoma surgery.

During the research for this dissertation two different approaches to improve upon the current antifibrotic drug therapies were evaluated. Firstly, development of novel drugs. Novel drugs often aim to influence the fibrotic response in a more specific manner compared to MMC (*e.g.*, by targeting TGF-β). In **chapter 2**, drugs that have been studied *in vivo* were systematically reviewed. While most drugs have a lower

toxicity compared to MMC, they often have a lower efficacy. Therefore, further research should focus on the optimization or refinement of novel drugs by optimizing the dosage, route of administration, application frequency, and development of combination therapies or novel drug delivery systems [44-49].
Refinement of the current MMC usage might be, for the time being, a better solution [50]. At the moment, several drug delivery systems (DDSs) loaded with an antimetabolite are being developed by other parties (see **chapter 6** for a complete overview) [51-69]. The work presented in this thesis aimed to develop a DDS loaded with MMC, to prevent postoperative fibrosis that would outperform the current gold standard one-time intra-operative application of MMC.

Two new (bio)degradable DDSs were developed and compared in **chapter 7**. Chosen prototypes were selected based on the texture, handling, and MMC release kinetics. Additionally, implants had to adjust to the circumference of the eye (have a certain flexibility). As a carrier, polycaprolactone (PCL) or poly-lactic-co-glycolic acid (PLGA) were used. Both carrier polymers showed a comparable bleb survival when compared to the gold standard treatment of MMC *in vivo*. After 90 days, the PLGA DDS released 99% of MMC *in vitro* and a higher degradation rate was observed when compared to PCL. Furthermore, DDSs with PLGA induced a shorter foreign body response compared to DDSs with PCL. However, animals implanted with a DDS developed a localized thin-walled bleb. Either caused by toxic side effects towards the conjunctiva from the release of MMC or the localized diffusion of AqH into the bleb forming a “ring of steel” causing thin walled blebs [70]. Further optimization regarding dosage, release, and dispersion of MMC will be required to minimize side effects and enhance healthy bleb development.

Postoperative outcomes can become more predictable in the future, by implementation of a DDS, vision-threatening complications can possibly be reduced. These improvements are further steps towards an increased safety profile of bleb-forming glaucoma surgery. Hopefully, this may lead to further acceptance of these procedures by both ophthalmologists and patients. If this happens, societies can make the move towards earlier implementation of bleb-forming surgery in the treatment armamentarium.

The clinical and economic impact of the research conducted for this dissertation is discussed in c**hapter 9**.

References

1. McKean-Cowdin, R., et al., *Severity of visual field loss and health-related quality of life.* Am J Ophthalmol, 2007. **143**(6): p. 1013-23.
2. Varma, R., et al., *An assessment of the health and economic burdens of glaucoma.* Am J Ophthalmol, 2011. **152**(4): p. 515-22.
3. *European Glaucoma Society Terminology and Guidelines for Glaucoma, 5th Edition.* Br J Ophthalmol, 2021. **105**(Suppl 1): p. 1-169.
4. Wolters, J.E.J., et al., *History, presence, and future of mitomycin C in glaucoma filtration surgery.* Curr Opin Ophthalmol, 2021. **32**(2): p. 148-159.
5. Schlunck, G., et al., *Conjunctival fibrosis following filtering glaucoma surgery.* Exp Eye Res, 2016. **142**: p. 76-82.
6. Conlon, R., H. Saheb, and I.I.K. Ahmed, *Glaucoma treatment trends: a review.* Canadian Journal of Ophthalmology, 2017. **52**(1): p. 114-124.
7. Lusthaus, J. and I. Goldberg, *Current management of glaucoma.* Medical Journal of Australia, 2019. **210**(4): p. 180-187.
8. Chen, D.Z. and C.C.A. Sng, *Safety and Efficacy of Microinvasive Glaucoma Surgery.* J Ophthalmol, 2017. **2017**: p. 3182935.
9. Busch, T., et al., *Learning Curve and One-Year Outcome of XEN 45 Gel Stent Implantation in a Swedish Population.* Clinical ophthalmology (Auckland, N.Z.), 2020. **14**: p. 3719-3733.
10. Theilig, T., et al., *Comparing the efficacy of trabeculectomy and XEN gel microstent implantation for the treatment of primary open-angle glaucoma: a retrospective monocentric comparative cohort study.* Scientific reports, 2020. **10**(1): p. 19337-19337.
11. Quaranta, L., et al., *Efficacy and Safety of PreserFlo(®) MicroShunt After a Failed Trabeculectomy in Eyes with Primary Open-Angle Glaucoma: A Retrospective Study.* Advances in therapy, 2021. **38**(8): p. 4403-4412.
12. Gillmann, K. and K. Mansouri, *Minimally Invasive Glaucoma Surgery: Where Is the Evidence?* Asia Pac J Ophthalmol (Phila), 2020. **9**(3): p. 203-214.
13. Coppens, G. and P. Maudgal, *Corneal complications of intraoperative Mitomycin C in glaucoma surgery.* Bull Soc Belge Ophtalmol, 2010(314): p. 19-23.
14. Jongsareejit, B., et al., *Efficacy and complications after trabeculectomy with mitomycin C in normal-tension glaucoma.* Jpn J Ophthalmol, 2005. **49**(3): p. 223-7.
15. Beckers, H.J., K.C. Kinders, and C.A. Webers, *Five-year results of trabeculectomy with mitomycin C.* Graefes Arch Clin Exp Ophthalmol, 2003. **241**(2): p. 106-10.
16. Patel, S. and L.R. Pasquale, *Glaucoma drainage devices: a review of the past, present, and future.* Semin Ophthalmol, 2010. **25**(5-6): p. 265-70.
17. Gedde, S.J., et al., *Treatment outcomes in the Tube Versus Trabeculectomy (TVT) study after five years of follow-up.* Am J Ophthalmol, 2012. **153**(5): p. 789-803.e2.
18. Tanner, A., et al., *One-year surgical outcomes of the PreserFlo MicroShunt in glaucoma: a multicentre analysis.* British Journal of Ophthalmology, 2022: p. bjophthalmol-2021-320631.
19. Pound, P. and M. Ritskes-Hoitinga, *Is it possible to overcome issues of external validity in preclinical animal research? Why most animal models are bound to fail.* J Transl Med, 2018. **16**(1): p. 304.
20. Ferri, N., et al., *Drug attrition during pre-clinical and clinical development: understanding and managing drug-induced cardiotoxicity.* Pharmacol Ther, 2013. **138**(3): p. 470-84.
21. Kaeslin, M.A., et al., *Changes to the Aqueous Humor Proteome during Glaucoma.* PLoS One, 2016. **11**(10): p. e0165314.
22. Ngumah, Q.C., S.D. Buchthal, and R.F. Dacheux, *Longitudinal non-invasive proton NMR spectroscopy measurement of vitreous lactate in a rabbit model of ocular hypertension.* Exp Eye Res, 2006. **83**(2): p. 390-400.
23. Morgan, J.E. and J.R. Tribble, *Microbead models in glaucoma.* Exp Eye Res, 2015. **141**: p. 9-14.
24. Evangelho, K., C.A. Mastronardi, and A. de-la-Torre, *Experimental Models of Glaucoma: A Powerful Translational Tool for the Future Development of New Therapies for Glaucoma in Humans-A Review of the Literature.* Medicina (Kaunas), 2019. **55**(6).
25. Kilkenny, C., et al., *Animal research: reporting in vivo experiments: the ARRIVE guidelines.* J Gene Med, 2010. **12**(7): p. 561-3.
26. Smith, A.J., et al., *PREPARE: guidelines for planning animal research and testing.* Lab Anim, 2018. **52**(2): p. 135-141.

27. Research, N.C.f.t.R.R.R.o.A.i. 2022 [cited 2022 19-12-2022]; Available from: https://www.nc3rs.org.uk/.
28. Bertens, C.J.F., et al., *Repeatability, reproducibility, and agreement of three tonometers for measuring intraocular pressure in rabbits.* Sci Rep, 2021. **11**(1): p. 19217.
29. van Mechelen, R.J.S., et al., *Wound Healing Response After Bleb-Forming Glaucoma Surgery With a SIBS Microshunt in Rabbits.* Transl Vis Sci Technol, 2022. **11**(8): p. 29.
30. Pereira, I.C.F., et al., *Conventional glaucoma implants and the new MIGS devices: a comprehensive review of current options and future directions.* Eye (Lond), 2021. **35**(12): p. 3202-3221.
31. Acosta, A.C., et al., *A newly designed glaucoma drainage implant made of poly(styrene-b-isobutylene-b-styrene): biocompatibility and function in normal rabbit eyes.* Arch Ophthalmol, 2006. **124**(12): p. 1742-9.
32. Batlle, J.F., A. Corona, and R. Albuquerque, *Long-term Results of the PRESERFLO MicroShunt in Patients With Primary Open-angle Glaucoma From a Single-center Nonrandomized Study.* J Glaucoma, 2021. **30**(3): p. 281-286.
33. Scheres, L.M.J., et al., *XEN(®) Gel Stent compared to PRESERFLO™ MicroShunt implantation for primary open-angle glaucoma: two-year results.* Acta Ophthalmol, 2021. **99**(3): p. e433-e440.
34. Baker, N.D., et al., *Ab-Externo MicroShunt versus Trabeculectomy in Primary Open-Angle Glaucoma: One-Year Results from a 2-Year Randomized, Multicenter Study.* Ophthalmology, 2021. **128**(12): p. 1710-1721.
35. Sherwood, M.B., et al., *A new model of glaucoma filtering surgery in the rat.* J Glaucoma, 2004. **13**(5): p. 407-12.
36. SooHoo, J.R., et al., *Bleb morphology and histology in a rabbit model of glaucoma filtration surgery using Ozurdex(R) or mitomycin-C.* Mol Vis, 2012. **18**: p. 714-9.
37. Doyle, J.W., et al., *Intraoperative 5-fluorouracil for filtration surgery in the rabbit.* Invest Ophthalmol Vis Sci, 1993. **34**(12): p. 3313-9.
38. Vassey, M.J., et al., *Immune Modulation by Design: Using Topography to Control Human Monocyte Attachment and Macrophage Differentiation.* Advanced Science, 2020. **7**(11): p. 1903392.
39. Wilcox, M. and O.A. Kadri, *Force and geometry determine structure and function of glaucoma filtration capsules.* Ophthalmologica, 2007. **221**(4): p. 238-43.
40. Choritz, L., et al., *Surface topographies of glaucoma drainage devices and their influence on human tenon fibroblast adhesion.* Invest Ophthalmol Vis Sci, 2010. **51**(8): p. 4047-53.
41. Bell, K., et al., *Learning from the past: Mitomycin C use in trabeculectomy and its application in bleb-forming minimally invasive glaucoma surgery.* Survey of Ophthalmology, 2021. **66**(1): p. 109-123.
42. Coppens, G. and P. Maudgal, *Corneal complications of intraoperative Mitomycin C in glaucoma surgery.* Bull Soc Belge Ophtalmol, 2010. **314**: p. 19-23.
43. Jongsareejit, B., et al., *Efficacy and complications after trabeculectomy with mitomycin C in normal-tension glaucoma.* Japanese journal of ophthalmology, 2005. **49**(3): p. 223-227.
44. Van Bergen, T., et al., *The Combination of PlGF Inhibition and MMC as a Novel Anti-Scarring Strategy for Glaucoma Filtration Surgery.* Invest Ophthalmol Vis Sci, 2016. **57**(10): p. 4347-55.
45. Sherwood, M.B., *A sequential, multiple-treatment, targeted approach to reduce wound healing and failure of glaucoma filtration surgery in a rabbit model (an American Ophthalmological Society thesis).* Trans Am Ophthalmol Soc, 2006. **104**: p. 478-92.
46. Martorana, G.M., et al., *Sequential Therapy with Saratin, Bevacizumab and Ilomastat to Prolong Bleb Function following Glaucoma Filtration Surgery in a Rabbit Model.* PLoS One, 2015. **10**(9): p. e0138054.
47. Kim, T.H., et al., *Co-treatment of suberoylanilide hydroxamic acid and mitomycin-C induces the apoptosis of rabbit tenon's capsule fibroblast and improves the outcome of glaucoma filtration surgery.* Curr Eye Res, 2008. **33**(3): p. 237-45.
48. Zuo, L., J. Zhang, and X. Xu, *Combined Application of Bevacizumab and Mitomycin C or Bevacizumab and 5-Fluorouracil in Experimental Glaucoma Filtration Surgery.* J Ophthalmol, 2018. **2018**: p. 8965709.
49. Andres-Guerrero, V., et al., *The Effect of a Triple Combination of Bevacizumab, Sodium Hyaluronate and a Collagen Matrix Implant in a Trabeculectomy Animal Model.* Pharmaceutics, 2021. **13**(6).

50. Alvarado, J.A., et al., *Ahmed Valve Implantation with Adjunctive Mitomycin C and 5-Fluorouracil: Long-term Outcomes.* American Journal of Ophthalmology, 2008. **146**(2): p. 276-284.e2.
51. Sahiner, N., et al., *Creation of a drug-coated glaucoma drainage device using polymer technology: in vitro and in vivo studies.* Arch Ophthalmol, 2009. **127**(4): p. 448-53.
52. Schoenberg, E.D., et al., *Effect of Two Novel Sustained-Release Drug Delivery Systems on Bleb Fibrosis: An In Vivo Glaucoma Drainage Device Study in a Rabbit Model.* Transl Vis Sci Technol, 2015. **4**(3): p. 4.
53. Merritt, S.R., G. Velasquez, and H.A. von Recum, *Adjustable release of mitomycin C for inhibition of scar tissue formation after filtration surgery*. Exp Eye Res, 2013. **116**: p. 9-16.
54. Ponnusamy, T., et al., *A novel antiproliferative drug coating for glaucoma drainage devices.* J Glaucoma, 2014. **23**(8): p. 526-34.
55. Li, H., et al., *Synthesis and biological evaluation of a cross-linked hyaluronan-mitomycin C hydrogel.* Biomacromolecules, 2004. **5**(3): p. 895-902.
56. Liu, Y., et al., *Crosslinked hyaluronan hydrogels containing mitomycin C reduce postoperative abdominal adhesions.* Fertil Steril, 2005. **83 Suppl 1**: p. 1275-83.
57. Xi, L., et al., *Evaluation of an injectable thermosensitive hydrogel as drug delivery implant for ocular glaucoma surgery.* PLoS One, 2014. **9**(6): p. e100632.
58. Donin, N.M., et al., *Sustained-release Formulation of Mitomycin C to the Upper Urinary Tract Using a Thermosensitive Polymer: A Preclinical Study.* Urology, 2017. **99**: p. 270-277.
59. Donin, N.M., et al., *Serial retrograde instillations of sustained release formulation of mitomycin C to the upper urinary tract of the Yorkshire swine using a thermosensitive polymer: Safety and feasibility.* Urol Oncol, 2017. **35**(5): p. 272-278.
60. Kimura, H., et al., *Injectable microspheres with controlled drug release for glaucoma filtering surgery.* Invest Ophthalmol Vis Sci, 1992. **33**(12): p. 3436-41.
61. Paula, J.S., et al., *Bevacizumab-loaded polyurethane subconjunctival implants: effects on experimental glaucoma filtration surgery.* J Ocul Pharmacol Ther, 2013. **29**(6): p. 566-73.
62. Du, L.Q., et al., *Effect of poly(DL-lactide-co-glycolide) on scar formation after glaucoma filtration surgery.* Chin Med J (Engl), 2013. **126**(23): p. 4528-35.
63. Swann, F.B., et al., *Effect of 2 Novel Sustained-release Drug Release Systems on Bleb Fibrosis: An In Vivo Trabeculectomy Study in a Rabbit Model.* J Glaucoma, 2019. **28**(6): p. 512-518.
64. Ang, M., et al., *Evaluation of sustained release of PLC-loaded prednisolone acetate microfilm on postoperative inflammation in an experimental model of glaucoma filtration surgery.* Curr Eye Res, 2011. **36**(12): p. 1123-8.
65. Kojima, S., et al., *Effects of gelatin hydrogel containing chymase inhibitor on scarring in a canine filtration surgery model.* Invest Ophthalmol Vis Sci, 2011. **52**(10): p. 7672-80.
66. Liang, L., et al., *Prevention of filtering surgery failure by subconjunctival injection of a novel peptide hydrogel into rabbit eyes.* Biomed Mater, 2010. **5**(4): p. 045008.
67. Kojima, S., et al., *Effects of Gelatin Hydrogel Loading Mitomycin C on Conjunctival Scarring in a Canine Filtration Surgery Model.* Invest Ophthalmol Vis Sci, 2015. **56**(4): p. 2601-5.
68. Maeda, M., et al., *Effects of Gelatin Hydrogel Containing Anti-Transforming Growth Factor-beta Antibody in a Canine Filtration Surgery Model.* Int J Mol Sci, 2017. **18**(5).
69. Han, Q., et al., *Effects of bevacizumab loaded PEG-PCL-PEG hydrogel intracameral application on intraocular pressure after glaucoma filtration surgery*. J Mater Sci Mater Med, 2015. **26**(8): p. 225.
70. Cordeiro, M.F., et al., *Effect of varying the mitomycin-C treatment area in glaucoma filtration surgery in the rabbit.* Invest Ophthalmol Vis Sci, 1997. **38**(8): p. 1639-46.

Chapter 9

Impact

9. Impact

Glaucoma, a degenerative disease of the optic nerve, is the second leading cause of blindness worldwide, and the leading cause of irreversible blindness. Approximately 65 million people suffered from glaucoma in 2020 [1]. Due to the aging population (that continues to grow) and the rise in risk factors such as myopia, diabetes and high blood pressure, it is expected that 112 million people will be affected by 2040 [1]. All current treatments aim to halt visual field loss by lowering intraocular pressure (IOP), the main risk factor for glaucoma, as a causative (neuroprotective) treatment is still unavailable [2]. Usually, a step-up approach is chosen in which is started with medical and/or laser therapy, reserving surgery for advanced cases. However, this may lead to suboptimal treatment as, even in the Western world, 10% of patients' progress to bilateral blindness during their lifetime [3]. Bleb-forming filtering surgeries have the highest IOP reducing potential, but they also require intense follow-up and have known complications. Additionally, substantial surgical skills are needed to obtain satisfactory results. As a result, surgical treatment is often postponed, as both ophthalmologists and patients are reluctant to choose this option.

An important problem with all bleb-forming surgeries is the high postoperative failure rate, which is predominantly caused by the fibrotic response in the filtering bleb. In this dissertation, we have investigated novel methods to reduce the failure rate and searched for more reliable and safer treatment options to further optimize bleb-forming glaucoma surgery. The research presented may not only be beneficial for glaucoma patients, but also for ophthalmologists/physicians, surgeons, scientists, laboratory animals, and the healthcare system.

9.1 Animal models and standardization

Before a drug or a medical device can be introduced into the clinic, it needs to be validated within an animal model. Researchers are both legally and ethically required to test a treatment within an animal model before further use in patients is allowed [4]. Despite the required preclinical validation, high attrition rates are encountered within drug development [5], which are partly accountable to the translational failure from an animal model towards humans [6]. Currently, animal research faces a lot of scrutiny due to changes in society. Ethics related to animal welfare have significantly improved during the last decade, and the process of acquiring approval to conduct a study with animals as test subjects has been intensified and regulated more strictly. In **chapter 2**, animal models that have been used for glaucoma filtration surgery research were reviewed. Throughout the years, a multitude of animals such as rats, mice, hamsters, rabbits, dogs, etc. have been used. Each animal model has its own strengths and limitations which need to be carefully considered before the onset of

an animal study. The systematic review within this thesis will help research groups with setting up their animal study and choosing the appropriate animal model for their specific research question. With a proper selection and set-up of an animal study, less animals will have to be used for research.
Currently, there is a lack of standardization between research groups worldwide regarding *in vivo* research, making it difficult to interpret and compare results between studies. Furthermore, different readout parameters, experimental protocols, and welfare requirements can affect the reproducibility and reliability of results. To reduce variation among research groups, it is paramount to standardize animal research. The results obtained in both **chapter 2** and **chapter 3** support this claim. Further standardization is key to reduce the use of animals and increase reproducibility and reliability across research groups worldwide. Organizations like the National Centre for the Replacement, Refinement & Reduction of animals in Research could offer a reliable means to provide specialized protocols for research groups worldwide.

9.2 Clinical impact

As already mentioned, current bleb-forming surgeries still have high failure rates and intense postoperative follow-up is required after these procedures. Additionally, possibly serious adverse events, such as bleb dysesthesia, hypotony, corneal edema, and blebitis/endophthalmitis may occur. All these risks make current glaucoma surgery burdensome and therefore unpopular for patients as well as surgeons. However, by postponing surgery, glaucomatous field loss may have progressed significantly due to conjunctival irritation/inflammation from long-term use of eye drops. Subsequent increase of growth factors in the aqueous humor (AqH) may further increase the fibrotic response leading to an increased failure rate when bleb-forming glaucoma surgery is finally undertaken [7]. Currently, roughly 10% of all bleb-forming surgeries still fail each year [8], accumulating to a failure rate of 40-50% after 5 years in long term studies [9-11].
Mitomycin C (MMC) is the gold standard treatment to reduce fibrosis after glaucoma filtration surgery. However, due to serious postoperative complications associated with the use of MMC such as endophthalmitis, cystic blebs, and leaking blebs, novel medications are now routinely investigated. Unfortunately, as shown in **chapter 2** and **chapter 6**, novel drugs, although safer, are in most cases less effective in reducing the fibrotic response compared to the gold standard treatment with MMC.

In this dissertation, several methods to reduce the fibrotic response after glaucoma filtration surgery were assessed. Firstly, the use of surface topographies in conjunction with a glaucoma drainage device to enhance forming of a robust well-functioning filtering bleb (**chapter 5**) and secondly, a degradable continuous-release

drug delivery system (DDS) filled with MMC (**chapter 7**) were evaluated. *In vitro* research has shown that surface topographies can alter the reaction of cells, *e.g.*, more, or fewer alternatively activated (M2) macrophages upon a surface [12]. The research presented in this thesis showed that surface topographies can modify the cellular response *in vivo*. However, we found an increased capsule thickness and presence of inflammatory cells after topographies were used. With further optimization, selection, and research for viable surface topographies, a reduced failure rate of bleb-forming surgeries with glaucoma drainage devices may be found. Surface topographies can be easily engineered onto a biomedical device, making it a viable method to implement with glaucoma drainage devices. However, further refinement and selection of surface topographies with SIBS is necessary.

The already mentioned gold-standard MMC is regularly used in the clinic as an antifibrotic drug during bleb-forming glaucoma surgery. MMC can either be applied intraoperatively with sponges, or injected postoperatively into the bleb (*e.g.*, in a bleb needling procedure). However, the use of MMC in Europe is off-label, resulting in unstandardized protocols, which may lead to unreliable and highly variable results between patients and clinics [13, 14]. The implementation of a DDS, loaded with MMC, during bleb-forming glaucoma surgery will help with standardizing the surgery and minimizing the risk for adverse events. In **chapter 7** two DDS designs were evaluated *in vivo*. Some adverse effects were found to be associated with the use of a DDS *in vivo* (*e.g.*, thin-walled cystic blebs). However, larger fluid-filled bleb cavities were seen during follow-up after using a DDS when compared to the gold standard, one-time intraoperative application of MMC. Although further optimization is required (*e.g.*, slower release of MMC or lower total dosage of MMC), the use of a DDS seems promising towards obtaining safer and more reliable methods to reduce fibrosis after bleb-forming glaucoma surgery.

The research presented within this thesis is another step forward towards safer and more successful bleb-forming glaucoma surgery, making early surgery more acceptable for patients and surgeons in the near future, and hopefully reducing the number of patients becoming severely visually impaired or getting blind from glaucoma.

9.3 Economic impact

It is problematic that healthcare professionals as well as patients tend to postpone surgical intervention until other options such as eye drops or laser surgery have failed, because of the aforementioned fear of considerable postoperative care and vision threatening complications [15]. Besides the large burden glaucoma has on

patients, the management of glaucoma puts a large strain on the current health care system. The medical costs (including office visits, glaucoma exams, visual field tests, medication, glaucoma surgeries, and cataract extraction), amount to approximately 400 to 1000 euros per person per year depending on disease severity [16, 17]. In 2020, it was estimated that approximately 65 million people suffered from glaucoma worldwide, which would account for medical costs of around 26 to 65 billion euros, which could even increase up to 45 to 112 billion euros by 2040 worldwide [1]. If the disease is not managed properly, costs can increase even more due to the need of home care for visually impaired patients. In the Netherlands, roughly 357.000 patients were diagnosed with glaucoma in 2021, an increase of approximately 5,5% compared to 2020 [18]. When considering medical costs of 400-1000 euros per patient per year, glaucoma treatment costs can yearly amount up to 357 million euros in the Netherlands alone.
Currently, topical medication is the first line of treatment in the management of glaucoma, accounting for roughly 55 to 61% of all health care costs [19]. Unfortunately, eye drops can be troublesome to instill and may cause side effects, which may lead to poor adherence [20]. It is estimated that 50% of patients will have stopped adhering to their treatment within the first year [21]. Nonadherence with medication and/or not reaching a target pressure that is sufficiently low causes further progression of visual field loss. When the disease progresses, additional medication is often prescribed, increasing both the costs and side effects caused by long-term use [19, 22]. Every 1 mmHg of reduction can save annually 10 million euros [23]. Therefore, with proper management of glaucoma, the total health care costs can be decreased by approximately 30-50% [17].

A shift in treatment paradigm would be required to reduce the healthcare costs for the management of glaucoma. In 2020, topical medication had a gross revenue of 4.8 billion dollars, while surgical glaucoma devices only had a gross revenue of 575 million dollars [21, 24]. In an ideal world, surgical intervention for glaucoma will be performed only once throughout a patient's life with no further need of additional medication or surgery to adjust IOP. Further implementation of safe and effective surgical methods may therefore be very cost effective. The implementation of the methods researched in this thesis, like surface topographies or using a DDS, may be helpful to reach this goal.

References

1. Kapetanakis, V.V., et al., *Global variations and time trends in the prevalence of primary open angle glaucoma (POAG): a systematic review and meta-analysis.* Br J Ophthalmol, 2016. **100**(1): p. 86-93.
2. Garway-Heath, D.F., et al., *Latanoprost for open-angle glaucoma (UKGTS): a randomised, multicentre, placebo-controlled trial.* The Lancet, 2015. **385**(9975): p. 1295-1304.
3. Mokhles, P., et al., *Glaucoma blindness at the end of life.* Acta Ophthalmol, 2017. **95**(1): p. 10-11.
4. Education, F.a.D.a.D.o.I.a.C. *Guidance Documents (Medical Devices and Radiation-Emitting Products)*. 2022 [cited 2022; Available from: https://www.fda.gov/medical-devices/device-advice-comprehensive-regulatory-assistance/guidance-documents-medical-devices-and-radiation-emitting-products.
5. Pound, P. and M. Ritskes-Hoitinga, *Is it possible to overcome issues of external validity in preclinical animal research? Why most animal models are bound to fail.* J Transl Med, 2018. **16**(1): p. 304.
6. Ferri, N., et al., *Drug attrition during pre-clinical and clinical development: Understanding and managing drug-induced cardiotoxicity.* Pharmacology & Therapeutics, 2013. **138**(3): p. 470-484.
7. Lusthaus, J. and I. Goldberg, *Current management of glaucoma.* Med J Aust, 2019. **210**(4): p. 180-187.
8. Beckers, H.J., K.C. Kinders, and C.A. Webers, *Five-year results of trabeculectomy with mitomycin C.* Graefes Arch Clin Exp Ophthalmol, 2003. **241**(2): p. 106-10.
9. Bowden, E.C., et al., *Risk Factors for Failure of Tube Shunt Surgery: A Pooled Data Analysis.* Am J Ophthalmol, 2022. **240**: p. 217-224.
10. Mariotti, C., et al., *Long-term outcomes and risk factors for failure with the EX-press glaucoma drainage device.* Eye (Lond), 2014. **28**(1): p. 1-8.
11. Souza, C., et al., *Long-term outcomes of Ahmed glaucoma valve implantation in refractory glaucomas.* Am J Ophthalmol, 2007. **144**(6): p. 893-900.
12. Vassey, M.J., et al., *Immune Modulation by Design: Using Topography to Control Human Monocyte Attachment and Macrophage Differentiation.* Adv Sci (Weinh), 2020. **7**(11): p. 1903392.
13. Bell, K., et al., *Learning from the past: Mitomycin C use in trabeculectomy and its application in bleb-forming minimally invasive glaucoma surgery.* Survey of Ophthalmology, 2021. **66**(1): p. 109-123.
14. Al Habash, A., et al., *A review of the efficacy of mitomycin C in glaucoma filtration surgery.* Clin Ophthalmol, 2015. **9**: p. 1945-51.
15. Bar-David, L. and E.Z. Blumenthal, *Evolution of Glaucoma Surgery in the Last 25 Years.* Rambam Maimonides Med J, 2018. **9**(3).
16. Varma, R., et al., *An assessment of the health and economic burdens of glaucoma.* Am J Ophthalmol, 2011. **152**(4): p. 515-22.
17. Traverso, C.E., et al., *Direct costs of glaucoma and severity of the disease: a multinational long term study of resource utilisation in Europe.* British Journal of Ophthalmology, 2005. **89**(10): p. 1245-1249.
18. M.M.J Nielen, M.J.J.C.P., A.M. Gommer, C. Hendriks. *Gezichtsstoornissen, Leeftijd en geslacht, Glaucoom*. 2021; Available from: https://www.vzinfo.nl/gezichtsstoornissen/leeftijd-en-geslacht/glaucoom.
19. Real, J.P., et al., *Direct costs of glaucoma: Relationship between cost and severity of the disease.* Chronic Illn, 2020. **16**(4): p. 266-274.
20. Beckers, H.J., et al., *Side effects of commonly used glaucoma medications: comparison of tolerability, chance of discontinuation, and patient satisfaction.* Graefes Arch Clin Exp Ophthalmol, 2008. **246**(10): p. 1485-90.
21. Downs, P., *2020 glaucoma pharmaceuticals market report a global analysis for 2019 to 2025*, M. scope, Editor. 2020.
22. Beckers, H.J., et al., *Adherence improvement in Dutch glaucoma patients: a randomized controlled trial.* Acta Ophthalmol, 2013. **91**(7): p. 610-8.
23. van Gestel, A., et al., *The long-term outcomes of four alternative treatment strategies for primary open-angle glaucoma.* Acta Ophthalmol, 2012. **90**(1): p. 20-31.

24. Freeman, B., *2020 glaucoma surgical device market report a global analysis for 2019 to 2025*, M. scope, Editor. 2020.

Summary

Summary

Glaucoma is the leading cause of irreversible blindness worldwide. The etiology and pathogenesis of this disease, in which the optic nerve slowly degenerates, are complex and not fully elucidated yet. The hallmark of the disease is progressive visual field loss. There is no causative treatment. Current treatments mainly focus on the reduction of (high) intraocular pressure (IOP), the main risk factor for developing glaucoma. To reduce visual field loss, patients are treated with IOP-lowering medications (usually eye drops), laser procedures, or glaucoma surgery. Unfortunately, despite treatment, glaucoma can still progress in patients. Twenty-five percent of patients will ultimately suffer from unilateral blindness and 10% from bilateral blindness at the end of their lives. For these patients, bleb-forming glaucoma filtration surgery (trabeculectomy or tube shunt surgery) has the highest IOP-reducing potential.

All bleb-forming procedures aim to create an alternative pathway for aqueous humor to exit the eye and reduce IOP. This is achieved by creating a hole/fistula between the anterior chamber and the subconjunctival/sub-Tenon's space (trabeculectomy), or by placing a drainage tube at this site. Aqueous humor will flow under the overlying conjunctiva and the accumulation of fluid there will create a small pouch, called a filtering bleb. However, surgery is often postponed due to fear of severe postoperative complications such as hypotony, bleb leakage, and endophthalmitis. Furthermore, despite the use of antifibrotic drugs in conjunction with filtering surgery (mostly mitomycin C (MMC)), approximately 10% of surgeries fail each year due to the formation of fibrosis and subsequent scarring of the filtering bleb, underlining the unmet need for refinement of current treatments or the development of new treatment modalities.

During the SEAMS project we aimed to develop novel biomedical devices and methods to implement within bleb-forming glaucoma surgery. The work presented within this dissertation can be divided into three sub-goals; validation of an animal model for glaucoma surgery research, development of a novel glaucoma drainage device, and development of a sustained drug delivery system loaded with MMC.

Before novel biomedical devices or drugs can be introduced into the clinic, a preclinical study needs to be performed to assess their safety and efficacy. **Chapter 2** offers a systematic review of currently used animal models and antifibrotic treatments for use in glaucoma filtration surgery research. Throughout the years, several types of animals have been used as models for this research, including mice, rats, rabbits, hamsters, dogs, and owl monkeys. Based on the systematic review,

small rodents (such as mice and rats) are ideally suited to test novel drug targets and to perform molecular studies on, due to readily available molecular tools such as transgenic/knock out animals and molecular analysis kits. Due to its large eye (similar to humans), strong fibrotic response, and ease of handling, the rabbit is ideally suited for the development of biomedical devices. Several types of drugs were evaluated in a pre-clinical setting. Although most drugs showed a higher safety profile compared to the gold standard treatment with MMC, a lower antifibrotic effect was often found. Therefore, further optimization regarding drug dosage, administration route, application frequency, and potentially the development of combination therapies or a drug delivery system (DDS) is needed before the current gold standard treatment with MMC can be replaced.

Standardization of animal research is essential to increase the reliability and reproducibility of experiments across different research groups worldwide. In **chapter 3**, three different tonometers, regularly used in animal research, were compared to find the most reliable device for use in rabbits. Amongst the three different tonometers, the iCare TonoVet had the lowest learning curve and showed the smallest inter- and intraobserver variation in rabbits. An approximately 25% mmHg lower IOP value was observed when rabbits were measured under sedation.

SIBS, or in full “poly(styrene-block-isobutylene-block-styrene)” is an innovative material that is currently used in coronary stents and in the PRESERFLO® MicroShunt, a glaucoma microshunt. Although it is made out of a biocompatible, non-erodible, thermoplastic polymer, bleb fibrosis still occurs in the clinic. To validate our rabbit animal model and find potential new targets for antifibrotic treatment modalities after implantation with a SIBS microshunt, rabbits were implanted with the PRESERFLO® MicroShunt and followed for 40 postoperative days to investigate bleb fibrosis (**chapter 4**). Macroscopically, all blebs failed within 2 weeks. Histologically, a wide influx of cells was visible, including macrophages, polymorphonuclear cells, foreign body giant cells, fibroblasts, and myofibroblasts. Novel methods that reduce the fibrotic response should consider the high variety of cells that attribute to the development of bleb fibrosis. Inhibition of the inflammatory response and the downregulation of fibroblasts can offer novel therapeutic avenues to downregulate both the fibrotic response and foreign body response towards a SIBS based implant.

Upon implantation of a biomedical device, a unique interface between the material and surrounding cells develops. One way to reduce fibrosis is by limiting or skewing the reaction of cells into a favorable (antifibrotic) reaction. Surface topographies have gained popularity within the biomedical community. Surface topographies have

shown to skew the cellular response *in vitro* and *in vivo*. However, their antifibrotic potential in bleb-forming glaucoma surgery hasn't been studied up until now. **Chapter 5** studies the effectiveness of surface topographies upon addition onto a modified microshunt. In this pilot study, a PRESERFLO® MicroShunt was modified with an endplate (with or without surface topographies), placed at the distal end of the tube. This study showed that bleb survival was extended by the addition of an endplate to the tube. An endplate with a smooth surface, induced less inflammation and encapsulation compared to the surface topographies, and extended bleb survival compared to the PRESERFLO® MicroShunt. Although one of the 3 topographies showed some promising results regarding bleb survival, results were inconclusive. Further *in vitro* research (currently ongoing) is necessary to select and validate proper surface topographies, optimized with SIBS, to be implemented onto a microshunt.

To prevent the formation of fibrosis in the filtering bleb, MMC is currently used as the gold standard antifibrotic treatment. The past, current and future use of MMC is discussed in **chapter 6**. MMC can be applied intraoperatively with sponges or injected directly into the bleb postoperatively. Although MMC is an effective drug, it is cytotoxic to surrounding tissue, which can lead to severe vision threatening complications. There is an ongoing search for novel antifibrotic drugs that can limit the fibrotic response. In **chapter 2**, a multitude of drugs that are under investigation have been reviewed. While most were safer compared to the current standard, they often lacked efficacy. Therefore, further research is needed to optimize these novel drugs. A drug delivery system (DDS) can release a low dosage of a drug over a certain period of time. In theory, after implementation of a DDS, a continuous, controlled, low dosage can be achieved. Another advantage of a DDS would be a limitation of cytotoxic side effects, while maintaining an effective dosage (see **chapter 6**). In **chapter 7**, two DDS designs were evaluated *in vitro* and *in vivo*. As carriers, either polycaprolactone (PCL) or polylactic-co-glycolic acid (PLGA) were used. *In vitro* release kinetics showed a comparable release for both the PCL-based DDS and the PLGA DDS. However, a secondary burst of MMC was noted around day 42 for the PLGA DDS, which was possibly caused by hydrolysis of the PLGA polymer. The antifibrotic efficacy *in vivo* was compared to the gold standard treatment of 0.4 mg/ml MMC, intraoperatively applied for 3 minutes. Both DDS designs were as effective as the gold standard treatment, but the PLGA DDS showed more favorable results when compared to the PCL-based DDS. Ninety-nine % of all MMC was released at day 90 *in vitro*, and the DDS showed a fast degradation rate with a shorter foreign body response. However, thin-walled blebs were noted in the early postoperative period, Therefore, further optimization in dosage, release and

dispersion of MMC into the bleb will be required to minimize side effects before the DDS can be used in patients.

Samenvatting

Samenvatting

Glaucoom is wereldwijd de belangrijkste oorzaak van onomkeerbare blindheid. De ziekte wordt gekenmerkt door een langzame degeneratie van de oogzenuw en hierbij passende progressieve gezichtsvelduitval. De etiologie en pathogenese van glaucoom zijn complex en nog steeds niet helemaal opgehelderd. Er is tot op heden geen behandeling voorhanden waarbij de ontstane gezichtsveldschade kan worden verholpen. Alle huidige behandelingen zijn gebaseerd op verlaging van de (meestal verhoogde) oogdruk, de belangrijkste risicofactor voor het ontwikkelen van glaucoom. Om gezichtsveldverlies door glaucoom zoveel mogelijk te beperken worden patiënten behandeld met oogdruk verlagende medicatie (meestal oogdruppels), laserbehandelingen of chirurgie. Ondanks behandeling kunnen patiënten echter helaas nog steeds achteruitgaan. Uiteindelijk zal, aan het eind van hun leven, 25% van alle glaucoom patiënten blind worden aan één oog en 10% aan beide ogen. Voor deze patiënten heeft filterblaasvormende glaucoomchirurgie (trabeculectomie of glaucoomimplantaat) de hoogste potentie om de oogdruk effectief te verlagen.

Alle filterblaasvormende procedures creëren een alternatieve route voor de uitstroom van kamerwater (inwendig oogvocht) uit het oog, waardoor de oogdruk wordt verlaagd. Dit wordt bereikt door het maken van een opening ofwel “fistel” tussen de voorste oogkamer en de subconjunctivale ruimte (trabeculectomie), of door een glaucoomimplantaat te plaatsen dat middels een flexibel buisje (tube) het kamerwater afvoert van voorste oogkamer naar de subconjunctivale ruimte. Het hier verzamelde kamerwater vormt een vloeistofreservoir, een zogenaamde filterblaas of “bleb”. Deze chirurgische procedures worden helaas vaak lang uitgesteld vanwege angst voor ernstige complicaties, zoals hypotonie (te lage oogdruk), filterblaaslekkage en infecties (endophthalmitis). Bovendien falen nog vrij veel operaties door de vorming van fibrose in het operatiegebied, waardoor de filterblaas verlittekent en de oogdruk weer oploopt. Ondanks het gebruik van fibrose remmende middelen (meestal mitomycine C (MMC)), faalt jaarlijks ongeveer 10% van deze operaties. Dit benadrukt dat er een onvervulde behoefte is aan verfijning van bestaande, of het ontwikkelen van nieuwe behandelingen.

Het doel van het SEAMS project was om bestaande chirurgische behandelingen te verfijnen en hierbij ook op zoek te gaan naar nieuwe chirurgische behandelopties. Het onderzoek binnen dit proefschrift is op te delen in 3 verschillende subdoelen. Validatie van een diermodel van glaucoomchirurgie, ontwikkeling van een nieuw glaucoom drainage implantaat en ontwikkeling van een medicatieafgifte systeem geladen met

Voordat een nieuw biomedisch implantaat of medicijn geïntroduceerd kan worden in de kliniek is een preklinische validatie noodzakelijk Hierdoor wordt zowel de veiligheid als de effectiviteit van een behandeling gewaarborgd. In **hoofdstuk 2** werd een systematische review uitgevoerd waarbij verschillende diermodellen van glaucoomchirurgie en antifibrotische medicijnen vergeleken zijn. Hieruit bleek dat vooral kleine dieren zoals ratten en muizen gebruikt worden voor de ontwikkeling van medicijnen, of voor fundamenteel (moleculair) onderzoek met betrekking tot de fibrotische reactie. Dit komt mede door de beschikbaarheid van moleculaire tools en transgene/knock-out dieren. Daarentegen is het konijn ideaal voor de ontwikkeling van nieuwe biomedische implantaten/apparaten door onder meer de grootte van het oog, de sterke fibrotische reactie en de hanteerbaarheid van het dier. Antifibrotische medicijnen die momenteel op diermodellen getest worden zijn veelal minder effectief dan de gouden standaardbehandeling met MMC, echter blijken ze vaak veiliger en hebben ze minder toxische effecten. Verdere optimalisatie omtrent dosering, administratie, applicatiefrequentie en de eventuele ontwikkeling van combinatietherapieën of medicijnen afgiftesystemen (drug delivery system, DDS) zal dan ook nodig zijn voordat de huidige gouden standaardbehandeling met MMC vervangen kan worden.

Standaardisatie van dierexperimenteel onderzoek is essentieel om de betrouwbaarheid en reproduceerbaarheid van dierexperimenten te verhogen. Drie verschillende tonometers die gebruikt kunnen worden voor dierexperimenteel onderzoek zijn vergeleken in **hoofdstuk 3**. Hieruit bleek dat de iCare TonoVet de laagste leercurve en de kleinste inter- en intraobserver variatie had voor het gebruik in konijnen. Verder werd een 25% mmHg lagere oogdruk gemeten na het gebruik van sedatie.

Poly(styrene-block-isobutyline-block-styrene) ofwel SIBS, is een innovatief materiaal dat op het moment gebruikt wordt in cardiale stents en in de PRESERFLO® MicroShunt, een minimaal invasief glaucoomimplantaat bestaand uit een kort en dun flexibel buisje zonder eindplaatje. Hoewel dit polymeer goed getolereerd wordt door het menselijk lichaam, treed er nog steeds fibrose op in de filterblaas. Om het konijnmodel voor glaucoomchirurgie te valideren en eventueel nieuwe opties voor therapieën te ontdekken, werden konijnen geïmplanteerd met de PRESERFLO® MicroShunt. Hierna werd de wondgenezing voor 40 dagen opgevolgd (**hoofdstuk 4**). Alle filterblazen faalden binnen 2 weken na implantatie. Histologische bepalingen lieten een verhoging van het aantal macrofagen, granulocyten, vreemd lichaam reuzencellen, fibroblasten en myofibroblasten zien. Nieuwe methodes om de fibrose te remmen zullen rekening moeten houden met de grote verscheidenheid aan cellen die belangrijk zijn bij de ontwikkeling van fibrotisch weefsel. Inhibitie van de

inflammatoire reactie en van fibroblasten kan nieuwe therapeutische wegen bieden om zowel de fibrotische reactie als de lichaamsvreemde reactie op een SIBS microshunt te verlagen.

De implantatie van een biomedisch implantaat zorgt voor een unieke interactie tussen het materiaal (polymeer)en het omliggende weefsel. Eén manier om fibrose te remmen is door de reactie van cellen op het materiaal te beïnvloeden of deze aan te sturen naar een gunstig scenario waarbij minder fibrose ontstaat. De laatste jaren is binnen de biomedische gemeenschap veel aandacht besteed aan het effect van oppervlaktetopografieën van een materiaal op cellen. *In vitro* onderzoek heeft laten zien dat oppervlaktetopografieën de cellulaire reactie kunnen beïnvloeden door bijvoorbeeld differentiatie van specifieke cellen aan te sturen. Binnen de glaucoomchirurgie is het echter nog onduidelijk welke oppervlaktetopografieën de fibrotische reactie kunnen remmen. In **hoofdstuk 5** is een pilotstudie uitgevoerd waarbij konijnen zijn geïmplanteerd met een gemodificeerde PRESERFLO® MicroShunt. Aan de MicroShunt werd een eindplaatje (overeenkomend met, maar kleiner dan de huidige conventionele glaucoomimplantaten) gefabriceerd, dat wel of niet voorzien was van oppervlaktetopografieën. Deze studie liet zien dat de filterblaasoverleving verlengd kon worden door de additie van een eindplaatje. Hoewel één van de drie geteste oppervlaktetopografieën in eerste instantie een positief effect leek te hebben, konden er uit dit experiment vanwege de beperkte data geen eenduidige conclusies getrokken worden over een mogelijk antifibrotisch effect. Het gebruik van een eindplaatje met een vlak en onbewerkt oppervlak liet minder inflammatie en inkapseling van de microshunt zien, met verbeterde filterblaasoverleving t.o.v. de PRESERFLO® MicroShunt. Verder *in vitro* onderzoek (nu gaande) is nodig voor de selectie en validatie van geschikte oppervlaktetopografieën voor implementatie op een microshunt.

Om de vorming van fibrose te remmen na een glaucoomoperatie is MMC vooralsnog de gouden standaard. In **hoofdstuk 6** is het historische, het huidige en het toekomstige gebruik van MMC toegelicht. MMC wordt op het moment meestal intra-operatief en soms postoperatief gebruikt om fibrose tegen te gaan. Hoewel MMC erg effectief is, is het gebruik van MMC geassocieerd met potentieel ernstige bijwerkingen die visusbedreigend kunnen zijn. Op het moment is veel onderzoek gericht op het testen van nieuwe antifibrotische medicatie (zie **hoofdstuk 2**). Hoewel de meeste geteste medicijnen veiliger zijn dan MMC, zijn ze meestal minder effectief in het remmen van de fibrotische reactie. Verfijning van het huidige gebruik van MMC heeft daarom tot nu toe de meeste kans van slagen. Een DDS kan een continue lage dosis afgeven op een gewenste locatie. Hierdoor kan een effectieve dosis in het weefsel gehandhaafd blijven met waarschijnlijk minder cytotoxische bijwerkingen. In

hoofdstuk 7 werden twee verschillende DDS-designs vergeleken met elkaar. Twee verschillende polymeermatrixen zijn hiervoor gebruikt, polycaprolactoon (PCL) en poly-lactaat-co-glycolzuur (PLGA). Het antifibrotische effect werd *in vivo* vergeleken met de gouden standaardbehandeling met MMC (eenmalig intra-operatieve applicatie van MMC). Hoewel beide designs even effectief waren in het behouden van een filterblaas t.o.v. de gouden standaard, toonde de PLGA DDS de meest veelbelovende resultaten. De PLGA DDS toonde een release van 99% binnen 90 dagen *in vitro*, had een hogere degradatiesnelheid en een kortere lichaamsvreemde reactie. Verdere optimalisatie van de DDS is echter nog nodig. Een dunwandige filterblaas werd soms gezien bij konijnen die geïmplanteerd werden met een DDS. Optimalisatie in de dosering, de release en diffusie (binnen de bleb) van MMC uit de DDS zal daarom nog noodzakelijk zijn om cytotoxische bijwerkingen te minimaliseren, alvorens de DDS geschikt kan zijn voor gebruik in patiënten.

Dankwoord

In november 2019 ben ik gestart als promovendus bij het SEAMS-project (Smart, Easy, and Accurate Minimally Invasive Glaucoma Surgery project). Allereerst wil ik natuurlijk mijn promotieteam bedanken. Zonder hen zou dit boekje nooit tot stand zijn gekomen. Om te beginnen met Henny, bedankt voor deze mooie kans. Ik ben je erg dankbaar voor alles wat je me hebt geleerd, inclusief de operatietechnieken die ik altijd met veel plezier heb uitgevoerd. Het was een voorrecht om onder jou te mogen promoveren.

Jarno, sinds mijn eerste dag heb jij mij begeleid als copromotor. Jouw strakke tijdsschema's en wekelijkse overleg, stipt om 8:00 uur 's ochtends, heb ik altijd erg gewaardeerd. We hebben altijd interessante discussies gehad over de resultaten en de voortgang van het project. Daarnaast stond je altijd voor me klaar wanneer ik hulp nodig had en je keek mijn manuscripten en andere teksten altijd grondig na.

Christian, ik herinner me nog goed het moment waarop je me vertelde dat er een functie als promovendus binnen de oogheelkunde beschikbaar was. Jij vond dat ik de perfecte kandidaat was voor die positie. Enige tijd later kwam ik je nog eens tegen in Roermond, waar je me opnieuw probeerde over te halen. Je zei dat ik tot de avond de tijd had om te solliciteren op die functie. Kennelijk met succes, want die avond heb ik mijn sollicitatie geschreven en verstuurd. Tijdens mijn tijd bij de oogheelkunde hebben we veel gelachen, gedronken en gegeten (ik wil niet weten hoeveel kilo döner er in al die jaren doorheen is gegaan). Je stond altijd klaar om me te helpen en mee te denken bij problemen. Ik wil je dan ook hartelijk bedanken voor de leuke tijden en je hulp.

Het SEAMS-project zou niet zijn wat het is zonder het consortium van onderzoekers van de Technische Universiteit Eindhoven, Santen InnFocus, de Universiteit Maastricht en het Universitair Medisch Centrum Maastricht. Theo, Frank, Marion, Leonard, Jaap, Jan, Albert, Sebastian, Ines en Phani, bedankt voor jullie input, de interessante werkdiscussies en de gezellige etentjes.

Ik heb het geluk gehad om met een aantal leuke collega's samen te werken, te beginnen met Marjolein, Linda, Floortje en Anke. Ik wil niet weten hoeveel duizenden coupes jullie hebben gesneden. Bedankt voor al jullie hulp en inzet bij het opzetten en uitvoeren van de histologie. Mijn tijd op kantoor zou een stuk saaier zijn geweest zonder jullie. Bedankt voor de gezellige sfeer en niet te vergeten de borrels na het werk.

Daarnaast wil ik alle onderzoekers bedanken: Wouter, Pascal, Suryan, Luigi, Wenting, Magali, Maartje, Joukje, Nienke, Lotte, Shuhe, Yu Yu, Birke, Marlies en Tos. We hebben een gezellige tijd gehad binnen de oogheelkunde.

Binnen het SEAMS-project heb ik in totaal met 167 konijnen gewerkt. Hoewel mijn geduld soms op de proef werd gesteld, was het een eer om met deze dieren te werken en ik zal hun bijdrage aan de wetenschap nooit vergeten.

Hoewel collega's essentieel zijn voor een goede tijd als promovendus, zijn familie en vrienden net zo belangrijk voor het waarborgen van je mentale gezondheid. Allereerst wil ik mijn vrienden bedanken voor alle leuke activiteiten, steun en interesse in mijn werk gedurende de afgelopen jaren. In het bijzonder wil ik Guus, Robin, Lorenzo en Chrissy noemen. We hebben veel leuke momenten samen beleefd die ik nooit zal vergeten. Het was altijd fijn om met jullie tijd door te brengen en te ontspannen.

Een lichte competitiedrang ten opzichte van mijn broer en zus heeft ertoe geleid dat ik na mijn hbo-studie ben gaan doorstuderen en uiteindelijk een PhD ben gaan doen. Tim, je stond altijd te "hakken" op je kamer, hoewel dat tegenwoordig wat minder is, blijft het een leuke herinnering. Zoë, van jongs af aan speelden we al dierenarts of dierenasiel, zoals je kunt zien heb ik veel aan die ervaring gehad. Daarnaast heb je me geleerd dat stress nooit goed voor je is, hoewel ik de manier waarop dat tot uiting kwam buiten beschouwing zal laten in dit boekje. Toch bedankt hiervoor. Gerry, ook jij verdient een bedankje. Je bent een welkome toevoeging aan onze familie. Toen Zoë je aan ons voorstelde, kon ik je nauwelijks verstaan vanwege je Belgische accent. Nu ik je goed kan volgen, zijn je verhalen zeker het luisteren waard en samen lachen we veel (soms ook ten koste van Zoë). Olivia, Fileine, Siem, Dinand en Maeve, ook al zijn jullie te jong om dit later te herinneren, ben ik trots om jullie oom te zijn. Ik waardeer de extra training die jullie me bieden door met mij vliegtuigje te spelen en ik zal dat zo lang mogelijk volhouden.

Marly, of zoals ik je beter ken, "mam". Ik ken niemand die zo altruïstisch is als jij en ik wil je bedanken voor al je hulp en liefde gedurende de jaren.

Hoiie he,
Ralph

Appendix

Curriculum vitae

Radulfus (Ralph) Johannes Stefanus van Mechelen was born on the 4th of June 1993 in Heerlen, the Netherlands. In 2011 he graduated from senior general secondary education (HAVO) at the Grotius College in Heerlen. Afterwards, he started a practical bachelor in life science at the Zuyd University of applied sciences. He graduated from his bachelor in 2015. He obtained his Master of Science degree in biomedical science from the University of Maastricht in 2017. He briefly worked at the Pediatrics department as a research associate up until December 2017. Hereafter, he obtained a position at the centrale proefdiervoorzieningen (CPV) Maastricht as a biotechnician. He started his PhD at the University eye clinic Maastricht in 2018 under supervision of prof. dr. Henny Beckers (this thesis). This was a cross-translational multidisciplinary international cooperation between Maastricht University, Maastricht University Medical Center +, Eindhoven University of Technology, and InnFocus Inc., a Santen company. The research was performed within the framework of the Chemelot Institute for Science and Technology (InSciTe).

Appendix

II

List of publications

Accepted manuscripts

- van Mechelen, R. J. S., Wolters, J. E. J., Herfs, M., Bertens, C. J. F., Gijbels, M., Pinchuk, L., Gorgels, T. G. M. F., & Beckers, H. J. M. (2022). Wound Healing Response After Bleb-Forming Glaucoma Surgery With a SIBS Microshunt in Rabbits. *Translational vision science & technology*, *11*(8), 29.

- van Mechelen, R. J. S., Wolters, J. E.J., Bertens, C. J. F., Webers, C. A. B., van den Biggelaar, F. J. H. M., Gorgels, T. G. M. F., & Beckers, H. J. M. (2022). Animal models and drug candidates for use in glaucoma filtration surgery: A systematic review. *Experimental eye research*, 217, 108972.

- *Bertens, C. J. F., ***van Mechelen, R. J. S.**, Berendschot, T. T. J. M., Gijs, M., Wolters, J. E. J., Gorgels, T. G. M. F., Nuijts, R. M. M. A., & Beckers, H. J. M. (2021). Repeatability, reproducibility, and agreement of three tonometers for measuring intraocular pressure in rabbits. *Scientific reports*, *11*(1), 19217. * shared co-author

- *Wolters, J. E. J., ***van Mechelen, R. J. S.**, Al Majidi, R., Pinchuk, L., Webers, C. A. B., Beckers, H. J. M., & Gorgels, T. G. M. F. (2021). History, presence, and future of mitomycin C in glaucoma filtration surgery. *Current opinion in ophthalmology*, *32*(2), 148–159. * shared co-author

- van Mechelen, R. J. S., Sudarsanam, P., Bertens, C. J. F., Tas, M. O., Gijbels, M. J. J., Pinchuk, L., de Boer, J., & Beckers, H. J. M. (2023). The Influence of Design Modifications and Microstructured Surface Topographies on Bleb Survival after Glaucoma Tube Shunt Implantation. Advanced biology, e2300051. Advance online publication.

- **van Mechelen, R. J. S.**, Wolters, J. E. J., Fredrich, S., Bertens, C. J. F., Gijbels, M. J. J., Schenning, A. P. H. J., Pinchuk, L., Gorgels, T. G. M. F., & Beckers, H. J. M. (2023). A Degradable Sustained-Release Drug Delivery System for Bleb-Forming Glaucoma Surgery. Macromolecular bioscience, e2300075. Advance online publication.

Manuscripts under review

- Pereira, I.C.F., **van Mechelen, R. J.S.**, Wyss H.M., Pinchuk, L., Beckers, H.J.M., & den Toonder J.M.J. (2023). Magnetically actuated glaucoma drainage device for regulating intraocular pressure after implantation.

Manuscripts unrelated to this thesis

- Barkhuizen, M., Vles, J. S. H., **van Mechelen, R.J.S.**, Vermeer, M., Kramer, B. W., Chedraui, P., Bergs, P., van Kranen-Mastenbroek, V. H. J. M., & Gavilanes, A. W. D. (2019). Preterm Perinatal Hypoxia-Ischemia Does not Affect Somatosensory Evoked Potentials in Adult Rats. *Diagnostics (Basel, Switzerland)*, *9*(3), 123.

- Barkhuizen, M., **van Mechelen, R.J.S.**, Vermeer, M., Chedraui, P., Paes, D., van den Hove, D. L. A., Vaes, B., Mays, R. W., Steinbusch, H. W. M., Robertson, N. J., Kramer, B. W., & Gavilanes, A. W. D. (2019). Systemic multipotent adult progenitor cells improve long-term neurodevelopmental outcomes after preterm hypoxic-ischemic encephalopathy. *Behavioural brain research*, *362*, 77–81.

- Barkhuizen, M., van Dijck, F. J. P., Jellema, R. K., Gussenhoven, R., Engelbertink, I., **van Mechelen, R.J.S.**, Cleutjens, J. P. M., Seehase, M., Steinbusch, H. W. M., Zimmermann, L. J., Gavilanes, A. W. D., & Kramer, B. W. (2018). The influence of anesthetics on substantia nigra tyrosine hydroxylase expression and tau phosphorylation in the hypoxic-ischemic near-term lamb. Pediatric research, 83(6), 1190–1199.